



Università degli Studi di Cagliari

**PhD IN SOIL DEFENSE AND CONSERVATION, ENVIRONMENTAL
VULNERABILITY AND HYDROGEOLOGICAL PROTECTION**

XXV Cycle

**REMOTE SENSING AND GIS-BASED MAPPING ON LANDSLIDE
PHENOMENA AND LANDSLIDE SUSCEPTIBILITY EVALUATION OF
DEBRESINA AREA (ETHIOPIA) AND RIO SAN GIROLAMO BASIN
(SARDINIA)**

Sector of Scientific Disciplines: *Applied Geology [GEO/05]*

Presented by:

Asmelash Abay Hagos

Doctoral Program Coordinator:

Prof. Felice Di Gregorio

Tutor:

Prof. Giulio Barbieri

Academic Year 2011/2012

ACKNOWLEDGEMENTS

The present Doctoral thesis is the final output of my three-year study. During the thesis work, I have acquired help from many individuals and institutions. Therefore, it gives me a pleasure to recognize all individuals and organizations who contributed to the success of this work.

This PhD study was made possible by the scholarship grant from the Italian Ministry of Foreign Affairs' Cooperation Office for Developing Countries. A special gratitude goes to the Italian Government for giving me such opportunity to follow my Study. I would like to express my thanks to my employer, Mekelle University, for allowing me leave of absence for my study abroad.

I am privileged to express my sincere thanks and appreciations to my promoter Prof. Ing. Giulio Barbieri, not only for his continuous and remarkable guidance in the academic aspect throughout my study but also for his efforts in persuading the Italian government to support my PhD study financially. His constant encouragement and invaluable advice starting from the beginning of the research until the end enables me to reach at this level. Thank you very much professor for your versatile and limitless help.

My warmest gratitude goes to the Applied Geology and Geophysics section, at the Department of Civil, Environmental Engineering and Architecture, University of Cagliari for allowing me the laboratory and office facilities during my stay there. My particular warmest gratitude goes to Mr. Mario Sitzia for his unforgettable help he did in both office and field works. It was difficult to complete my field work of Sardinia project without the help of Mario using his personal car. I am also indebted to Mr. Piero Marras, for he allows me to use his car with him during some of the field days in the Sardinian project. Other Colleagues at Cagliari University who helped me in various aspects such as Mr. Luigi Noli and Tonio Trogu are highly appreciated.

I am thankful to Earth Science Department of Cagliari University for permitting me to use the laboratory facilities. Special appreciations go to Prof. Marco Marchi for helping me in analyzing the petrographic and chemical tests; Prof. Stefano Columbu for valuable help in the laboratory analysis of physical tests of rocks and Mr. Salvatore Noli for his help in the thin section preparation. I am grateful to Prof. Marcella Palomba, of the National Research Council of Cagliari for her support in the X-ray diffraction analysis of the clay samples.

The following institutions and individuals therein, are highly acknowledged :(1) The Geotechnical Laboratory of Cagliari Province, special gratitude go to Dr. Salvatore Pistis and his colleagues for the free access to carry out geotechnical tests of soils (2) Tekeze Deep Water Wells Drilling P.L.C, particularly to Mr Teklewoini Asefa (board director), Mr. Mulugeta G/Tsadik (General manager) and Mr. Asefa Marse (Operation department head) for allowing me car during my field work in the Debresina area (3) The USGS-Northern

California Earthquake Data Centre and USGS/NASSA for allowing the free access to use the earthquake data and Aster images of the study area respectively (4) The National Meteorology Agency of Ethiopia for their permission to use the rainfall data of the area (5) The Information Network Security Agency (INSA) of Ethiopia for providing me the SPOT image of the study area (6) The Geological Survey of Ethiopia (GSE) for providing me some Landsat images and other reference materials. My particular thanks to Mr. Leta Alemayoh for the reference materials he gave me during my data collection (7) The Tarmaber Woreda Administrations for their cooperation during the field work.

I am highly indebted to the academic board members of the PhD courses in “Soil Defense and Conservation, Environmental Vulnerability and Hydrogeological Protection”, at the Doctoral School in Environmental and Land Engineering and Sciences of Cagliari University for their yearly evaluation and valuable comments on the status of this PhD thesis. My particular appreciation goes to Prof. Felice Di Gregorio, Programme Coordinator of the PhD, for his encouragements.

It gives me a special privilege to extend my earnest thanks to my friends Dr. Abdelwassie Hussien and Tesfaye Asresahagne for both academic and social experiences and support that they shared me while we were together at home, University office and field works.

I am highly indebted to Dr. Mulugeta Fiseha, Earth Science Department of Addis Ababa University; Dr. Miruts Hagos, Earth Science Department of Mekelle University; Mr. Fethanegest W/Mariam from Axum University for their comments on some of the chapters of the thesis. I am also thankful my colleagues of the Earth Science Department of Mekelle University, particularly to Dr. Kifle W/Aregay for aerial photos and some images he provided me; Dr. Tesfamichael G/Yohanes & Dr. Kassa Amare for their valuable encouragements.

Finally, I would like to thank my wife, Yalem, for her courageous patience and hardship of taking home responsibility during my absence. Similarly, I want to extend my fatherly love to my children Sofonias, Danait and Soliana for they show good understanding and patience about my absence for the study. I sincerely thank to all my beloved family for they are all the bases for my success.

Above all, I would like to thank ‘Almighty God’ who made it possible to begin and finish this work successfully.

Dedications

- To my late mother Alganesh Mesele, because “Mother’s love never fades”

And

- To my wife, Yalem Fiseha and my children Sofonias, Danait and Soliana for none of this work would have been possible without thier love and patience.

ABSTRACT

The thesis presents GIS based spatial data analysis for landslide phenomena and susceptibility mapping which is carried out in Debresina area of the Afar rift margin (in Ethiopia) and in Rio San Girolamo basin at the margin of Campidano graben (in Sardinia, Italy). Both of these distant study areas are prone to various types of landslide and landslide-generated hazards with tremendous damages such as loss of human lives, failure of infrastructures, and damage on agricultural fields and on the natural environment. Landslides and related hazards have no geographic boundaries. They occur in both developed countries (like Italy) and in developing countries (like Ethiopia) causing a continuous threat to human beings all over the world.

The objectives of this study in both project areas were therefore: (1) to generate maps of landslide inventory and various landslide causative factors, and evaluate their contribution to the occurrences of landslide and its frequency in the respective study areas, (2) to evaluate the landslide susceptibility and prepare maps of both study areas using various GIS based methods and compare their results, (3) to recommend landslide hazard mitigation strategies based on the final findings of the study for both respective project areas.

The study accomplished: (1) characterization of 160 and 108 landslide occurrences in Debresina and R.S.Girolamo areas respectively (2) remote sensing and field investigations of the landslide causative factors (3) laboratory investigations of some physical, mineralogical and geotechnical properties of rocks and soils, and (4) GIS-based data analysis and landslide susceptibility evaluation using Overlay Mapping (OM), Frequency Ratio (FR), Analytical Hierarchal Process (AHP) and Global Limit Equilibrium (GLE) methods. Besides, methods like the Kinematic Analysis and Melton Ratio are also applied to further appraise the effect of geological structures in the Debresina area and to identify the type of debris flow, debris flood and normal flood in the R.S.Girolamo respectively.

Though the utilized landslide causative factors vary depending on the applied methods and the specific condition of the study areas, a total of seven landslide causative factors such as lithology, proximity to faults and to drainages, land use, slope, aspect and elevation were selected and prepared in GIS for landslide susceptibility mapping in the Debresina area. Six similar causative factors are also used at the R.S.Girolamo area excluding proximity to fault.

Results of the study revealed that: (I) the major final triggering factor for the September 2005 landslide event of Debresina area is most probably earthquake besides to the saturation and active gully erosion while in R.S.Girolamo are rainfall and active gully erosion (II) More than 77% of the landslide occurrence in Debresina area is contributed by complex/composite slide and debris/earth slide while about 75% landslide occurrences in R.S.Girolamo is covered by debris flow (III) all the methods (OM, FR and AHP) more or less give similar

indication that an area is susceptible to slope failure in Debresina area if it is covered by lithology of colluvium-eluvium, debris deposits, various tuffs and clay soils, have slope range of 10° - 40° , land use of river course, arable and bare rock, have proximity to fault of 0-600m and to drainage 0-300m, have elevation of 2000-2500m and with an aspect to East and Southeast. Whereas the R.S. Girolamo area is prone to landslide if it has a lithology of alluvium, talus, granite and colluvium; have a slope class $>26^{\circ}$, have land use of river coarse, forest and bare rock, have proximity to drainage of 0-100m, with elevation of 450-600m and having an aspect of facing North, Northwest, Northeast and Southward (IV) the top landslide causative factors in Debresina area are lithology (34.2%), proximity to fault (24.5%), proximity to drainage (16.2%) while in the R.S. Girolamo the main landslide influencing factors are proximity to drainage (41%), lithology (24%) and land use (13%), (V) the prediction accuracy of the OM, FR and AHP methods in both study areas is compared based on Area under the Curve (AUC) method and results verified that the percentage of prediction accuracy of the methods in general is higher at the Debresina area than in R.S.Girolamo. This could be mainly attributed to the prevalent landslide types in each study areas. Hence, it can be suggested that the applicability of these methods for the susceptibility analysis flow-like landslides (e.g. debris flow) and rock falls/topples are relatively lower than in the other types of landslide types (VI) in the GLE method of circular failure surface, the reduction of the SF from the dry slope to the saturated slope condition for the Debresina area is 43-45%, but in the case of R.S.Girolamo the reduction of SF reaches up to 64-71%. This evidenced that the triggering impact of water for slope failure is greater in R.S.Girolamo than in Debresina area (VII) the overall study results of the various methods presented in this thesis have shown the great potential of GIS-based landslide predictions and can therefore be used as a basic data for preliminary slope management and land-use planning of the respective study areas.

The state of prevention towards the hazards is quite different in both areas, owing to the developmental difference of the two countries, Ethiopia and Italia. Thus, in R.S.Girolamo landslide and related hazard prevention measures are better institutionalized and, hence, with better territorial management and public awareness of the hazard. Whereas in Debresina area, no responsible institution exists to date and the territorial management is poor, and people have no idea how to prevent landslide hazards. Based on the obtained susceptibility maps and considering the economic, cultural and technological differences of the two study areas, landslide hazard mitigation strategies and remedial measure options are recommended

Keywords: Landslide susceptibility, Causative factors, GIS-Overlay Mapping (OM), Frequency Ratio (FR); Analytical Hierarchical Process (AHP); Global Limit Equilibrium (GLE); Debresina (Ethiopia) & R.S.Girolamo (Sardinia)

ACKNOWLEDGEMENTS	I
ABSTRACT	IV
LIST OF FIGURES	XII
LIST OF TABLES	XVIII
ACRONYMS	XX
Part I: General	1
1. General introduction	1
1.1 Objective of the research	2
1.1.1. General objective	2
1.1.2 Specific objectives	2
1.2 Methodologies and approaches	2
1.2.1 Literature review	4
1.2.2 Data collection	4
1.2.3 Laboratory works	8
1.2.4. Data evaluation and GIS-based modeling of landslide susceptibility	8
1.3 Structure of the Thesis	9
2. Theoretical backgrounds.....	11
2.1 Definition of landslide hazard and terminologies.....	11
2.2 Factors influencing the slope stability	11
2.2.1 Geological factors	12
2.2.1.1 Types and properties of soils and rock materials	12
2.2.1.2 Discontinuities	13
2.2.1.3 Weathering of geologic materials	14
2.2.2 Topographic and morphometric factors	15
1.2.2.1 Slope gradient	15
2.2.2.2 Aspect	15
2.2.2.3 Elevation	16
2.2.2.4 Drainage factors	16
2.2.2.5. Basin relief and basin ratio.....	16
2.2.2.6 Melton’s ratio (R).....	17
2.2.3 Land use factor.....	17

2.2.4. Hydrological factors.....	18
2.2.4.1 Precipitation	18
2.2.4.2 Groundwater	19
2.2.5. Seismicity factors.....	19
2.3 Types and mechanisms of slope failures	20
2.3.1 Slides.....	21
2.3.2 Falls.....	21
2.3.3 Topples.....	21
2.3.4 Lateral spreads	22
2.3.5 Flows.....	22
2.3.6 Complex movements.....	23
2.4 Methods of slope failure assessment.....	23
2.4.1 Assumptions.....	23
2.4.2 Qualitative method.....	25
2.4.3 Quantitative method.....	25
2.4.3.1 Statistical and probabilistic methods.....	25
2.4.3.2 Deterministic method.....	29
2.4.4 Semi-quantitative methods.....	31
Part II: Debresina area (Ethiopia)	33
3. General characteristic of the study area and Afar Rift margin	33
3.1 General overview of the Afar Rift margin	33
3.1.1 Geological and structural setting.....	33
3.1.2. Physiography and climate	38
3.1.3 Seismicity of Rift margin.....	42
3.1.4. Landslide status and regional trends at the Rift margin	44
4. Description of the Debresina area and data preparation	48
4.1 Background and problem definition of Debresina landslide.....	48
4.2 Location of the study area.....	53
4.3 Triggering factors	54
4.3.1. Hydro meteorological triggering factors.....	55
4.3.1.1 Rainfall (RF)	55
4.3.1.2 Spring and seepage.....	59

4.3.2 Earthquake (EQ)	62
4.4 Field survey and laboratory tests	64
4.4.1 General	65
4.4.2 Properties of rocks	66
4.4.3 Chemical, physical and geotechnical properties of rocks	72
4.4.3.1 Geochemical tests of rocks	72
4.4.3.2 Physical and geotechnical properties of rocks	74
4.4.2 Physical and geotechnical properties of soils.....	80
4.5 Landslide inventory and input data preparation and mapping.....	85
4.5.2 Landslide inventory mapping.....	85
4.5.3 Input map preparation	86
4.5.3.1 Slope	86
4.5.3.2 Aspect	87
4.5.3.3 Elevation	89
4.5.3.4 Proximity to fault factors	90
4.5.3.5 Proximity to drainage.....	91
4.5.3.6 Land use	93
4.5.3.7 Lithology.....	94
5. GIS-based Landslide Susceptibility Assessment and Mapping of Debresina area	96
5.1. GIS based Overlay Mapping techniques (OM)	96
5.1.1. Principles and background of the method.....	96
5.1.1.1 Weighed Slope map	97
5.1.1.2 Weighed Land Use map.....	99
5.1.1.3. Weighed Litho-technical map.....	100
5.1.2. Results and Discussion.....	102
5. 2. Frequency Ratio method.....	105
5.2.1 Methodology	105
5.2.2. Results and Discussion.....	106
5.2.2.1 Correlations between landslides and causative factors using FR-probability model.....	106
5.3. Analytical Hierarchical Process (AHP) method	113
5.3.1 Methodology	113
5.3.1. Results and Discussion.....	119

5.4. Verification and comparison of the results of OM, FR and AHP methods	124
5.5 General characteristics and slope stability analysis of the September-2005 landslide event.....	127
5.5.1. General characteristic of the event.....	127
5.5.2 Slope stability analysis using kinematic approach.....	132
5.5.3 Slope stability analysis using Global Limit Equilibrium (GLE) method.....	134
5.5.3.1 Global Limit Equilibrium (GLE) methods and general principles	134
5.5.3.2 Selected methods and software	137
5.5.3.3 Simplified slope cross-section and input parameters	138
5.5.3.4 Results and Discussion.....	140
6. Landslide hazard mitigation strategies and remedial measures	148
6.1. General	148
6.2 Non-structural mitigation strategies	149
6.2.1. Public awareness and education.....	149
6.2.2 Pre-disaster preparedness.....	150
6.2.3 Post-disaster recovery	150
6.2.4 Establishment of early warning systems	150
6.3 Structural and physical landslide hazard mitigation measures	151
6.3.1 Land use planning	151
6.3.2 Promote afforestation practice and minimize deforestation.....	152
6.3.3 Drainage.....	152
6.3.4 Gully treatment and reducing stream erosion	153
6.3.5 Providing retaining wall structures	153
7: Conclusions and recommendations.....	155
7.1 Conclusions	155
7.2 Future research works	161
Part- III: Rio San Girolamo area (Sardinia, Italy)	163
8. General characteristic of the study area and the Campidano Rift	163
8.1. Regional geological and structural setting	163
8.2. Physiography and climate.....	165
8.3 Landslide status and regional trends at the Rift margin	166
8.3.1 Spatial distribution and number of landslides	167
8.3.2 Type of movement	168

8.3.3 Regional distribution of landslide types by lithologies	168
8.3.4 Damages caused by the landslides	169
8.3.5 Landslide Index (LSI)	170
8.4. Background and problem definition of R.S. Girolamo basin	170
9. Description of the Rio San Girolamo area and data preparation.....	174
9.1 Location of study area	174
9.2 Triggering factor	175
9.3 Properties of rocks and soils.....	182
9.3.1 General.....	182
9.3.2. Field survey and laboratory tests of geologic materials.....	183
9.3.2.1 Lithological, physical and geotechnical properties of rocks	184
9.3.2.2 Physical and geotechnical properties of soils.....	193
9.4. Landslide inventory and input data preparation and mapping	196
9.4.1. Landslide inventory mapping.....	196
9.4.2 Input map preparation	197
9.4.2.1 Slope gradient	198
9.4.2.2 Slope aspect	199
9.4.2.3. Elevation	200
9.4.2.4 Proximity to drainage.....	201
9.4.2.5. Land use	202
9.4.2.6 Lithology/Litho-technical mapping	204
10. GIS-based Landslide Susceptibility Mapping and analysis of R.S. Girolamo area	207
10.1. GIS-based Overlay Mapping techniques.....	207
10.1.1. Methodology	207
10.1.1.1. Weighed Slope map	208
10.1.1.2 Weighed Land use map.....	209
10.1.1.3. Weighed Litho-technical map.....	210
10.1.2 Results and Discussion.....	212
10.2. Frequency Ratio (FR) method	214
10.2.1 Methodology	214
10.2.2. Results and Discussion.....	214
10.2.2.1 Correlations between landslides and causative factors using FR-probability model	214

10.3. Analytical Hierarchy Process (AHP) method	221
10.3.1 Methodology	221
10.3.2. Results and Discussion.....	222
10.4 Verification and comparison of the results of OM, FR and AHP methods for R.S. Girolamo area	225
10.5. General characteristics of the event and deterministic slope stability approach.....	228
10.5.1. General characteristic of the event, focusing on that of October 2008	228
10.5.1.1 Rock fall/topples and kinematic approach	229
10.5.1.2 Debris slide	231
10.5.1.3 Debris flow/flood	232
10.5.3 Slope stability analysis using Global Limit Equilibrium (GLE) method.....	235
10.5.4 Results and Discussion.....	235
11. Landslide hazard mitigation strategies and remedial options.....	244
11.1. General	244
11.2 Non-structural mitigation strategies	244
11.2.1 Pre-disaster preparedness.....	244
11.2.2 Post-disaster recovery	245
11.2.3 Establishment of early warning systems	245
11.3 Structural and physical landslide hazard mitigation measures	245
12. Conclusions and Recommendations.....	246
12.1 Conclusions	246
12.2 Future research works	249
Remarks on the similarities and differences of the two distant study areas.....	251
References	254
Annexes:	265

LIST OFFIGURES

Fig 1.1 Flowchart of study methodologies & approaches.....	3
Fig 3.1:Stratigraphy of the Afar region	35
Fig 3.2:DEM of the Afar area showing geomorphological and structural divisions	37
Fig 3.3:Typical geological section illustrating the nature of crustal attenuation across the western Afar margin.	39
Fig 3.4:Average annual Temperature of Afar Rift, including border highland and Rift margins.....	41
Fig 3.5:Average Annual Rainfall of Afar Rift, including border highland and Rift margins	41
Fig 3.6:Location of earthquake epicenters for the years 1961-2008	43
Fig 3.7:Seismic risk map of Ethiopia for100 year return period, 0.99 probabilities.	44
Fig 3.8:Compiled locations of some landslide occurrences in Ethiopia	46
Fig 4.1:Location of the study area using DEM	54
Fig 4.2:Average monthly rainfall of four stations	56
Fig 4. 3 (a).Annual rainfall of the study area (from 1962 -2008) & (b) comparison of cumulative rainfall of the years 1989, 1995, 1997, 1998, 2000 and 2005	58
Fig 4. 4: Comparison of the monthly rainfall of 2004, 2005 and 2006 and the average monthly rainfall for 44 years (Debresina station).....	59
Fig 4 5:Recorded maximum daily RF in each months of the year 2005.....	59
Fig 4. 6:Ponded rain water on the hummocky topography further triggering the sliding earth (a) At the Gifaita Gebriel (south of Debresina town) (b) At Yizaba locality.	60
Fig 4.7:Triggering and reactivating effect of water on the landslide of Debresina area.....	61
Fig 4.8:Conceptual model of the geo-hydrological conditions of the study area and its effects on the slope failure	62
Fig 4.9:Location of EQ epicenters on September 2005 in relation to the study area.....	64
Fig 4 .10: Rough sketch of major formations of the study area high lighting regional correlation with the Ethiopian plateau stratigraphy	66
Fig 4.11: Thin section photomicrographs of different lithologies of Alaje formation	68
Fig 4.12: The various lithologies of Alaje formation	68
Fig 4.13: Diagram Showing section at the Alaje formation at locality of Nib Amba	69
Fig 4.14:Tarmaber basalt (a).Field photograph showing the cliff forming along which the Tunnel is found (b) Photo: S6- CN1.25: (c) Photo from thin section (S6-3CN10).....	70
Fig 4.15:The various types of recent sediments.....	71
Fig 4. 16: Plots of chemical result of the samples on Total alkali-versus-silica" (or TAS) diagram).....	73
Fig 4.17:Graph used to convert the Schmidt hammer rebound number to UCS.....	76
Fig 4.18:Specimen shape requirements for irregular lump test type	77
Fig 4.19:Rose diagram of strike trends of discontinuities showing their relative prevalence for (a). Alaje basalts and (b) Tarmaber basalts.....	79
Fig 4.20: Clay minerals identification of the study area based on Casagrande plasticity chart.....	84

<i>Fig 4.21: Landslide inventory map of Debresina area, Ethiopia</i>	<i>86</i>
<i>Fig 4.22:Slope gradient map of the study area.....</i>	<i>87</i>
<i>Fig 4.23:Percentage areal coverage by the different slope classes.....</i>	<i>87</i>
<i>Fig 4.24:Aspect map of the study area</i>	<i>88</i>
<i>Fig 4.25:Percentage of areal coverage by the different classes of Aspects.....</i>	<i>88</i>
<i>Fig 4.26:Elevation map showing the various classes of Debresina area</i>	<i>89</i>
<i>Fig 4.27:Percentage areal coverage by the different classes of elevation</i>	<i>90</i>
<i>Fig 4.28:Map showing proximity to fault classes.....</i>	<i>91</i>
<i>Fig 4.29:Diagram showing proximity to fault versus areal coverage.</i>	<i>91</i>
<i>Fig 4.30: Map illustrating proximity to drainage classess for Debresina area</i>	<i>92</i>
<i>Fig 4.31:Proximity to drainage versus areal coverage</i>	<i>92</i>
<i>Fig 4.32:Land use map of study area</i>	<i>93</i>
<i>Fig 4.33:Percentage of areal coverage by the different land use classes.....</i>	<i>94</i>
<i>Fig 4.34:Lithological map of the Debresina area</i>	<i>95</i>
<i>Fig 4.35:Percentage of areal coverage by the different lithologic units</i>	<i>96</i>
<i>Fig 5.1: Schematic diagram of the Overlay Mapping process, raster maps are made on 30 by 30 grid cells.</i>	<i>97</i>
<i>Fig 5.2: Percentage of areal coverage of the various slope classes.....</i>	<i>98</i>
<i>Fig 5.3: Weighed slope map of the study area.....</i>	<i>98</i>
<i>Fig 5.4: Rasterised weighed land use map of the study area</i>	<i>100</i>
<i>Fig 5.5: Graph and equation showing how to calculate the normalized weight of the field</i>	<i>101</i>
<i>Fig 5.6: (a) weighed litho-technical map of study area and (b) their areal coverage in percent</i>	<i>102</i>
<i>Fig 5.7: GIS-model builder of Overlay Mapping technic for landslide susceptibility mapping</i>	<i>103</i>
<i>Fig 5.8: Landslide susceptibility zonation of Debresina area based on Overlay Mapping Method.....</i>	<i>104</i>
<i>Fig 5.9: Areal coverage of the four Landslide Susceptibility Index (LSI) classes by Percent based on Overlay mapping method.</i>	<i>104</i>
<i>Fig 5.10: Histogram showing the FR value of the various lithologies of the study area.....</i>	<i>108</i>
<i>Fig 5. 11: Photograph showing the landslide occurrences in thick colluvium deposit (a, c, & d) and in fractured rhyolitic ignimbrite rocks (b).....</i>	<i>109</i>
<i>Fig 5.12: Some of the SE- facing landslide main scarp (indicated by 'a' & arrows) along the thick colluvium-eluvium deposits.....</i>	<i>109</i>
<i>Fig 5.13: Relationship of FR values with proximity to fault.....</i>	<i>110</i>
<i>Fig 5.14: Relationship of FR values with proximity to drainages.</i>	<i>110</i>
<i>Fig 5.15: The relationship between slope angle and FR- values.....</i>	<i>111</i>
<i>Fig 5.16: Areal coverage of the four Landslide Susceptibility Index (LSI) classes by Percent based on FR- method.</i>	<i>112</i>
<i>Fig 5.17: Landslide susceptibility zonation of Debresina area based on FR-method.....</i>	<i>113</i>
<i>Fig 5.18: Relative influences of parameters on the landslide of Debresina</i>	<i>121</i>

Fig 5.19: Landslide susceptibility zonation of Debresina area based on AHP- method.....	123
Fig 5. 20: Areal coverage of the four Landslide Susceptibility Index (LSI) classes by Percent based on AHP- method.....	124
Fig 5.21: Cumulative frequency diagram showing success rate curve for susceptibility maps produced by FR, OM and AHP models.....	125
Fig 5.22: Histogram showing the relative distribution of landslide classes, for the OM, FR and AHP methods	126
Fig 5.23: Histogram of the percentage of prediction accuracy based on Area Under the Curve (AUC) method.....	127
Fig 5. 24: Simplified geological cross-section across the main landslide.....	129
Fig 5.25: Photographs showing some characteristics of the landslide of September 2005.....	130
Fig 5.26: The nature of the various deposits and slope instability at the Robi river course and its two flanks.	131
Fig 5.27: Landslide occurrences and their impacts on Zone-V around Armania	132
Fig 5.28: (a) diagram showing the major landslide occurred in September 2005 overlapped with the Rift margin faults (b) Photograph of the landslide scarp following the trends of: (I) NNE-SSW (II) NNW-SSE & (III) E-W trending Rift margin faults	133
Fig 5.29: Stereographic plots of NNE-SSW, NNW-SSE trending rift margin faults and east facing slope to indicate what kinematic failures are possible.....	133
Fig 5.30: Various definitions of the Safety Factor (SF).	136
Fig 5 31: Constructed simplified geological cross-section selected for the slope stability analysis	139
Fig 5.32: Sample interpreted global minimum Safety Factor using Janbu simplified method.....	142
Fig 5 33: Global minimum Safety Factors for various loading conditions	142
Fig 6.1: Construction of retaining wall along the road cut Debresina-Armaniya main asphalt road to mitigate the potential slope failure.....	153
Fig 6.2: Photo showing the landslide occurrences around the foundation of the national electric grid pole at the Armaniya, specific name of Tikure Chika	154
Fig 8.1: Regional geological map of southern and central Sardinia, including study area.....	164
Fig 8.2: Geological cross-section across the Campidano graben based on aeromagnetic data	165
Fig 8.3: Geomorphological and structural divisions of southern and central Sardinia/ from DEM	166
Fig 8.4: Landslide inventory map of Sardinia.....	167
Fig 8.5: Percentage of landslides by type of movement in Sardinia.....	168
Fig 8.6: Landslide percentage by lithological classes, in the Sardinia region, Italy	169
Fig 8.7: Number of landslides by type of damage.	169
Fig 9.1: Location map of Rio San Girolamo	174
Fig 9.2: Average monthly rainfall of four stations, namely, Capoterra (85-yrs), Uta (38-yrs), Decimomanu (68-yr), and Elmas (14-yrs).....	176
Fig 9.3: Annual rainfall of the Capoterra for the years 1922 -2010 (85-years).....	176
Fig 9.4: The maximum daily rainfalls that resulted in the flooding and/ or debris flow hazards in the study area	177

Fig 9.5: Comparison of the monthly maximum rainfall of 1985, 1999, 2005 and 2008 and the average monthly rainfall for 84 years (Capoterra station).....	178
Fig 9.6: Rainfall intensity-duration relationship of the event of Oct.22/2008 for some stations including the study area	179
Fig 9.7: Average rainfall Intensity-Duration relationship for the event of October 22/2008 for six stations including the study area	180
Fig 9.8: Debris flow nature and effect of Oct. 22/2008 event.....	181
Fig 9.9: The figure demonstrates accumulations of debris materials after the 2008 event of R.S. Girolamo.	182
Fig 9.10: Position of the 'PMN' and 'SVI' formation in relation to the regional stratigraphic Succession of Paleozoic metamorphic basement.....	183
Fig 9.11: Paleozoic metamorphic basement exposure	184
Fig 9.12: Various granitic exposures showing: (I). Fractured granitic intrusion (SBB) (II). Weathered granitic intrusion (VLD), (III). Basic dikes within the Santa Barbara unit (IV). Fractured granitic and their accumulated debris material	186
Fig 9.13: The various types of quaternary(unconsolidated sediments).....	187
Fig 9.14: Calculated minimum, maximum and average values of Unconfined Compressive Strength (UCS) of rocks from Schmidt hammer rebound.....	188
Fig 9.15: Degree of weathering versus unconfined compressive strength of granitic rocks of the study area	189
Fig 9.16: Strength variation of rocks for parallel and perpendicular point load measurements to the grain/foliation alignment.....	190
Fig 9.17: Summary Unconfined Compressive Strength from Point load.....	190
Fig 9.18: Rose diagram of strike of discontinuities showing their relative prevalence in (a). Granitic intrusion and (b) Metamorphic basement	192
Fig 9.19: The hydraulic conductivity value of various soils of the study area as Calculated by Hazen's formula	196
Fig 9.20: Landslide inventory map of R.S. Girolamo, Sardinia, Italy.	197
Fig 9.21: Landslide types and their percentage of area coverage	197
Fig 9.22: Slope gradient map of the study area.....	198
Fig 9.23: Percentage of areal coverage by the different slope classes	199
Fig 9.24: Slope aspect map of the study area.....	200
Fig 9.25: Percentage of areal coverage by the different classes of aspects, R.S. Girolamo, Sardinia.....	200
Fig 9.26: Elevation map showing the various classes of R.S. Girolamo area.....	201
Fig 9.27: Percentage of areal coverage by the different classes of elevation	201
Fig 9.28: Drainage proximity map of the R.S. Girolamo area	202
Fig 9.29: Proximity to drainage versus areal coverage, R.S. Girolamo, Sardinia.....	202
Fig 9.30: Land use map of the study area	203
Fig 9.31: Percentage of areal coverage by the different land use classes.....	204

Fig 9.32.Lithologic map of the study area.....	205
Fig 9.33: Percentage of areal coverage by the different lithologic units	205
Fig 10.1:Percentage of areal coverage of weighted slope classes based on PAI weighing system	208
Fig 10.2:Weighed slope map of the study area.....	209
Fig 10.3: Rasterised weighed Land use map of the study area	210
Fig 10.4:Histogram of areal coverage of each weighed of litho-technical classes based on PAI weighing system	211
Fig 10.5:Weighed Litho-technical map of study area.....	212
Fig 10.6: Landslide susceptibility zonation of R.S. Girolamo area based on Overlay Mapping Method	213
Fig 10.7:Areal coverage of the four Landslide Susceptibility Index (LSI) classes based OM method.....	213
Fig 10.8:Histogram showing the FR values of various lithologies of the study area.....	216
Fig 10.9:Photographs showing the various lithologies and landslides.....	217
Fig 10.10: Rock fall derived talus deposits at the foot of the fractured granite rock exposure and NNW-SSE trending lineaments	217
Fig 10.11:The relationship between slope gradient and FR values	218
Fig 10.12:The relationship between elevation and FR values.....	219
Fig 10.13:Areal coverage of the four Landslide Susceptibility Index (LSI) classes by Percent based on FR- method....	220
Fig 10.14:Landslide susceptibility zonation of R.S. Girolamo area based on FR method.....	220
Fig 10.15 Relative influences of causative factors on the landslide of R.S.Girolamo	222
Fig 10.16:Landslide susceptibility zonation of R.S.Girolamo area based on AHP- method.....	225
Fig 10.17: Areal coverage of the four Landslide Susceptibility Index (LSI) classes by Percent based on AHP- method	225
Fig 10.18: Cumulative frequency diagram showing success rate curve for susceptibility maps produced by FR, OM and AHP models.....	226
Fig 10.19: Histogram showing the relative distribution of landslide classes, for the OM, FR and AHP methods for R.S. Girolamo area.....	227
Fig 10.20: Histogram showing the percentage of prediction accuracy comparison of the three methods based on Area Under the Curve (AUC) method for R.S. Girolamo area	228
Fig 10.21: Typical slope profile along :(a). the right side of the R.S. Girolamo & (b) a small creek at the Santa Barbara sub-catchment.....	229
Fig 10.22: Rock falls from the jointed granitic rocks, at the steep slope of the study area (S.Barbara Sub-catchment) .	230
Fig 10.23: Stereogram plots of joints of the study area.....	231
Fig 10.24:Debris slide from the granitic sources (a) and metamorphic sources (b).....	231
Fig 10 25: Characteristics of landslide initiated debris flow at the left side of the river San Girolamo.....	232
Fig 10.26: Micro-catchments identified as debris flow, debris flood and fluvial floods in the R.S. Girolamo area, based on Melton ratio methods.....	234
Fig 10.27: Scatter plot using Melton Ratio and watershed Length with class limits for debris flow, debris flood and fluvial flood.	235

<i>Fig 10.28: Global minimum Safety Factors using circular failure surface with Janbu simplified method.</i>	<i>237</i>
<i>Fig 10.29: Histogram illustrating minimum Safety Factor for the various loading conditions</i>	<i>237</i>
<i>Fig 12.1: Mean monthly rainfall comparison of the two study areas, Debresina & R.S. Girolamo</i>	<i>252</i>
<i>Fig 12.2: Histogram showing the percentage of prediction accuracy comparison of the three methods based on Area Under the Curve (AUC) method for R.S. Girolamo and Debresina areas</i>	<i>253</i>

LIST OF TABLES

<i>Table 1.1: Field litho-technical data collection format.....</i>	<i>6</i>
<i>Table 4.1: Past landslide records.....</i>	<i>57</i>
<i>Table4.2: Comparison of annual and long term avearege rainfalls for the landslide occurrence years (Debresina station)</i> <i>.....</i>	<i>57</i>
<i>Table4.3: Summary of laboratory and related works.....</i>	<i>65</i>
<i>Table 4.4: Geo-chemical test results of the rocks of Debresina.....</i>	<i>72</i>
<i>Table 4.5: Calculated UCS of rocks from Schmidt hammer rebound.....</i>	<i>75</i>
<i>Table 4.6: Example showing how the unconfined strength (UCS) is calculated from point load test for the Tarmaber</i> <i>basalt.....</i>	<i>77</i>
<i>Table 4.7: Summary of unconfined compressive strength from Point Load.....</i>	<i>77</i>
<i>Table4.8: Discontinuity characteristics and estimation of hydraulic conductivity of rock masses in Alaje formation</i>	<i>80</i>
<i>Table4.9: Grain-size characteristics, Atterberg limits and classification of soils of Debresina area.....</i>	<i>81</i>
<i>Table4.10: Shear strength parameters of soils (from direct shear test) of Debresina area, Ethiopia.....</i>	<i>82</i>
<i>Table4.11: Identified minerals using XRD method.....</i>	<i>83</i>
<i>Table5.1: Weights of the different classes of slope gradients PAI guideline)......</i>	<i>98</i>
<i>Table5.2: Areal coverage of various Land uses and their assigned weights based on PAI weighing system</i>	<i>99</i>
<i>Table5.3: Example of calculated Litho-technical weights in three stations.</i>	<i>101</i>
<i>Table5.4: Frequency Ratio (FR) of landslide occurrences.....</i>	<i>106</i>
<i>Table5.5: Illustrative pair-wise comparison matrix of elements in the AHP.....</i>	<i>116</i>
<i>Table5.6: The fundamental scale of absolute numbers/Scale of Relative Importance</i>	<i>116</i>
<i>Table5.7: Random Consistency Index (RI).....</i>	<i>118</i>
<i>Table5.8 (a): Pair-wise comparison matrixes, principal Eigenvectors (relative weights) and Consistency Ratios of</i> <i>various parameters (causative factors) and the data layers.....</i>	<i>120</i>
<i>Table5.8 (b): Pair-wise comparison matrixes, principal Eigenvectors (relative weights) and Consistency Ratios of</i> <i>classes within the various parameters (causative factors) and the data layers.....</i>	<i>121</i>
<i>Table5.8 (c): Evaluation of the consistency of the preferences used for rating the parameters and classes.....</i>	<i>122</i>
<i>Table5.9: Percentage Comparison of area occupied by each landslide susceptibility class and the susceptibility index</i> <i>values between OM, AHP & FR model..</i>	<i>126</i>
<i>Table5.10: Summary of GLE methods.....</i>	<i>137</i>
<i>Table5.11: Results of global minimum Safety Factor (SF) calculated using SLIDE software for the various combinations</i> <i>of conditions, Debresina area (Ethiopia).</i>	<i>140</i>
<i>Table8.1: Distribution of landslides in the provinces.....</i>	<i>167</i>
<i>Table 8.2: Landslide Index values.....</i>	<i>170</i>
<i>Table 8.3: Types of landslides (by %) as compared with total landslide coverage in Italy.....</i>	<i>171</i>
<i>Table 9.1: Rainfall intensity-duration data of the event of October 22/2008.</i>	<i>178</i>

<i>Table 9.2: Summary of field and laboratory works</i>	<i>184</i>
<i>Table 9.3: Example showing how the Unconfined Strength (UCS) is calculated from the Point Load test for the R.S.Girolamo area.....</i>	<i>189</i>
<i>Table 9.4: Discontinuity characteristics and estimation of hydraulic conductivity of rock masses in granitic rock.....</i>	<i>193</i>
<i>Table 9.5: Grain-size characteristics, Atterberg limits and classification of soils of R.S.Girolamo area</i>	<i>194</i>
<i>Table 9.6: Shear strength parameters of soils (from direct shear test) of R.S. Girolamo area</i>	<i>195</i>
<i>Table 10.1: Weights of the different classes of slope gradients of R.S. Girolamo using PAI weight.....</i>	<i>208</i>
<i>Table 10.2: Areal coverage of various Land uses and their assigned weights, R.S.Girolamo</i>	<i>209</i>
<i>Table 10.3: Example of calculated litho-technical weights in two stations of R.S Girolamo.....</i>	<i>211</i>
<i>Table 10.4: Frequency Ratio (FR) of landslide occurrences of R.S. Girolamo.....</i>	<i>215</i>
<i>Table 10.5 (a): Pair-wise comparison matrixes, relative weights of various parameters (causative factors) and the data layers of R.S Girolamo</i>	<i>222</i>
<i>Table 10.5 (b): Pair-wise comparison matrixes, principal Eigenvectors (relative weights) of classes within the various parameters (causative factors) and the data layers of R.S. Girolamo.....</i>	<i>223</i>
<i>Table 10.5 (c): Evaluation of the consistency of the preferences used for rating the parameters and classes.....</i>	<i>224</i>
<i>Table 10.6: Percentage of area occupied by each landslide susceptibility class Compared to the Landslide Susceptibility Index values between OM, AHP & FR model.....</i>	<i>227</i>
<i>Table 10.7: Results of global minimum Safety Factor (SF) calculated using SLIDE software for the various combinations of conditions, R.S. Girolamo area (Sardinia)</i>	<i>236</i>

ACRONYMS

ACT	Action by Churches Together
AGS	Australian Geomechanics Society
AHP	Analytical Hierarchal Processing
AUC	Area Under Curve
BP	Before Present
DEM	Digital Elevation Model
DIGITA	Dipartimento di Geoingegneria e Tecnologie Ambientali
EBCS	Ethiopian Building Codes standards
EQ	Earthquake
FAO	Food and Agricultural Organization
FCC	False Color Composite
FR	Frequency Ratio
GIS	Geographical Information System
GLE	Global limit equilibrium
GWT	Ground Water Table
IFFI	Inventario Fenomeni Franosi in Italia
ISPRA	Istituto Superiore per la Protezione e la Ricerca Ambientale.
LSL	Landslide Susceptibility Index
NMA	National Meteorological Agency
OM	Overlay Mapping
PAI	Piano per l'Assetto Idrogeologico
PGA	Peak Ground Acceleration
RF	Rainfall
RS	Remote Sensing
SF	Safety Factor
SWIR	Short Wave Infrared
TIR	Thermal Infrared

UNISDR	United Nations International Strategy for Disasters
VES	Vertical Electrical Sounding
VNIR	Visible and Near-Infrared
XRD	X-Ray Diffraction

Part I: General

1. General introduction

This study entitled as” Remote sensing and GIS based mapping on landslide phenomena and landslide susceptibility “is carried out in Debresina area (in Ethiopia) and Rio San Girolamo basin (in Sardinia, Italy). Debresina is a highland district located in the Afar Rift margin of Ethiopia while Rio San Girolamo is also highland district situated in the margin Campidano graben of Sardinia region (Italy). Both of the Debresina (Ethiopia) and Rio San Girolamo (Sardinia) sites are prone to various types of landslide and related hazards.

As it is well known, the surface of the earth is always under dynamic change due to various geo-processes causing a continuous threat to human being. Geo-processes become natural hazards when they threaten life and property. Most geo-hazards/natural hazards are naturally occurring, and some others man-made. The term natural hazard refers to all occurrences of a natural phenomenon, which threatens or acts hazardously in a defined space and time (Varnes, 1984: Crozier, J.M & Glade, T., 2004). According to the United Nations International Strategy for Disasters (UNISDR, 2009), natural hazard is a natural process or phenomenon that may cause loss of life, injury or other health impacts, property damage, loss of livelihoods and services, social and economic disruption, or environmental damage.

Natural hazards have no geographic boundaries they occur in both developed countries (like Italy) and in developing countries (like Ethiopia). Landslides are among the natural hazards that constitute a critical and continuous threat to human beings all over the world. As discussed in the literature review part of this thesis, there are various types of landslides and the factors that control their potential occurrence are also too many. These controlling factors of the various slope failures could more or less be similar in the world. However, the dominance of one factor may be different from locality to locality. Hence, the resulting types of landslide could also be different. However, the response to the degree of damage is different comparing both developed and developing environments. In developed societies, hazards can cause great damage to property with associated high costs while in developing areas loss of life and injury are often more common although it does not mean that developing countries do not suffer heavy economic losses due to natural disasters or vice-versa (Bell, 1999). This is obviously attributed to the differences in the knowledge of people, economic stability, quality of life, culture, amount of funds and investments, experience and quality of landslide investigation, level technology that exists between these developed and 3rd world countries. Surprisingly, although better

conditions are available in the developed world (like Italy) than in the low income countries (e.g. Ethiopia), the loss of both life and infrastructures are still in an increasing trend.

This study will therefore, assess and evaluate the various landslide controlling factors, the potential of the landslide occurrences, as well as similarities or difference will be drawn in the various environments of these two distant study areas namely Debresina (in Ethiopia) and Rio San Girolamo (Sardinia).

1.1 Objective of the research

1.1.1. General objective

The overall objective of this thesis is to assess the occurrence of landslides, correlating them with various landslide causative factors; mapping and evaluation of landslide susceptible areas in both Debresina area (Ethiopia) and Rio San Girolamo (Sardinia-Italy) using GIS based semi-quantitative and quantitative techniques.

1.1.2 Specific objectives

The specific objectives of the research in the two respective study areas include:

- (1) To identify and characterize the landslide occurrences and generate landslide inventory map
- (2) To prepare the maps of various causative factors and evaluates their contribution to the occurrences of landslide and their frequency in the respective study areas
- (3) To evaluate the landslide susceptibility and prepare maps of both study areas using various GIS based methods and compare their results
- (4) To recommend landslide hazard mitigation strategies which can serve to the local community based on the final maps of the respective study areas

1.2 Methodologies and approaches

Under this section, only the general over view of the approaches and methodologies used in the course of data collection and analysis are described. However, the details of the specific methodologies and approaches used are described in the various steps of each respective chapter.

All the methods and approaches used in this research included (Fig1.1): (a) literature review (b) data collection using Remote sensing and field investigations (c) laboratory works, and (d) data analysis and evaluations using GIS based Overlay Mapping (OM), Frequency Ratio (FR), Analytical Hierarchical

Processing (AHP) and Global Limit Equilibrium (GLE) slope stability analysis methods and (e) development of landslide susceptibility map and zonation.

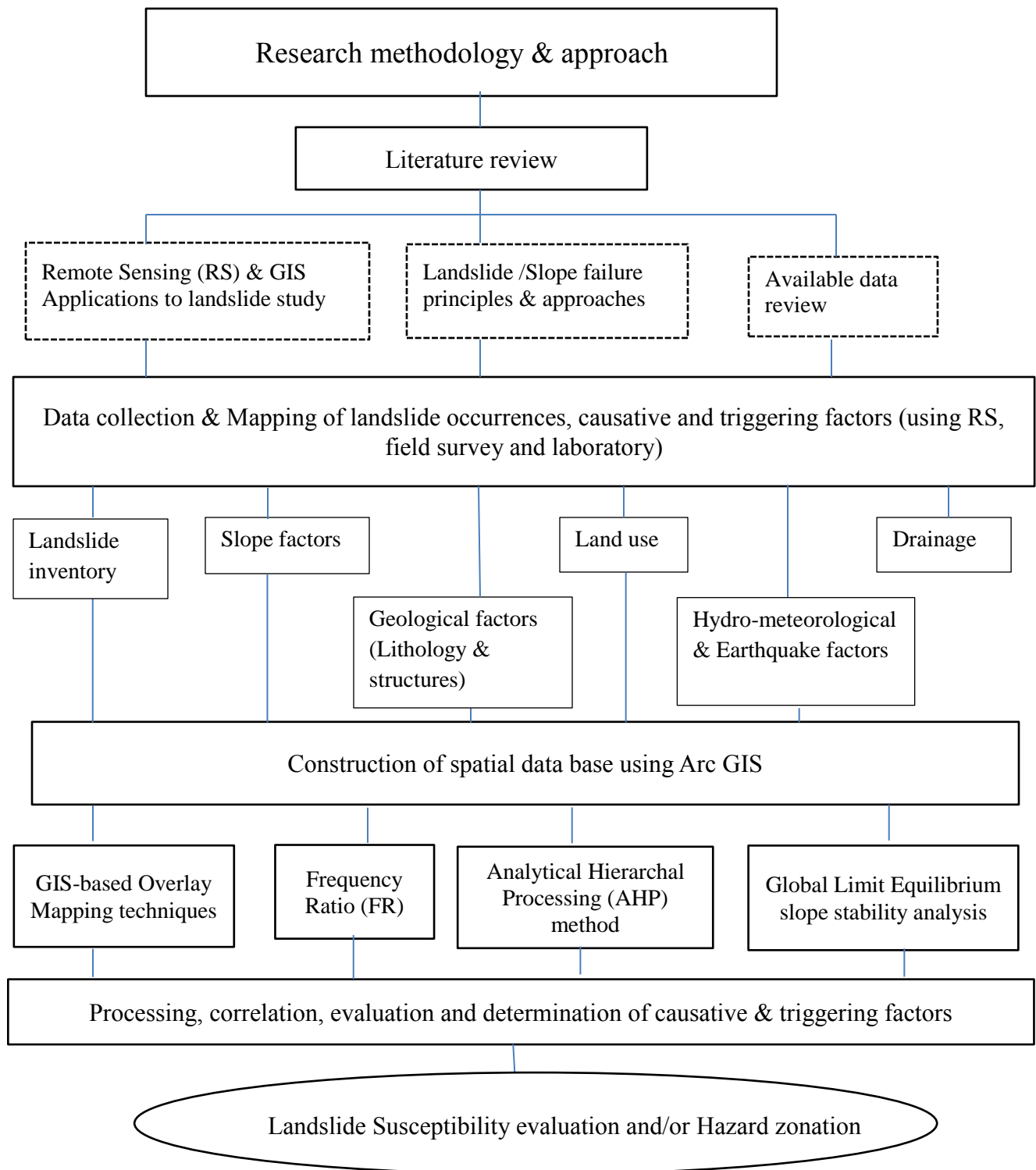


Fig 1.1: Flowchart of study methodologies & approaches

1.2.1 Literature review

Literature review is fundamental step in the research works to know what similar works or methods are available and what are not available in the area of interest. It involved: (1) search for available information on landslide records (2) search for satellite images, DEM and topographical data for the study areas (3) compilations of geological, topographical, hydro-metrological and geotechnical records (4) comprehensive review of literature on (4.a) causes and mechanisms of landslide and on various methods and considerations of slope instability assessments (4b) on the application of remote sensing and GIS on landslide, and (5) earthquake data collection in the Debresina area

1.2.2 Data collection

A. Remote sensing based data collection

Aster images of Level 1B acquired in the month of July each respective years of 2002, 2003, 2005, 2006, 2007, and 2008; Landsat images of 2001 and 2005, SPOT images, 30m-DEM, aerial photos 1984 (scale 1:50,000) and Google Earth have been used to map the landslide occurrences and distribution as well as to identify and visually interpret the various causative factors such as the geology (lithology & structures), land use, slope, drainage in the Debresina area. Likewise, interpretation of orthophoto of 2003, 2006, Ikonos satellite image of 2005, Google Earth, 10-DEM, topographic maps and existing regional geological maps have been used at the R.S. Girolamo area.

The interpretability of features from satellite images relies in the first place on the spatial resolution of the images in relation to the size of the features which are characterizing the area under consideration and which can be recognized or identified. Thus, size of the features to be detected, contrast and scale are important considerations in using remote sensing. For instance in the case of Debresina area, only the VNIR portion of ASTER images were considered in the analyses because of their higher resolution compared with the SWIR and TIR portions. False Color Composite (FCC) using the 3N, 2, 1 bands in red, green, blue respectively and band ratio have been used to visually identify the landslide scars. The images have been processed with various enhancement techniques (such as various band composition, filtering techniques, band ratio) in order to get a good contrast between the landslide distributions, geological features and various land uses. The images have been analyzed and interpreted suing ENVI4.5 and Arc GIS. Landslide scars, geological structures, rock outcrops, and various land use patterns have been digitized from the all the image sources using ArcGIS9.3 and converted into shape files. Supervised image classification has been also applied using

some training points to support the evaluation and preparation of the different interpreted input thematic maps.

B. Field investigations

The next stage was to carry out the fieldwork in the study areas. Field works have been carried out to verify the interpreted inventory and landslide causative factors map as well as for detailed field measurements and sample collection in both study areas. Thus, the field investigations included:

- Inventory of landslide occurrences and describing of the characteristics of landslides in the areas of study
- Geological/litho-technical and geotechnical characterization of rocks and soils
- Land use data collection and verification
- Detailed examination of the major landslide along selected representative landslide-affected slopes,
- Rock and soil sampling for laboratory physical, geotechnical tests, chemical, mineralogical, diffractometric analysis

The other causative factors, like slope factor and drainage have been determined from the DEM, topographic and field measurements of the two respective areas. Especially, the small sized landslide scars that were difficult to identify with the satellite images, as well as the depth & travel distance of the small sized landslides have been measured at the field. The landslides were described and classified following both Varnes (1978), and Cruden and Varnes (1996) classification systems.

One of the parameters for landslide classification is the material involved (Varnes, 1978). Hence, a detailed measurement and examination of physical and geo-mechanical properties have been conducted on the lithology and the litho-technical map preparation. Criteria like degree and depth of weathering, spacing and orientation of joint, strength of rocks, hydraulic properties have been collected based on the data collection format modified from the guideline of the Italian Geological Services (Amantii M, et al, 1992) to prepare the litho-technical maps for the investigation of slope instability. Geophysics (VES) has been also carried out in the major landslide of Debresina area to estimate the depth of overburden.

Field data has been collected in several stations with focuses to the main landslide using the following and indexed in to four classes (slope instability increases from class I- class IV)

Table 1.1: Field litho-technical data collection format (modified from Amantii M, et al, 1992, 1992)

	Parameters	Class-I	Class-II	Class-III	Class-IV
I	Degree of weathering				
II	Depth of weathering				
III	Spacing of discontinuities				
IV	Orientation of discontinuities				
V	Compressive strength				
VI	Hydraulic properties				

Slope instability

And parameters like degree of cementation, thickness and compactness are also considered during field description and measurements for the unconsolidated lithology.

The depth of weathering is estimated from gully and ridge exposure. Schmidt hammer, compass and GPS have been used to measure the in situ compressive strength of rocks, joint characteristics and locations respectively.

The other important parameters in the slope stability data collection are the hydraulic properties of the geologic materials. The hydraulic properties of rocks and soils are therefore estimated from field joint characterization and laboratory grain size analysis respectively using the various empirical formulas. For example, Hazen formula (1.1) is the most commonly used method for determining permeability of soil in correlation to grain size (Burt G.L, 2007) as grain size is one of the key factors affecting the permeability. Permeability of soils can also be estimated on the basis of soil classification, i.e. if the soil classification is known, this can be a first order check on the permeability magnitude (Burt G.L., 2007). Hence, soils of the study area have been classified using the results of the laboratory analysis and their hydraulic properties have been estimated.

$$K = C(d_{10})^2 \quad 1.1$$

where K = hydraulic conductivity (cm/sec): d_{10} = particle diameter corresponding to 10 percent finer by dry mass on the grain size distribution curve (cm): C = Hazen's factor ($\text{cm}^{-1} \text{sec}^{-1}$), which is proposed to be 100.

The shallow groundwater conditions are also assessed from springs and seepages conditions at various measuring points along the sections of the geologic formations. However, it was not possible to compare the empirically obtained results with borehole data as there are no such data in both study areas. For example, the water supply of the people of Debresina is supplied for nearly 99% from spring sources.

The Rock mass permeability has been estimated from the discontinuity characteristics. Where there is no available instrument for field test of the rock mass, its permeability can be estimated using the fracture analysis data. The permeability of a jointed rock mass is usually several orders higher than that of the intact rock. The rock mass permeability of the rocks in the study area has been estimated using the Snow (1965) and Louis (1974) formula as cited in A. El-Naqa (2000) for opened fractures of the hard rocks (equations 1.2 and 1.3) and that of the Hock and Bray (1981) as in equation 1.4.

$$K = \frac{ge^3}{12s\mu} \quad 1.2$$

where:

K = hydraulic conductivity of the rock mass (m/s);

e = Joint opening (m)

g = acceleration due to gravity (m/sec²)

μ = kinematic Viscosity fluids (for water equals 1×10^{-6} m²/sec)

s = joint spacing (m).

However, the reciprocal of fracture spacing is equal to the fracture frequency (λ), so the above equation can be written as:

$$K = \frac{\lambda ge^3}{12\mu} \quad 1.3$$

$$K = \frac{e}{s} K_f + K_r \quad 1.4$$

K_f = permeability coefficient of infilling material

K_r = permeability of intact rock

Equations (1.2 and 1.3) give the highest permeability coefficient for open fractures while equation (1.4) gives the lowest permeability coefficient for infilled joint systems.

Considering the roughness of fracture walls that diverts the flow, Louis' equation (equation 1.2) can be reduced to the following form (Carlsson and Olsson 1992), as stated in A. El-Naqa (2000).

$$K = \frac{ge^3}{12sC\mu} \quad 1.5$$

$$C = (1 + 8.8\zeta^{1.5}) \quad 1.6$$

The function C designates the influence of the relative fracture roughness on the hydraulic conductivity. The term ζ represents the relative roughness of the joint and is normally of the magnitude of 0.4-0.5 for natural

fractures (A. El-Naqa, (2000). This gives a value for C approaching 4, which shows that the conductivity in a rough fracture is 25% of that in smooth fractures as indicated by the same author.

To understand the causative parameters and triggering mechanisms of landslides, a geological x-section have been made along the representative sliding profile for detailed geological and geotechnical evaluations. Soil and rock samples were collected from the affected portion for laboratory investigations.

1.2.3 Laboratory works

Both soil and rock samples have been collected from the sliding part of the study areas to examine their physical, geotechnical, mineralogical properties. The soil tests, such as Atterburg limits (Liquid Limit, Plastic Limit and Plastic Index), granulometric analysis, direct shear test, unit weight, moisture content and some free swelling have been carried out in the Geotechnical laboratories of Water Resources Bureau of Tigray (Ethiopia) and Cagliari Province (Sardinia, Italy) using ASTM and European standards. X-ray Diffraction tests have been also performed on selected clay soils in the DIGITA of Cagliari University to estimate the type of clay mineralogy.

Petrographic (thin sections), physical (density, water absorption), Point Load test of the rock samples have been determined at the Earth Science and Territorial Engineering departments of the University of Cagliari. Chemical tests have been also performed in Spain to determine the type of volcanic rocks.

1.2.4. Data evaluation and GIS-based modelling of landslide susceptibility

Inventory of landslides and seven landslide causative factors such as lithology, proximity to fault, Land use, Slope steepness, Aspect, Elevation and Proximity to drainage have been prepared and processed using ArcGIS9.3. The relationships of each causative factor with the landslide distributions were evaluated, and GIS based landslide susceptibility map of the area were defined and zoned. In doing these above mentioned processes four types of approaches, namely the Overlay Mapping (OM) (type of indexed method), Frequency Ratio (FR) probability method, Analytical Hierarchical Process (AHP) method and the Global Limit Equilibrium (GLE) slope stability analysis method were applied. The first three methods have been executed with help of ArcGIS 9.3, while GLE has been analyzed using the SLIDE software. Further, the impacts of faults on the Debresina landslide and identification of debris flow types in the R.S.Girolamo have been done using Kinematic Slope Analysis and Melton Ratio methods respectively.

The FR model is a popular quantitative method which has been recently applied with satisfactory results in several works intending to create landslide susceptibility maps (Narumon I. et al, 2010). The spatial data base

and the input maps have been constructed using GIS techniques, and the FR method has been applied to quantitatively describe the relationship between the landslide causative factors and the past landslide occurrences, as well as to prepare the landslide susceptibility map of the study area. The FR index of each landslide causative factor has been calculated with the help of spatial analyst techniques of ArcGIS. The weighted sums of FR values of all classes have been used to produce a landslide susceptibility map.

Similarly, the Analytic Hierarchical Process (AHP), which was developed by Saaty (1980), has been used to evaluate the factors and produce the landslide susceptibility map of the area. It is one of the multi-criteria decision-making methods in which each weighted causative factor is linearly overlapped to generate the landslide hazard susceptibility map of the area. The results have been discussed and compared in order to evaluate the prediction accuracy between these methods.

Global Limit Equilibrium method has been also applied at selected sections of the landslide area to calculate the global minimum safety factor. In this method the impact of seismicity and groundwater on slope stability has been entertained.

Finally, possible suggestions on mitigation measures have been forwarded depending on the nature of slope failures and the social and economic conditions of the site in particular and the country in general.

1.3 Structure of the Thesis

This thesis is carried out in two distant historical countries, namely Ethiopia (in Debresina area) and in Sardinia-Italy (R.S. Girolamo catchment). The thesis is organized in three parts and 12 separate chapters.

Part I: consists of chapters 1 and 2. Chapter-1 discusses about the overall objective of the research work and the methodologies followed to achieve the objectives and results. While Chapter -2 presents a literature review on causes and mechanisms of slope failures and on basic assumptions and methods of landslide assessment and predictions. In this chapter, the factors influencing landslide such as geology, topographic factors, drainage factors, land use, hydrologic factors, and seismicity have been discussed. Moreover, landslide inventory mapping and landslide susceptibility modelling are explained.

Part II: particularly discusses about the Ethiopian project area (Debresina area) and consists of Chapters 3, 4, 5, 6 and 7. Chapter -3 summarizes the general characteristics of the Afar Rift margin including the Debresina site of Ethiopia, while Chapter-4 focuses on the detail field and laboratory based descriptions, data preparation and mapping of the landslide controlling factors at the Debresina area. Chapter-5 concentrates on the landslide susceptibility mapping of Debresina area using three different GIS based approaches for

landslide susceptibility mapping: GIS based -Overlay Mapping method, FR method and AHP method as well as slope stability analysis using GLE-method. Obtained results are compared and evaluated, and a landslide susceptibility map is presented for the study area. Chapter-6 presents landslide hazard mitigation strategies, which could be adopted to minimize losses from such hazards in the Debresina area of Ethiopia and in other parts of Rift margins of the country where similar conditions prevail. Chapter 7 of thesis focused on the conclusions and recommendations of Debresina area.

Part-III: Particularly concentrates about the Sardinia project area (R.S. Girolamo) and consists of chapters 8, 9, 10, 11, and 12. Chapter -8 presents the general characteristics of the Campidano rift margin including the R. S. Girolamo site of Sardinia while Chapter-9 focused on the detail field and laboratory based description, data preparation and mapping of the landslide controlling factors at the R.S. Girolamo area. Similarly, Chapter-10 concentrates on the landslide susceptibility mapping of R.S. Girolamo area using three different GIS based approaches for landslide susceptibility mapping: GIS based-Overlay Mapping method, FR method and AHP method. Obtained results are compared and evaluated, and a landslide susceptibility map is presented for the study area. While Chapters-11 and 12 discusses on the mitigation measures and conclusion and recommendations of the R.S. Girolamo area respectively.

Finally, the similarities and differences of the Ethiopian (Debresina) and the Sardinian/Italian (R.S. Girolamo) areas are compared at the end without specific chapter.

2. Theoretical backgrounds

Under this chapter, the theoretical concepts, terminologies, causes and mechanisms of landslides as well as methods of associated hazard assessments are discussed.

2.1 Definition of landslide hazard and terminologies

A natural hazard has been defined by UNESCO (Varnes, 1984) as the probability of occurrence within a specified period of time and within a given area of a potentially damaging phenomenon. Landslides are recognized as one of the most significant “natural hazards” in many areas throughout the world (Crozier and Glade, 2005). Instead of the fact that landslide is defined by various authors, there are still some differences among them in defining and classifying landslides, especially the flow type landslides (debris flow, earth flow and avalanche). This is due to the fact that landslides are usually characterized by various causes, movements and morphology, and involving different soil materials. Globally, landslides cause billions of dollars in damage and thousands of deaths and injuries each year. For example, only in the United States the total economic losses of landslides (direct and indirect) are of about US\$2 billion per year (Schuster R.L, et al, 2001). The term ‘landslide’ incorporates a wide variety of slope failures, such as rock/soil slides, deep-seated slides, mud flows, debris flows, rock falls (Varnes, 1978; Pierson and Costa, 1987; Hutchinson, 1988; Cruden and Varnes, 1996; Hungr et al, 2001). The term landslide means “the movement of a mass of rock, debris or earth down a slope” (Cruden, 1991).

2.2 Factors influencing the slope stability

The equilibrium status of a natural slope can be affected by several direct or indirect factors. In every slope there are forces which tend to promote downslope movement and opposing forces which tend to resist movement. A change in any one or a combination of these factors can alter the equilibrium condition of slope, decreasing its stability and sometimes leading to the slope failure. This change may be caused by natural processes such as the faulting, rivers undercutting the toe of a slope or bank scouring by debris flows etc. and also anthropogenic activities such as excavation, cultivation or removal of material may also cause change in slopes. Varnes (1978) pointed out that there are a number of external or internal causes which may be operating either to reduce the shearing resistance or to increase the shearing stresses.

Slope instability factors can be causative factor or triggering factor. Causes may be considered to be factors that make the slope vulnerable to failure, that predispose the slope becoming unstable while the trigger is the

single event that finally initiates the landslide. Some of the major factors which influence the slope stability are described below.

2.2.1 Geological factors

Geology is vital component in landslide modelling, stability study and protection design of landslides. Thus, a critical understanding of the geological conditions of the area is crucial for any slope stability investigation. The factors that control the mode of initial failure in rock slopes mainly include rock mass fabric, lithology contrasts, and geologic structure in the source slope (e.g. Hutchinson J.N, 1987; Cruden, et al, 1996; Guzzetti, et al, 1996; Chigira, 2000). The important geological factor that should be considered in landslide hazard investigation is summarized below as stated by numerous authors.

2.2.1.1 Types and properties of soil and rock materials

The mechanical properties of rocks may be influenced by particle size, properties of crystals and their preferred orientation (Chowdhury, 2010). Factors inherent in the nature of the materials which include the types and orientations of minerals and their degree of interlocking may have an influence on engineering characteristics of slopes, as it causes a marked anisotropy in the strength and deformation characteristics of soil/rock masses (Selby, 1993; Abramson et al, 1996) as cited in Woldearegay K.(2005).

The type of material within a sloped terrain is also important factor. For example unconsolidated materials, such as soil and sediment, tend to be more prone to slope failure than rocks.

Lithological contrasts

Sliding is frequently facilitated by the presence of bedding plane, shears resulting from tectonic processes (e.g., Evans, et al, 1987; Wang W.N, 2003), gouge zones, or weak primary interlayers such as tuffaceous zones (Fauque L., et al, 2002), shale, marl, or clay inter-beds (Hendron A.J, 1985). Such unstable bedding layers can occur when slope failures on bedding planes is triggered when either pore water pressures develop at the interface between two different alternating strata, or the strength of the clay deposit is weakened by water infiltrating through the overlying regolith layer (Krejci et al, 2002). According to Chowdhury (2010), recognition of the following points is of paramount interest for slope studies:

(a) Sequences of weak and strong beds (inter-bedded weak and strong layers): weak rocks like clay-shales and clay-stones are often critical in the development of slope instability.

(b) Thin marker beds such as coal and clay seams and carbonaceous shale: these beds are often missed in routine investigations. Their presence is useful in establishing stratigraphic correlations and in determining the extent of previous tectonic and landslide activity.

(c) Old failure surfaces or shear zones: the fact that shear strength along such surfaces is reduced to a low residual value due to large deformations must always be borne in mind

(d) Highly altered and permeable regolith overlaying relatively low permeability substrate (Sidle and Ochiai, 2006): the presence of water in the permeable layer may develop pore-pressures within the masses forming the slopes thereby causing slope instability

2.2.1.2 Discontinuities

Discontinuities represents a plane of weakness within a rock mass across which the rock material is structurally discontinuous and possess little or no tensile strength, varying in size from small fissures on the one hand to huge faults on the other (Bell, 2007). It is of paramount importance to study the properties of discontinuities because they influence the stability, the deformation and permeability of the slopes. The summarized notes are given from Hudson, et al, (1997), Bell (2007) and Price (2009).

Joint Roughness

The surfaces of mechanical discontinuities may be smooth and planar or exhibit varying degrees of roughness. For a particular rock the greater the roughness of the surface the greater the resistance of the discontinuity to shearing. If normal stresses are relatively low then shear movement along a rough surfaced discontinuity must be accompanied by dilation in normal direction.

Discontinuity Wall strength

A full evaluation of discontinuity shear strength requires not only assessment of roughness but also of wall strength. Accordingly, it is necessary to measure wall rock strength. This is almost impossible by conventional laboratory testing because of the extremely small size of the samples but option may be to use impact testers to the discontinuity surface. Thus, Schmidt hammer is one of the simplest interment used to estimate the wall strength of joint in the field.

Aperture and discontinuity infill

Aperture is the perpendicular distance between the adjacent rock surfaces of the discontinuity. This will be a constant value for parallel and planar adjacent surfaces, a linearly varying value for non-parallel but planar adjacent surfaces, and completely variable values for rough adjacent surfaces (Hudson, 1997). It affects the rock mass properties as separation largely controls the frictional strength along the joint as well as the flow of

water and the rate of weathering of the wall-rock. Open joints with large apertures have low shear strength and are also associated with high permeability and storage capacity.

Openness of discontinuities in outcrops may be either wholly or partially filled by material from either weathering in situ or from outside. Thus, bedding planes opened by weathering may be filled with clay. Such infilling will clearly affect the shear strength of the discontinuity. If the infill is weak, the discontinuity shear strength may be less than that of the discontinuity with walls in contact. If the infill results from mineralization (e.g. quartz or calcite), the infill may be stronger and more bonded to the rock (Price, 2009). In general, filling affects the shear strength, deformability and permeability of the discontinuities.

Orientation

The importance of discontinuities in any particular project depends partly on their orientation relative to directions of imposed stresses. In the much more detailed surface mapping required for engineering geological purposes dip direction/dip measurements is generally used. The orientation of major joint set relative to an engineering structure largely controls the possibility of unstable conditions or excessive deformations developing.

Spacing and Frequency

Spacing is the perpendicular distance between two discontinuities from the same set (Hudson et al, 1997; Price 2009) and is relevant to problems of slope stability, tunnel stability, excavation, groundwater flow and foundation bearing capacity (Price, 2009). The shape and size of rock blocks depends upon the spacing of the discontinuities bounding them. The larger and more closely spaced the discontinuities are, the more influential they become in reducing the effective strength of a rock mass. It controls the mode of failure. For instance, a close spacing gives low mass cohesion and circular mode of failure.

2.2.1.3 Weathering of geologic materials

Weathering implies decay and change in state from an original condition to a new condition as a result of external processes and weakens rocks (Price, 2009). Two main types of weathering are recognized: physical weathering, in which the original rock disintegrates to smaller-sized material with no appreciable change in chemical or mineralogical composition, and chemical weathering, in which chemical and/or mineralogical composition of the original rock and minerals are changed (Clark and Samal, 1982).

The rate at which weathering proceeds depends not only on the impact of the weathering agents but also governed by the mineralogical composition, texture, porosity and strength of the rock on the one hand, and the incidence of discontinuities within the rock mass on the other hand (Bell, 2007). Soil depth and type,

which resulted from weathering, are affected by several factors including climate and parent rock mineralogy. Weathering depends on the original mineralogy, the nature of climate and biological environment (Crozier, 1986).

Weathering is a long-term background process which causes material to lose its strength through time. Because weathering brings about changes in engineering properties, in particular it commonly leads to an increase in porosity with a corresponding reduction in density and strength, these changes being reflected in the amount of discoloration (Bell, 2007). Weathering also affects the permeability of geologic materials. An increase in the mass permeability frequently occurs during the initial stages of weathering due to the development of fractures, but if clay material is produced as minerals breakdown, then the permeability may be reduced (Bell, 2007).

2.2.2 Topographic and morphometric factors

2.2.2.1 Slope gradient

Slope angle controls the gravitational driving most geomorphic work and thus debris flow initiation and debris transport (Jakob, 1996). In general the steeper the slope, the more the risk of landslide due to the higher shear induced by gravity, although various types of landslide are related to certain slope range. For example, the initiation of debris flow is related to the slope of the source areas, with typical values between 27° and 38° (Takahashi, 1981; Hungr et al., 1984; Rickmann and Zimmermann, 1993). Watershed slope is important feature and is usually used to represent the geomorphologic and landslide characteristics of discriminate analysis on debris flow streams. However, watershed slope is multi-value distribution, a set of 0 ~ 90 degrees watershed mean slope is a most commonly used parameter to represent watershed slope property (Tien-Chien, et al, 2012). The occurrence of various debris processes such as debris initiation, transportation and deposition has been studied in relation to slope of catchments (e.g. Takahashi, 1981; Hungr et al, 1984; Rickmann and Zimmermann, 1993). Although different studies indicated different ranges of slope in each steps of the debris processes, generally speaking slope angle of initiation of debris flow > slope angle of transportation > than angle of deposition.

2.2.2.2 Aspect

The aspect of a slope is defined as the horizontal direction to which a slope faces. In other words, it shows the direction of maximum slope of a surface. It can influence landslide initiation.

The amount and distribution of precipitation received on a particular slope differs with respect to the various orientations it could have. Aspect related parameters such as exposure to sunlight, drying winds, rainfall (degree of saturation), and discontinuities may control the occurrence of landslides (Dai & Lee, 2002). This means that slopes similar in inclination, materials and geology may behave differently depending on their aspect which may control moisture, seepage and pore water pressures and so on. However, the direct correlation between aspect and landslides is not yet clear (Van Westen, et al, 2006).

2.2.2.3 Elevation

The influence of elevation on the mechanism of land sliding is often attributed to be indirect. In general, precipitation, weathering processes, erosion and resulting weathering depths, soil thickness, land use are influenced by elevation. The strong statistical relationship between elevation and landslide occurrence has been mentioned in several studies (e.g. Gritzner, et al, 2001; Dai and Lee, 2002). The more intense erosion and weathering, the more will be the influence of elevation on landslides. Thus, considering elevation as one of the causative factors is reasonable from the perspective of other elevation affected processes that control landslides.

2.2.2.4 Drainage factors

In addition to rainfall, erosive action of streams also contributes to slope instabilities. Streams erode sides of their valley which leads to instability of the slope area surrounding it (Bathrellos, et al, 2009). This is due to undercutting action of streams. The closer the slope is to streams, the more likely will it get water and develop pore pressure. Streams may adversely affect stability by eroding slopes or by saturating the lower part of the material which results in an increase in ground water level. Therefore, distance to stream is one of the information to be collected in most landslide susceptibility zonation

2.2.2.5. Basin relief and basin relief ratio

Basin relief is the difference in elevation between the highest and lowest points in a basin, and is therefore an indication of the potential energy in a basin. It indicates the overall steepness of drainage basin and is an indication of intensity of degradation processes operating on slopes of the basin (Pradeep, et al, 2011). The relief aspects of the sub basins play an important role in drainage development, surface and sub-surface water flow, permeability, landforms development and erosion properties of the terrain (Bagyaraj and Gurugnanam, 2011). As indicated in the same authors, a higher relief values indicates the gravity of water flow, low infiltration and high runoff conditions and the ruggedness number indicates the structural complexity of the

terrain. Relief is closely related to basin slope (Salisbury, 1962) in Jakob (1996) and basin size; it may therefore be normalized by dividing it by other dimensions of the basin.

Relief ratio is defined as the ratio of relief and horizontal distance between the highest and the lowest point of the basin (Jakob, 1996). Authors such as Schumm (1954, 1956) and Ahnert (1970, 1972) as cited in Jakob (1996), employed quantitatively the relief in several studies and they concluded that sediment yield was closely related to the ratio of the basin relief. In morphometric study, basin relief ratio also incorporates the function of slope. Steeper channels are more likely to convey all debris to the areas of deposition with little intermittent storage; however, basins with steep overall slope but with pronounced local concavities can promote debris flow deposition preventing the debris from reaching the fan (Jakob, 1996).

2.2.2.6 Melton's Ratio (R)

Melton's ratio is originally developed by Melton (1957, 1965) as cited in Jackson (1987), and is defined as the watershed relief divided by the square root of watershed area. It is a useful tool to differentiate flood and debris flow prone watersheds and their respective fans (Jackson et al, 1987; Wilford et al, 2004; de Scally and Owens, 2004; Andrew and Davies, 2011)

$$R = H_b(A_b)^{-0.5}$$

where H_b is the basin relief and A_b is the basin area.

Other morphometric factor used in the catchment debris flow and flooding study includes Stream Power Index (SPI) and Topographic Wetness Index (TWI). SPI is among the morphometric factors that could be used to identify the erosive effects of concentrated surface runoff while TWI has been used to describe the spatial soil moisture patterns (Wilson and Gallant, 2000). The locations with higher TWI host more favorable conditions for landslide formation (Conoscenti et al, 2008). Hence, it is useful conditioning index in landslide susceptibility studies.

2.2.3 Land use factor

Land use and land use changes caused by human and natural factors, are one of the causative factors which may influence the mass movements and sediment supply susceptibility of a catchment.

Improper slope land cultivation, removal of vegetative cover, and road construction can contribute to the occurrence of landslides and debris flows in a catchment. A description of the types and density of vegetation

and land use provides information on the possible effects of land use on surface-water runoff and erosion (Richard, 2005).

Land development may remove vegetation and expose soils, promoting erosion, increasing sediment yield and decreasing natural slope stability within the drainage basin and often creates impervious surfaces that increase the rate and volume of runoff (Richard, 2005). Also, Garfi, et al, (2006) recognizes vegetation cover as a significant control on the sediment generation processes acting within fan catchments. Once this vegetation is removed slopes increasingly become prone to erosion through mass movements or water flows. Conversely, the presence of vegetation can alter the severity of debris flows by contributing additional vegetative debris to the flow (Selby, 1974). Landslide hazard evaluation must address such development-induced land use conditions where applicable.

2.2.4. Hydrological factors

Hydrology plays a crucial role in landslide initiation. Some of the major significant hydrologic processes include spatial and temporal distribution of rainfall, water recharge and discharge areas, lateral and vertical movement within the regolith, and the likes.

2.2.4.1 Precipitation

The most common trigger of landslide is sufficient water input during precipitation events. Landslides triggered by rainfall occur in most mountainous area of the world. The mobilization of debris material during debris flow events is related either to the onset of sediment transport due to water runoff or to slope failures caused by an increase in pore-water pressures. Shallow debris-flows are often triggered by intense rainstorms of short duration whereas deep-seated landslides are triggered by antecedent rainfall (high cumulative rainfall) over days or weeks often combined with intense rainfall over a much shorter period (Chowdhury, 2010).

Both the runoff formation and slope instabilities are a function of rainfall intensity and cumulative precipitation or water input in another way. Therefore, a critical combination of rainfall intensity and duration has been proposed by numerous authors (e.g. Caine, 1980; Wilson and Wieczorek, 1995; Crozier, 1999; Guzzetti, et al, 2000; Glade et al, 2000; Aleotti, 2004; Guzzetti et al, 2004; Guzzetti., et al, 2007 & 2008; Dahal, et al, 2009; Brunetti M.T., et al, 2010) as criterion to define the threshold value of rainfall above which shallow landslide and debris flows can occur in several specific regions. The term "rainfall threshold" usually indicates a minimum value or maximum of rainfall necessary to trigger a natural process of instability; the "minimum" is considered the lower level below which the process is not triggered; the "maximum" is the level beyond which the process always occurs (Crozier, 1996). Rainfall thresholds may be used for

developing landslide warning systems based on weather information in general and rainfall magnitudes in particular.

2.2.4.2 Groundwater

Groundwater is another factor that plays role in landslide initiation. Geology in turn influences the flow of groundwater, its direction, pressure and gradient at any point within a slope. Chowdhury (2010) states that water can influence the strength of the materials by: (1) chemical alteration and solution, (2) reduction of apparent cohesion due to capillary forces, which disappear on submergence or saturation, (3) increasing pore water pressures with consequent reduction of shear strength. The same author also mentioned that increase of pore water pressures due to the flow of groundwater is an important factor in the development of slope failures and the occurrence of landslides. In particular the presence of groundwater under pressure often facilitates severe slides of the flow type.

Hodge and Freeze (1977) coupled a hydrogeological groundwater model and a slope stability model and showed the influence of the saturated permeability distribution within a slope on its stability. The results showed that a positive pore pressure can develop in a heterogeneous stratigraphy and that this can result in slope instability. Iverson and Reid (1992) included seepage forces in their calculation of potential slope failure to reveal the physics of the influence of ground water flow on the effective stress pattern in slopes. Their results showed that shear stresses are influenced by groundwater flow. Thus, groundwater flow increases the slope failure potential and its effect is highest for seepage areas. These researchers also showed a large influence of the saturated permeability distribution within slopes on slope stability.

When water bearing sand and gravels overlie more impermeable soils (or bedrock), the ground water is usually perched. Rainfall seeps in the ground by gravity until it reaches the less permeable stratum. Groundwater builds up above the impermeable stratum and flows laterally to the slope face where it emerges as a line of seepage or spring. Perched groundwater commonly occurs in layered strata such as alluvium, colluvium materials. Landslides caused by aggressive erosion from seepage are common. Where natural springs and seepages lines occur, the soil above the spring line is typically at marginal stability. Therefore the area near the spring outlet is likely to become unstable. Spring flows may be seasonal and only active during the wet season (Cornforth, 2005).

2.2.5. Seismicity factors

Earthquake is one of the principal triggering factors of landslides that cause great hazard to both of life and properties loss. The vibration released during earthquakes can cause failure of slopes which were previously

stable. The possibility of an earthquake in triggering a landslide event depends on the shaking of the ground rather than on the actual magnitude of the earthquake (Muthu and Petrou, 2007). The vibrations released during a quake can cause resettlement of the soil skeleton which in turn causes expulsion of water.

Rock falls and slides of rock fragments that form on steep slopes are common earthquake induced landslides although other type of landslide is also possible, including highly disaggregated and fast-moving falls, more coherent and slower-moving slumps block slides, and earth slides, and lateral spreads and flows that involve partly to completely liquefied material (Keefer, 2002).

Earthquakes reduce stability by imparting both a shearing stress and a reduction in resistance to slope material. Earthquake wave propagation has three principal effects (Crozier, 1986; Alexander, 1993) which includes (1) the direct mechanical effect of horizontal acceleration, which provides a temporary increment to shearing stress 2). The cyclic loading which weakens inter-particle bonding causing liquefaction and (3) the reduction in inter-granular bonding by sudden shock irrespective of the degree of saturation.

According to Cornforth (2005) earthquake induced landslides can be grouped into: a) failure of marginally stable slopes which include ancient landslide terrain, actively eroding river banks, man-made cuts and fills on steep terrain, talus slopes, weathered rock faces, and stratified volcano slopes b) translational slide movements in clay soils-which commonly occurred in clay slopes were under normal static conditions, but become unstable when subjected to horizontal earthquake shock c) liquefaction of cohesionless soils-common in course grained soils (sands).

2.3 Types and mechanisms of slope failures

There are various types of landslides depending on the type of material and motion involved in the process. Hence, classification of landslides usually takes into account the type of material involved and the type of movement mechanism (Dai and Lee, 2002). Various systems of landslide classification have been proposed by various researchers (e.g. Varnes, 1978; Hutchinson, 1988; Cruden and Varnes, 1996; Hungr et al, 2001).

The most widely used classification is the one developed by Varnes (1978) which takes into account both the type of material and the type of movement in combination for the classification of landslides into different types. This classification distinguishes five types of mass movement (fall, topples, slides, spreads, and flows) and combinations of these principal types along with different types of material (bedrock, coarse soils, and predominant fine soils).

2.3.1 Slides

A slide is a downslope movement of soil or rock mass occurring predominantly on the surface of rupture or on relatively thin zones of intense shear strain (Varnes, 1996). Mass movement slides develop in contact with the underlying surface. The slide can be rock-slides or debris-slides when rocks or debris slide down a pre-existing surface, such as a bedding plane, foliation surface, or a joint surface. Sliding mass may or may not experience considerable deformation and could be translational, rotational or a combination of both, which is called a compound slide (Bell, 1999).

Rotational slides are usually where sliding material moves along a curved surface and develop from tension scars in the upper part of a slope, the movement being more or less rotational about an axis located above the slope (Varnes, 1978). Translational slides occur when the mass displaces along a planar or undulating surface of rupture, sliding out over the original ground surface (Varnes, 1996). The movement is frequently, structurally controlled by discontinuities and variations in shear strength between layers of bedded deposits, or by the contact between firm bedrock and overlying detritus. Translational slides tend to be more superficial than compound slides (Bell, 1999).

The scale of rockslides could range from small-scale discontinuity controlled plane or wedge failures to large-scale failures. According to various authors (e.g. Terzaghi, 1950; Goodman and Kieffer, 2000) as stated in Woldearegay K. (2005), factors governing large-scale slope stability are primarily: (a) the stress conditions, including the effects of water, (b) the geological structures, in particular the presence of large-scale features, (c) the geometry of the slope, and (d) the rock mass strength. Failure modes in large-scale rock slope instabilities could be planar shear, wedge failures or quasi-rotational shear failures.

2.3.2 Falls

A fall starts with the detachment of soil or rock from a steep slope along a surface on which little or no shear displacement takes place. The material then descends mainly through the air by falling, bouncing, or rolling (Varnes, 1996). Fall movement is very quick, and typically involves slope angles range from 45° to 90° and includes rock falls, debris falls, and earth falls.

2.3.3 Topples

Topples is the forward rotation out of the slope of mass of soil or rock about a point or axis below the Centre of gravity of the displaced mass. Toppling is sometimes driven by gravity exerted by material upslope of the displaced mass and sometimes by water or ice in cracks in the mass (Varnes, 1996).

2.3.4 Lateral spreads

Spread is defined as an extension of a cohesive soil or rock mass combined with a general subsidence of the fractured mass of cohesive material into softer underlying material (Varnes, 1996). The dominant mode of movement is lateral accommodated by shear or tensile fractures (Varnes, 1978). Lateral spreads involve the horizontal displacement of the surface and are distinctive because they usually occur on very gentle slopes or flat terrain. They are more common in fine grained soils, such as clay, especially if the soil has been remodeled or disturbed by construction, or similar activities. Loose cohesionless sediments commonly produce lateral spreads through liquefaction. Liquefaction can occur spontaneously because of changes in pore-water pressure or in response to earthquake vibrations. Lateral spreads typically damage pipelines, utilities, bridges, and other structures having shallow foundations. The movement of lateral spreading is usually complex, being predominantly translational, but also show rotational movement and liquefaction, and consequent flow may also be involved (Varnes, 1978; Bell, 1999).

2.3.5 Flows

Flow and flow like landslide have various types of definitions and many classification exist on literature. For example, according to Bell (1999) flows consist of slurry of loose rocks, soil, organic matter, air and water moving down-slope. They are distinguished from slides by having higher water content and are thoroughly deformed internally during movement (Hutchinson, 1995). A flow is a spatially continuous movement in which surfaces of shear are short-lived, closely spaced, and usually not preserved. The most referred and accepted of all definitions is that of Varnes (1978). Flows are rapid movements of material as a viscous mass where inter-granular movements predominate over shear surface movements and these can be debris flows, mudflows or rock avalanches, depending upon the nature of the material involved in the movement (Varnes, 1978).

Although some popular definitions of landslides are given by several authors (Varnes,1978; Pierson and Costa ,1987), there is no unique terminology to distinguish between different flow types which reflects to some extent the complexity of these phenomena.

Some of the various definitions of the flow like mass movements (debris flow, mud flow, earth flow, and debris avalanche) as defined by various authors are given below.

- **Debris flow** is a very rapid to extremely rapid flow of saturated non plastic debris in a deep channel (Hungre, et al, 2001) and mixture of fine material (sand, silt, clay) and coarse material (gravel and boulders), with a variable quantity of water, that forms a muddy slurry which moves downslope

(Vanes, 1978; Dikau et al, 1996)

- **Mud flow** is a very rapid to extremely rapid flow of saturated plastic debris flow in a channel, involving significant greater water content relative to the source material, and the distinction between mud flow and debris flows perhaps is not of primary importance, as both have hyperconcentrated flow (Hungr, et al, 2001).
- **Debris avalanche** is a very rapid to extremely rapid shallow flow of partially or fully saturated debris on a steep slope, without confinement in an established channel (Hungr, et al, 2001). It begins as more or less shallow surficial sliding failure on a slope and continues into a rapidly moving flow.
- **Earth flow** is rapid or slower, intermittent flow like movement of plastic clayey earth (Hungr, et al, 2001). However, it is very difficult to distinguish mud flow from earth flow in terms of textural composition but it is significantly different in term of water content and flow velocity (Hungr, 2001).
- Another term, **debris flood**, has been applied by Aulizky (1980) to the cases of massive bed load transport characterized by clay rich colluvial debris and alluvial materials. Thus debris flood is very rapid, surging flow of water, heavily charged with debris, along a steep channel and can continue moving in channels with flatter slopes than those required for debris flow and thus is observed on larger streams

2.3.6 Complex movements

A complex landslide is a combination of at least two types of movement, such as falling, toppling, sliding, spreading or flowing.

2.4 Methods of slope failure assessment

So many various statistical, probabilistic and physical based or deterministic methods and approaches for landslide susceptibility study have been proposed and used. But no common agreement exists either on the methods for or on the scope of producing susceptibility maps (Brabb, 1984; Varnes, 1984; Carrara, et al, 1991, 1995; Soeters and van Westen, 1996; Aleotti and Chowdhury, 1999; Guzzetti, et al, 1999). According to Guzzetti (2005), these operational and conceptual differences among others include: (i) the general underlying assumptions (ii) the methods and tools favoured for the analysis and the susceptibility assessment.

2.4.1 Assumptions

Irrespective of the existing conflicting views existing among experts, the following are widely accepted assumptions (Varnes, 1984; Carrara, et al, 1991; Hutchinson, 1995; Turner and Schuster, 1996; Guzzetti et al, 1999; Guzzetti, 2005):

- (1) Slope failures leave discernible morphological features that can be recognized, classified and mapped in the field or through remote sensing, chiefly stereoscopic aerial photographs (Varnes, 1978; Hansen, 1984; Hutchinson, 1988; Cruden and Varnes, 1996; Dikau et al, 1996).
- (2) Landslides are controlled by mechanical laws that can be determined in a qualitative or quantitative manner. Conditions that cause landslides (factors directly or indirectly linked to slope instability), can be collected and used to build predictive models of landslide occurrence (Hutchinson, 1988; Dietrich, et al, 1995).
- (3) The past and present are keys to the future (Varnes, 1984; Carrara et al, 1991; Hutchinson, 1995). The principle implies that future slope failures will be more likely to occur under the conditions which led to past and present instability. Hence, the understanding of past failures is essential in the assessment of landslide hazard (Varnes, 1984; Carrara et al, 1995; Hutchinson, 1995; Guzzetti et al, 1999).
- (4) Landslide occurrence, in space or time, can be inferred from heuristic investigations and analysis of environmental information or inferred from physical models. Therefore, a territory can be zoned into susceptibility classes ranked according to different probabilities (Carrara et al., 1995; Soeters and van Westen, 1996; Guzzetti, et al, 1999). Most important steps and procedures in most methods of landslide susceptibility assessment follow (Guzzetti, 2005):
 - (a) Landslide inventory mapping of the target region or a subset of it
 - (b) The identification and mapping of the physical factors which are directly or indirectly correlated with slope instability (the instability factors, or independent variables).
 - (c) Ranking and assigning weights to the instability factors depending on their relative impact in generating slope failures
 - (d) The classification of the land surface into domains of different levels of susceptibility
 - (e) The assessment of the model performance

Review of the previous works (e.g. Varnes, 1984; Carrara, et al, 1995; Soeters and van Westen, 1996; van Westen et al, 1997; Aleotti and Chowdhury, 1999; Guzzetti et al, 1999) depicts that methods for ranking landslide factors and assigning different susceptibility levels can be generally grouped either (a) direct or indirect method or (b) qualitative, quantitative, methods or a combination of them (semi-quantitative). Nowadays, all approaches such as qualitative, quantitative and semi-quantitative methods are friendly working with GIS environment.

2.4.2 Qualitative method

Qualitative method is subjective and demonstrates the hazard zoning in descriptive (qualitative) terms (Validnia M.H., et al, 2009); such techniques depend highly on experience, knowledge and previous works on the study area. In this approach, information is analyzed and evaluated on logical and judgment based argument.

Heuristic approach

This method is one of the qualitative based method used in landslide susceptibility assessment. This method is proposed for the first time by Amatesi (1977) for the identification of geo-environmental and anthropogenic factors that determine the landslide or slope instability. According to him the environmental factors are divided into passive and active. The passive factors (e.g. geological and geomorphological factors) are relatively constant over short time while the active ones (e.g. climate, land use) are subject to considerable variations in the short term. According to this method causative factors of the landslide for the study area are first selected, and each causative factor is considered as a parameter map. Then the relative importance of each parameter map for slope instability is evaluated depending experience of the expert knowledge and previous works on the study area (e.g. Anbalagan, 1992), or statistics of landslide distribution and analysis (e.g. Dai, et al, 2001 ; Lee, et al, 2004 ; Lee, 2005). In this approach, information is generally analyzed and evaluated on logical and judgment based argument. After the weight is assigned to each factors, the various maps are summed based on their corresponding attribute values using ArcGIS to get the final landslide susceptibility zoned maps of the study area. The landslide susceptibility zoning is provided in descriptive (qualitative) terms (Validnia M.H., et al, 2009). The limitation of this method is its subjectivity in weighing the factors.

2.4.3 Quantitative method

This method produce numerical estimates (probabilities) of the occurrence of landslide phenomena in any hazard zone (Guzzeti F., et al, 1999, 2005) and such approach is based on mathematically objective structures (Neaupane K.M. and Piantanakulchai M., 2006). It includes the various statistically and probabilistic based models, physical based models or deterministic or geotechnical approach.

2.4.3.1 Statistical and probabilistic methods

The statistical analysis approaches and technique for landslide analysis is introduced by Carrara (1983), which nowadays has been widely used for landslide prone area zonation due its feasibility, high efficiency, low cost and a better understanding upon spatial factors influencing slope instability. Landslide susceptibility mapping

using either multivariate or bivariate statistical approaches analyses the historical link between landslide-controlling factors and the distribution of landslides (Guzzetti, et al, 1999).

Bivariate Statistical Analyses (BSA) involve the idea of comparing a landslide inventory map with maps of landslide influencing parameters in order to rank the corresponding classes according to their role in landslide formation. The main idea of this analysis is to determine the densities of landslide occurrences within each parameter map and its parameter map classes, and to derive data driven weights based on the class distribution and the landslide density (Süzen and Doyuran, 2004). With these weights, causative factor maps can be combined to obtain a landslide susceptibility map.

Multivariate Statistical Analyses - many literatures presents different multivariate statistical approaches with potential use for landslide susceptibility and hazard assessment, including linear regression and discriminant analysis (Carrara, 1983; Yin and Yan, 1988; Carrara, et al, 1991; van Westen, 1993; Carrara, et al, 1995) and logistic regression (e.g. Carrara, et al, 1991; Ayalew and Yamagishi, 2005; Guzzetti, et al, 2006; Chen and Wang, 2007). Multivariate statistical analyses of causal factors controlling landslide occurrence may indicate the relative contribution of each of these factors to the degree of susceptibility within a defined land unit (Long, 2008). These analyses are based on the presence or absence of stability phenomena within the units (Van Westen, 1993).

Several researchers suggested that statistical analyses are more appropriate for susceptibility zoning at medium scales (1:50,000 to 1:25,000) because of their potential to minimize expert subjectivity (Soeters and van Westen, 1996; van Westen et al, 2006). However, if we didn't do adequate consideration with the mechanics of the physical process involved, and correlation of the causative factors and landslide susceptibility, statistical methods are liable to result in very coarse and even misleading regression. With this in mind, some cross check procedures were proposed to minimize these drawbacks and increase the quality of landslide susceptibility assessments with the statistical approaches through: (a) proper validation and reduction of simulation uncertainty (Chung and Fabbri, 2003; Chung, 2006; Guzzetti, et al., 2006; van den Eeckaut, et al, 2006), and (b) introduction of expert knowledge to the statistical models used (Van Westen, et al, 2003).

Weights of evidence

The Weight of Evidence (WOE) modeling is a quantitative method that has been widely used originally in the mineral exploration. Some authors such as Bonham-Carter, et al, (1989), used this approach for mapping the gold mineralization in Canada.

It uses the Bayesian probability model and recently the method has been applied to landslide susceptibility evaluation in several case studies (Van Westen, 1993; Sentz and Ferson, 2002; Van Westen, et al, 2003; Süzen and Doruyan, 2004; Barbieri & Cambuli, 2009).

Weight of Evidence is a data-driven process that uses known landslide occurrences (training points) as model training sites to produce predictive probability maps from multiple weighted evidences (Raines 1999). Training points (landslide occurrences) are used in Weight of Evidence to calculate prior probability, weights of each of the evidential thematic classes, and posterior probabilities of the predictive factors

Prior probabilities and posterior probabilities are the most important concepts in the Bayesian approach. Prior probability is the probability that a terrain unit contains the response variable (e.g. landslide) before taking landslide predictive factors (B) (e.g. causative factors) into account and its estimation is based on the response variable (landslide occurrences) density for the study area.

The prior probability that an event (landslide, LS) occurs per unit area is calculated as the total number of events over the total area (equation-1). This initial estimate can be modified (i.e. increased or decreased) by the introduction of other available class of the predictive variables (B) (equ's 2 & 3). while a posterior probability is then estimated according to the response variable (landslide) density for each class of the predictive factors.

The method calculates the positive weight (W^+) (eq'n.4) and negative weight (W^-) (eq'n.5) for each class of landslide predictive factor (B) based on the presence or absence of the landslides (LS) within the area.

$$P_{\text{Prior}} = \frac{\text{LS_area}}{\text{Total area}} \quad (1)$$

$$P\{LS|B\} = P\{LS\} \frac{P\{B|LS\}}{P\{B\}} \quad (2)$$

$$P\{LS|B^-\} = P\{LS\} \frac{P\{B^-|LS\}}{P\{B^-\}} \quad (3)$$

$$W^+ = \ln \frac{P\{B|LS\}}{P\{B|LS^-\}} \quad (4)$$

$$W^- = \ln \frac{P\{B^-|LS\}}{P\{B^-|LS^-\}} \quad (5)$$

where, P = probability and ln = natural log. Similarly, B = class of the landslide predictive factor and sign ‘-’ shows the absence of the class and/or the predictive factor; LS is presence of landslide, and LS⁻ is absence of a landslide.

A positive weight (W^+) implies that the predictable variable is present at the landslide locations and the magnitude of this weight is an indication of the positive correlation between the presence of the predictable variable and the landslides. A negative weight (W^-) implies the absence of the predictable variable and shows the level of negative correlation.

The ratios of the probabilities of ‘event’ (e.g. landslide) presence to that of ‘event’ absence are called odds (Bonham-Carter 1989). The Weight of evidence for all the predictive factors (causative factors) is combined using the natural logarithm of the odds (logit), in order to estimate the conditional probability of landslide occurrence. When several predictive factors are combined, areas with high or low weights correspond to high or low probabilities of presence of the event (landslide) (Thierry, et al. 2007).

Some researchers (e.g. Thierry, et al, 2007) states that Weight of Evidence depends on the assumption of conditional independence between variables, and hence if not verified it may lead to an overestimation of the spatial probabilities. This is because many factor variables have some dependence naturally (e.g. altitude and land use; slope and internal relief etc.)

Frequency ratio (FR) probability model

The FR probability model is a quantitative method, which comprises the analysis of the relationship between landslide occurrence and factors causing the failure. When evaluating the probability of occurrence of a landslide within a certain area and in a specific period of time, it is crucial to recognize the conditions that can favor the landslide and the process that could trigger the failure. The application of the FR probabilistic model is based on the assumption that future landslides will occur under circumstances similar to those of past landslides (Lee, et al, 2004). FR approach is based on the observed relationships between distribution of landslides and each landslide-related factor to reveal the correlation between landslide locations and the factors in the study area (Lee and Pradhan, 2006).

The use of GIS is very important to apply the FR method in that it helps: (1) to prepare all the necessary input thematic maps, (2) to apply the map overlay technique of the various thematic maps (3) to calculate all the areas of landslide and non-landslide for each class of each factor

The frequency is calculated from the analysis of the relation between landslides and the attributed factors. The FR can be calculated for each class of the parameter (equation 6), and then the Landslide Susceptibility Index (LSI) is determined by summation of each factor’s ratings (Lee and Min, 2001; Lee and Pradhan, 2006) as expressed in (equation7):

$$FR = \frac{\text{area of landslide in class} / \text{area of all landslide}}{\text{area of class} / \text{entire map}} \quad (6)$$

$$LSI = Fr_1 + Fr_2 + Fr_3 + \dots + FR_n \quad (7)$$

Some authors (e.g. van Westen, 1993; Guzzetti, et al, 1999; Dai et al, 2002) indicated this method is most appropriate at medium and large-scale landslide studies. This method is one of the methods applied in this study and will be further explained in detail in the respective chapters.

2.4.3.2 Deterministic method

Deterministic methods are other quantitative method that depends on engineering principles of slope instability expressed in terms of the factor of safety. They depend on classical slope stability theory and principles such as infinite slope; limit equilibrium and finite element techniques and require standard soil parameter inputs such as soil thickness, soil strength, groundwater pressures, slope geometry (Fell R., et al, 2008).

Recent studies have shown also that the best approach for spatial prediction of landslides is the application of deterministic slope stability models, combined with steady state or transient models for hill slope hydrology (Mehrdad S., et al, 2011). In this regard deterministic models provide the best quantitative information on landslide hazard that can be used directly in the design of engineering works or in the quantification of risk.

However, their application is restricted to over small areas at large scales (Van Westen, 2004) due to: (1) their requirement of large amount and detailed input data, (2) their substantial degree of simplification of the landslide types and depths (Van Westen, et al, 2005) (3) the oversimplification of the geological and geotechnical model, and difficulties in predicting groundwater pore pressures and their relationship to rainfall (Fell R., et al, 2008).

Limit equilibrium theory

Limit equilibrium theory is often used to analyse the stability of natural slopes. A number of methods and procedures based on limit equilibrium principles have been developed for this purpose. The aim of limit equilibrium studies is to analyse the stability of any mass of soil or rock assuming incipient failure along a potential slip surface. This approach often enables the solution of many problems by simple statics provided some simplifying assumptions are made (Chowdhury, 2010):

- a failure surface of simple shape is assumed and the material above this surface is considered to be a 'free body'

- the driving and resisting forces are estimated enabling the formulation of equations concerning force equilibrium or moment equilibrium (or both) of the potential sliding mass
- a number of repeated calculations and trial slip surfaces are necessary to find the critical (potential) slip surface. After a number of trials have been performed, it is possible to locate the most dangerous position for the potential slip surface. This surface is one which gives the minimum factor of safety for the slope in conventional terms, and is theoretically the critical slip surface
- for homogeneous slopes without discontinuities of any kind, it is usual to assume the shape of the slip surface before trials are conducted, e.g., circular, log-spiral etc. In the former case, we can avoid defining factor of safety at a point.
- in almost all conventional limit equilibrium methods, the factor of safety is considered as, or implied to be, a constant all along the failure surface

Two classes of conventional limit equilibrium methods can be distinguished on the basis of the shape of potential slip surfaces (Chowdhury, 2010): (1) Methods in which the surface is assumed to consist of one or more plane segments (2) methods in which the slip surface may be of curved, composite or arbitrary shape. Planar failure surfaces have special relevance to stability problems concerning hard rock slopes in which failures often occur along discontinuities. While failures along curved slip surfaces are common in most slopes of cohesive soil. Such failures may also occur in some soft rocks (Hoek and Bray, 1974, 1977) as cited in Chowdhury, (2010). Composite failure surfaces often occur in non-homogeneous slopes consisting of different types of soil or rock or both.

Conceptually a major shortcoming of limit-equilibrium methods is that (1). incipient failure is assumed which is justified only for a real factor of safety of one (2). A calculated factor of safety equal to one will most often not correspond to a state of incipient failure for the real slope. This because the real factor of safety is strongly influenced by many variables associated with geological details, material parameters, pore water pressures and stress-deformation characteristics of the mass of soil or rock. It may also be influenced by factors such as initial stresses, stress and strain distribution, discontinuities, stress level and, of course, progressive failure. Therefore, performing sensitivity analyses of the influence of changes in significant variables on the factor of safety is desirable in limit equilibrium, because the calculated factor of safety is based on a number of simplifying assumptions which their influence is often difficult to quantify (Chowdhury, 2010).

The infinite slope stability model

Planar infinite slope analysis has been widely applied to the determination of natural slope stability, particularly where the thickness of the soil mantle is small compared with the slope length and where

landslides are due to the failure of a soil mantle that overlies a sloping drainage barrier (Amantii M, et al, 2002). The drainage barrier may be bedrock or a denser soil mass. In this case, soil depth is obviously the depth to the drainage barrier. However, a translational failure plane may develop at any hydraulic conductivity contrast where positive pore water pressure can develop. Therefore, the depth to the failure plane may be much less than the depth to competent bedrock.

The infinite slope model generally relies on several simplifying assumptions which may cause some limitation to its application (Ritter, 2004). It assumes that:

- failure is the result of translational sliding
- the failure plane and water table are parallel to the ground surface;
- the failure plane is of infinite length
- failure occurs as a single layer.

The principal disadvantage of infinite-slope analysis is that mechanical one-dimensionality precludes accurate assessments of slopes in which groundwater flow or topography produce forces that vary in directions other than the slope-normal direction (Iverson and Reid, 1992).

2.4.4 Semi-quantitative methods

Qualitative methods depend critically on expert opinions and demonstrate the hazard zoning in descriptive (qualitative) terms. Some qualitative approaches, however, incorporate the idea of ranking and weighting, and may evolve to be semi-quantitative in nature. The semi quantitative estimation for landslide risk assessment is found useful in the following situations (AGS¹, 2000): i) as an initial screening process to identify susceptible/hazards; ii) where the possibility of obtaining numerical data is limited. Semi-quantitative approaches consider explicitly a number of factors influencing on stability (Chowdhury and Flentje, 2003). A range of scores and settings for each factor may be used to assess the extent to which that factor is favorable or unfavorable to the occurrence of instability. The application of the Analytical Hierarchy Process (AHP) method, developed by Saaty (1980), is one of the best examples for such semi quantitative methods of landslide susceptibility mapping. Several authors (e.g. Barredo et al, 2000; Mwasi, 2001; Nie, et al, 2001 and Yagi, 2003, Woldearegay, K., 2005; Long N.T., F.De Smedt, 2011) have been utilized to landslide susceptibility mapping. Being partly subjective, results of these approaches vary depending on knowledge of experts. Hence, qualitative or semi-quantitative methods are often useful for regional studies (Soeters and Van Westen, 1996; Guzzetti, et al, 1999). This approach may be applicable at any scale or level of analysis, but

¹ AGS=Australian Geomechanics Society

² PAI= Piano per l'Assetto Idrogeologico

Debresina area (Ethiopia) & R.S. Girolamo basin (Sardinia)

more reasonably it is used in medium scales. Nowadays, such a semi-quantitative approach can efficiently use spatial multi-criteria techniques implemented in GIS that facilitate standardization, weighting and data integration in a single set of tools (Castellanos A., 2008). The semi quantitative AHP approach with help of GIS will be more explained and considered later in the respective chapters.

Part II: Debresina area (Ethiopia)

3. General characteristic of the study area and Afar Rift margin

3.1 General overview of the Afar Rift margin

The Afar depression and its Rift margins are one of the most potential regions for geo-hazards including earthquake, volcanic hazard, landslide, flooding, drought and land degradation. The lowland part of the Afar depression is mainly known for its volcanic hazard, earthquake and drought. Also the central and northeastern parts are known for high sediment concentrated flooding hazard. While the Rift margins are vulnerable to landslide, seismic, and land degradation. The western Afar Rift margins have an estimated length of about 550km from Ankober area (southern end) to Dallol area (its northern end). This part of the Rift margin is densely populated and contains several towns, infrastructures such as the asphalted roads, large bridges, road tunnels, large dams/reservoirs, newly proposed railway routes and other investments and touristic areas.

In this chapter the regional geological and structural setting, over all seismicity and geomorphological aspects of the Afar region is presented to give the insights to the general trend of landslide occurrences in the Rift margins and highlands of Ethiopia.

3.1.1 Geological and structural setting

The basement rocks of Ethiopia upon which all the younger formations were deposited contains the oldest rocks in the country, the Precambrian, with ages of over 600 million years (Tefera, 1996). They contain a wide variety of sedimentary, volcanic and intrusive rocks with various degree of metamorphism. For example, the Precambrian sequences in the south and west of the country has been strongly metamorphosed than those found in the northern part of the country. For much of the early Paleozoic time, Ethiopia was in a state of steady uplift which caused widespread erosion in all but the Northern provinces where deposits partly of glacial origin have been noted towards the end of this period. Subsidence followed in the Mesozoic with a large shallow sea spreading initially over the Ogaden province and eventually extending further north and west as the land continued to subside. Sandstone was deposited on the old land surface and deposition of mudstone and limestone followed as the depth of water increased (Tefera, 1996). This sequence was followed by general uplift and drying out of lake beds to leave gypsum and anhydrite precipitates. Similar cycles also continued at the Ogaden province during the Tertiary period.

Regional tectonic activity associated with rifting events in the Red Sea, Gulf of Aden and East African Rift Valley during the late Tertiary caused faulting and fracturing together with widespread volcanism. Vast quantities of flood lava sequences peaked between about 31-29Ma with the emplacement of up to 2000m of lavas and ignimbrites along the Nubian and Arabian margins of the southern Red Sea (Ebinger, et al, 1993; Hofmann et al, 1997; Wolfenden, et al, 2005). The volcanic rocks are made up of repeating sequences of basaltic lava flows overlain by rhyolites including ignimbrites, air fall tuffs and lavas (Afar consortium, 2012).

This was accompanied by the eruption of large amounts of ash and coarser fragmental material, forming the Trap Series. Several shield volcanoes, also consisting of alkali basalts and fragmental material, and then developed around the eastern edge of the Lake Tana depression. More recent volcanism is associated with the development of the Rift Valley, activity being concentrated within this structure and along the edge of the adjoining plateau. These Eocene to early Miocene volcanic rocks (Trap basalts) are found mainly round the edge of the Afar Depression on the Ethiopian and Somalian Plateau. According to Beyene & Abdelsalam (2005), these Traps are highly weathered and dissected by faults.

The Miocene igneous rocks of the Afar region are divided into the per-alkaline granites (26-22Ma), the Trap basalts (25-15Ma), the Mabla rhyolite series (14-10Ma) and the Dalha series (8-6Ma) (Varet, 1978). As indicated in (Fig 3.1), the per-alkaline granites are situated along the eastern and western margins of the Afar Depression and in the north. They intrude the late Proterozoic basement, the Mesozoic marine sequences and the older volcanic sequences (Varet, 1978). While the Trap basalts are part of the flood basalt sequences that overlie the Mesozoic sediments and are in places intruded by the peralkaline granites (Afar consortium, 2012). The Mabla Series erupted from north-south trending vents and consists of rhyolites and ignimbrites with some minor basalt flows (Varet, 1978). According to Varet (1978) the Dalha Series consists of basaltic fissural flows up to 800m thick with some rare sedimentary rocks and ignimbrites inter-bedded between the flows.

The other most extensive volcanic sequences are the Afar Stratoid series which have significant areal coverage of the Afar depression. Individual basalt flows are between 1 and 6m thick and the whole Series is up to 1500m thick (Afar consortium, 2012). Varet (1978) also indicated the existence of non-conformity between the trap series and the Dalha Series indicating a period of erosion and lowered magmatic activity between them.

In the east and west of the Afar depression are the transverse volcanics and marginal centers. These are east/northeast trending volcanic centers around 4 million years old and are intercalated with the top of the

Afar Stratoid Series (Afar consortium, 2012). The Marginal centers are summit calderas with trachytic and rhyolitic sequences (Barbieri & Varet, 1977; Varet 1978).

Finally, the recent units include the axial volcanic ranges and the quaternary sediments. The quaternary axial volcanics ranges are characterized by fissure eruptions and shield volcanoes with basaltic flows and alkaline and per-alkaline silicic rocks and occur along northwest-southeast trending narrow rift zones (Afar consortium, 2012). The axial volcanic ranges are underlain by thin ocean-type crust which young from the marginal to the central zones in a similar way to mid-oceanic ridges. This depicted that the axial volcanic ranges represent oceanic spreading centers (Varet, 1978; Tefera, et al, 1996).

The Quaternary sedimentary rocks of the Afar depression are mainly fluvial/lacustrine, having thicknesses up to 200m in places (Varet, 1978; Fig.3:1).

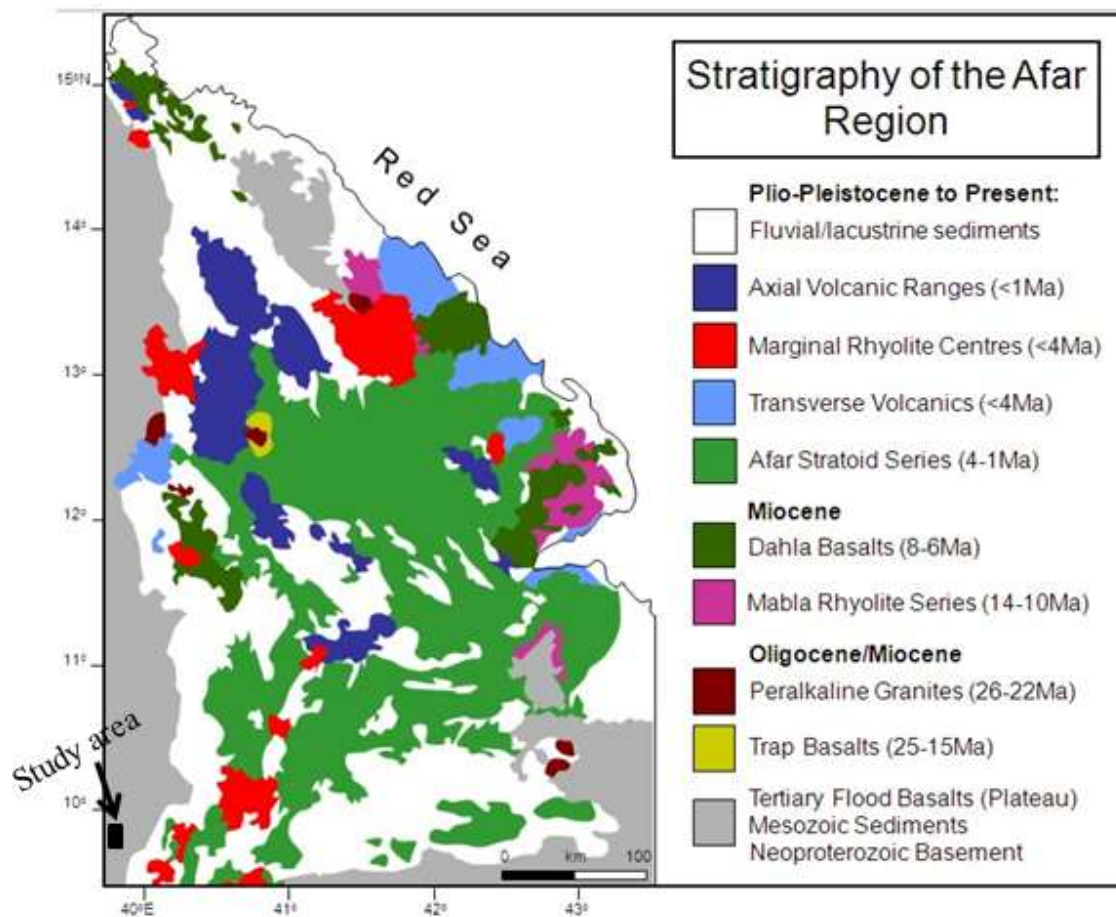


Fig 3.1: Stratigraphy of the Afar region (after Varet, 1978 and Beyene and Abdelsalam, 2005)

Based on geology, structural trends and geographic positions, the Afar depression can be divided into three regions: northern, east-central and southern (Hayward & Ebinger, 1996; Tesfaye, et al, 2003).

a) The Northern Afar rift

The northern Afar region (also known as the Danakil depression) is a low lying area dropping in elevation from around 200m in the north to 120m below sea level in its center (Afar consortium, 2012). It is bound to the west by the Ethiopian plateau and to the east by the Danakil block. It is dominated by young axial volcanic ranges that are typically produced by basaltic fissure eruptions and shield volcanoes aligned in Northwest-Southeast belts, parallel to the regional tectonic of the Red Sea (Barbieri and Varet, 1977; Varet and Gasse, 1978). The northern Afar depression also hosts Miocene to Holocene evaporites and fluvial sedimentary rocks (Tesfaye, 2003 and references there in).

b) The central sector Afar rift

The central sector (Fig 3.2) dominated by graben and horst structures and bounded to the west and east by axial volcanic ranges is occupied by Pliocene flood basalts and quaternary sedimentary rocks. The flood basalts, which are inter-bedded with less common and more silicic layers and volcanic centers, are collectively termed the “Afar stratoid series” (Varet and Gasse, 1978). Available age data indicate that the stratoid series was emplaced between 4.0 and 1.0 Ma (Barbieri, et al., 1977). Quaternary extension is distributed across the whole area with many faults in different orientations forming narrow and overlapping northwest-southeast trending grabens that are typical of the region (Hayward & Ebinger, 1996; Tesfaye, et al, 2003) and its average crustal thickness is about 25km (Hayward & Ebinger, 1996). One best example is the Dobi graben which is characterized by the high angle normal faults and sinistral strike-slip faults (Hayward & Ebinger, 1996; Beyene, 2004). This area is an active zone that shallow earthquakes occurrences are common. The Tendaho graben is one of the largest active site in the central sector of the Afar depression (Tesfaye, et al, 2003).

c) Southern Afar rift

The Southern Afar Rift is bounded by the Somalian Escarpment in the south, the Ali-Sabieh Block in the east, the Tendaho–Gobaad discontinuity in the north and the Main Ethiopian Rift to the west (Fig 3.2). This zone is a transition zone between the central Afar and the Main Ethiopian Rift and it is structurally characterized by: (1) North to Northeast trending dominant structures in the West, and East-West trending in the East (Beyene & Abdelsalam, 2005) (2) Northwest-trending transfer fault zones which can be traced to discontinuities in the

western Ethiopian escarpment (Hayward & Ebinger, 1996). (3) The kinematically distinct Gulf of Aden normal faulting pattern (trending due to East-Southeast) found in the Southern part (Tesfaye, et al, 2003) (4) Escarpment with a length of about 250km and an average crustal thickness of about 26km (5) Unfaulted Pliocene-Recent (3.3-0Ma) fluvio-lacustrine sediments and basalts between the basins flanks and the escarpment that runs up to a distance of more than 50km (Varet, 1978).

In general in this zone the three important structures, namely the NW-SE trending structures (parallel to the general trend of the Red sea); NE - SW trending structures (parallel to the main Ethiopian rift) and the E-W trending (parallel to the Gulf of Aden) are joined. The western bounding rift margins, where the study area is situated is characterized by this three important regional structures controlling the deep seated landslides along the rift margins, e.g. the Debresina landslide of September 2005.

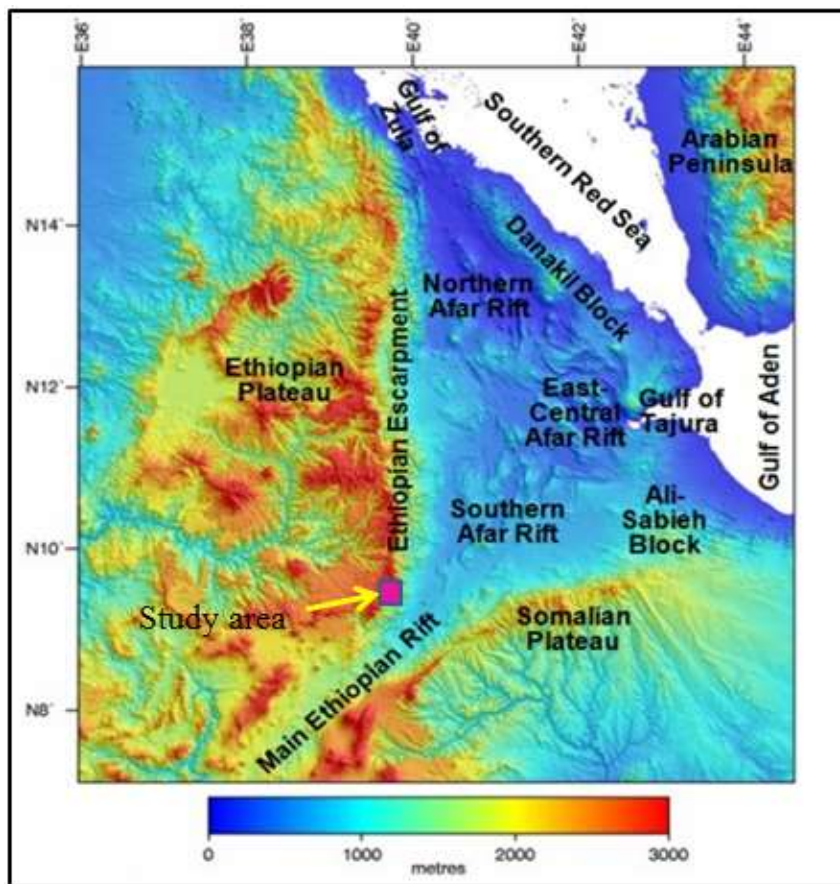


Fig 3.2: DEM of the Afar area showing geomorphological and structural divisions
(Adopted from: <http://www.see.leeds.ac.uk/afar/websitepages/structurepages/structuregeol.htm>)

3.1.2. Physiography and climate

The triangular-shaped Afar depression covers an area of 200,000 km² (Beyene & Abdelsalam, 2005) is bounded on the west by the Ethiopian plateau and marginal escarpments, on the south by the southeastern plateau (Somali plate), and on the northeast by the Danakil horst (Fig 3.2). The physiography of the Afar area is dominantly controlled by the tectonic and geologic features of the area. Both the northwestern and the eastern highland plateaux forming the shoulders of the Afar depression sharply fall into lowland plains towards the center of the Afar depression and their altitude recedes to lowlands and eventually reach sea level at the Gulf of Zula and the Gulf of Tajura (Beyene & Abdelsalam, 2005). From physiographic point of view, the Afar area and its peripheral highlands can be grouped into three regional physiographic divisions. These are (a) Border Plateau, (b) Marginal escarpment and (c) Rift floor (Fig 3.2).

(a) Border plateau

The plateau occupies the western and Southern part of the Afar rift valley. The western part of these plateaus belongs to the northwestern (Ethiopian) plateau while the southern part belongs to Southeastern (or Somalian) plateau. The northwestern portion of the plateau covers part of Tigray and Amara regions which include Semien Mountains and Lake Tana, which is the source of the Blue Nile. They typically comprise the flat-top topography with some undulating ridge chains and deeply dissected intermountain valleys. These plateaus near to the escarpment are dominantly covered by the Tertiary volcanic rocks (mostly basalts) although some exposure of Mesozoic sedimentary rocks and localized quaternary sediments are also found in the flat areas. The plateaus are also a water divide areas where either water is flowing towards the Afar drainage system or other drainage systems of the country. The annual average rainfall of the plateau is roughly 1250mm (Fig 3.5) while its mean temperature varies from 6 to 26°C (Fig 3.4).

(b) Marginal escarpment

The escarpment generally comprises an upper vertical cliff line, below which very steep slopes develop into terraced and faceted slopes which end on the rift valley plain. Similar to the plateau the escarpments are also divided into the northwestern and southwestern Ethiopian plateau.

The western margin is formed by down-warping of the Afar Depression and subsequent faulting and rift-ward tilting of faulted blocks (Zanettin and Justin-Visentin, 1975) as cited in (Beyene & Abdelsalam, 2005; Fig 3.3). The faulted blocks are rift-ward tilted and eroded by dense drainage networks. Elevation drops from 3000–2500 m at the ridgeline of the Ethiopian Escarpment to 800–100 m in the lowlands of the Afar depression (Mohr, 1983). At its lower section of these marginal areas, scattered and discontinuous basins are common.

For example, the western margins of the Afar depression are bounded by a seismically active, right-stepping, en echelon system of discontinuous grabens that extend for about 500 km such as Borkena, Maglala-Renda Coma, Dergaha-Sheket, Guf-Guf, -Menebay-Hayk (Mohr and Rogers, 1966; Mohr, 1967a, 1974a, 1974b) as cited in Tesfaye, et al (2003). The distance (width) of these grabens from the escarpment to the basin flanks is more than 50km, and are essentially unfaulted Pliocene-Recent (3.3-0Ma) fluvio-lacustrine sediments and basalts (Varet, 1978). These marginal grabens are interpreted to have been initiated during the early phase of Afar Rift tectonics (Tesfaye, 1999, 2003). Geologically, the elevated part of this physiographic unit is covered by the Tertiary volcanic and Mesozoic sedimentary rocks and part of their lower flank are covered by Quaternary volcanic and sediments (fluvio-lacustrine and colluvium deposits). The lower slopes of the escarpment have been variably incised by drainage lines such that they now comprise a series of spurs and valleys trending near perpendicular to the escarpment.

Generally, due to the steep slope and intense faulting and fracturing, these areas are characterized by high weathering, erosion and slope instabilities. Unlike its western margin, the southern Afar margin has no marginal basins developed adjacent to the Somalian plateau.

The rift escarpment has an estimated annual average rainfall of 850 to 1400mm (Fig 3.5) and temperature ranging from 20 to 27°C (Fig 3.4)

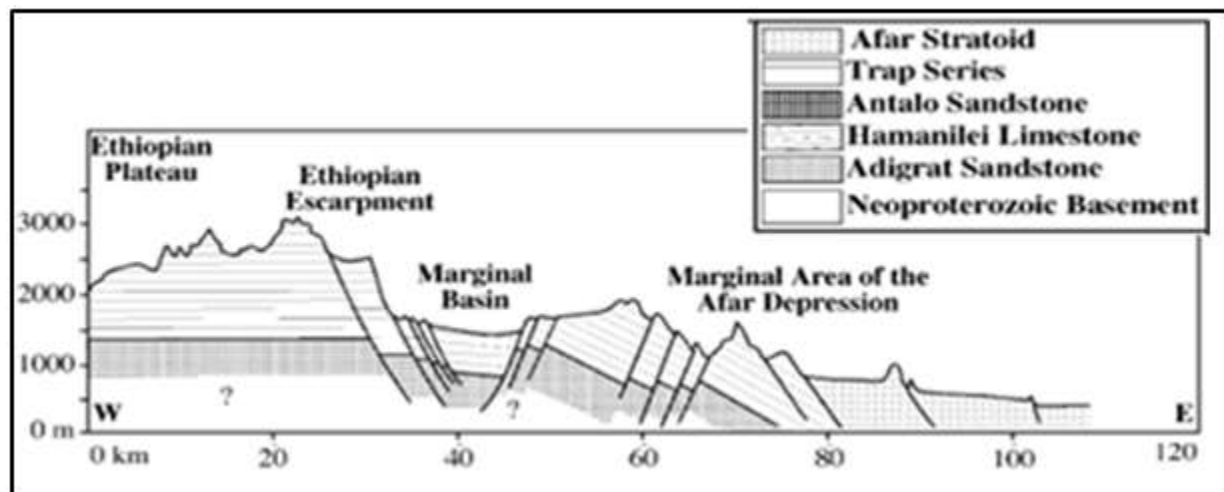


Fig 3.3: Typical geological section illustrating the nature of crustal attenuation across the western Afar margin (modified from Beyene & Abdelsalam, 2005)

(c) Rift floor

The Afar rift floor is the lowest physiographic region in the Afar area which includes the Danakil desert at north east part, and Dallol area at the northern part. There is a significant drop in elevation from the plateaus that stand well above 3500 m to the lowest point in northern Afar at -146m (Tesfaye, et al, 2003). This tectonic depression, which is due to the breakup of the Afro-Arabian plateau in the Oligocene-Miocene, is still active (Barbieri, et al., 1975; Hoffman et al, 1997). It is represented by gentle to flat topography, recent volcanic and tectonic activities, presence of discontinuous graben and horsts. Its mean elevation varies from 70m in the Northern part, 450 m in the central and 700m in the southern part of the rift floor (Tesfaye, et al, 2003).

It is covered by recent volcanic rocks (Afar stratoid, more recent axial zone volcanic), salt deposits and sediments (Zanettin, 1992). It is characterized by fracturing, active volcanism and diking until now. The presence of many volcanoes in the region, including Erta Ale and the Dabbahu Volcano in the middle of the depression, also finds its cause in these plate movements (http://en.wikipedia.org/wiki/Danakil_Depression). Its average annual rainfall is estimated to less than 250mm (Fig 3.5).

From climate point of view, the Afar rift valley is characterized by an arid and semi-arid climate with low and erratic rainfall in general. It is one of the hottest places year-round in the country with the temperature varying from around 25°C during the rainy season to 48 °C during the dry season. (http://en.wikipedia.org/wiki/Danakil_Depression), averaging to about 31°C (Fig 3.4). Rainfall is bi-modal throughout the region with a mean annual rainfall below 500 mm in the semi-arid western escarpments and decreasing to 150mm in the arid zones to the east. Afar is increasingly drought prone (<http://www.epa.gov.et/Download/Regional/Climate/Change>) (Fig 3.5). Usually areas nearby to the rift escarpments are affected by sediment rich flash flooding that comes from the heavy rainfall of the escarpments and highlands while the central and eastern parts are prone to drought.

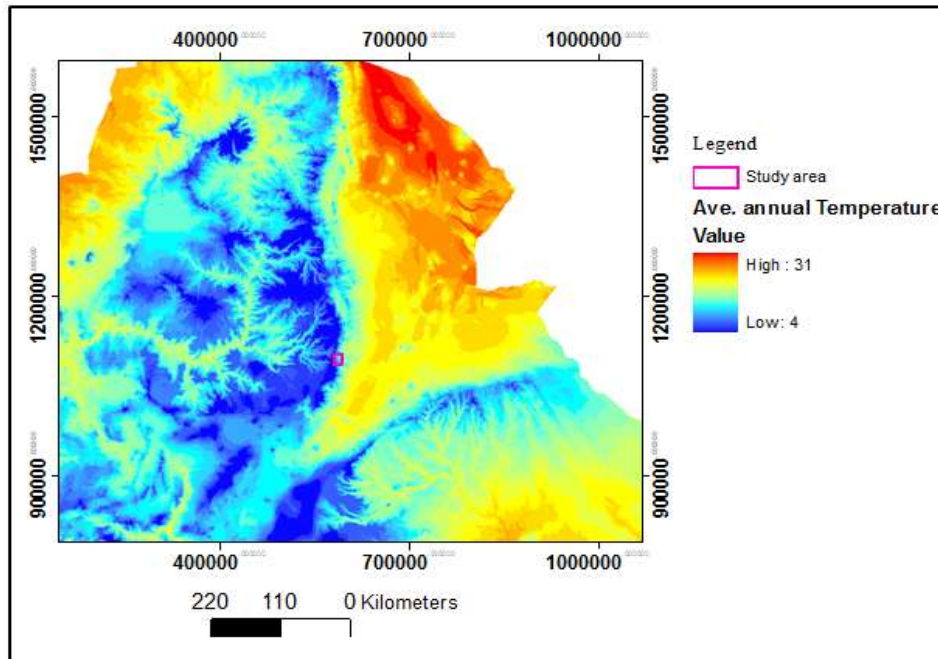


Fig 3.4: Average annual Temperature (in $^{\circ}\text{C}$) of Afar Rift, including border highland and rift margins (modified from the Average annual Temperature of Ethiopia)

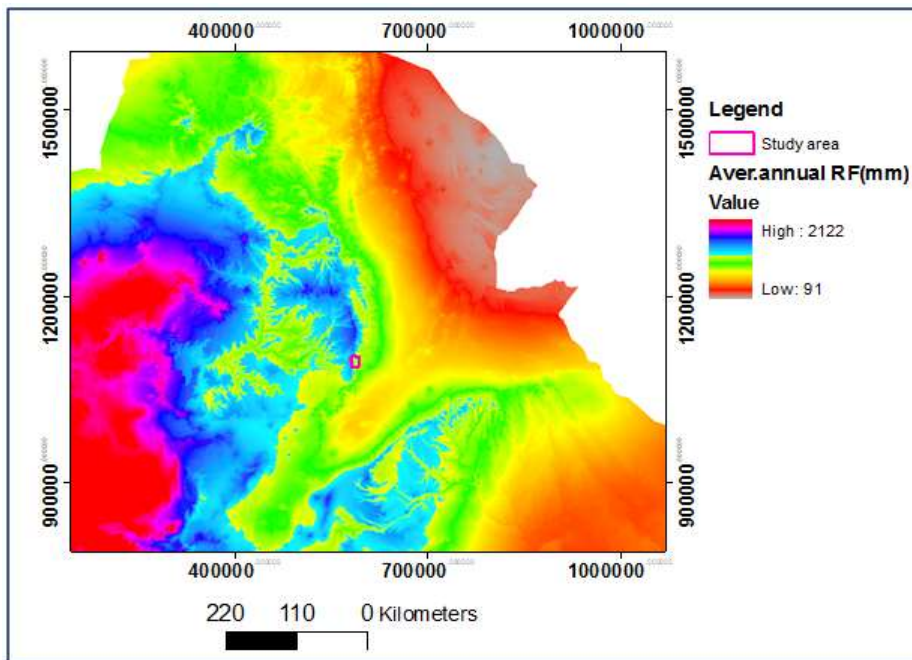


Fig 3.5: Average annual Rainfall (in mm) of Afar Rift, including border highland and rift margins (extracted from the average annual RF- map of Ethiopia)

3.1.3 Seismicity of Rift margin

The knowledge of plate tectonics is very important to estimate and locate the earthquake risk. The 300 km wide Afar depression is a diffuse extensional province marking a triple junction, where the plate boundaries represented by the Red Sea (Arabia-Nubia), the Gulf of Aden (Arabia-Somalia) and the main Ethiopian rift (Nubia-Somalia) meet. The Afar depression and Main Ethiopian Rifts as well as their marginal highlands are prone to significant level of seismic hazard due to the presence of the active regional tectonic and volcanic activities in the region. The seismo-volcanic activity in Afar depression is correlated to faulted zones of Wonji Fault Belt and the volcanic ranges of N.Loggia, Tat'Ali, Ertale and Alayta (Al-Arifi, et al, 2012). The Wonji Fault Belt is the axial rift zone of the Main Ethiopian Rift. The volcanic ranges in the depression are generated by basaltic fissures eruptions arranged in NW-SE and N-S directions. To the east of the depression and extreme west of the Gulf of Aden, the median valley of the Gulf of Tadjura is also marked with seismic activity (Al-Arifi, et al, 2012).

The historical seismicity of Ethiopia and neighboring east African countries has been studied by Gouin (1979), Kebede, et al (1991), Asfaw (1996), Midzi V., et al, (1999) and others. Gouin (1979) compiled a catalogue of earthquake and produced the first seismic hazard map of Ethiopia. The same authors indicated that some of the seismo-volcanic activity in Afar depression and main Ethiopian rift has caused casualties and damage. For example, according to (Gouin, 1979; Kebede,1991; Asfaw, 1986; Midzi,V., et al,1999; Al-Arifi, et al, 2012) such occurrences include, the 1906 Main Ethiopian rift earthquake ($M=6.8$), the 1961 Kara kore (western margin of Afar depression) earthquake which completely destroyed the town of Majete and severely damaged Kara kore town ($M_s = 6.6$), the 1969 Serdo earthquake ($M_s = 6.3$) in the central Afar in which 24 people were killed and 167 injured, the 1989 Dobi graven earthquake ($M_s = 6.5$) which destroyed several bridges on the highway connecting the port of Assab to Addis Ababa which caused damages in the Afar depression marginal highlands.

Seismicity released during lateral dike intrusions in the Manda-Hararo-Dabbahu rift of Afar in September 2005 provides indirect insight into the distribution and evolution of tensile stress along this magma assisted divergent plate boundary. During dike intrusions, seismicity migrates over distances of 10-15km at velocities of 0.5-3.0km/h away from a single reservoir in the center of the rift segment, confirming the analogy with a slow spreading mid-ocean ridge segment (Al-Arifi, et al, 2012). The past and recent seismo-volcanic activities in Afar depression that caused casualties and damage to properties are indicative of a geologically hazardous area. The geologic hazards are expected to reoccur in the future in the area relative to the plate movements at the triple junction, which caused RRR motions (Al-Arifi et al, 2012). The ongoing volcanism, recent faulting

(dominantly normal faulting), and shallow earthquakes are evidence for ongoing extensional deformation in the region (Barbieri, et al, 1975; Varet and Gasse, 1978; Mohr, 1978b; Ebinger and Hayward, 1996).

Fig 3.6 shows the distribution of earthquake epicenters in the Afar depression and its marginal highlands for the period 1961 to 2008, having magnitude $M_b \geq 3.5$ as obtained from the USGS-Northern California Earthquake data Centre. As indicated in figure the distributions of the epicenters are more concentrated towards the Northeast of the Afar depression and northwest of the rift margin than southeast flank.

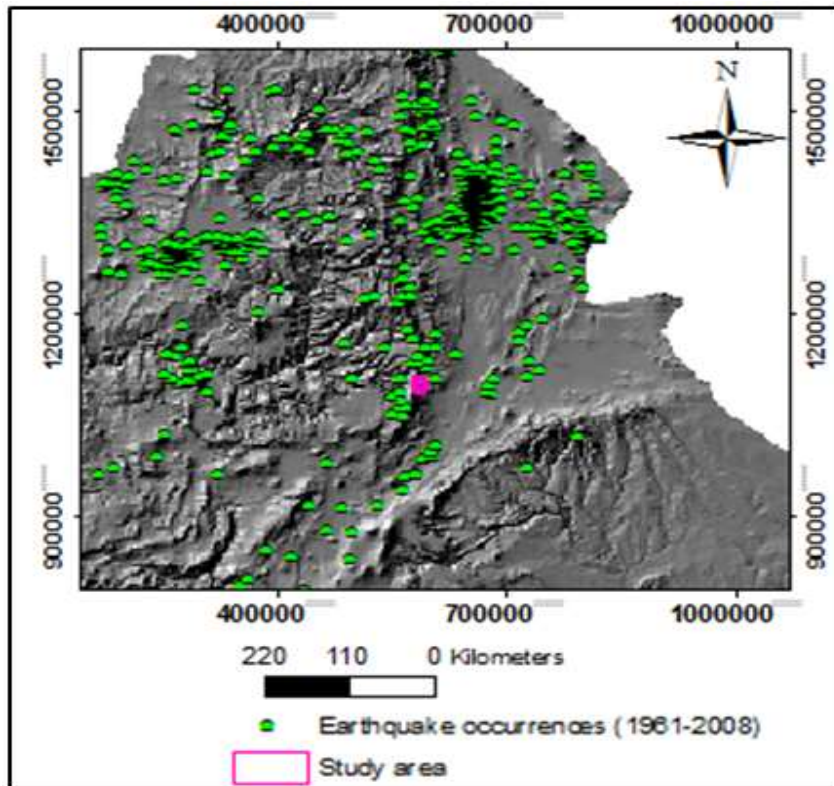


Fig 3.6: Location of earthquake epicenters for the years of 1961-2008 (min. values ≥ 3.5)

Although there is no study to date that shows the triggering effect of earthquake on the landslide of Ethiopia, earthquake is believed to be the second landslide triggering factor next to rainfall in Ethiopia, especially at the rift margins. Earthquakes are recurrent events in Ethiopia, especially along the Rift system, where magnitudes greater than five are not rare (Gouin, 1979; Ayele, 1995). Widespread evidence of seismic triggering of landslides, which mostly generate at first rapid movements such as rock falls, rock slides, and debris-mud flows, is provided by the historical record of earthquakes and related surface effects (Gouin, 1979) as stated in Bekele, et al (2009). It is common to find clear field evidence for the occurrences of both large and small scale landslides at the rift margins of Ethiopia although there is no documented evidences when and how they

happened. However, according to some local information, some are occurred by the heavy rainfall while others are occurred in relation to the earthquakes.

Various types of maps such as seismo-tectonic maps (compilation of seismic, geodetic and geological information) and seismic zoning (compilation of seismic and earthquake engineering information) can be produced to characterize the seismicity and evaluate their hazard on life and properties. For example, Laike Mariam (1986) has carried out a probabilistic seismic hazard analysis to obtain the hazard map for Ethiopia and the neighboring countries (Fig 3.7) and the study area is located in the high seismic risk.

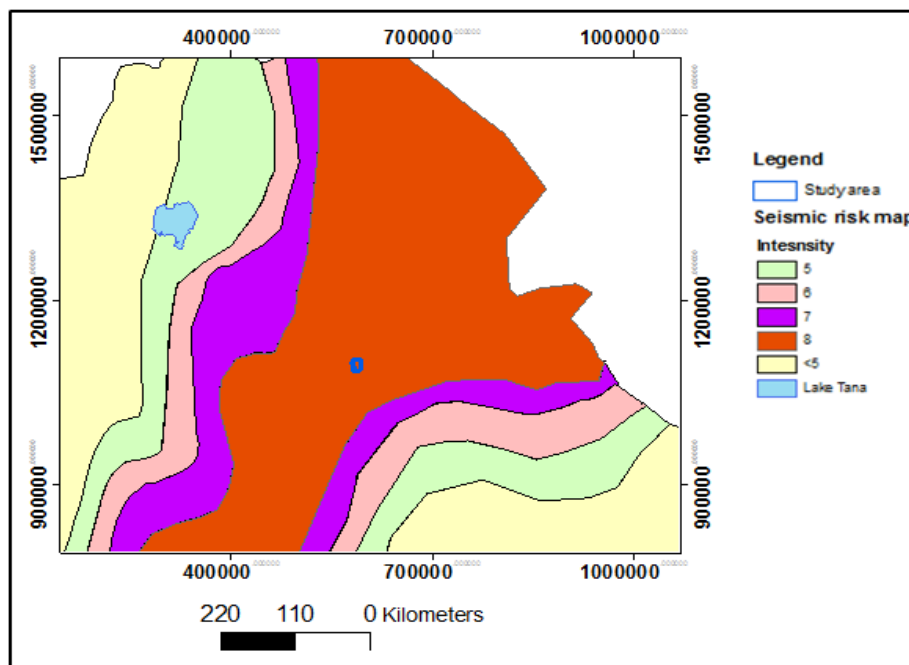


Fig 3.7: Seismic risk map of Ethiopia for 100 year return period, 0.99 probabilities (digitized & extracted from Laike Mariam A., 1986).

3.1.4. Landslide status and regional trends at the Rift margin

To visualize the regional trends of the landslide occurrences and their controlling mechanisms, previous works were referred (e.g. Ayalew, 1999; Woldearegay, 2005) and located on the hillshade map of Ethiopia (Fig 3.8). Most of the landslides are found associated with the highlands and rift margins where high concentrations of people, towns, infrastructures, utilities are available. Besides to landslide, these areas are also vulnerable to high rainstorm and flooding, earthquake, severe erosion and environmental degradation. On the other hand the lowlands are characterized by flat topography, low rainfall, and high seismo-volcanic phenomenon. However, the low lands, especially those far from the marginal highlands, are less hazardous as

compared to the rift margins because of the less population density and relatively sparse distribution of level of infrastructures

As stated in the previous sections of this chapter, the highlands and the rift margins are with features that favor the conditions of slope instabilities. Some of these main regional characteristics of these features include:

- (1) Formed by series of regional step forming normal faults which could in turn: (a) are water paths for regional ground water flow that enhances slope instability (b) can trigger local earthquakes (c) facilitates high differential weathering and deteriorating the geotechnical properties of the geologic materials
- (2) The intersection of the NE-SW fault systems (parallel to the marginal faults of main Ethiopian rift valley), NW-SE faults (which are parallel to the marginal Afar rift systems) and the E-W faults (which are parallel to the Gulf of Aden rift systems) are the major controlling factor for the large and deep seated landslide along the rift margins. The E-W marginal fault systems are also controlling the drainage system of the margins.
- (3) Found at the border of the seismo-tectonically active Afar rift valley, which can easily be reactivated by the volcanic eruption, diking and associated earthquakes?
- (4) The presence of the fragile lithologies (e.g. paleosols and lacustrine deposits, agglomerates, ignimbrites, various tuffs) as intercalation at the volcanic rocks as well as the presence of considerable thickness of colluvium/slope and fault deposit at the foot of the steep slopes also highly influencing the stability condition following the regional trend of the rift margins
- (5) Characterized by high rainfall and steep slope enhances high run off and erosion favoring slope instability in the area.
- (6) Highly dissected by the drainage systems following the faults and lineaments and hence characterized by deep gorges
- (7) Features that act as drainage structures between highlands and the lowlands and several springs are emerging either following the hydraulic differences of the various lithological stratifications (contact springs) or following the geological structures (fracture springs).The high fluctuation of their discharge between the dry season and the wet season enhances further slope instability

(8) Densely populated and high human impact on the local environment degradation. Intense agricultural activities and tree cutting are common and are daily activities in the steep slopes, aggravating the slope instability

(9) Improper slop cuts during the construction of road infrastructures that connect the concentrated towns found along these areas

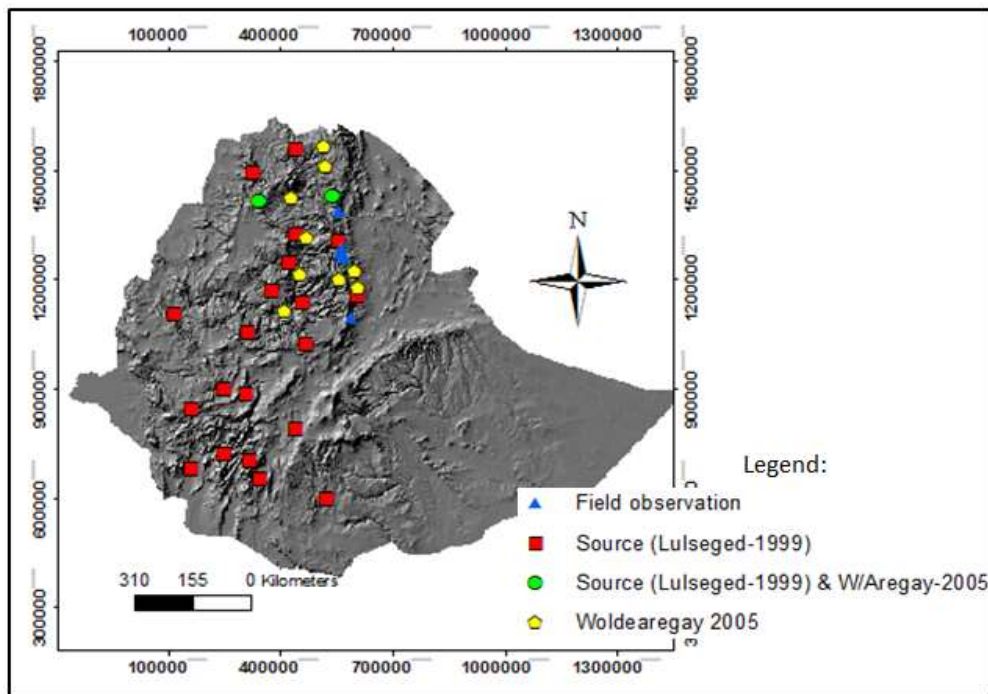


Fig 3.8: Locations of some landslide occurrences in Ethiopia (compiled from Ayalew L., 1999; Woldearegay K., 2005; and my field observations)

Generally the regional trend of the landslide occurrences at the rift margin coincides with the regional trend of the border faults, spatial distribution of high rainfall, and high concentration of seismic epicenters, and drainage systems of the rift margins. Shallow landslides are also aligned with road cuts crossing the marginal areas.

4. Description of the Debresina area and data preparation

4.1 Background and problem definition of Debresina landslide

Landslides are one of the most widespread and frequent hazards on earth causing tremendous disasters and losses of billions of dollars each year. In recent years it has become obvious that landslides represent a far greater hazard globally than had been previously assumed, both in terms of economic losses and fatalities (Petley, et al, 2005a; Petley, 2006). These events are frequently recurring geological hazards that damage socio-economic and cultural activities, communication and transport services, basic facilities and utilities like power, drinking water and irrigation supply systems. For instance, a World Bank Report (2005) indicates that (a) 3.7 million km² of land area of the globe is exposed to landslides (b) about 300 million (5% of world population) are exposed to landslide (c) about 820,000 km² is identified under high risk category which has a population of 66 million at high risk. Statistics from the Center for Research on the Epidemiology of Disasters (CRED.<http://www.cred.be/>) shows that landslides are responsible for 17% of all fatalities from natural hazards worldwide.

Many papers have been published on the socio economic impacts of landslide on human lives and infrastructure. Little attention has been, however, paid to the effect of landslide on the natural environment (Schuster and Highland, 2007). Landslides are destructive agents which has the capacity in modifying and changing the landscape.

Landslide costs are often underestimated, since the related damages are erroneously attributed to the triggering process, such as earthquakes and typhoons (Schuster, 1996). Given the ongoing pressure of increasing populations and expansion of urban areas into unstable hill slopes, the cost to society of landslides will increase in years to come (D. Calcaterra, et al, 2003) and hence the human and economic costs of landslides have increased dramatically in recent years. On the other hand, landslide is relatively one of the natural hazards that its impact can be significantly reduced if proper land use planning and design is applied. For example, a study in the State of New York (U.S.A.) showed that improved procedures of slope design from 1969 to 1975 have reduced the cost of repairing landslide damage to highways by over 90 percent (Hays, 1981).

The Ethiopian highlands and rift margins are suffering from landslides and related geo-hazards such as sediment concentrated flooding, erosion, and land degradation resulting in loss of human life and property and severe damage to agricultural lands. These highlands and rift margins are characterized by complex

geology, rugged and variable morphology, steep fault escarpments, high rainfall conditions and seismically active zones which generally give rise to favorable conditions for the slope failure hazards. They are also densely populated and intensively cultivated. According to the demographic profile of Ethiopia 2011, the Ethiopian populations are estimated to be more than 86 million, from which about 80 % lives in rural areas with a subsistence farming which is entirely dependent on natural resources. As estimated from the 90m DEM, about 58 % of the country is categorized as a mountainous and hilly areas having more than 1500m altitude. About 90 % of the population and 90% arable lands, as well as 60% of all the live stocks of the country are found in these highlands including the rift margins (Gete Zeleke (2010). Apart from this, the Ethiopian highlands are home of several historical /cultural heritages and monuments from many thousands of years to the present.

Although land sliding has been recognized as a widespread phenomenon in the Ethiopian highlands and rift margins, there is no inventory study at regional level. Hence their social, economical and environmental impacts in the country are not well documented. Nevertheless, the existing case studies (e.g. Ayalew, 1999; Temesgen, et al, 2001; Ayalew L. and H. Yamagishi, 2004; Tenalem A., and Barbieri G., 2005; woldearegay k., 2005) depicts that landslides have been affected human lives, infrastructures, agricultural lands and natural environment in the various parts of the highlands and rift margins of Ethiopia. In the years 1990-1998 alone, landslides or landslide-generated hazards have claimed about 300 human lives, damaged over 100 km asphalt road, demolished more than 200 dwelling houses and devastated in excess of 500 hectares of land in different areas of the highlands of Ethiopia (Ayalew L,1999). According to the press reports of Walta information Centre of 2000, 2002, 2003 as cited in (woldearegay k., 2005), 135 human lives have been lost, about 3500 people were displaced and an estimated 1.5 Million US Dollar worth property has been damaged in the highlands of Ethiopia in the years 1998-2003.

Landslides triggered due to torrential rainfall have killed 11persons and seriously injured 8 persons and also destroyed 102 homes in the Detta Woreda district of Gamo Goffa Zone in southern Ethiopia in August 2003 (Addis zemen newspaper, Aug 31/2003). The report quoted Abraham Choso, the then Woreda administrator, as saying seven of the dead were men and four were women. According to the humanitarian news (Addis Ababa, August 26, 2010), at least 19 people died and more than 20 were injured by a landslide in Mersa town of the Amhara region (<http://www.eastafricaforum.net/2010/08/29/landslide>). The landslide occurred late on Tuesday 24/2010 following heavy rains in the Mersa area that is located some 500km north of Addis Ababa along the Afar Rift margin. The press release of 26 June 2010 (http://www.et.emb-japan.go.jp/art_eco6.html) indicated also that a 144 million Ethiopian birr grant has been provided by the Japan government to rehabilitate the damaged Goha Tsion-Dejen road of the Abay gorge which has 45km length and is now under

investigation. This road is under landslide threats since early times (Ayalew, 1999; Ayalew, et al, 2004). Even the recently built asphalt road is under continuous landslide damage incurring high maintenance cost. Several other roads such as the Addis Ababa-Desse-Mekelle main asphalts are threatened by the slope failures when crossing the landslide susceptible landscapes of the rift margins. For example areas like the Debresina-Armanya; Kombelcha-Dessie; wuchale-Wurgessa-Mersa; Alamata-Korem-Maichew-Alaje; Adigrat-Mugulat-Bizet and so on are some of the areas that have been affected by various slope failures during every rain season along this road. It is common to see landslide destructing retaining walls and breaks the roads causing traffic interruption along many other roads crossing the rift margins and highlands during the rainy season. Significant amount of reservoir site studied at the foot of these mountains and escarpments (e.g. in the Raya valley, Kobo- Girana valley etc.) are suspended for the fear of the huge landslide driven debris that might fill reservoirs.

Some of the landslide enhancing factors in the Ethiopian highlands include among others, population growth, land use change (notably deforestation), urbanization, uncontrolled farming activities, road cuts. More than 99.7% of human food comes from the land, which basically depends on the productivity and quality of the soil (FAO, 1998). However, soil is diminished and degraded by the mass wasting and erosion from the highland and rift margin of Ethiopia. The slope failure at the rift margin and highlands are also main sources of debris-flows that have potential to erode and destruct the agricultural lands at the flat areas of the intermountain valleys. Due to the increase of pressure on land, many rural people are moving into areas which are potentially endangered by slope instability hazards (woldearegay, 2005). Currently, many towns and cities are expanding into landslide-prone areas without any prior slope instability hazard assessment and risk analysis. For this reason, the economic, social and environmental significance of the landslides and related hazards are becoming serious concerns to the general public and to the planners and decision-makers at various levels of the government in the highlands of Ethiopia (woldearegay, 2005).

The Debresina area is one of the most landslide prone areas located in the Afar rift margin of Ethiopia. Landslide occurrences and casualties have long history in Debresina area. Information obtained from local people indicated that landslide occurrences and casualties were common since the 1950's at the localities known as Armaniya, Nib Amba, work Amba, Tach and lay Indode, Shotel Amaba of the Tarmaber woreda. Most of the landslides occurred during the rainy season but some (e.g. landslide events of work Amba and Nib Amaba) has been triggered by seismic activities (Leta, 2007) and their time of occurrence is estimated to be in the 1960's (local information). This is also evidenced by the clearly seen presence of recent and old landslide scars in the areas. In these areas, specifically at the localities yizaba and Shotel Amaba, a massive and complex landslide has occurred in September 2005. Although landslide occurrences are common in the

rift margins, there is no landslide reported as large as this landslide event in Ethiopia so far. The general trend of the failure planes of this massive landslide is controlled by the NNW-SSE and NNE-SSW rift margin fault planes, having a failure landmass of length of more than 5km and width of 3km (from crown to toe) and surface area of greater than 15km².

Similar to other most landslide cases, there is no clear cut on the exact date of occurrence of this landslide. For example, Gebresilassie (2007) mentioned that the major landslide was occurred in 13 September 2005. However, other interviewed persons such as Ato Dereje Geta (whose house is totally destroyed by the then landslide at Yizaba), Ato Yeshe Dagna (the then Woreda agricultural expert who was on the site for fieldwork at that time) and Ato Firew Mekonen (the then head of the Woreda government communication office) said that the major landslide occurred on September 28/2005. Another interviewed person, Ato Meles Adamu (Agricultural expert in Tarmaber Woreda) said also that the main landslide occurred in September 10-12 /2005 indicating there is ambiguities on when it occurred. However, all information sources agreed on the existence of a minor crack at the beginning of September in Ethiopian calendar, and its duration for two weeks.

According to the aid reports of Action by Churches Together (ACT, 2006) and the information of the local authorities, this event has caused losses of over 900 hectares of arable lands, displacement of more than 4049 peoples, destruction of more than 1250 dwelling local houses and over 75% crop harvesting failure specifically in the localities named Yizaba and Shotel Amba. Local information also indicated that 4 mills, unknown numbers of water sources for both drinking and traditional irrigation have been destroyed. The prevalence of landslide hazards in such terrains could certainly have major role in aggravating the food insecurity problem of the country as most people living here are farmers who are dependent on subsistent agriculture.

Gebresilasie (2007) estimated the cost of the damage attributed by the 2005 landslides to be about 14 million Ethiopian birr in Yizaba locality only. In fact, if we consider the indirect cost of all the environmental destruction including the downstream arable lands lost by the huge landslide driven debris flow, the cost would have been more than threefold of the mentioned one. Gebresilassie (2007) also tries to assess the social impact of the landslide in Debresina by interviewing local peoples and mentioned a loss of about 350ha farm and grazing land, 44ha of forest and bush land, more than 26 residential houses and lots of houses are cracked in various localities of the Debresina area from the years 1953 to 2000. In fact, it is very difficult to consider the numbers and figures obtained from the local oral legend, but the idea can generally imply the presence of a frequent and casual landslide in the area since long.

In the study area significant amount of cultivable lands are being destroyed frequently and the number of landless farmers is increasing from time to time. For this reason several farmers are moving into sloppy areas which are potentially endangered by landslide hazards or are migrating to nearby towns. Besides, the local villages and towns in the study area are expanding into landslide-prone areas without any prior landslide hazard assessment and risk analysis. Moreover, landslides are posing serious challenges to infrastructure. The Addis Ababa-Desse-Mekelle main asphalted road crossing the study area has been damaged many times due to the first time failures and/or reactivated old landslides at the areas between Debresina-Armanya towns. Even during the fieldwork of this research, a new crack has been observed at the places between Sar-Amba and Armaniya just for a length of 500m. On the 14th of August 2010, two houses were partially damaged by the then landslide which is found at about 150m downstream of this cracked road indicating that it is still active. Similarly, some cracks are observed in the foundation of two of the high tension electric poles that pass near the Armaniya area.

As outlined above, landslide and related problems and risks are still continuing with an increasing trend to damage life and properties, and devastate infrastructure and the environment at various localities of the rift margin and highland of Ethiopia including in the study area. This is due to the facts that:

- Several towns in Ethiopia, including the study area, are located at the rift margin and highlands where landslides occur episodically in these environments. Due to this, the communities living in such areas are at high risk during intense and prolonged rainfall and seismic tremors.
- There are no recorded data of landslide occurrences throughout the country in general and the study area in particular. That is, no systematic databases center on mass movements that records/compiles or distributes or prepares inventory maps, hazard zonation maps at different scales for use by various stakeholders, vulnerability and risk assessment studies, classification and prioritization of the risks, prevention, mitigation, preparedness, response and risk reduction measures.
- No information, data-bases, maps, techniques and technologies exist in this field although there are haphazard few efforts from individual researchers. For this reason farming activities, urbanization and intensification of infrastructures in the sloppy area is still going and aggravating further landslide occurrence.
- The level of awareness of local people and the local administrators is very low. Hence, little attention is given at all level to the existence of landslides and their losses while planning and implementing activities related infrastructures and environment. Instead most of the actions taken by the decision-makers, at various levels of the government, focus on emergency issues.

- No National Disaster Management Authority exists in Ethiopia with the context of: (1) taking initiatives by issuing national guidelines on landslides that could help in preparation of plans for management of landslides (2) providing proactive awareness and preparedness to people by monitoring the expected risk

Therefore, this study is designed to understand and evaluate the various causative and triggering factors for the landslides of the area and identify the landslide prone zones that could be used as an input for the developmental land use planning of the area and other similar areas in the rift margin and highlands.

4.2 Location of the study area

The study area is located in north central Ethiopia and it is part of the Tarmaber Woreda of the Amara region, located at the eastern edge of the Ethiopian highlands just at the foot of the Tarmaber tunnel which is the outlet from the central Shewan highland to the Afar rift valley. The study area is bordered on the south by part of Ankober, on the west by the Jemma basin, on the northwest-north by Molale, and Mehalmeda, on the northeast and eastern part by Showa Robit. The Administrative center of the Woreda is Debresina while other small towns like Armaniya, Chira Meda along the Addis Ababa - Desie main road and Mezezo along the Debresina- Mehalmeda road are found.

Geographically it is located NE of Addis Ababa between UTM coordinates 580000 to 593500 mE and 1085000 to 1103800 mN (Fig 4.1). The total study area covers an area of 218 km². Debresina, capital of the Woreda is found at approximately 190 km on the main road from Addis to Dessie.

Except the main roads of Debresina-Armaniya and Debresina - Mezezo, the area is exceptionally inaccessible due to the rugged relief, vertical slopes and gorges, which are the dominant topographic features of the area, which make it difficult even to walk on foot.

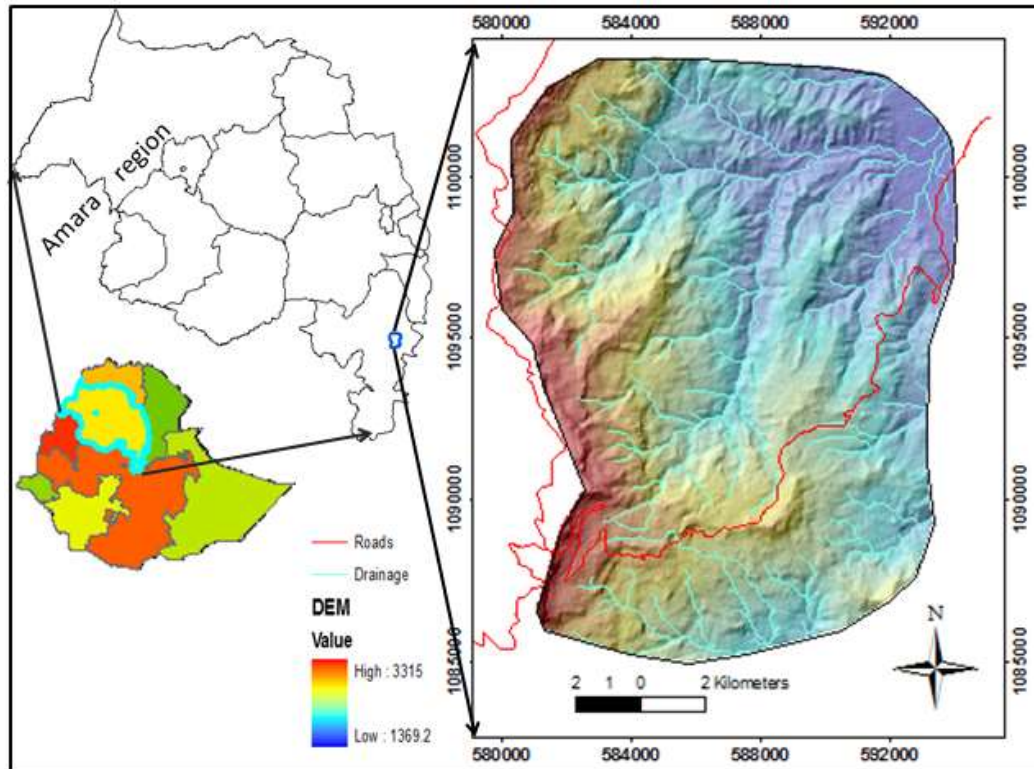


Fig 4.1: Location of the study area using DEM

4.3 Triggering factors

A trigger is an external stimulus such as high rainfall, earthquake shaking, volcanic eruption, rapid stream erosion that causes a nearly immediate response in the form of a landslide, by rapidly increasing the stresses or by reducing the strength of the slope materials (E.M,Wilde, et al, 2002). Both natural and human induced changes in the environment can trigger landslide. As mentioned in chapter 3, the study area is characterized by high rainfall and earthquake tremors in association to the Afar rift volcanism and diking phenomena.

Rainfalls and earthquakes are the major landslide triggering factors in the world. Their relationship to the occurrence of landslides can be well addressed when there is a long time records series of the events. However, their relationship is not defined in Ethiopia to date due to the absence of recorded data. Comparing both rainfall and earthquake, it is relatively easy to get data of the amount of rainfall than obtaining any type of earthquake data in Ethiopia. However, the rainfall data is not also complete. For instance, it is difficult to get the intensity and duration of rainfall data which are the main components in the slope stability assessment. So, the problem is not only restricted to the recorded relation but also on the data availability of the triggering factors. For this reason it is impractical to empirically quantify the relationship with the landslide although there is no doubt on their triggering effect.

As it is also indicated in available studies in Ethiopia (e.g. Ayalew, 1999; Ayenew and Barbieri, 2005; Woldearegay, 2005), rainfall is one of the major triggering factor of slope instability and it facilitates the landslide process in the highlands of Ethiopia. This is evidenced by the fact that most landslides usually have occurred in the wet season. However, some of the landslides are also triggered by earthquakes, especially in the rift margin and nearby highlands (e.g. Abebe, et al, 2009 and other oral witnesses obtained from the local community). Available data indicated that considerable number of earthquake occurred from March to October creating a time overlap with the wet seasons making another complication in identifying the triggering factor. Ayalew (1999) stated that in Ethiopia most landslides are occurring more frequently in September than in July. The same author also indicated that there are some occurrences of more violent landslides in June, October and November where negligible amount of rainfall is available, mentioning the cases of Wudmen and Sawla localities along the way to Jimma.

Rainfall (from National Meteorology Agency of Ethiopia) and earthquakes (from the United States Geological Survey) data were collected to assess their triggering effect on the landslide of the study area.

4.3.1. Hydro meteorological triggering factors

Rainfalls are common triggering factors of landslides in many mountain regions. Several researchers (e.g. Caine, 1980; Guzzetti, et al, 2008) have proposed a dependency of the minimum level of rainfall duration and intensity which might set off shallow landslides and debris flows. However, it is not only the amount of precipitation but rather the amount of water that infiltrates and moves into the ground to cause a failure.

The analysis and description of the triggering effect of the rainfall and geo-hydrological condition of the study area is provided below.

4.3.1.1 Rainfall (RF)

To assess and see the effect of rainfall to the landslide occurrences of the area, a monthly rainfall of four meteorological stations situated inside and just outside of the study area namely, Debresina (44 years), Debrebirhan (45 years), Mezezo (17 years) and Shewarobit (17 years) are analyzed. The Debresina station is found within the area of interest and has highest rainfall (Fig 4.2) indicating that the rift margins receive more rainfall than the central high lands represented by Debrebirhan station. Mezezo station, which lies near to the rift margin than the station of Debrebirhan records more rainfall. Obviously, the lowland area is represented by the Shewa Robit meteorological station which has the lowest rainfall amount. The reason for the high rainfall of the rift margins is attributed due to the

orographic effect. Localized landslide occurrences are common in every rainfall period in the rift margin including Debresina area, especially along stream banks and road cuts.

Debresina area is one of the areas receiving a high rainfall in the country having a bimodal rainfall, with peak precipitation in the months of June to September, and with minor rainfall in the months of February to May (Fig 4.2). As the cases in every corner of the world, rainfall is one of the potential triggering factors for the slope failure in the Debresina area.

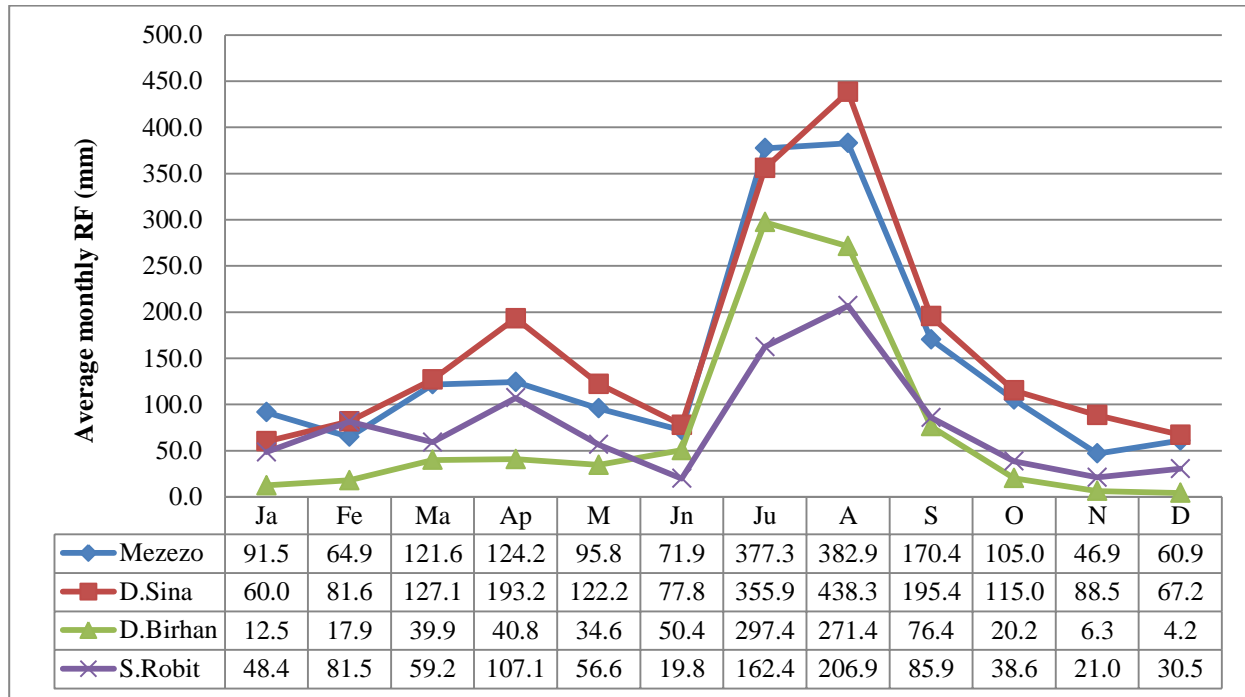


Fig 4. 2: Average monthly rainfall of four stations: Ja =January; Fe=February; Ma = March; Ap = April; M = May; Jn = June; Ju= July; A = August; S = September; O = October; N = November; D = December

The maximum, minimum and average annual rainfall in the study area (Debresina station) is 3409 mm, 959.4 mm and 1922 mm respectively. The maximum annual rainfall is recoded in the year 1997, while the minimum in the year 1991. The monthly maximum RF is always in the months of July and August for all the recorded data. More than 50% of the annual average RF is obtained in the months of July and August while 23% of it is obtained in the months of March to May where the minor rainfall peaks occurred.

As has been explained in the inventory mapping of the past landslides by this study, more than 160 landslide occurrences including very large and small size landslides are identified. However, it was not possible to know the time of occurrences except for the September 2005 big landslide event. G/silassie (2007) has tried to define the period of landslide occurrence in the area for some of the years (Table 4:1) by interviewing local people.

Table 4.1: Past landslide records

S.N	Locality name	Time of occurrence	Damage
1	Yizaba, Gishrit locality	1995	1575m ² wood land was affected
2	Yizaba, Aynemariam locality	1995,1998 & 1999	Some residential units cracked and 3ha of bush land damaged
3	Shotel-Amba	1953 & 1998	Residential units, farmland and grazing areas were affected by both periods
4	Weibila	1995 & 1997	18 residential units and 30 hectare of farm land and grazing land was affected by the 1995 landslides
5	Sina/Aregai	October, 1971	35-40 hectare of forest land was destroyed
6	Armania	1953, 1979 & 1997	The asphalt road has been affected in all the three landslide events. Still active and a tensional cracks are observed at the roadside
7	Nib-Amba	1953, 1997 & 2000	>100ha of farm land, grazing area destroyed
8	Sholla-Meda	July, 2000	20ha of farm land, grazing area and settlement
9	Lay Indode	September, 2000	It destroyed 8 residential unit & 30ha of farm land and grazing land. It is still active and has been reactivated event rainy season
10	Tach Indode	1999 & September, 2000	It destroyed an estimated of 40ha of grazing land and farm land. It is still active and has been reactivated event rainy season.
11	Yizaba, Shotel Amba, Armania,Ainemariam	September 2005	Over 900ha arable lands destroyed, more than 4049 peoples displaced, more than 1200 dwelling local houses destructed & over 75% crop harvesting failure specifically in the localities named Izaba and Shotel Amba

(Sources: 1-10 from G/silassie (2007: #11 from Action by Churches Together (ACT) (2006) and local authorities

Most of the landslide provided in Table 4.1 does not have known month or date of occurrences and thus, it is very difficult: (1) to conclude all the landslide occurrences in the rift margins and highlands occurred in the peak wet season (2) to derive the threshold rainfall for the landslide initiation. Nevertheless, crudely speaking all the landslides given in table 4.1 have been occurred when the annual RF is greater than the long term average rainfall (Table 4.2). The annual and the long term average rainfalls are compared in Table 4.2 for the landslide years identified by the interview above.

Table4.2: Comparison of annual and long term average rainfalls for the landslide occurrence years (Debresina station)

Years	1971	1979	1993	1997	1998	1999	2000	2005
Annual RF (mm)	2773.4	1945.7	2437.5	3409.2	2185.8	2140.9	2282.3	1994
Long term average annual rainfall of Debresina station is 1922.28mm								

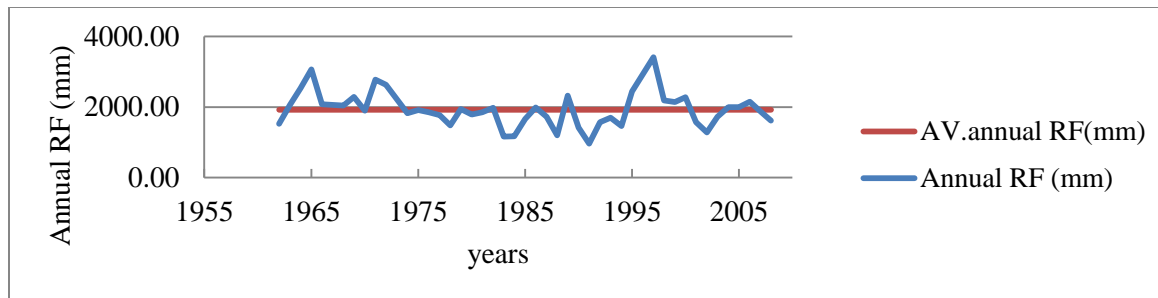


Fig 4.3a: Annual rainfall of the study area (from 1962 -2008)

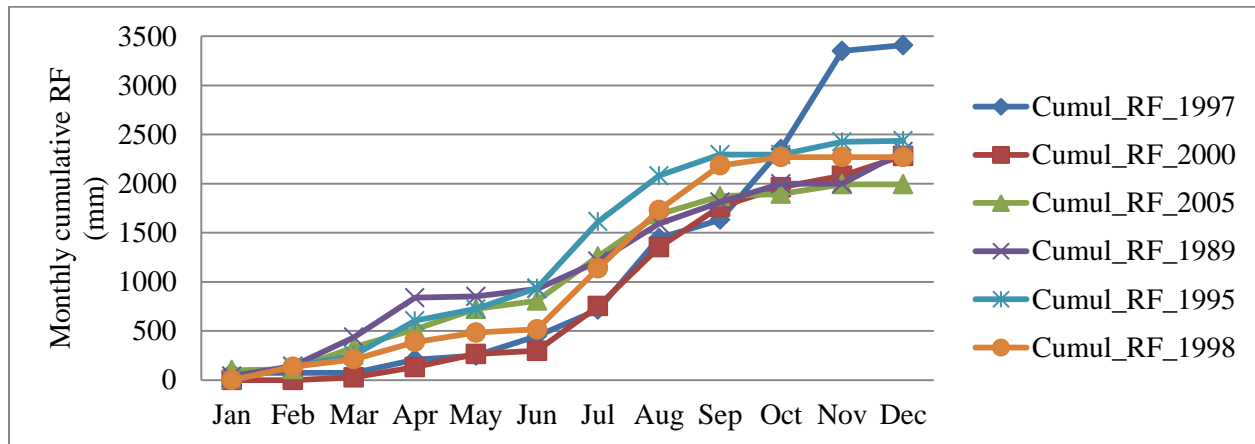


Fig 4.3b: Comparison of cumulative rainfall of the years 1989, 1995, 1997, 1998, 2000 and 2005 (data from Debresina weather station) of the large-scale landslide area, Ethiopia.

However, there were lower occurrences of major landslides between the years of 1974 to 1994 (Fig 4.3a) where the amounts of annual rainfalls were lower than the long term average except for 1989. Cumulative monthly RF of the years having maximum annual rainfalls (Fig 4.3b), monthly distribution of rainfalls of the three consecutive years of 2004, 2005 and 2006 (Fig 4.4) and the daily maximum of 2005 (Fig 4.5) are also compared and analyzed to see the triggering effect of rainfall to landslides, with emphasis to the event of September 2005. As explained in chapter one, there are no clear agreements among different sources on the initial date of the September 2005 landslide, varying from September 13 to 28/ 2005 as explained above. Analysing of the RF data showed that: (1) the daily maximum RF of the year 2005 is recorded on 8th of August but the massive landslide occurred after around mid of September (2) the monthly peaks are recorded in the months of July and August for all the years, including 2005 (3) the overall annual average of 2005 is less than some years with maximum annual average RF such as 1989 (2326mm), 1995 (2437mm), 1997 (3409mm), 1998 (2271) and 2000 (2282mm) and so on. The cumulative values are plotted and compared in Fig 4.3b. The evaluation of these rainfall values depicts that the possibility of large scale landslide could have been existed in the earlier years (e.g. in 1997) than in 2005 if rainfall only was the triggering factor. Therefore, the final triggering factor of the September 2005 landslide event was most probably the then earthquake although rainfall has also the additional effect.

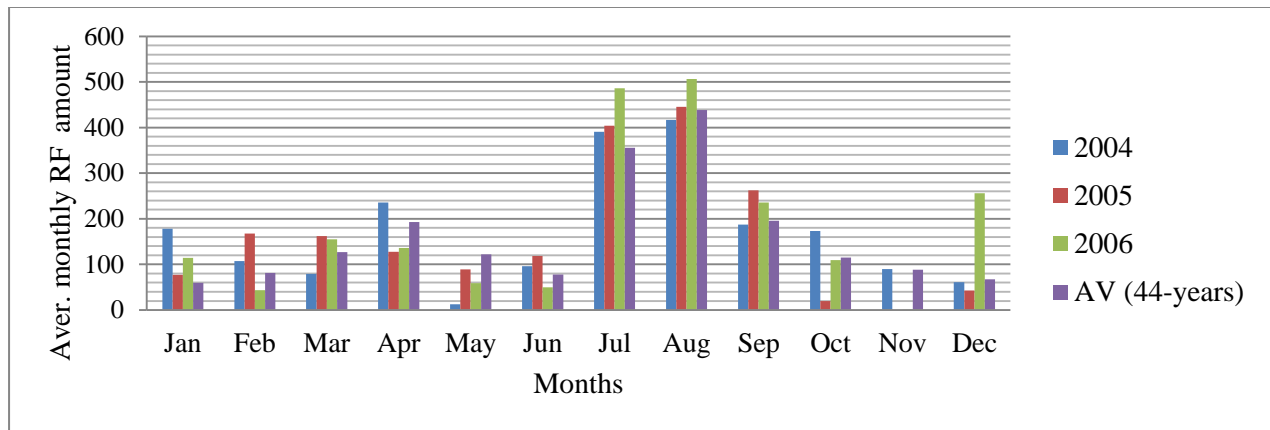


Fig 4.4: Comparison of the monthly rainfall of 2004, 2005 and 2006 and the average monthly rainfall for 44 years (Debresina station)

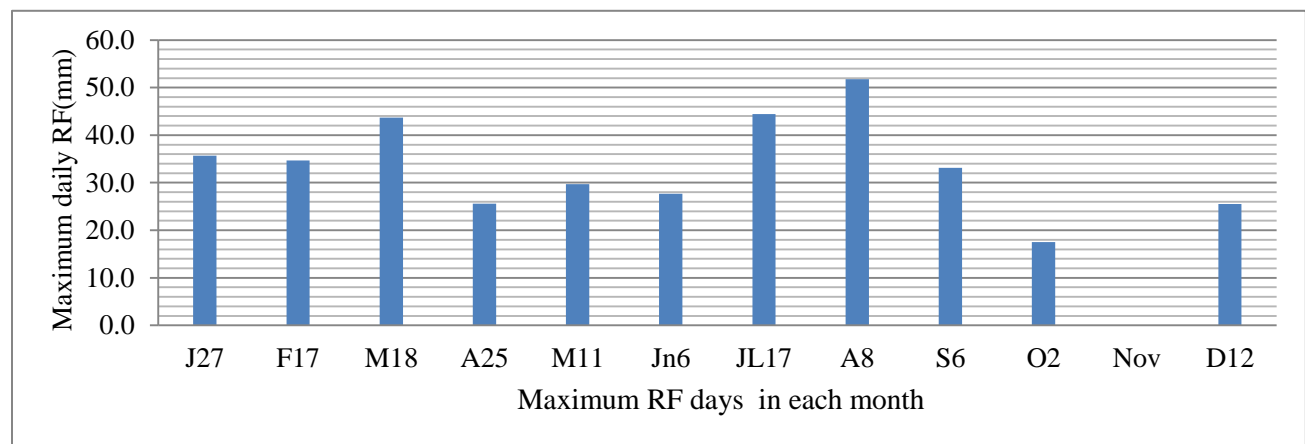


Fig 4.5: Recorded maximum daily RF in each months of the year 2005 (J27 = January 27th; F17 = February 17th; M18 = March 18th; A25 = April 25th; M11 = May 11th; Jn6 = June 6th; JL17 = July 17th; A8 = August 8th; S6 = September 6th; O2 = October 2nd; Nov = November with no RF; D12 = December 12th)

4.3.1.2 Spring and seepage

The prevalence of landslides in the volcanic terrain of Ethiopian highlands has been reported by previous authors (Ayalew, 1999; Ayenew and Barbieri, 2005; Woldearegay, 2005). For example, Woldearegay (2005) has reported that 55.4 % of the total 368 landslides occurrences are found in the volcanic terrain of the highlands of Ethiopia. The study area is totally covered by the disturbed tertiary volcanic terrain and their weathered products (quaternary sediments). Due to the cross cutting extensional tectonics (normal faults), the rocks are intensively fractured and weathered. In such areas, understanding the nature of fractures and discontinuities are amongst the most important geological factors to understand the geo-hydrological situation of the area. In fact, the geohydrology of the rift margin volcanic terrain in Ethiopia is very complex. This is because the stratigraphy and tectonics of the interface zone is complex (rocks are laterally discontinuous,

aquifer composition are heterogeneous, aquifer hydrodynamics characteristics are variable) (Kebede, et al, 2008).

An assessment and inspection of the geo-hydrological condition of the site carried out during the fieldwork in both the dry and the wet season and the observations (Figs 4.6 to 4.8) indicate that:(a)The upper sections of the slopes are covered by fractured and permeable Tarmaber basalts and marginal faults which in general act as zones of rainwater recharge to the down-slope and underlying masses, (b) The soft and low permeable paleosol and intercalated sediments, underlying altered Alaje formation, and the residual soils, retard vertical flow of water and promote lateral flow of water parallel to the slope surfaces and hence encourages water pressure build-up within the slopes (3).The colluvium-eluvium (coarse-grain dominated soils) at the gentler sections of the foot slopes enhance recharge, while the fine-grain dominated soils at the lower sections of the slopes retard drainages and hence promote rise in water level within the slopes during heavy rainfall seasons (Fig 4.8). As it can be seen from the figures below ponded water infiltrates into the slope and increases pore water pressure and decreases the shear strength, thereby causing instability to the slopes (Fig 4.6). The excessive surface run-off through drainages aggravates the erosional activity on the slopes (Fig 4.7). Therefore, the hydrogeologic conditions which indicate the drainage network and the nature of distribution of surface and sub-surface water are important for landslide occurrences.



Fig 4.6: Ponded rain water on the hummocky topography further triggering the sliding earth (a) at the Gifaita Gebriel (south of Debresina town) (b) at Yizaba locality.

These are evidenced by the springs and seepages which are commonly observed following the fractures or lithological contacts where fractured rock overlay the impermeable layer at various elevation levels in the study area. It is also observed that about 99% of the water supply of the area is obtained from spring and no

hand dug or drilled water wells exist in the area. In many of the landslide-affected sites, springs and seepage zones were observed to emerge along more fractured zones of the rocks or along the coarser soil horizons (Fig 4.7b, c). Perched ground water occurs commonly in layered strata, such as colluvium, alluvium and fills built from various source materials.

Most of the contact springs in the study area erodes the more permeable soil at their outlet and undermines the slope above, and are a zone of loose soil which can easily cause instability. The availability of several springs at the foot of the slided portion indicates that the aggressive erosion of such spring has caused a landslide in the area. The number and quantity of springs or seepage areas shows a high contrast between the wet and dry season as it was observed from the field trip in both seasons.

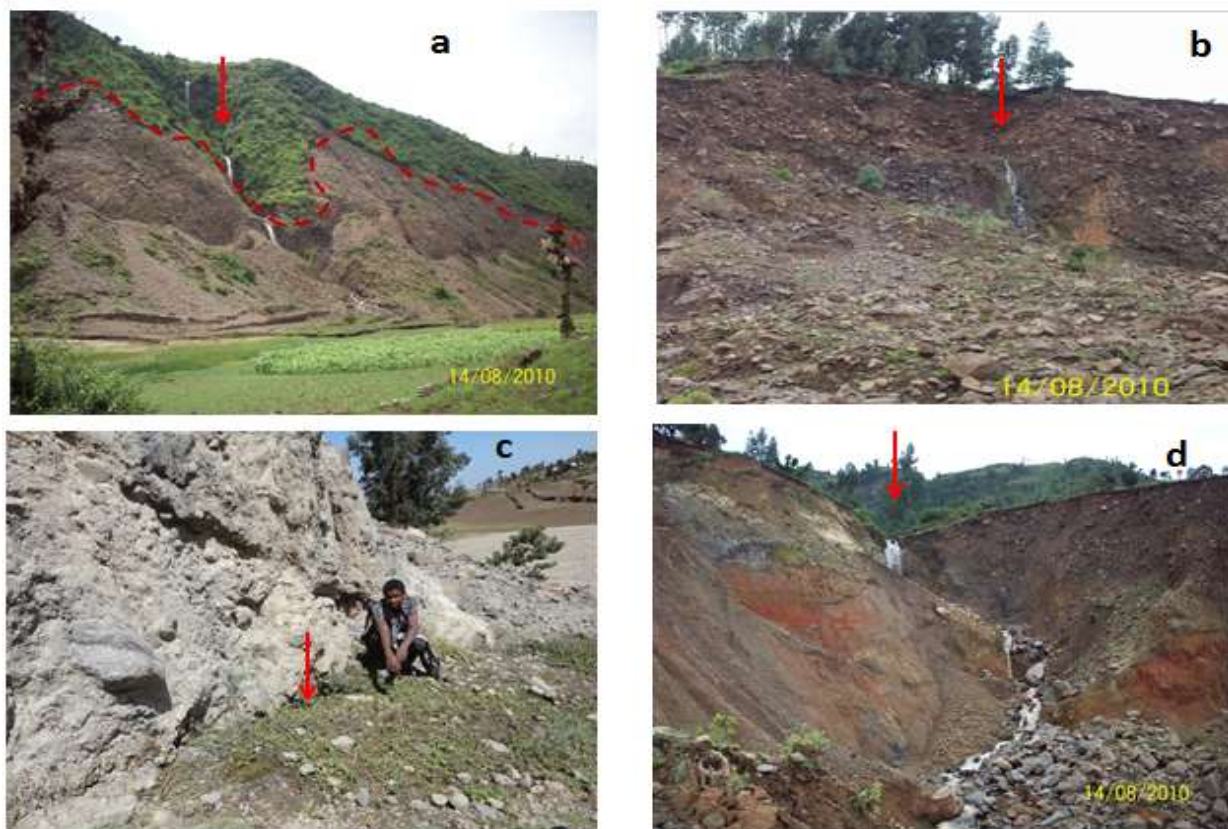


Fig 4.7: This diagram shows the triggering & reactivating effect of water on the major Sept.2005 landslide of the localities of Yizaba and Shotel Amba:(a) Surface run off along the west-east flowing streams (b) Spring water at the contact of the top layer (colluvium) and underlying altered Alaje tuff (c) Seepage at the foot of the landslide scarp (d) The aggressive deep gully erosion triggering the instability. (Photoes: a, b & d are taken in mid of Aug. 2010 while photo 'a' is taken in Jan.2012)

Most known landslide occurrences, including the complex landslides of 2005, took place in September and some in October in the area as seen in Table 4.1. Ayalew (1999) made similar observation that quite

significant landslide occurs in September-October in the Ethiopian highlands. The same author considered that this is related to the open cracks which were formed early in September and at the beginning of October and some sub-surface erosional features, including natural pipes. When water enters these open tensional cracks or pipes during periods of high precipitation, a rapid pore water pressure may be built up. This phenomenon, together with the effect of surface erosion around the lower parts of the slopes and an increase in bulk density at the top, is likely to give rise to sudden and catastrophic failures (Ayalew, 1999). Most of the time, such landslides are followed by small slumps over a number of days until the equilibrium is re-established (Ayalew, 1999). Similarly, the September landslide of Yizaba and Shotel-Amba of Debresina stays for two weeks until it attains the equilibrium.

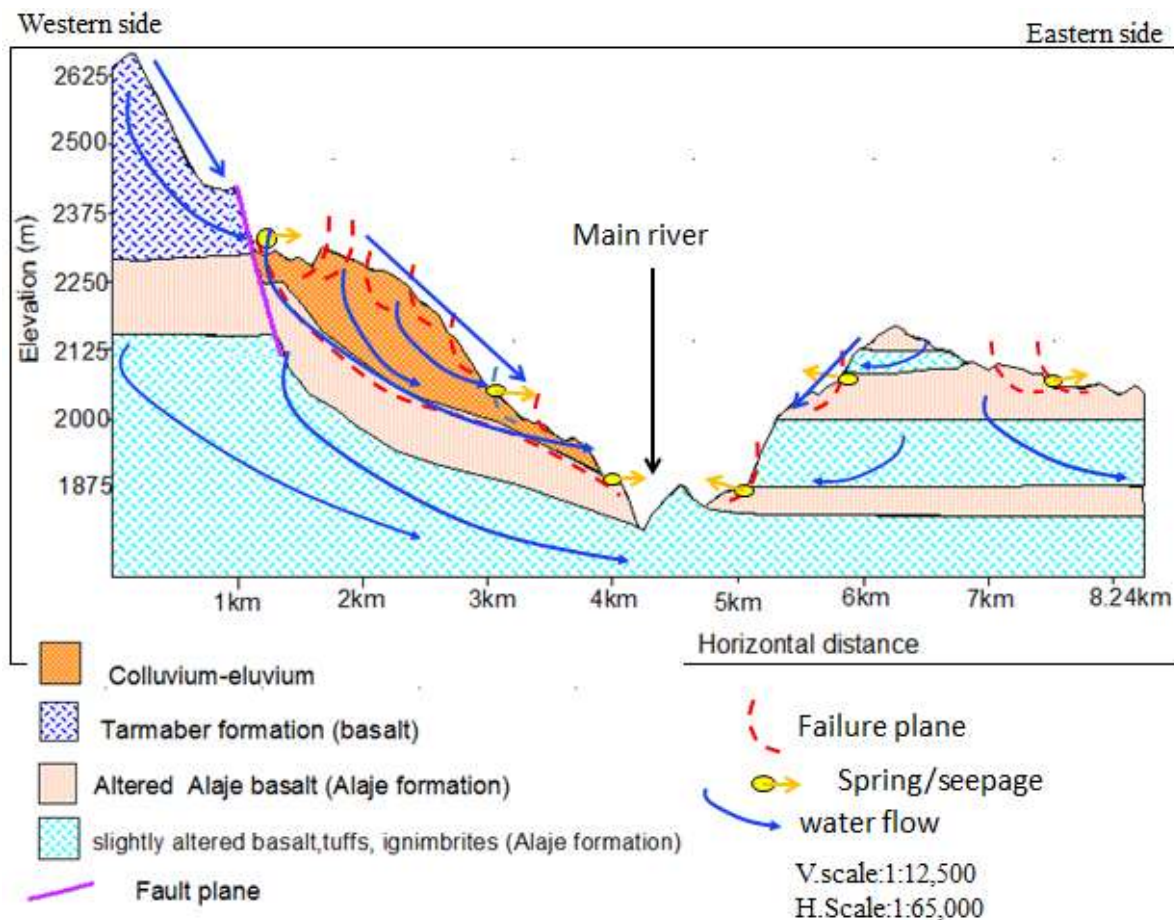


Fig 4.8: Conceptual model of geo-hydrological conditions of the study area and its effects on the slope failure

4.3.2 Earthquake (EQ)

The earthquake shocks may be responsible for triggering new landslides and reactivating old landslides. The vibrations due to earthquake may induce instability, particularly in loose and unconsolidated material on steep slopes.

The Afar rift margin, where the Debresina area is situated, is known for its earthquake occurrences. Most of the earthquake ranges from small to medium level (Ayele, et al, 2007). Although not registered, the occurrences of landslide in association with Afar earthquake in the area are common as evidenced by local dwellers. For example, as obtained from local information, there was a landslide occurrence around the Nibamba Gebriel and Sina Aregawi contemporaneous with the 1961 Kara-Kore earthquake.

An earthquake data is collected for the years 1960 to 2008 from the United States Geological survey (USGS) and Addis Ababa geo-observatory center for the whole of the country and neighboring east African countries. The data from the USGS includes date and depth of occurrences, magnitude, Geographic location while that of the Addis Ababa university was not that much helpful as it lacks the required information.

For example as per the collected data, only in the year of 2005 (i.e. from 4th of June to the 4th of October), 169 earthquake occurrence are registered in the localities of Dabbahu and Hararro (located between latitudes 11.72 to 12.75 degree N and longitude 40.29 to 40.70 degree E). More than 96% of these occurrences took place from September 14 to 29/2005 during which the landslide of Debresina has occurred (Fig 4.9). The epicentral depth of this earthquake was at 10km. Several researchers, such as Wright et al., (2006), Yirgu et al., (2006), Ayele et al., (2007, 2009), Rowland et al., (2007), Grandin et al., (2009), also reported that a major diking episode occurred in various localities of Afar depression in September 2005, causing a number of associated earthquakes of magnitude greater than 3.5 mb. Interviews with local people also confirmed that the then volcanic explosion and earthquake shake was felt by some people around the study area.

Similarly, there was another EQ occurrence on September 9, 16, 17 and 19/2005 around the locality known as Ankober which is 60-80km south of Debresina area as registered in the Addis Ababa Geo-observatory (Fig4.9). Thus, the most probable triggering factor for some of the initial cracks of the September 2005 large landslide occurrence could be the earthquake associated to the dike episode at Dabbahu and Manda-Hararo or to that of the Ankober (at the rift margin). However, it was not possible to check the strong motion of the then EQ whether it can trigger landslide in the Debresina area or not due to lack of data.

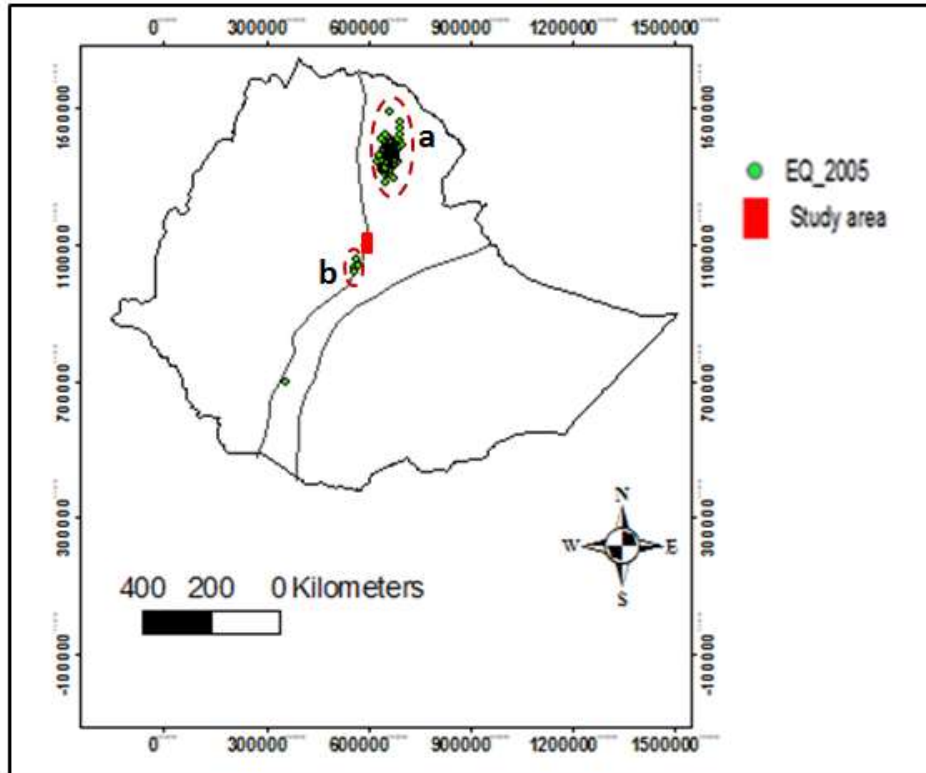


Fig 4.9:Location of EQ epicenters on Sept. 2005 in relation to the study area (a) occurrence of EQ in Sept. 2005 (between 170-300km NE of the study area) at the localities Dabbahu, Manda-Hararo (b) occurrence of EQ in Sept. 9,16, 17 and 19/2005 at the localities Ankober (found at about 60-80km South of the study area).

4.4 Field survey and laboratory tests

Geology is one of the major landslide causative factors in the study area. For this reason, some physical chemical, mineralogical and geotechnical tests have been carried out on the rocks and soils of the study area. Summary of activities are provide in Table 4.3.

Table4.3: Summary of laboratory and related works

Tests on rocks		
S.N	Type of test	Number of samples/tests
1	Petrographic tests	13
2	Geochemical tests	13
3	Physical tests (density, water absorption)	66 tests on 16 samples
4	Point load tests	23
5	Schmidt hammer reading measurements	>372
Physical, index and geotechnical tests on soils		
1	Atterburg limit (LL,PL, PI)	21
2	Grain size test	13
3	Free swell	8
4	Moisture content	11
5	Direct shear test	25
6	Unit weight	11
7	X-ray diffraction test	5
8	Geophysical VES points, field survey	More than 12

4.4.1 General

The geology of the highland and rift volcanic rock is studied by a number of authors (e.g. Mohre, 1962; Zanettin, et al, 1974 and 1978; Kazmine, 1975; Mohr, 1983; Pik R. et al, 1998; Kiefer, et al, 2004).

The Northwestern Ethiopian and Afar Rift valleys are composed of (from top to bottom): Tarmaber formation. Alaje formation, Aiba formation, and Ashenge formation (Mohr P., 1983).

The Debresina area is dominated by a Tertiary volcanic terrain consisting of Alaje formation (51%), Tarmaber formation (17.4% by Quaternary sediments (28 %) and youger ignimbrite (4 %). The Alaje formation belongs to the fissural flood basalts while the Tarmaber are the shield volcanoes (Mohre, 1983 and reference there in) and it is represented by interlayered silicic rocks and transitional basalts, but some time only by silicic rocks, mostly slightly Peralkaline Rhyolite (Zanettin, 1992). In the study area the Alaje formation is composed of basalts, rhyolitic/trachytic ignimbrites, tuffs, and agglomerates while the Tarmaber formations are dominantly basalts. A small part of the study area is covered by the younger ignimbrite which overlies the Tarmaber. Whereas the Quaternary sediments consists of alluvial, colluvial-eluvial deposits, fine residual soils.

The lithological the field description supported by some laboratory test results and photographs are given below where as the detail lithological map of the study area is provided in chapter4 as an input map for the landslide assessment. A very rough sketch is provided in Fig. 4.10 only for the major formations to give a high light with the regional geological stratigraphy.

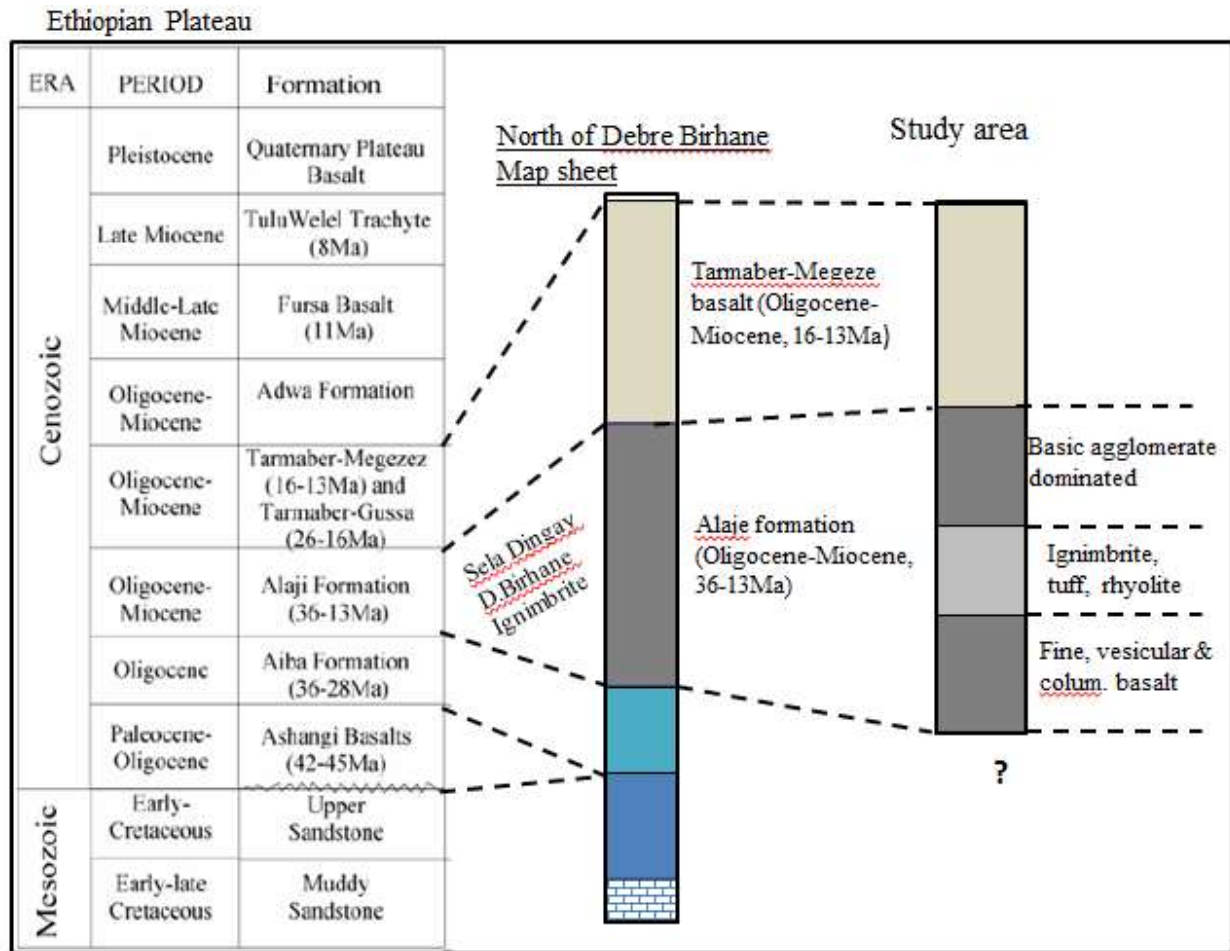


Fig 4.10: Rough sketch of major formations of the study area high lighting regional correlation with the Ethiopian plateau stratigraphy (modified from the Geological map of Debrebirhan area, 2009)

The geological and geotechnical properties of the rocks and the soils are more discussed and elaborated based on the field and laboratory works as follows.

4.4.2 Properties of rocks

Lithologically the Alaje formation found in the study area consists of basalts, agglomerates of basaltic composition, ignimbrites, tuffs, rhyolites and trachyte. These cover the moderate to gently sloppy areas of the middle, southern and northeastern part of the study area

Alaje basalt and basaltic agglomerates

The Alaje basalt is characterized by various layers of basalts separated by highly weathered basic tuff layer. Its texture varies from fine to medium. The fine and vesicular basalts are intensively fractured by non-directional joints (Fig 4.12, d). The aphanitic basalt is fine grained, black/dark/gray, irregularly fractured,

columnarly jointed and rarely shows a massive appearance that forms a steep morphology. It is strongly deformed as seen at the road and river cut exposures. Petrographic analysis shows that the aphanitic basalt has an average composition of groundmass 80%, plagioclase 15%, olivine 5%, pyroxene 3% and opaque minerals up to 2%. The groundmass is dominated by laths of plagioclase, clinopyroxene, and volcanic glass (Fig 4.11).

The basic tuffs and agglomerates are part of the Alaje formation, mostly found at the upper part just in contact with overlying Tarmaber basalts. They contain fragments of vesicular variety of dark colored porphyritic to aphanitic basalts and ignimbrite cemented by white ash. When checked by the geological hammer, it is loose and highly weathered with angular rock fragments from cobble to pebble size; in lower slope they are highly weathered. From field observation, slope failures are very common in this rock at the study area

It is loose and highly weathered with angular rock fragments from cobble to pebble size and forming low slope angle than other rocks (Fig12, a).

Alaje rhyolite/trachytic ignimbrite, tuff

This trachytic rhyolite is also part of the Alaje formation found intercalated with the basaltic rocks. At places, it forms small cliffs vertically jointed and at places it is highly shattered by the tectonic effect of the rift faulting. It is fine to medium grained, light yellowish color. Several landslide occurrences are also observed in this type of lithology.

Thin section studies shows that the ignimbrite of the study area varies from low grade rhyolite (less compacted or less welded) to high grade rhyolites (well compacted or welded ignimbrite) and has an average composition of glass 55%, plagioclase 15%, rock Sanidine 10%, rock fragment 10%, quartz 5%, hornblende 3%, iron oxide 1% (Fig 4.11).

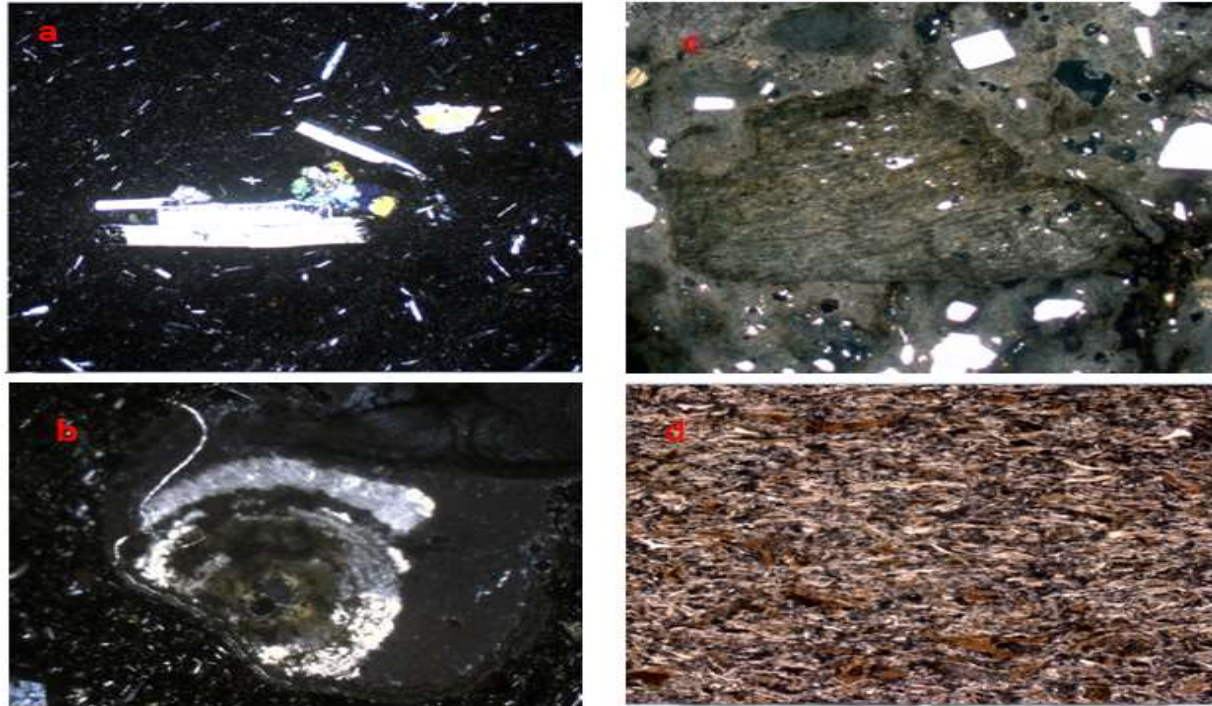


Fig 4.11: Thin section photomicrographs of different lithologies of Alaje formation showing (a) S3-2CN2.5 (for aphanitic basalt) (b) S4-2CN2.5 (vesicular Basalt)-shows presence of calcite (c) S1-2CN1.25 shows the alteration at the contact and less compaction of the welded tuff (d) S11-OB2, 5OP (show eutaxitic texture)

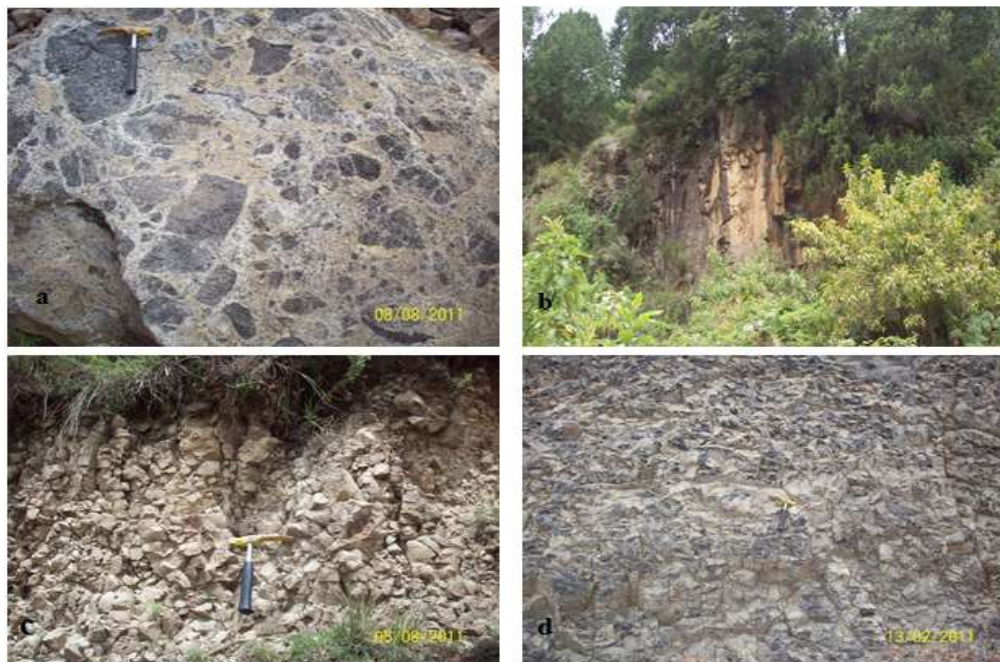


Fig 4.12: The various lithologies of Alaje formation: (a) Basaltic agglomerates (b) Cliff forming rhyolite (c) Shattered rhyolitic ignimbrite (d) Intensively fractured basalt



Fig 4.13: Diagram showing section at the Alaje formation at locality of Nib Amba: S5 (altered basic tuff ?), S2 (ignimbrite), S1 (rhyolitic welded tuff), S3 (columnar aphanitic basalt), S4 (vesicular& amygdaloidal basalt) from bottom to top respectively.

Paleosols and some tertiary sediment are haphazardly observed in all the Alaje formations depicting the time gap among successive eruptions. They control the flow of the perched water flow and hence also some of the slope failure.

Tarmaber Formation (basalts)

The Tarmaber Megezez formations are dominantly basaltic in composition. These rocks are mainly exposed on the western part of the study area generally forming a vertical cliffs and ridges trending in the N-S direction and some E-W offsets (Fig 4.14). The texture of Tarmaber-Megezez basalt varies between fine, medium to coarse grained, and is with a fresh color dark gray to weathered color of light yellow, light brown and reddish. Field observation and thin section result showed that medium to coarse type basalt has an average composition of groundmass 40%, plagioclase 30%, pyroxene (augite) 10%, olivine 12% and opaque minerals 10% and with an estimated porphyritic index of 20% (Fig 4.14, Photo-S₆). Plagioclase and olivine grains are altered to sericite and iddingsite respectively. The groundmass is dominated with plagioclase and pyroxene microlaths with some opaque. Similarly petrographic studies of fine to medium Tarmaber basalt (with phenocrysts of olivine-plagioclase and opaque) portray an average composition of groundmass 45%, plagioclase 30%, pyroxene 4%, olivine 10% and opaque minerals 8%. Plagioclase and olivine are altered to sericite and iddingsite respectively. The groundmass is composed of microcrystals of olivine, plagioclase, and opaque minerals.

From the field observation, they are affected by 2-3 sets of joint sets, with vertical to sub-vertical dip angles and nearly N-S, E-W and NE-SW general trends. Relatively they are less affected by the landslide but some rock falls are observed at the foot of the cliffs.

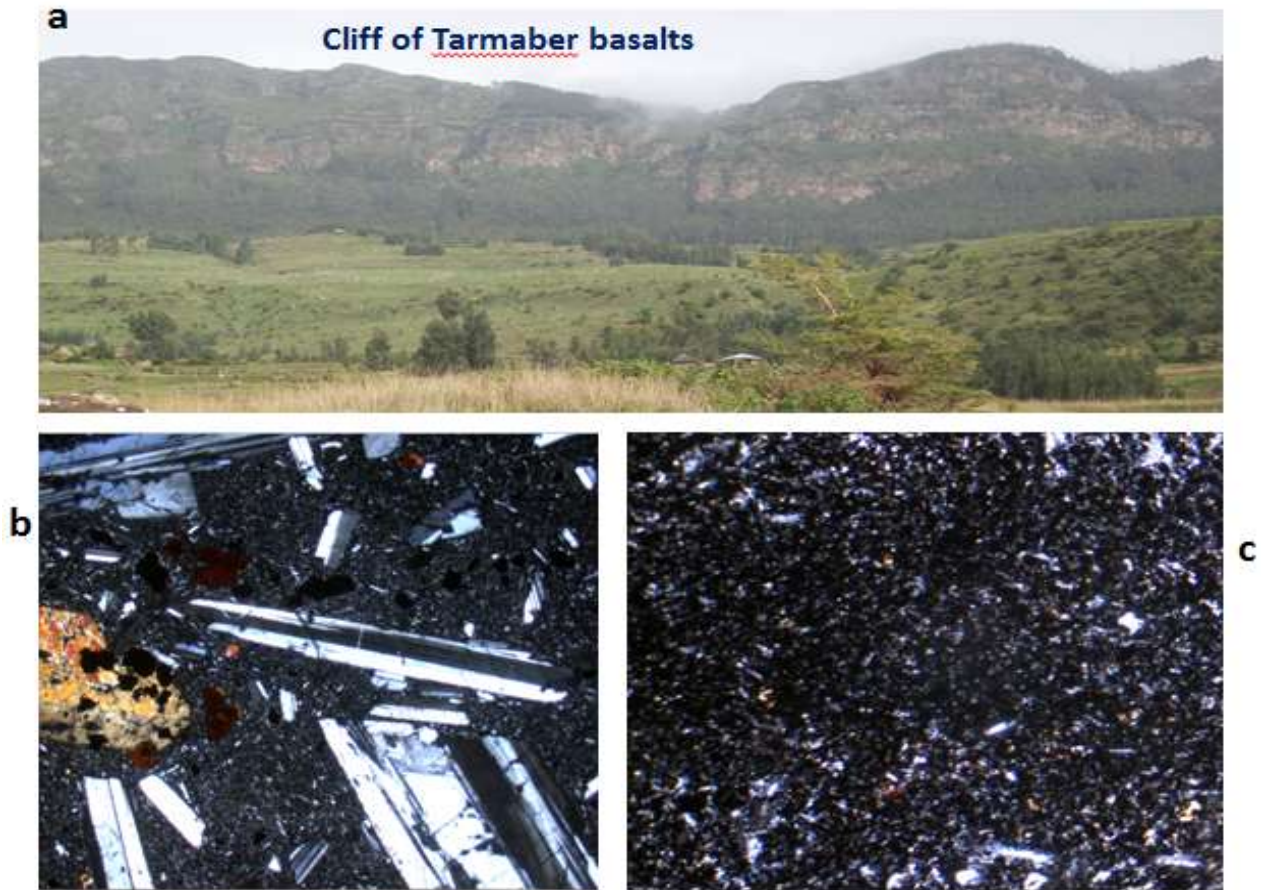


Fig 4.14: Tarmaber basalt (a) Field photograph showing the cliff forming along which the Tunnel is found (b) Photo: S6- CN1.25 showing plagioclase, olivine, opaque phenocrysts (c) Photo from thin section S6-3CN10 showing the groundmass (composed of glasses, clinopyroxine, plagioclase and opaque)

Quaternary/recent sediments

These sediments consist of the alluvial deposits and colluvium-eluvium deposits. The alluvial deposits dominantly lie at the eastern part of the catchment where there is relatively flat topography available and also following the river beds and river banks. Those alluvial found at the flat flood plain varies from clayey sand to silty sand with gravels and cobbles while those found at the river bed and banks are dominated by coarser materials such as sands, gravels , and big boulders (Fig 4.15,a). This indicates that the streams that initiate their flowing from the slided land are very rich in debris and are with erosive power damaging farmland and other infrastructures.

While the colluvium-eluvium is found at the foot of the stepped cliffs, ridges and flat hill tops. They are mixed and loose sediments deposited by old landslide, reworked breccia, and sheet floods consisting of fine to boulder sized soils. Most of the time, these are cultivable lands. Some of the seepages and/or springs that drain from the highlands disappear to these thick colluvium and reappear following the lower morphology breaks or the stream banks. These are the most susceptible lithology to both reactivated and first failure landslides

The fine dominated residual soils with no noticeable gravity movements are mapped and described separately. The altered Alaje basalt, when exposed at the surface is categorized with these groups. These types of soils are commonly found around the Sar Amba-Armania road and are prone to landslide, even though they are found in the flat topography (Fig 4.15, c & d).



Fig 4.15: The various types of recent sediments) (a) debris deposits at the river floor (b) eluvium dominated (c) colluvium-eluvium dominated (d) altered Alaje basic tuffs (residual soil)

4.4.3 Chemical, physical and geotechnical properties of rocks

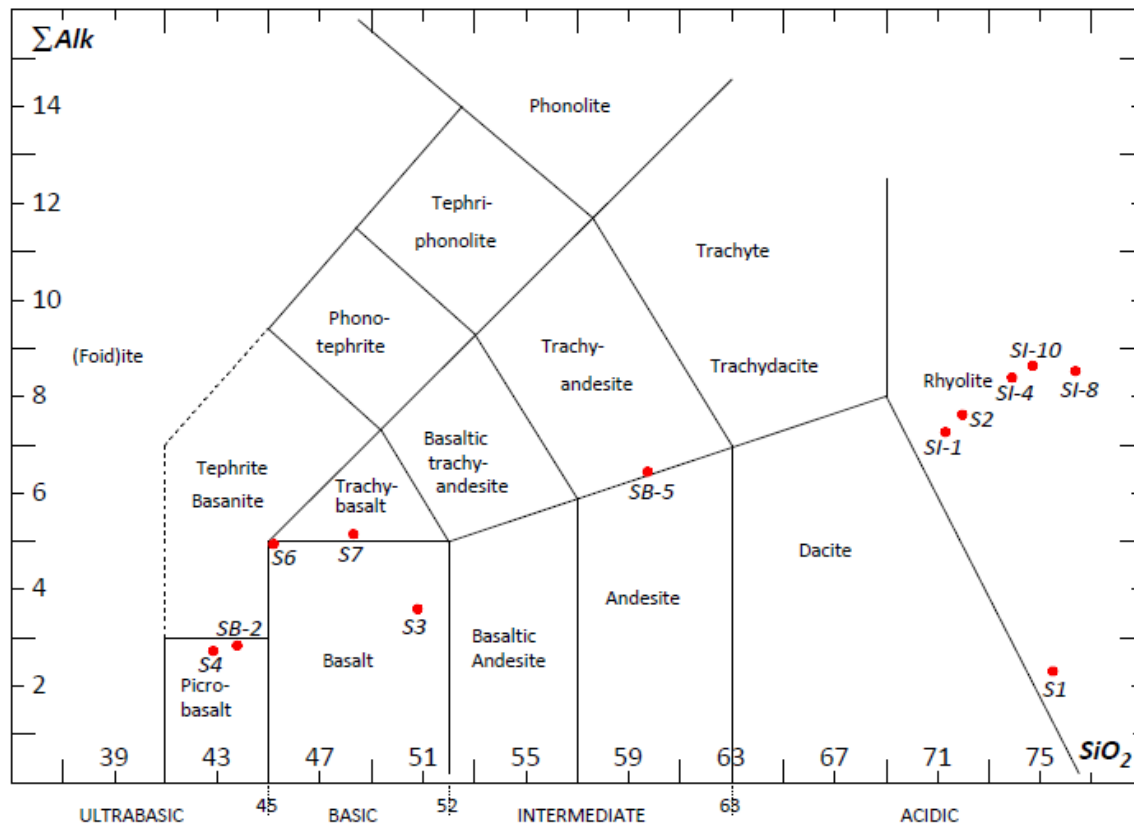
4.4.3.1 Geochemical tests of rocks

Table 4.4: Geo-chemical test results of the rocks of Debresina

#	1	2	3	4	5	6	7	8	9	10	11	12
Sample	S1	S2	S3	S4	S6	S7	SI-1	SI-4	SI-8	SI-10	SB-2	SB-5
<i>Le Bas</i>	K-Rh	K-Rh	K-Ba K- PiBa	K-Ba	TrBa	K-Rh	K-Rh	K-Rh	K- Rh K- PiBa	Ts		
<i>De La Roche</i>	----	alRy	AnBa	AnBa	Hw	LtBa	alRy	alRy	alRy	alRy	AnBa	Ry
Middle most	K	K	Na	Na	Na	Na	HK	K	K	K	Na	K
SiO ₂	75.49	71.96	50.78	42.87	45.17	48.31	71.31	73.89	76.34	74.68	43.78	59.69
TiO ₂	0.36	0.30	2.62	2.42	3.87	3.55	0.23	0.25	0.23	0.24	3.60	0.88
Al ₂ O ₃	6.65	11.19	14.42	13.59	16.78	15.72	11.60	10.63	12.18	10.54	12.56	12.69
Fe ₂ O ₃	2.13	2.34	11.90	8.79	13.11	11.72	3.33	4.37	1.58	4.18	14.38	6.29
FeO	0.00	0.00	0.00	0.00	0.00	0.00	0.00	0.00	0.00	0.00	0.00	0.00
MnO	0.04	0.05	0.18	0.21	0.19	0.20	0.07	0.09	0.04	0.09	0.20	0.20
MgO	0.52	0.21	5.32	3.19	3.51	3.81	0.09	0.08	0.05	0.07	4.93	1.54
CaO	1.49	0.39	9.26	10.16	7.68	7.49	0.69	0.23	0.20	0.18	8.34	1.24
Na ₂ O	0.77	2.89	2.62	2.12	3.27	3.52	2.23	3.96	4.42	4.14	2.16	2.70
K ₂ O	1.55	4.74	0.98	0.62	1.68	1.66	5.04	4.45	4.11	4.51	0.69	3.76
P ₂ O ₅	0.05	0.02	0.32	0.36	0.60	0.53	0.01	0.03	0.01	0.01	0.40	0.14
L.O.I.	9.83	4.41	1.18	13.75	2.20	1.56	4.07	0.83	0.69	0.58	8.53	9.97
Sum	98.88	98.50	99.58	98.08	98.07	98.06	98.67	98.81	99.85	99.22	99.57	99.10
S.I.	10.87	2.11	26.91	22.88	17.20	19.36	0.87	0.64	0.50	0.56	23.60	11.21
D.I.	75.84	87.11	31.48	25.29	37.60	39.59	84.18	88.40	95.28	88.98	23.99	66.71
A.I.	0.44	0.88	0.37	0.31	0.43	0.48	0.79	1.07	0.96	1.11	0.34	0.67
CIPW norm (Fe₂O₃/FeO=0.15)												
Q	60.16	34.65	3.52	3.69	0.00	0.00	35.53	32.20	33.60	33.23	1.64	21.64
C	1.11	0.64	0.00	0.00	0.00	0.00	1.25	0.00	0.12	0.00	0.00	2.26
Or	9.16	28.01	5.79	3.66	9.93	9.81	29.78	26.30	24.29	26.65	4.08	22.22
Ab	6.52	24.45	22.17	17.94	27.67	29.78	18.87	29.90	37.40	29.10	18.28	22.85
An	7.09	1.82	24.69	25.73	26.15	22.19	3.34	0.00	0.92	0.00	22.54	5.24
Ac	0.00	0.00	0.00	0.00	0.00	0.00	0.00	1.50	0.00	1.44	0.00	0.00

Ns	0.00	0.00	0.00	0.00	0.00	0.00	0.00	0.44	0.00	1.00	0.00	0.00
Di	0.00	0.00	8.78	9.67	3.08	4.89	0.00	0.03	0.00	0.02	6.78	0.00
Ed	0.00	0.00	7.03	8.83	3.61	4.68	0.00	0.81	0.00	0.70	6.71	0.00
Sl	0.00	0.00	15.81	18.50	6.69	9.57	0.00	0.84	0.00	0.73	13.49	0.00
En	1.30	0.52	9.18	3.46	0.90	5.37	0.22	0.19	0.12	0.16	9.14	3.84
Fs	2.37	2.77	8.43	3.63	1.21	5.90	4.27	5.69	1.84	5.48	10.38	7.46
Hy	3.67	3.30	17.60	7.09	2.11	11.28	4.49	5.87	1.96	5.64	19.52	11.29
FO	0.00	0.00	0.00	0.00	4.50	1.29	0.00	0.00	0.00	0.00	0.00	0.00
Fa	0.00	0.00	0.00	0.00	6.67	1.57	0.00	0.00	0.00	0.00	0.00	0.00
Ol	0.00	0.00	0.00	0.00	11.16	2.86	0.00	0.00	0.00	0.00	0.00	0.00
Mt	0.37	0.40	2.05	1.52	2.26	2.02	0.57	0.00	0.27	0.00	2.48	1.08
Il	0.68	0.57	4.98	4.60	7.35	6.74	0.44	0.47	0.44	0.46	6.84	1.67
Ap	0.11	0.04	0.74	0.83	1.40	1.22	0.03	0.07	0.03	0.03	0.92	0.32

SAL	84.03	89.57	56.17	51.02	63.74	61.78	88.78	88.40	96.32	88.98	46.53	74.20
FEM	4.82	4.31	41.18	32.54	30.97	33.69	5.53	9.20	2.70	9.29	43.24	14.37



Le Bas et al. (1986)

Fig 4.16: Plots of chemical test result on Total alkali-versus-silica" (or TAS) diagram (after Le Bas et al, 1986)

The laboratories results are plotted on the TAS diagram and the results show that:

- Two samples (S6, and S7) which belong to the Tarmaber basalts (shield basalts) and the SB-5 (basaltic agglomerate) are alkaline basalts. The alkaline Tarmaber basalts are also with more Titanium oxides than that of Alaje basalts.
- Three other samples such as, S3 (aphanitic basalt) belongs to Alaje formation (sub alkaline basalt) while SB-2 (medium grained basalt) and S4 (vesicular and amygdaloidal basalt) are with alkaline affinity and magnesium rich ones (Fig 4.13)
- The rhyolite ignimbrite samples such as SI-1 (near Mezezo town): SI-4 and SI-8 (from Ainemariam locality), SI-10 (from Yiza bamariam locality, S-1 (from Kola Nibamba locality) are taken from the failed slope and the results are shown in Fig 4.16. Except S1, which is low in alkaline, all others are more or less similar rhyolites
- Sample taken from the altered Alaje basic tuff has a very high loss on ignition (>21 L.O.I) showing that it is completely altered (Fig 4.13). For this reason it was not possible to identify and plot on the TAS diagram. However, high alteration indicates its susceptibility to the slope failure

Basaltic samples S4, SB-2 and SB-5 and ignimbrite/welded tuff samples such as S1, S2 and SI-1 have also high loss on ignition showing their degree of weathring. This in turn implies these are relatively susceptible to landslide

4.4.3.2 Physical and geotechnical properties of rocks

Some physical (density, water absorption) and unconfined compressive strength tests are carried out on some of the rocks. The unconfined compressive strength is estimated both from the point load and the Schmidt hammer test. The physical tests and point load tests are carried out at the laboratory of the department of earth science of Cagliari University.

Unconfined strength (point load & Schmidt hammer tests)

Rock strength is one of the parameters used in the litho-technical characterization of rock masses. In this work, Schmidt hammer and point load test were used to estimate the uniaxial compressive strength of rocks of the study area. These methods are economical and useful to reasonably estimate the rock strength. These tests give reasonably accurate results besides to their economic and fast behavior. Numerous studies have demonstrated and have reached a widespread agreement that, these tests provide comparable results with those obtained from a much more complicated and expensive uniaxial compression test if we used them

carefully and strictly. The Schmidt hammer gives a measure of the bounce of the hammer against the rock wall and this measure is converted into the corresponding value of uniaxial compression using the graph shown in Fig 4.17.

During the fieldwork more than 372 Schmidt hammer readings are taken in various rock units in 31 locations, 12 reading at each point and the values are averaged out. Densities of rocks are also determined in the laboratory as it is one of the factors used to convert the Schmidt hammer rebound values into the corresponding values of uniaxial compressive strength. Finally, the unconfined compressive strength of the rocks is calculated (Table 4.5) considering the average rebound number, position of hammering, and the density of rocks. The Schmidt hammer measurements are taken only in the rocks whose degree of weathering varies from grade-I (fresh rock) to grade -III. Rock units weathered to grade IV and above do give nearly zero-value of rebound reading and are considered as engineering soil.

Table 4.5: Calculated UCS of rocks from Schmidt hammer rebound

S. No	Rock	No. of readings/station	UCS (Mpa)		
			minimum	Maximum	Average
1	Rhyolitic ignimbrite	105	40	94	64
2	Ignimbrite/welded tuff	75	18	72	33
3	Tarmaber basalt	90	106	210	145
4	Alaje basalt	195	22	100	50

The highest average value of the UCS as measured from the Schmidt hammer reading is recorded by the Tarmaber basalt while the least value by the welded tuff.

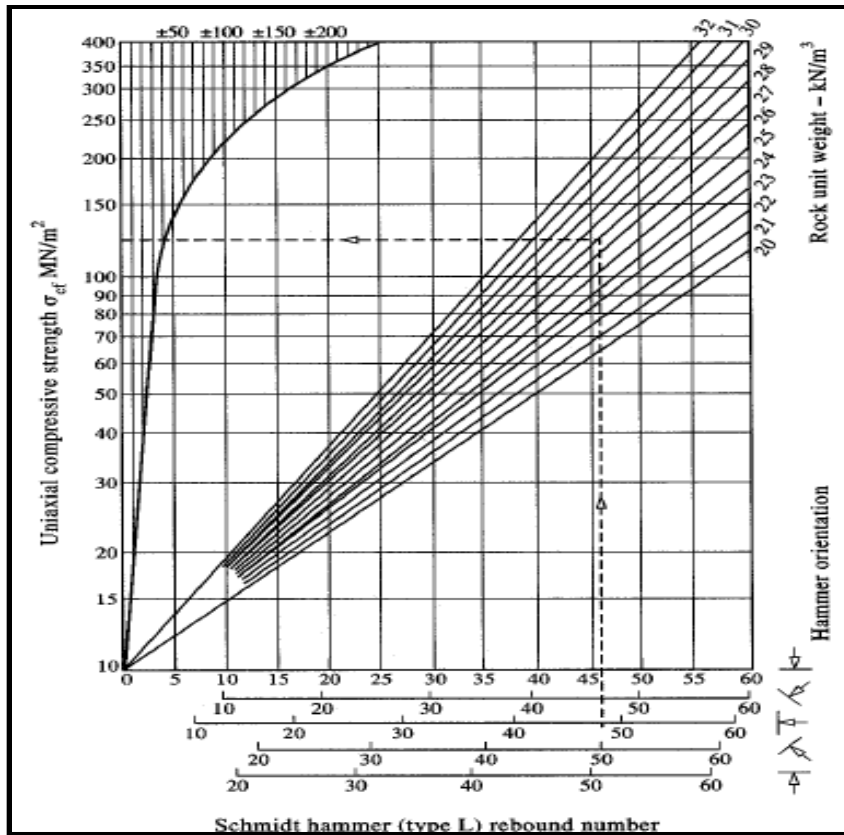


Fig 4.17: Graph used to convert the Schmidt hammer rebound number to UCS

Some rock samples are also collected and tested using the Point load strength test to determine and compare the unconfined strength with that of the Schmidt hammer. The point load strength test is an index test for strength classification of rocks and is often used as an indicator of the unconfined compressive strength (Hudson and Harrison, 2007). The point load strength testing is done following the procedures outlined in ISRM (1985). It can be conducted on rock cores (diametrical and axial test type), on regular shaped block (block test) and on irregular shaped block (irregular lump test). In this work irregular rock samples are collected for the test and calculations (Table 4.6) are carried out by applying the size correction and equivalent core diameter based on the recommendation of ISRM (1985). The point load test shows that no strong mechanical anisotropy is seen in the volcanic rocks indicating there is no much orientation of grains present in all the rock samples.

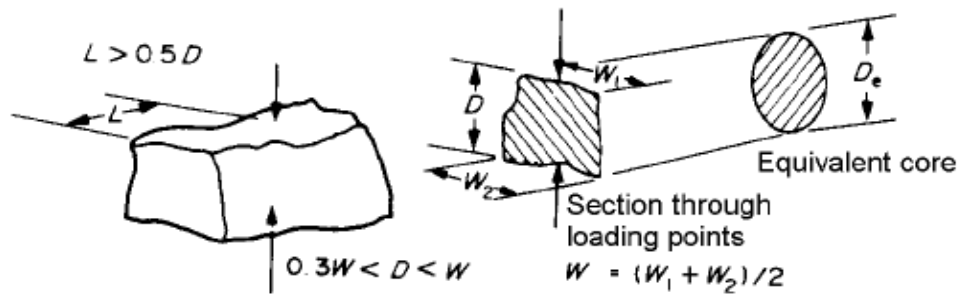


Fig 4.18: Specimen shape requirements for irregular lump test type (after ISRM, 1985)

Table 4.6: Example showing how the unconfined strength (UCS) is calculated from point load test for the Tarmaber basalt

S. code	W mm	D mm	P KN	$\frac{De^2}{\pi} = \frac{4Dw}{\pi}$ mm ²	$De = \sqrt{\frac{4Dw}{\pi}}$ mm	$I_s = \frac{p}{De^2}$ KN/mm ²	$F = \left(\frac{De}{50}\right)^{0.45}$ mm	$I_{s50} = \frac{I_s}{F}$ Mpa	UCS Mpa
SB-3	55	41	9.5	2872.6	53.6	0.003	1.03	3.4	81.9
SB-3a	55	20	9.5	1401.3	37.4	0.007	0.88	6.0	142.8
SB-3b	61.5	28	10	2193.6	46.8	0.005	0.97	4.4	106.2
SB-4	42	30	7	1605.1	40.1	0.004	0.91	3.9	94.7
SB-4a	39	24	6.5	1192.4	34.5	0.005	0.85	4.6	110.8

(W = average width of sample; D = thickness of sample; P = applied load; De = equivalent diameter of sample; Is = point load strength; F = size correction factor; Is (50) = point load strength index)

Table 4.7: Summary of unconfined compressive strength from point load

S. No	Rock	No. of samples	UCS (Mpa)		
			minimum	maximum	average
1	Rhyolite/ ignimbrite	7	40	191	103
2	Ignimbrite/welded tuff	7	25	174	76
3	T. basalt	5	82	143	107
4	A. basal	2	34	48	41

Similar to the Schmidt hammer, comparing the average compressive strength, obtained from the point load index, the Tarmaber basalt has the highest average values (107Mpa) and Alaje basalt the lowest (Table 4.7).

In both the Schmidt hammer and point load, the highest average value is recoded by the Tarmaber basalt and also the lowest average values recoded in the basalt and welded tuff although there is reversing of orders in

both methods. In the field, slope failure is common in both welded tuff and altered Alaje basalt next to the colluvium-eluvium.

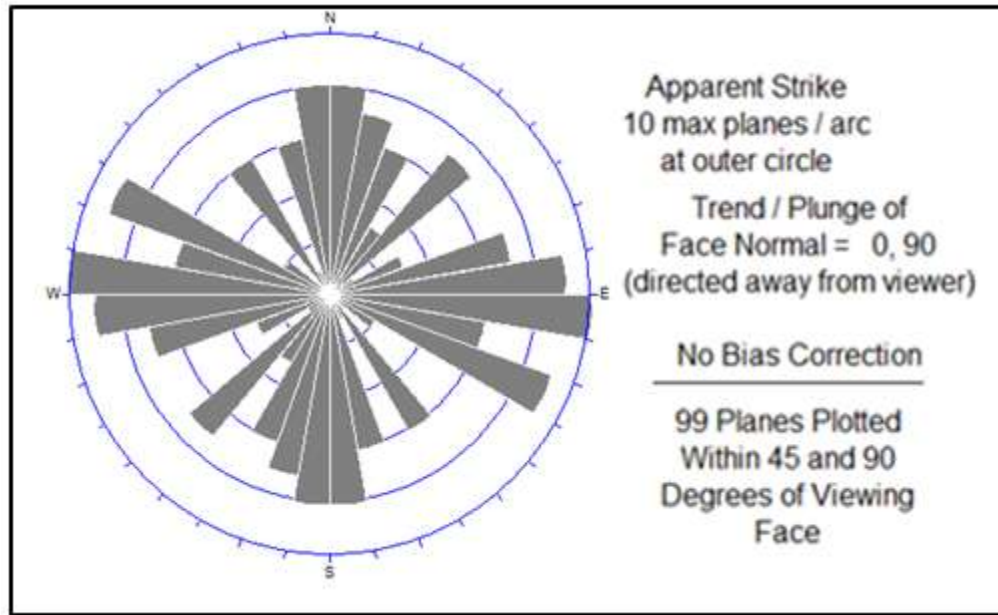
Hydraulic properties of rocks

The hydraulic characteristics of rock masses is usually governed by the hydraulic properties of fractures as the flow through the intact rock matrix is so low that significant fluid movement can only take place through the fractures. Several studies (e.g. Kirlyay, 1969; Snow, 1968; Louis, 1974) have suggested a methodology to estimate the hydraulic conductivity of the fractured rocks using mathematical formulae in which the terms in these formulas can be collected by a detailed field mapping survey of the discontinuities as stated in A. El-Naqa (2000).

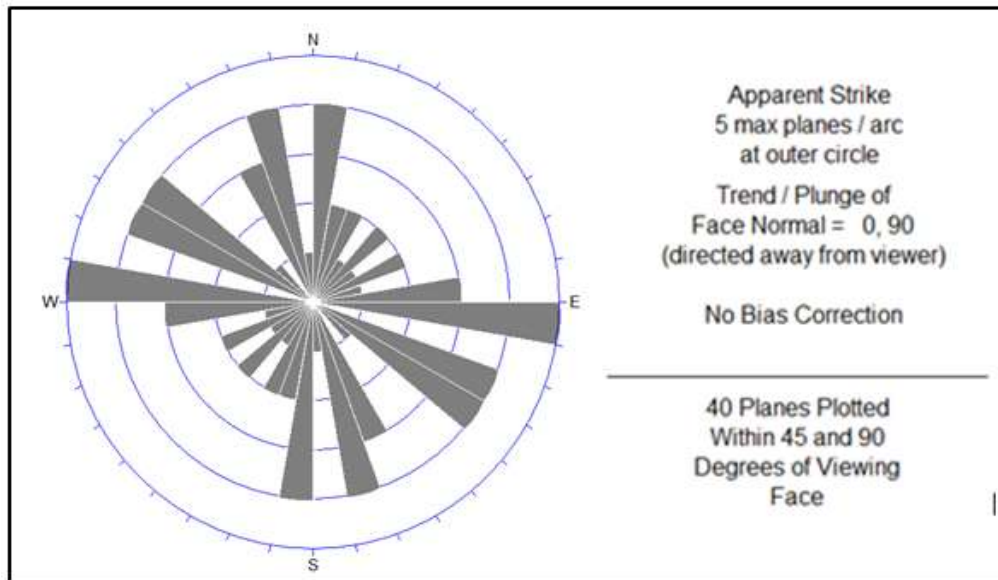
Therefore, to characterize the hydraulic conductivity of such a rock mass the fracture characteristics should be investigated and defined. To estimate the hydraulic conductivity of the fractured rock masses of the study area, the characteristics of the discontinuities such as orientation, spacing, opening and the likes are collected during the litho-technical mapping of the area together with other joint characteristics.

About 173 discontinuity measurements (dip angle, dip direction, spacing, and opening) in 21 stations are carried out. The characteristics of the discontinuities are summarized below. To realize the general trends of the discontinuities, some of the collected data are plotted on rose diagram (Fig 4.19, a & b). In this case, the rose diagram for some of the measured discontinuities in the area is prepared using the dip angle and dip direction. The rose diagram depicts that the number of joints direction wise and frequency in a group-interval is represented along the radial axis, the length of petals becoming a measure of relative dominance of the trend. The directions are grouped into 10° interval (Fig 4.19). The strike petals possess a mirror image about the center of the rosette.

The estimation of hydraulic conductivity of rock mass in different directions can lead to different results due to different fracture parameters such as spacing and aperture values (A.El-Naqa.2000). The methodology of Snow (1969) and Louis (1974), as stated in A. El-Naqa (2000) was used which is based on: (a) selection of typical outcropping rocks, (b) recording of geometrical characteristics of discontinuities, and (c) calculation of the hydraulic conductivity of a single joint and of the rock mass as a whole. The discontinuity parameter measurements involving orientation, number of joints sets, spacing, aperture, roughness, fill material, and hydraulic conditions were prepared following the norms given by guideline of Italian geological services (Amanti, et al, 1992) and also the International Society of Rock Mechanics (ISRM, 1978).



(a)



(b)

Fig 4.19: Rose diagram of strike trends of discontinuities showing their relative prevalence for (a) Alaje basalts and (b) Tarmaber basalts

Two to four sets of systematic joints are recognized in the rock masses of the Alaje and Tarmaber formations besides to the non-directional fractures. The systematic sets of joints are mostly dipping vertical to sub vertical. The dominant trends of the joint sets are N-S dominantly dipping toward East but some towards west; E-W dipping to both either North or south wards; NE-SW dominantly dipping towards SE and NW-SE dominantly dipping towards NE. Sample geometrical characteristics and discontinuity measurements are

carried out for the Alaje formation and are provided in Table 4.8, from which the hydraulic conductivity of the rock masses of the study area is estimated using the equations 1.2 to 1.6 provided in chapters-1(section 1.2.2).

Table4.8: Discontinuity characteristics and estimation of hydraulic conductivity of rock masses in Alaje formation

Parameter	Discontinuity sets			
	J1	J2	J3	J4
Orientation	N-S (trending)	E-W	NE-SW	NW-SE
Spacing(m)	0.03 to 2.2m (Ave. = 0.31m)	0.05 to 1.6 and (Av. =0.54)	0.02 to 1.9 & A = 0.23	0.08 to 0.70, & 0.29
Opening (m)	0.0015-0.002	0.001-0.005	<0.001	0.001-0.003
K(m/sec)	0.00577	0.05170	0.000971	0.020795

Summarized results in Table 4.8 shows the estimated hydraulic conductivity of the rock masses in the Alaje formation varies from 9.71×10^{-4} m/sec to 5.17×10^{-2} m/sec with an average value of 1.98×10^{-2} m/sec. Similarly the hydraulic conductivity of the fractured T. basalt in the area is estimated using the same calculation and the result varies from 8.5×10^{-4} m/sec to 1.40×10^{-2} m/sec.

4.4.2 Physical and geotechnical properties of soils

To evaluate the physical and geotechnical properties of soils, laboratory tests such as grain-size distribution analysis, Atterberg tests and direct shear tests were performed on soil samples collected from landslide-affected areas

Atterberg limits and particle size distribution of soils

The Atterberg limits of a fine grained (clayey or silty) soil represents the water content at which the property of the soil changes. The Atterberg limits (liquid limit, plastic limits and plastic index) are referred to as index tests because they serve as an indication of many physical properties of the soil, including compressibility, strength, permeability, and shrink or swell potential. They also provide a relative indication of the plasticity of the soil (i.e. the ability of a silt or clay to retain water without changing state from a semi-solid to a viscous liquid). These index tests were conducted in the geotechnical laboratory of Tigray water resources Bureau (Ethiopia) and geotechnical laboratory of Cagliari province (Italy). After the liquid (LL) and plastic (PL) limits, and Plastic index (PI) are determined, results are typically presented and summarized in Table 4.9. These results indicate that these soils have: (I) liquid limit that ranges from non-plastic (NP) to 72%, (II) plastic limit that varies from non-plastic (NP) to 45%, and (III) plasticity index that ranges from non-plastic to

33%. Similarly, grain size analysis of the soils is done at the geotechnical laboratory of Tigray water resources Bureau (Ethiopia). Results are summarized in Table 4.9.

Based on grain size analysis and Atterberg limits, soils are classified as using United Soil Classification System (USCS) and the dominant soil type includes SC, SM, CL (CI), and MH with some CH type of soil.

Table4.9: Grain-size characteristics, Atterberg limits and classification of soils of Debresina area

S.N	Sample code	%gravel	%sand	%silt	%clay	LL	PL	PI	USC
1	S-1	-	58.2	39.4	2.4	NP	NP	NP	SM
2	S-2	-	26.7	40.3	33	40	25	15	CL
3	S-3	-	24.8	54.6	20.5	31	14	17	CL
4	S-4	-	40	35.6	24.4	37	17	20	CI
5	S-5	-	8.3	40.2	51.4	54	30	24	MH
6	S6	-	19.8	60.9	19.2	45	26	19	CI
7	S7	-	10	50.3	39.7	53	31	22	MH
8	S8	-	59.5	33.2	7.3	43	32	11	SM
9	S9	-	8	70.8	21.2	41	25	16	CI
10	Sc-2	-	-	-	-	60	27	33	CH
11	Sc-3	-	-	-	-	51	25	26	CH
12	Sc-4	-	-	-	-	NP	Np	NP	SM
13	Sc-5	-	-	-	-	45	23	22	CI
14	Sc-6	-	-	-	-	54	33	21	MH
15	Ayne-1	4.3	63	18	15	52	29	23	SC
16	Meh-1	3.4	53	15	29	62	32	30	SC
17	Red-5	-	7	69	24	49	33	16	ML
18	Grey-6	-	5	64	31	NP	NP	NP	SM
19	Sinab.	-	-	-	-	52	38	14	MH
20	Indo.w	-	-	-	-	72	45	27	MH
21	W.beret	-	-	-	-	57	35	22	MH

(LL= Liquid Limit; PL= Plastic Limit; USC = Unified Soil Classification; SM = silty sand; CL/CI= lean clay; MH= elastic silt; SC = clayey sand; NP = non plastic)

Shear strength parameters of soil

The Shear strength of soil is also assessed using the direct shear test (ASTM-D3080) test of 25 soil samples to calculate the safety factor of the area from a reconstructed sample (Table 4.10). Analysis results show that the cohesion, c , value of the soils of the study area varies from 0.02 to 107 KPa and the angle of internal friction, ϕ , varies from 23 to 42 degrees. The test is conducted at 1kg, 2kg and 3kg vertical forces, for each soil samples, and the value of shear stress at failure is plotted against the normal stress for each test. The shear strength parameters are then obtained from the best line fitting of the plotted points.

Table 4.10: Shear strength parameters of soils (from direct shear test) of Debresina area, Ethiopia

	Code	c (KPa)	ϕ (deg)	γ (KN/m ³)	w%
1	S-1	4.71	37.68	-	-
2	S-2	4.71	26.23	-	-
3	S-3	4.71	29.23	-	-
4	S-4	18.34	37.72	-	-
5	S-5	9.02	42.5	-	-
6	S-6	32.04	26.2	-	-
7	S-7	17.85	37.82	-	-
8	S-8	45.99	32.32	-	-
9	S-9	19.81	35.32	-	-
10	Ayne-1	97.66	28.39	18.82	28.84
11	Meh-1	107.48	35.17	16.27	25.24
12	Red-5	99.4	38.66	16.67	37.17
13	Grey-6	88.75	31.17	16.75	30.58
14	S10	15.89	23	17.45	36
15	S11	31.97	34	18.04	31
16	S12	14.32		17.26	28
17	S13	31.38	32	18.24	35
18	S14	34.81	32	17.84	33
19	S15	22.56	32	15.29	30
20	S16	44.72	35	15.88	35
21	S17	0.02	32.1	-	-
22	S18	1.68	39.3	-	-
23	S19	25.77	35.9	-	-
24	S20	6.15	34.5	-	-
25	S21	9.33	35	-	-

Permeability of soils

The hydraulic conductivity of the soils of the study area is estimated based on the soil classification. That is soils are classified using the Unified soil classification (USCS) and the corresponding permeability values are estimated from the developed standard tables (ASTM and BS standards). Results of the USC (Table 4.9) show that the soil types include MH, CL, SM, SC, and CH types of soils. Accordingly, comparison of classified soils with standard permeability values depict that SC soil has less than 10^{-6} m/sec, and that of CL, ML and MH have permeability values of less than 10^{-7} m/sec. However, for some of the soils, especially the silty sand (SM) soils, the permeability is also calculated using the Hazen's formula indicated in chapter-1 (equation 1.1). The calculated results of the Hazen's formula indicated that the permeability of the SM soil varies from 6.76×10^{-4} to 8.1×10^{-5} m/sec and the CL soil has more than 4×10^{-6} m/sec.

Clay mineralogical identification

Clay soils are one of the causative factors for some of the slope failures in Debresina area. The purpose of the test was to identify the mineral contents present in the soil qualitatively and see their influence in the slope stability problem of the study area. Of the clay mineral identification techniques such as x-ray diffraction (XRD), differential thermal analysis (DTA), electron microscope and Atterburg limits, it is advisable to use at least two of any of the methods for identification of clay mineral(s) present in a soil (Fell R., et al, 2005). In this study XRD and Atterburg limits are applied. As a result, identification was conducted for five soil samples (Sc-1, Sc-3, Sc-7, Sc-8, and Sc-9) at Rock and Mineral Testing Laboratory of the department of geo-engineering (DIGITA) in Cagliari University using an X-ray diffraction method. According to these tests minerals like Halloysite/kaoline, Plagioclase, K-feldspar, quartz, smectite? Or vermiculite or chlorites are identified by the XRD methods (Table 4.11). The soil samples are taken from soils derived from weathered volcanic ash, tuff (non-crystalline parent material) and the infilling clay materials of joints and fault zones.

Table 4.11: Identified minerals using XRD method

Sample code	Identified minerals	Sampling area
SC-1	Halloysite/Kaolinite, quartz and Smectite (?) or vermiculites?	From Kobastil (Mezezo)
SC-3	K-feldspar, plagioclase, quartz,	From Nib Amba
SC-7	Kaolinite, Dickite, K-feldspar, plagioclase and Smectite (?) or vermiculites? Or chlorites	From Yizaba, brown color
SC-8	Kaolinite, plagioclase, and quartz	From Yizaba, black color
SC-9	Smectite (?) or vermiculites? Chlorite, quartz	From Armania, black color

The mineral groups such as smectite or vermiculite or chlorite have more or less similar XRD property and was not possible to identify between these minerals unless supported by Glycolation and heating.

Apart from the XRD, clay minerals can be identified from the Atterberg limits. As shown in (Fig 4.20) the position of the soil on the Casagrande plasticity chart can give an indication of which clay minerals are present. It should be noted that most soils contain several clay minerals, and hence the Atterberg limits may not fall exactly in the shaded zones. Atterburg limits of soils of the study area are analyzed and the results are plotted on the Casagrande plasticity chart, with PI in the vertical and LL in the horizontal axis.

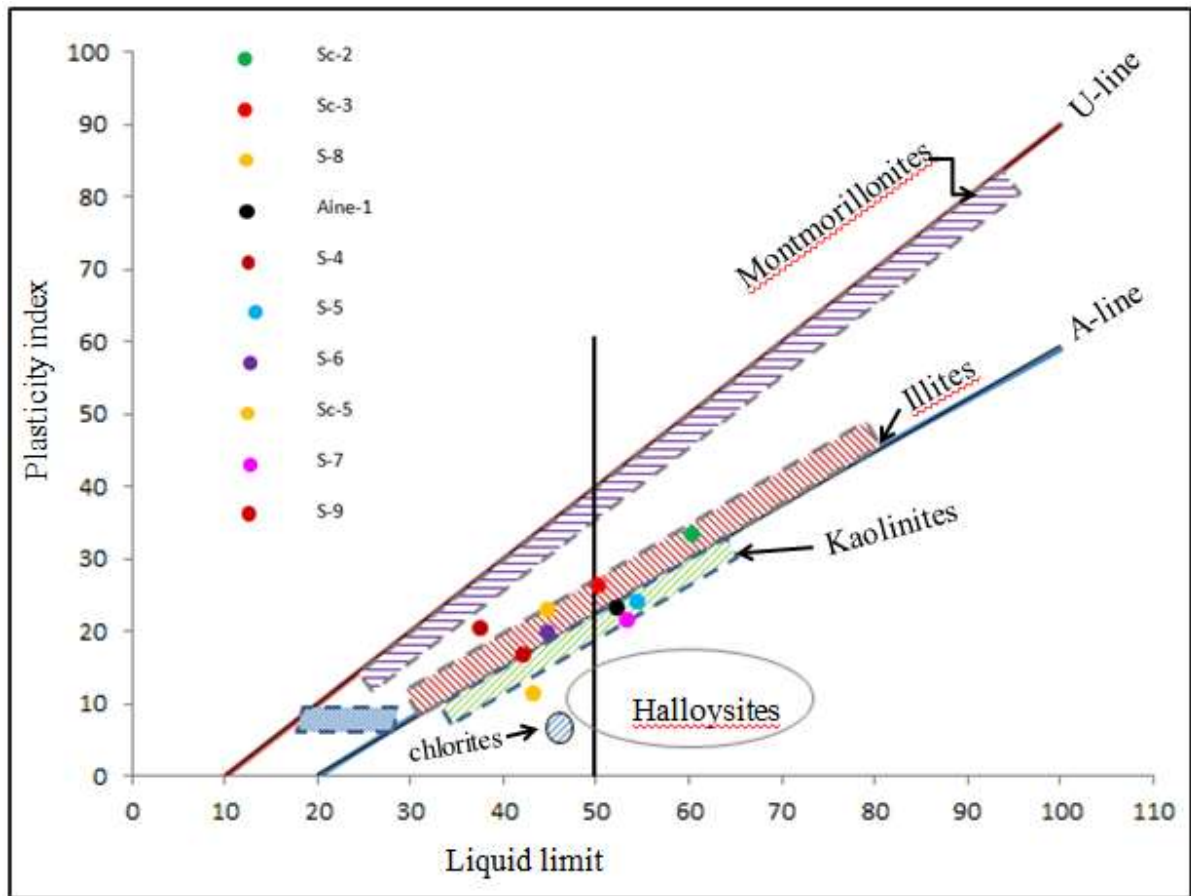


Fig 4.20: Clay minerals identification of the study area based on Casagrande plasticity chart (based on Holtz and Kovacs, 1981).

As indicated in Fig 4.20, five of the samples fall on the illites group, 3-of them fall on the Kaolinite, 1-is between illite and montmorillonite and 1-between kaolonite and halloysite. Thus, illite groups of clay mineral followed by Kaolinite are the dominant one in the study area.

Some clays show expansive nature while some others are with dispersive in nature. The presence of either types of clay soil affects the stability in negative way. Dispersive soils are those which by the nature of their mineralogy, and the chemistry of the water in the soil, are susceptible to separation of the individual clay particles and subsequent erosion of these very small particles through even fine fissures or cracks in the soil under seepage flows.

Some silicate clay minerals do not have a crystalline structure, even though they are fine grained and display claylike engineering properties and are known as allophane and are present in most soils (Fell R., et al, 2005). Mitchell (1976) as cited in Fell R., et al, (2005) indicates they are particularly common in some soils formed from volcanic ash because of the abundance of “glass” particles. The results of the petrographic and chemical

tests of the parent rocks (ignimbrite, rhyolitic and welded tuffs) show that the major groundmass component is glass depicting the favorability for allophane soil development in the study area.

Oxides, which are common in tropical residual soils and soils derived from volcanic ash, also occur widely in soils and weathered rock as fine-grained particles which exhibit claylike properties (Fell R., et al, 2005). Examples are, gibbsite, haematite and magnetite, limonite (amorphous iron hydroxide), and Bauxite (amorphous aluminum hydroxide).

4.5 Landslide inventory and input data preparation and mapping

4.5.2 Landslide inventory mapping

The delineation of landslide occurrences is vital for the prediction of future patterns of instability directly from the past distribution of landslide occurrences. With this consideration, the landslide distribution of the study area is determined through image interpretation (Aster image of various years, Landsat images, and Google Earth) and direct field survey, and then digitized directly into inventory map using GIS9.3. The minimum, maximum and average areas of the mapped landslide in the study area is approximately 0.001182km², 14.5km² and 0.188km² respectively. Complex and composite types, debris and earth slides, rock slide, debris flow and some rock falls are common types of landslides in the area. For example, the massive landslide of September 2005 is a complex and composite types consisting of various types of movements in sequence and in different parts of the displaced mass and with a mixed rocks, earth and debris materials.

More than 160 landslides are identified, out of these 90 are debris/earth slide, 39 are rock slide, 18 are earth slide, 12 are complex/composite slide and 1 is debris flow. However, considering the landslide areal coverage, 58.2 % is covered by complex/composite slide; 19.3% by debris/earth slide; 13.3% by debris flow; 7.2% by rock slide and 2% by earth slide. The inventory map is an input map used in the Frequency ratio method for analysis and verification of the susceptibility of the landslide occurrences prediction in the study areas.

These slope failures were related to geological, topographical, and climatic conditions. Thus, they can often facilitate the prediction of locations and conditions of future landslides. For this reason, it is important to determine the location and area of the landslide accurately when preparing the landslide susceptibility maps.

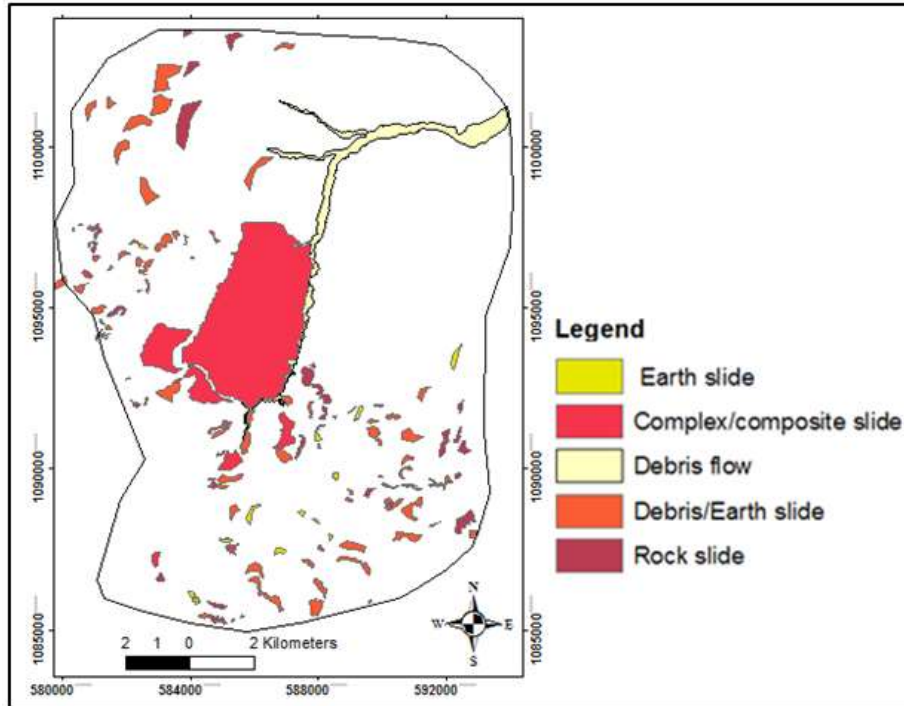


Fig 4.21: Landslide inventory map of Debresina area, Ethiopia

4.5.3 Input map preparation

Based on the site conditions and existing experiences of various landslide studies, seven relevant causative factors are selected as inputs for the models of landslide susceptibility mapping and to determine the degree of influence for each causative factor and their sub-classes i.e. lithology, distance from faults, land use, slope gradient, slope aspects, distance from streams, and elevation.

4.5.3.1 Slope

Considering only the slope factor, steeper slopes have a greater chance of land sliding in general but landslides are also common in the gentler slopes depending on the other environmental factors. Slope angle is very regularly used in landslide susceptibility studies since land sliding is directly related to slope angle (e.g. Dai et al, 2001; Lee, 2005; Woldearegay, 2005; Yalcin, 2008; Long, et al, 2010). The slope map of Debresina area is derived from the 30m DEM using the slope function of the spatial analyst of ArcGIS 9.3. The slope map is in the form of a raster having the same pixel size as the DEM. A map of slope classes is generated by grouping the slope angles into six different classes (Fig 4.22): (1) slope class with $<5^{\circ}$, (2) slope class with $5-10^{\circ}$ (3) slope class with $10-25^{\circ}$ (4) slope class with $25-40^{\circ}$ (5) slope class with $40-55^{\circ}$ and (6) slope class with $>55^{\circ}$.

Locally there are vertical to sub vertical fault cliffs of basaltic, trachytic/rhyolitic ignimbrite in each slope classes which are common areas for the occurrences of the landslides but these cannot be represented at the current resolution of the map.

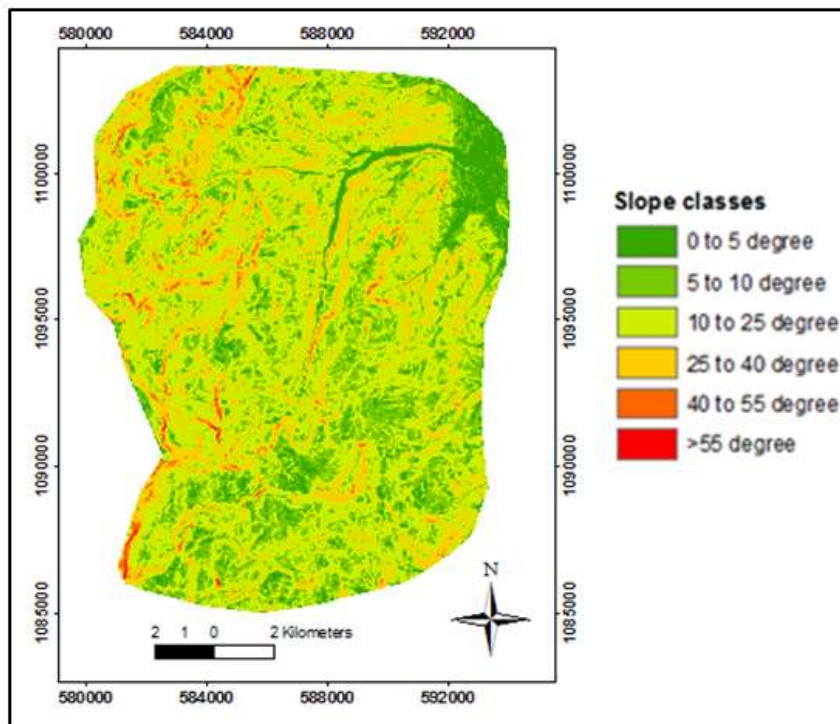


Fig 4. 22: Slope gradient map of the study area

Fig 4.23 below reveals that slope classes 5-10° and 0-5° and 25-40° are the dominant ones in terms of areal coverage. Most landslide occurrences are found in the slope ranges of 5 to 40 degrees.



Fig 4.23: Percentage of areal coverage by the different slope classes

4.5.3.2 Aspect

Aspect is considered as a landslide controlling factor by several other studies (e.g. Van Westen and Bonilla 1990; Saha et al. 2005; Yalcin, 2005).

Aspect in general refers to the orientation to which a mountain slope faces. The aspect of a slope can make very significant influences on its local climatic factors such as amount of rainfall which in turn influences the occurrences of landslides. Aspect related parameters such as exposure to sunlight, drying winds, rainfall (degree of saturation), and discontinuities may control the occurrence of landslides (Dai & Lee, 2002).

Hence, the slope aspect of the study area is derived from the 30m DEM. The derived aspect map was further reclassified into 8 distinctive classes (Fig 4.24). Most of the landslides are concentrated in the east and south east part of the slope aspect. More than 57 % of the total area is covered by the aspects of south east (SE), east (E) and south(S) (Fig 4.25).

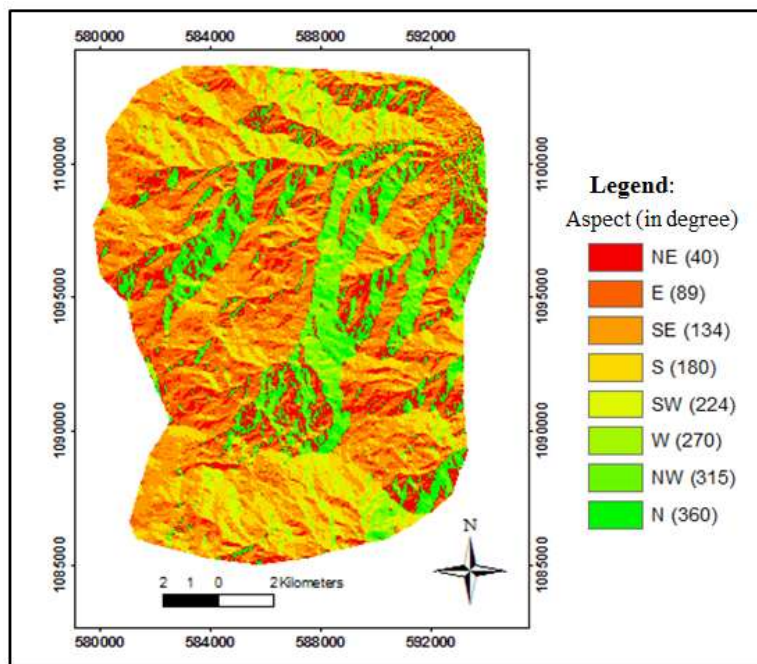


Fig 4.24: Aspect map of the study area

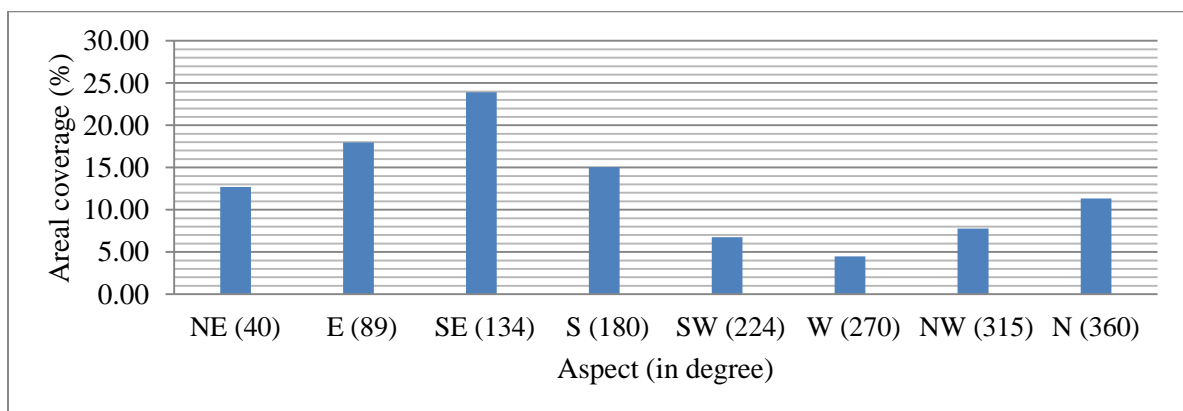


Fig 4.25: Percentage of areal coverage by the different classes of Aspects

4.5.3.3 Elevation

Elevation is useful to categorize the local relief and locate points of maximum and minimum heights within terrains. To correlate landslide occurrence for different relief classes, the elevation map has been prepared from the 30m DEM map using the spatial analyst of ArcGIS 9.3 and categorized into 5-class ranges (Fig4.26). Elevation influences to landslide are often displayed as indirect relationships or by means of other factors (Long, 2008). For example in the study area, lithological variations and degree of weathering that plays an important role in land sliding, is closely related with elevation.

The minimum elevation is 1368m, while the maximum is 3200m. Elevation classes in the range of 1500-2000 and 2000-2500m covers 44.5% and 32.5 % of the total area respectively, while elevation greater than 3000m has smallest areal coverage (Fig 4.27). About 86% of the landslides are initiated at elevation between 1500 to 2500m. This could be due to the lithological differences that the major part of the area below 2500m elevation is covered by the Alaje formation which consists of various tuffs, ignimbrite and weathered basalts liable to landslide.

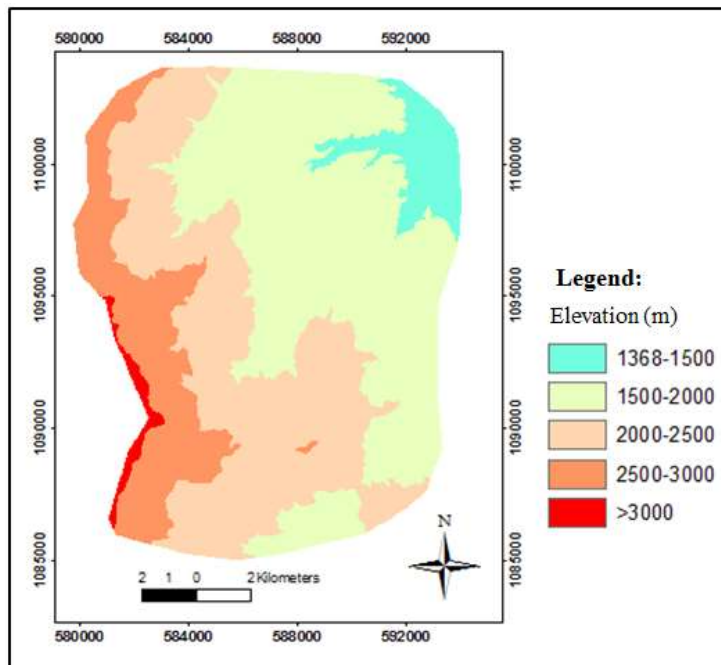


Fig 4.26: Elevation map showing the various classes of Debresina area

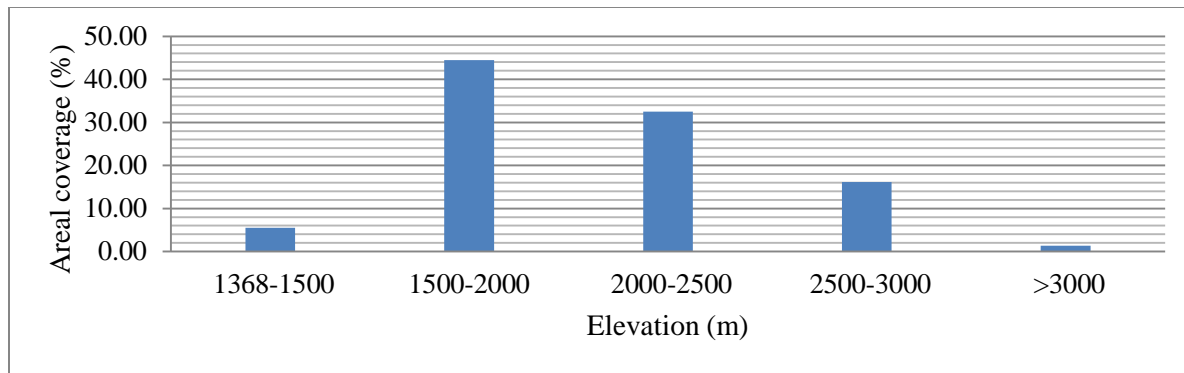


Fig 4.27: Percentage of areal coverage by the different classes of elevation

4.5.3.4 Proximity to fault factors

Fault map of the study area was prepared and compiled from various data sources (Aster and Landsat images) and previous works. The images have been interpreted using ENVI4.5 by applying different enhancing and band composition techniques, identifying the various features and digitizing them using ArcGIS9.3. The Afar rift margin is worldwide known for its extensional tectonic movement and characterized by normal faults. Thus, faults are very important factor for the landslide evaluation of the study area. This is due to the fact that they are not only weak zones, but also mostly characterized by: (a) deeper weathering, resulting in greater thickness of soil masses, (b) higher potential for concentrated groundwater flow, which can act as lubricant and also can produce water pressures causing landslides. With this in mind, the fault proximity maps are produced to evaluate its contribution to the landslide (Fig 4.28). About 66% of the landslide are located within a radius of less than 400m and cover 56% of the total area (Fig 4.29)

The major fault trends in the study area can be grouped into three i.e. (1) those faults that belong to the NNE-SSW directed extension marginal faults (2) those faults that belong to the NNW-SSE directed extension marginal faults and (3) those that belong to the East-west trending systems.

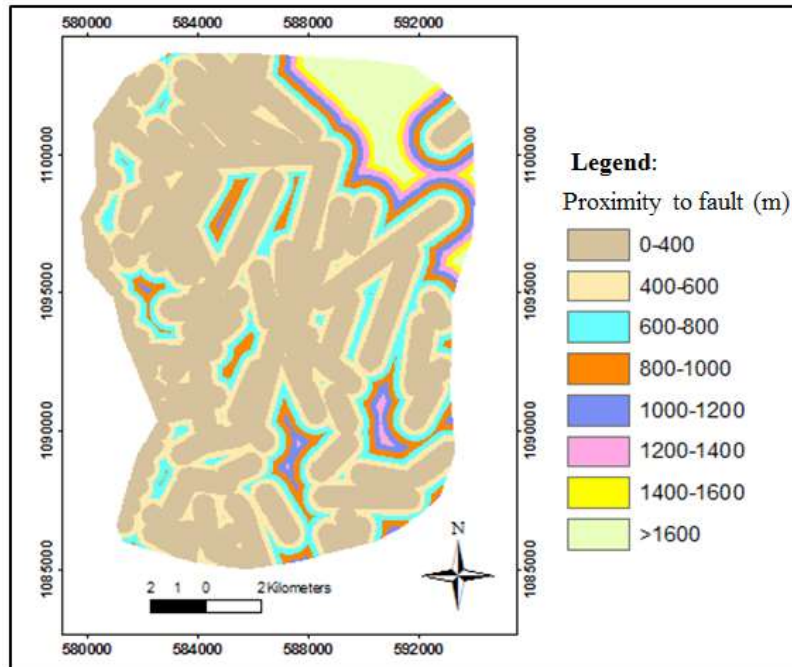


Fig 4.28: Map showing proximity to fault classes

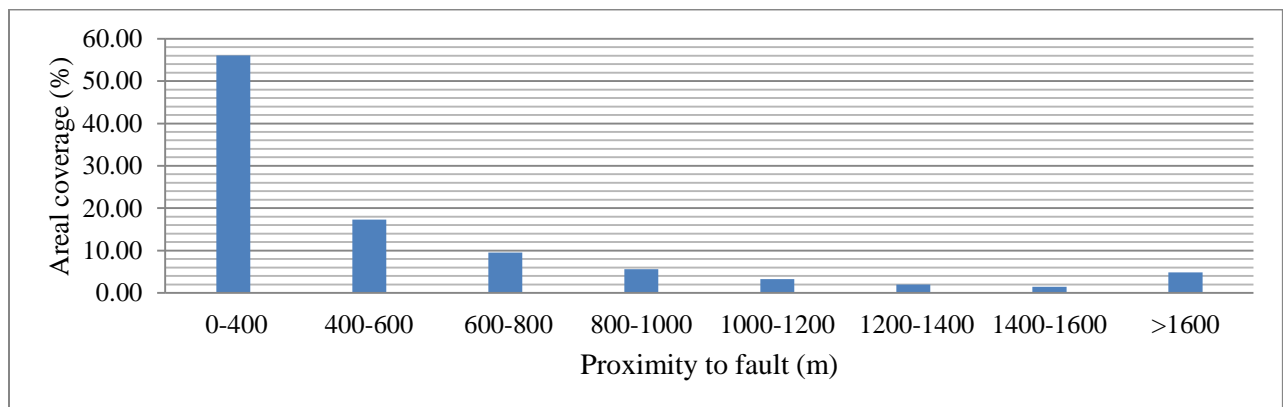


Fig 4.29: Diagram showing proximity to fault versus areal coverage.

4.5.3.5 Proximity to drainage

Streams may negatively affect stability by eroding the slopes or by saturating the lower part of the material (e.g. Dai et al., 2001) and hence distance to stream is one of the controlling factors for the stability of a slope (Yalcin, et al., 2011).

The drainage map has been prepared from the 30m DEM, using the Archydro 9.3 and digitized from the topographic map of 1:50,000 scale for comparison. Most drainage system of the area is created following the geological structures. The tectonic morphology of the study area is greatly modified by stream incisions,

which finally could influence slope stability through over steepening the lower sections of the slopes and removal of materials that provided support at the toe. For this reason the drainage proximity is considered as one causative factor in the landslide susceptibility study. The study area was divided into six different drainage proximity zones (Fig 4.30) and about 52.7% of the study area is found within 300m distance from the drainage and about 70% of the landslides occur in these areas.

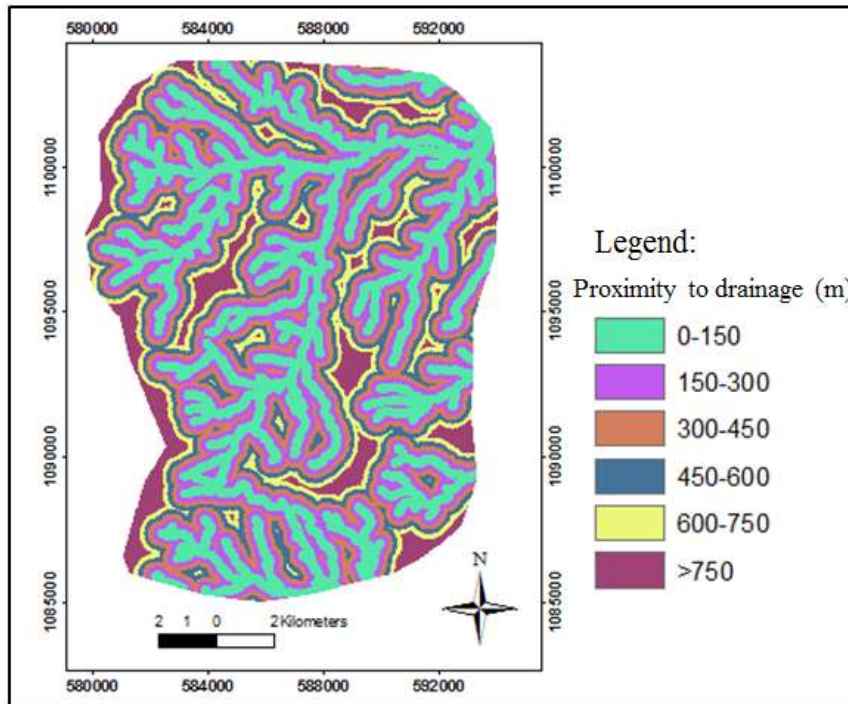


Fig 4.30: Map illustrating proximity to drainage classes for Debresina area

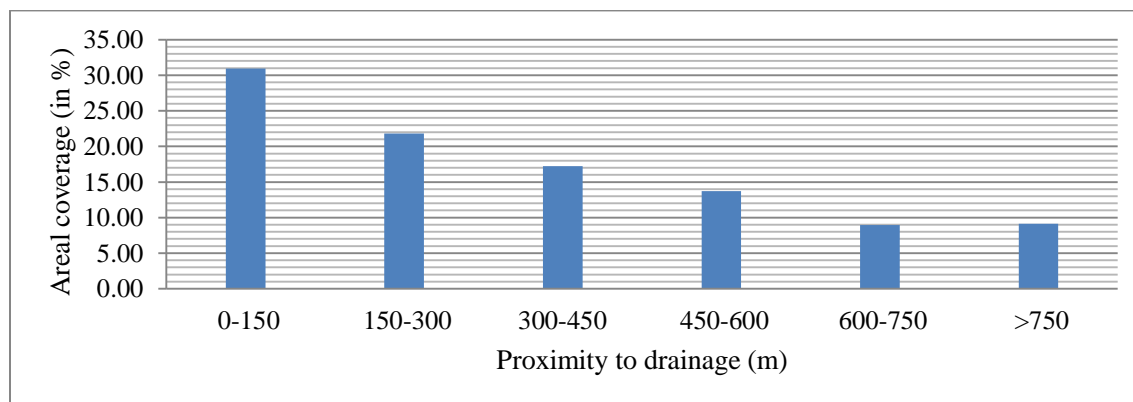


Fig 4.31: Proximity to drainage versus areal coverage

4.5.3.6 Land use

Land-use is another causative factor considered in the landslide evaluation of the area. Similarly, Aster and Landsat image, Google Earth, topographic maps of 1:50,000 and field surveys have been used in preparing the land use map (Fig 4.32). The major land use pattern in the area comprises heterogeneous agricultural areas, arable land, bushes & shrubs, bare land/sparse vegetation, forest, river bed and urban/semi-urban areas. Lower regions (up to slopes less than 30 degrees) have comparatively higher human influence. People in this region are still actively involved in agriculture, moving into steep slopes and cultivating without constructing proper terraces. This has created slope failure and soil erosion causing disasters in the study area.

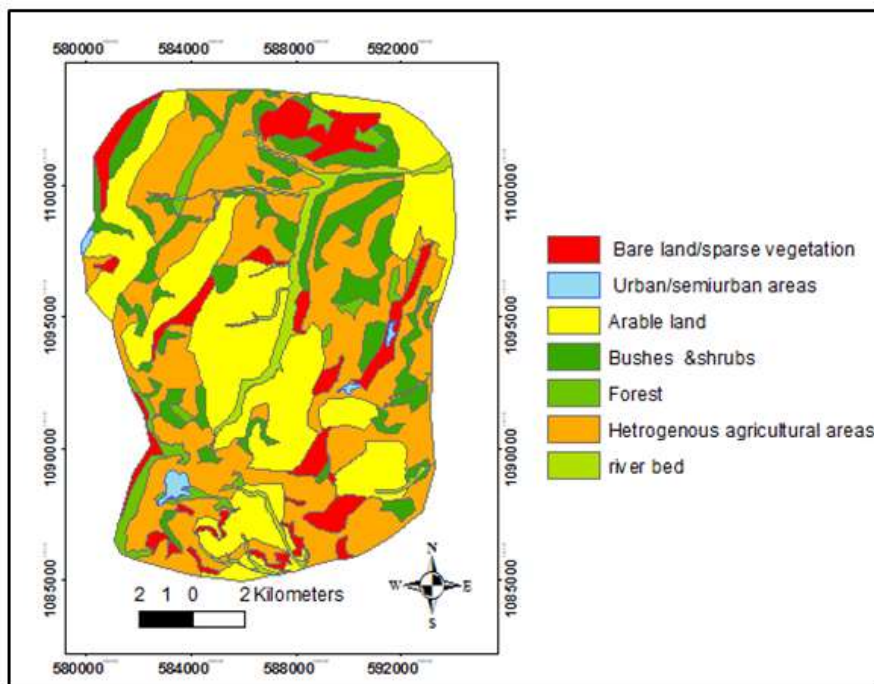


Fig 4.32: Land use map of study area

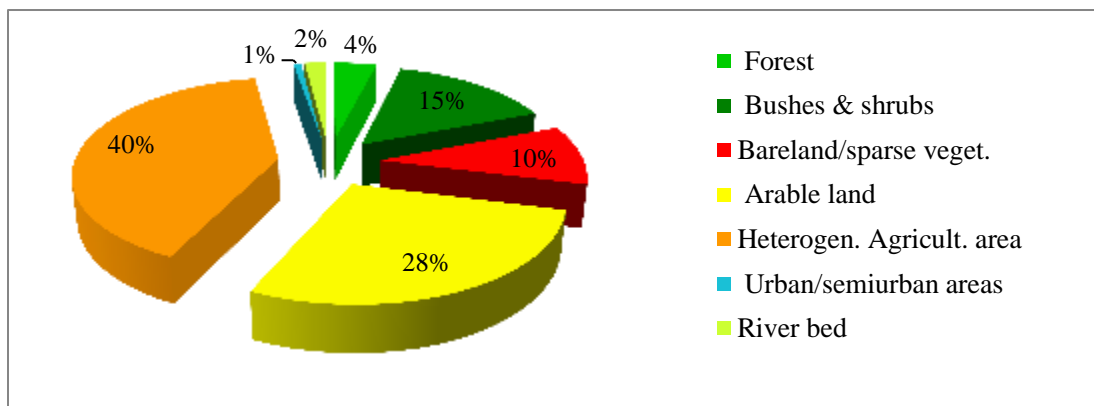


Fig 4.33: Percentage of areal coverage by the different land use classes

4.5.3.7 Lithology

Lithology is one of the most important parameters in landslide studies because different lithological units have different susceptibility degrees (Dai, et al., 2001; Yalcin and Bulut, 2007) and need detail consideration. It is strongly accepted that lithology significantly influences the occurrence of landslides, because lithological variations often lead to a difference in the strength and permeability of rocks and soils. Thus, the lithological map of the study area has been prepared from the interpretation of Aster image (Level-1B) of various years, Landsat images of 2001 and 2005, and Google Earth, supported by the existing regional geological map of Debrebirhan sheet (1:250,000 scale), comprehensive field surveys and some laboratory works as described in the previous chapters (sections 1.4 and 4.3).

Lithology basically involves the composition, texture, degree of weathering, as well as other details that influence the physico-chemical and engineering behaviors such as permeability, shear strength, etc. of the rocks and soils. These characteristics in turn affect the slope stability.

The main lithological units from bottom to top can be grouped as Alaje formation (basalts, rhyolitic/trachytic ignimbrites, tuffs, and agglomerates), Tarmaber formation (basalts), quaternary sediments (alluvial, colluvial-eluvial deposits, fine residual soils) (Fig 4.34). The Alaje formation especially the ignimbrites and the tuffs, are highly altered and weathered.

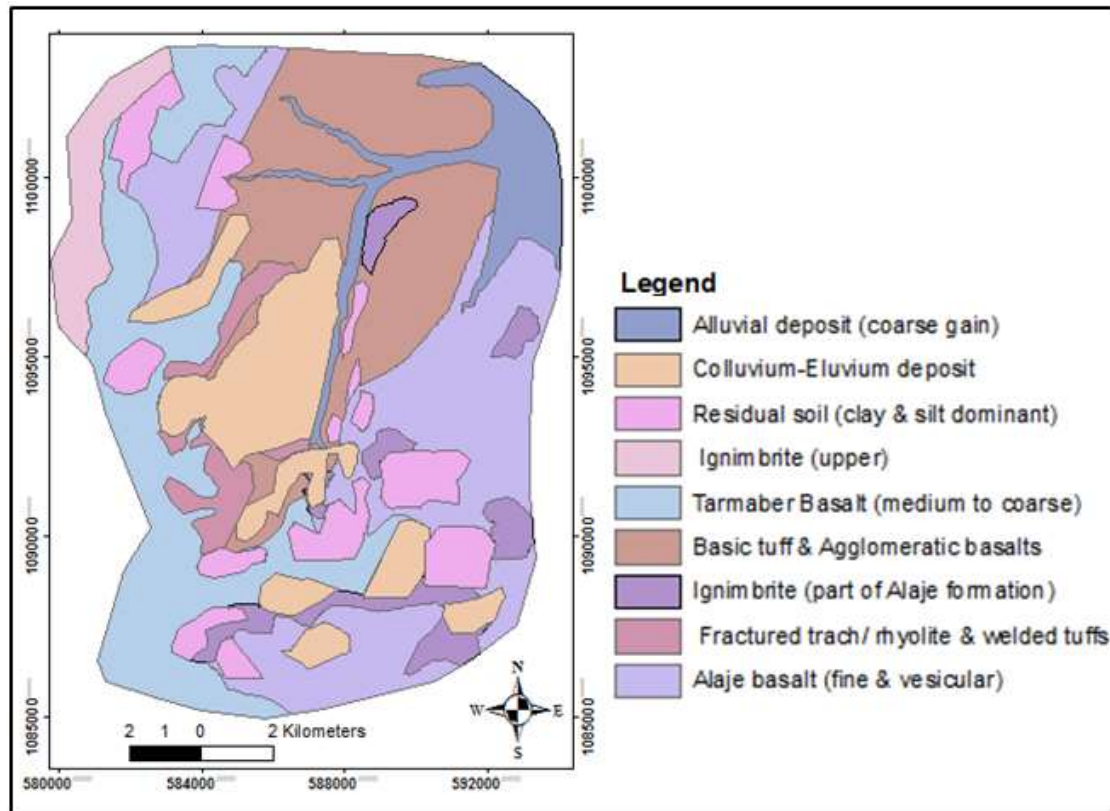


Fig 4.34: Lithological map of Debresina area

About 64 % of the area is covered by three lithologies namely Alaje basalt, basaltic agglomerate (part of Alaje formation) and Tarmaber basalt (Fig 4.35). However, about 50% of the landslide is occurring in the colluvium-eluvium sediments.

The physico-mechanical parameters, which has been explained in the previous chapters have been described and measured in 184-GPS points during the field work based on the modified format of guideline of the Italian geological services (Amantii M., et al, 1992).

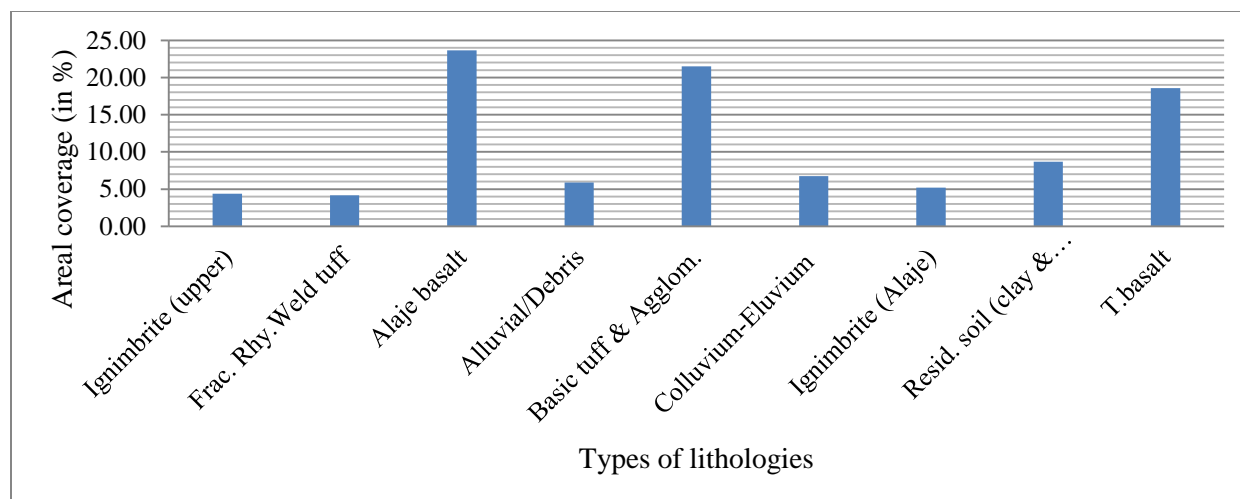


Fig 4.35: Percentage of areal coverage by the different lithologic units

5. GIS-based Landslide Susceptibility Assessment and Mapping of Debresina area

5.1. GIS-based Overlay Mapping techniques (OM)

5.1.1. Principles and background of the method

The Overlay Mapping method is a type of heuristic (indexed) approach utilized also by the regional government of Sardinia (Italy) in PAI² to study and evaluate hazards and risks, with their mitigation measures in the region. As a semi-quantitative method, it involves the knowledge of expertise and indexing method. This method considers only three main environmental factors such as Slope, Litho-technical and Land use factors in the evaluation process of the slope instability of an area. The parameters like Proximity to geological structures, (faults and lineaments), Aspect, and Altitude are not directly considered as a separate factor in the OM analysis. However, the impacts of such parameters, for example the detail characterization of the geological discontinuities, in general are considered during the Litho-technical mapping of the area of interest. In this method, the input maps, especially the Litho-technical mapping requires a detail field geo-mechanical characterization.

After detail mapping and classification of the factors into classes or sub-classes was accomplished, numeric weights were assigned to each factors/classes considering their field findings and impact to the slope instability. According to this method, the highest weight value is given to the factor that has less impact to the slope instability while the lowest weight value is assigned to the factor that has more impact to the instability. After assigning weights for each parameter is made, the various thematic maps are prepared in grid formats (raster format) to process the GIS based Overlay Mapping. The resulting weighed map represents the potential instability of the area. The various processes of data preparation of the input maps and overlay mapping are done with the help of ArcGIS 9.3 and the flow chart of the procedures and activities to be followed by this method are given in Fig 5.1.

² PAI= Piano per l'Assetto Idrogeologico

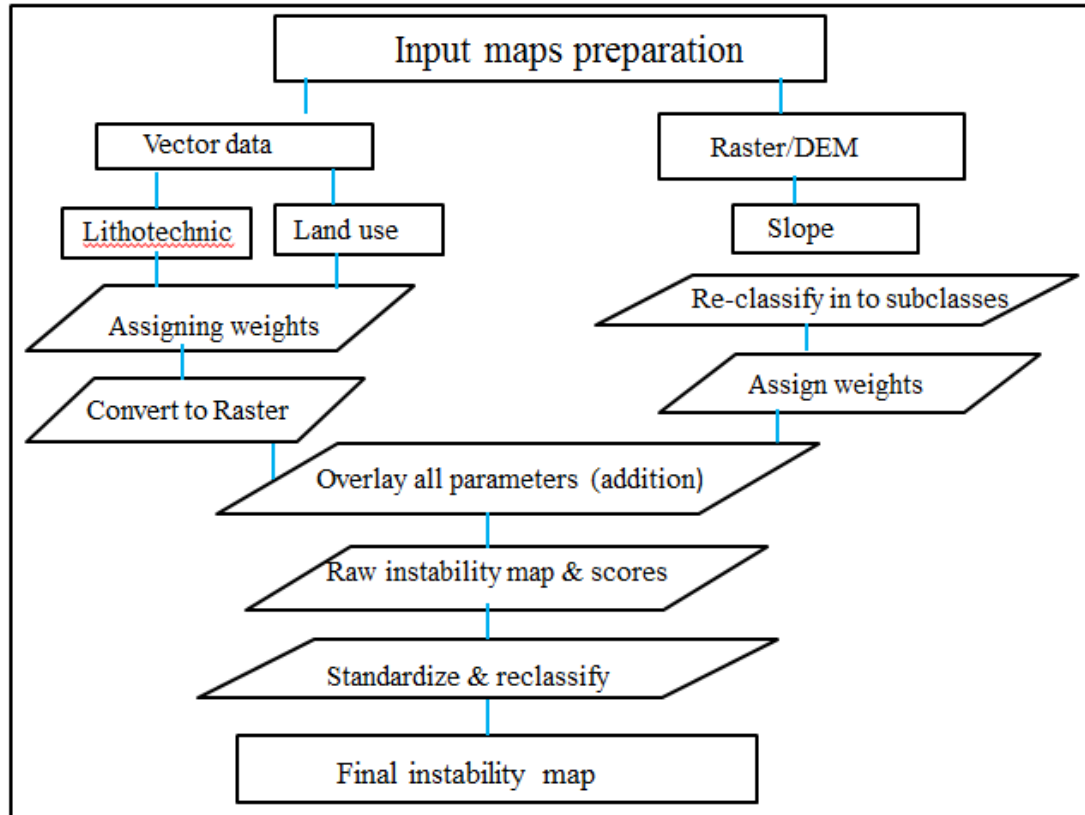


Fig 5.1: Schematic diagram of the Overlay Mapping process, raster maps are made on 30 by 30 grid cells.

During this fieldwork detail litho-technical and land use maps of the area of interest are prepared as described in chapter 4. In this part, the processes, procedures or activities related to the landslide susceptibility mapping of overlay techniques and the results will be discussed.

5.1.1.1 Weighed slope map

The Slope gradient is a very important factor in the study of landslide as explained in section 4.5.3. According to the PAI guideline of Dovera et al (2000), Slope gradients of the study area are categorised into five classes and assigned weights varying between -2 and +2 (Table 5.1). The maximum areal coverage (i.e., 32.6 %) falls in the middle slope class range of 21-35%, while the minimum coverage (11.5%) lies in the slope class range of 0-10%. About 51 % of the study area is covered by the slope range of 21-50% (Table 5.1 and Fig 5.2).

Table 5.1: Weights of the different classes of slope gradients PAI guideline (Dovera et al 2000)

Slope classes (deg)	Equivalent Slope classes (%)	Weights	Areal coverage (%)
0 - 6	0 - 10 %	2	11.5
7 - 11	11 - 20 %	1	20.8
12 -19	21 - 35%	0	32.6
20 - 26	36 – 50 %	-1	18.9
> 26	> 50 %	-2	16.2

As can be seen from Fig 5.3, steep slope gradients or cliffs represented by the reddish color, are localized following the Rift valley faults. These are assigned by the weighed value of -1 and -2 (Table 5.1) as per the PAI guideline, which means that they have a maximum potential for landslide. These areas are also indicators of fault cliffs where landslide occurrences are common.

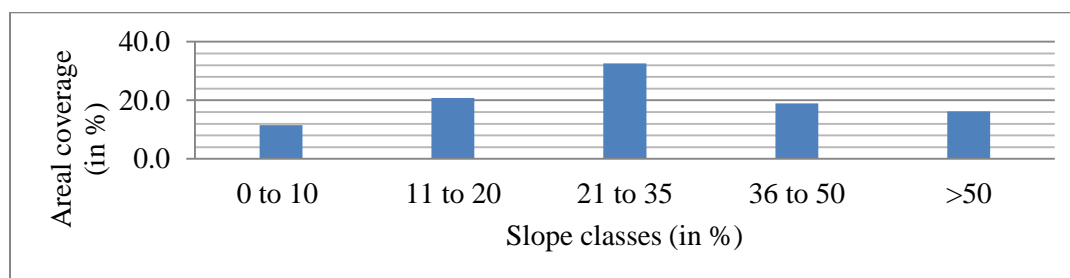


Fig 5.2: Percentage of areal coverage of the various Slope classes

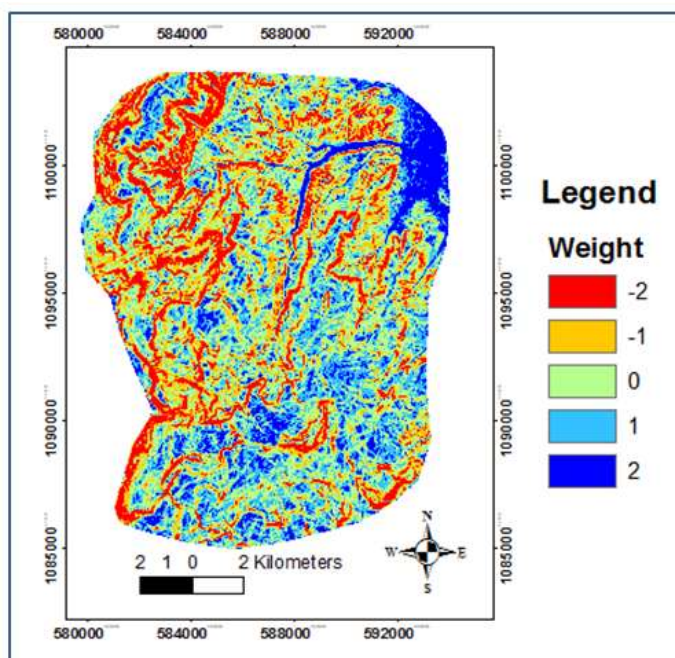


Fig 5.3: Weighed Slope map of the study area

5.1.1.2 Weighed Land Use map

Surface processes that enhance landslide such as runoff and erosion are highly controlled by the land use condition of the catchment. Thus, land use is the other factor that is considered in the slope stability problem analysis of the area.

After the land use map has been prepared in the way already explained under section 4.5.3, the weighing system of PAI guideline, which is similar to the FAO publications, is used for the nomenclature and classification of the various units of land uses. Seven land use classes are identified, with heterogeneous agricultural areas and arable (crop) lands being the main land use units covering 40% and 28% respectively (Table 5.2). Landslide occurrences are pronounced at the arable lands and river courses compared to the other types of land use classes.

Table 5.2: Areal coverage of various Land uses and their assigned weights based on PAI weighing system

Land use classes	Area (in %)	Weight
1. Forest	3.95	2
2. Bushes & shrubs	15.07	1
3. Bare land/sparse vegetation	9.92	-1
4. Arable land	28.0	-2
5. Heterogeneous agricultural areas	40.27	0
6. Urban/semi urban areas	0.72	0
7. River bed	2.02	-2

Similar to the Slope gradient, PAI guideline (Dovera et al, 2000) is used to assign weights for the various land use classes varying between +2 (e.g. forest land use) and -2 (e.g. arable land, river bed) and the weight values for the rest of the classes can be refereed in Table 5.2. Then, the land use map is rasterized using the weighted value and prepared in a way suitable for the Overlay Mapping process (Fig 5.4).

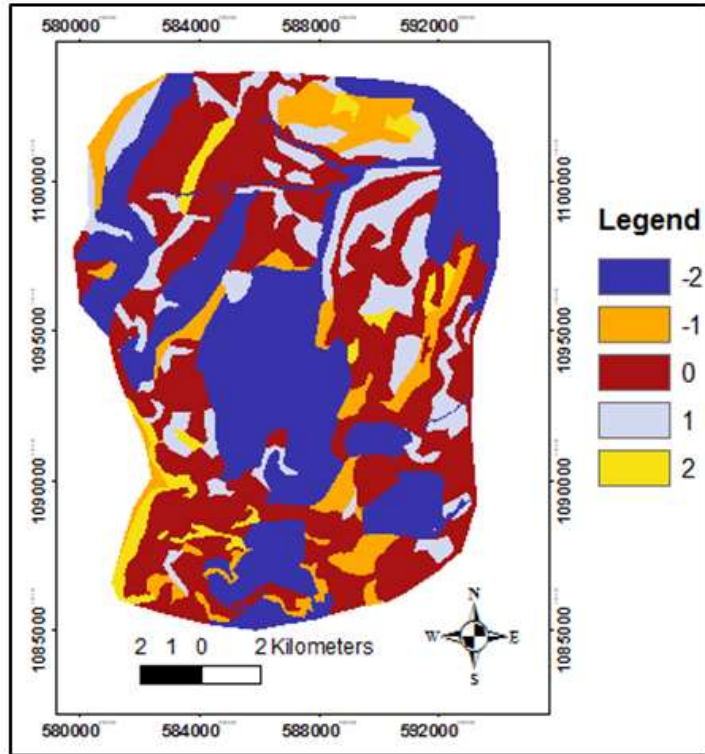


Fig 5.4: Rasterised weighed Land use map of the study area

5.1.1.3. Weighed Litho-technical map

According to Overlay Mapping method, Litho-technical factor is one of the most decisive factors in the slope instability assessment and need detail consideration. It incorporates several lithological and mechanical parameters to be addressed. The evaluation of the litho-technical parameters and the division into classes was performed following the instructions in the guideline of the Italian Geological Services for the implementation of a mapping of geological hazard related to slope instability phenomena (Annex). All parameters examined were divided into 4 classes, with a degree of influence to landslide descending from class-I (most stable) to class-IV (the most unstable).

Following the above mentioned guideline (Amantii M., et al, 1992), all the litho-technical parameters have been collected in 184 field station points and a weight has been assigned. As stated in the previous chapter, the geo-mechanical parameters to be collected in each station vary depending on the type of lithology encountered. For example, the collection of six parameters (degree of weathering, depth of weathering, spacing of discontinuities, orientation of discontinuities, compressive strength and hydraulic properties) are carried out if the encountered lithology is hard rock. The weight to be assigned for each of the 6-parameters varies from 1 to 4. This means that the possible minimum and maximum weighed values in one station are 6

and 24 respectively. However, the minimum and maximum lithological threshold weights of PAI are 1 and 9 respectively. Hence, for homogenizing the evaluation to that of PAI, it is necessary to normalize the field values with respect to the PAI weight in order to calculate the overall weighed lithological influence on the potential instability as per the guideline (Fig 5.5 and Table 5.3).

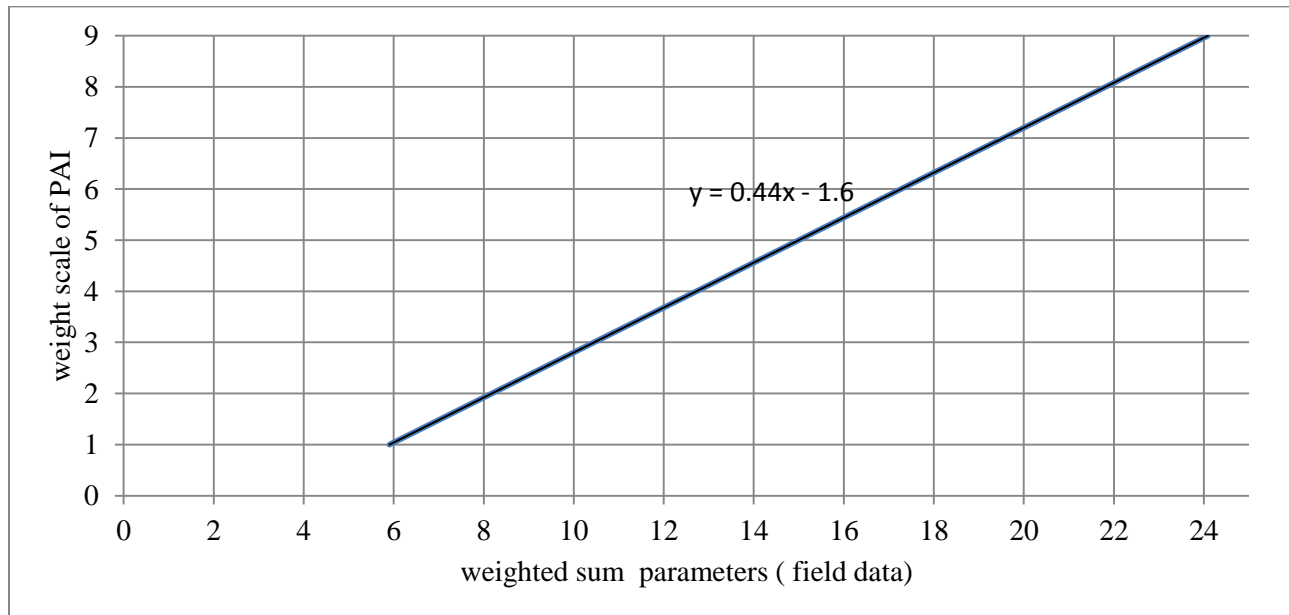


Fig 5.5: Graph and equation showing how to calculate the normalized weight of the field data

Table 5.3: Example of calculated Litho-technical weights in three stations.

Lithology	Alaje basalt					
Stations	90		92		96	
GPS locations	590550 (mE)	1090077 (mN)	590494 (mE)	1089887 (mN)	585896 (mE)	1087895 (mN)
	Classes	weight	Classes	weight	Classes	weight
Degree of weathering	IV	1	II	3	III	2
Depth of weathering	IV	1	I	4	IV	1
Spacing of discontinuity	III	2	III	2	III	2
Orientation of discontinuity	II	3	III	2	II	3
Compressive strength	IV	1	IV	1	IV	1
Permeability	IV	1	III	2	IV	1
Sum of weights	9		14		10	
Weight of PAI	2.4		4.6		2.8	

In a similar way as shown in the above table, all the weights are calculated in the 184 stations and the weighed litho-technical map has been produced (Fig 5.6,a), which is the major input map for the Overlay Mapping method. To produce weighted litho-technical polygon map, it is necessary to convert the weighed

point data to polygon map. In fact, it is clear that it is very difficult to know the exact radius of impact of each point data and changing them to polygon accordingly. In this work, to convert the point data to polygon, first all the weighted data are prepared in Excel using their x-y coordinates and the weighed value of the lithologies as z-value and is converted into point shape file using ArcGIS. Then applying the principle of Thiessen polygon, the feature points are converted into output features of proximal polygons using the weighed lithological values. Then after some editing and crosschecking, the polygon litho-technical map is rasterized for the Overlay Mapping process (Fig 5.6, a)

About 55% of the total area is covered by lithologies having a weighted value of 1 to 3 (Fig 5.6,b). This means that most lithologies of the study area are decomposed and liable to slope instability problems.

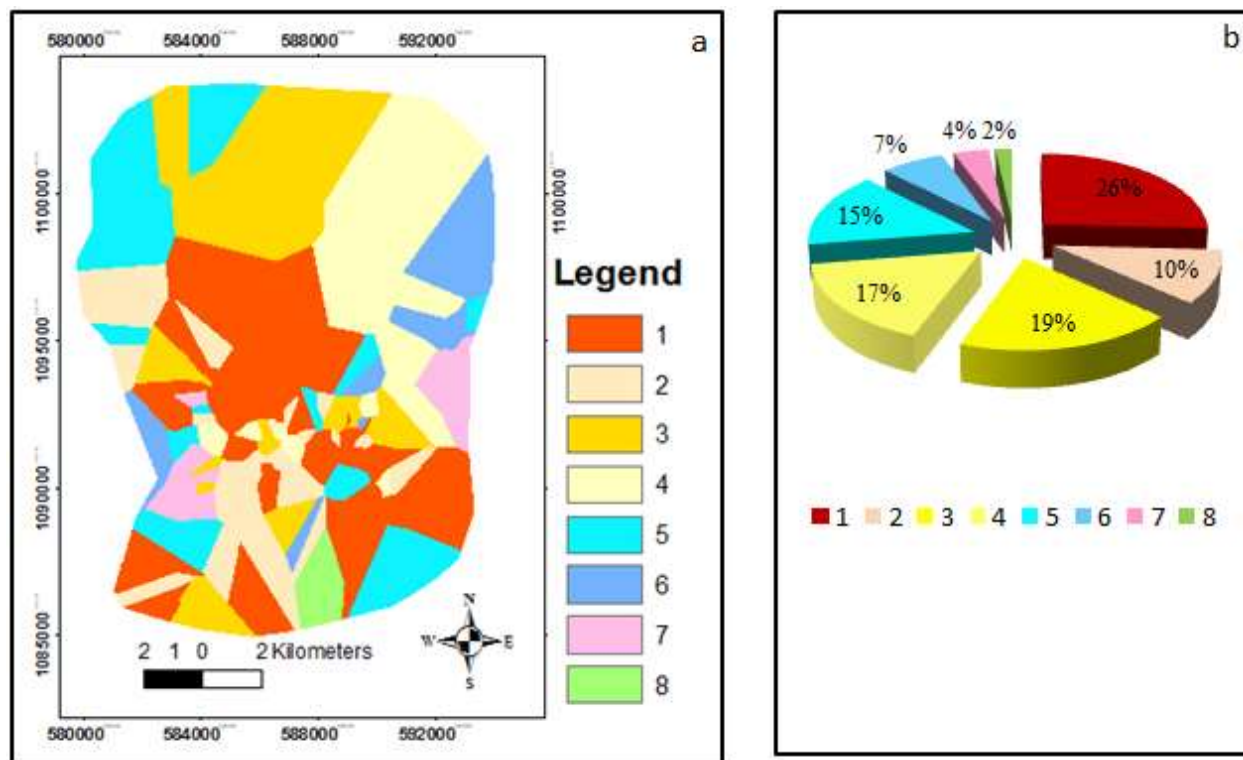


Fig 5.6: (a) Weighed Litho-technical map of study area and (b) their areal coverage in percent (the numbers 1, 2, 3 ...8 represents the weighed values of the lithology)

5.1.2. Results and Discussion

To prepare the landslide susceptibility of the study area based on Overlay Mapping approach: (1) Selection and mapping of the causative factors such as Slope gradient (Fig 5.3), Land use (Fig 5.4) and Litho-technical (Fig 5.6, a) is performed, (2) Thematic data layers are categorized among different classes and corresponding weights are assigned (3) the Overlay Mapping is obtained using the model builder of ArcGIS 9.3. The flow chart used for the overlay model preparation of the study area is shown in Fig 5.7.

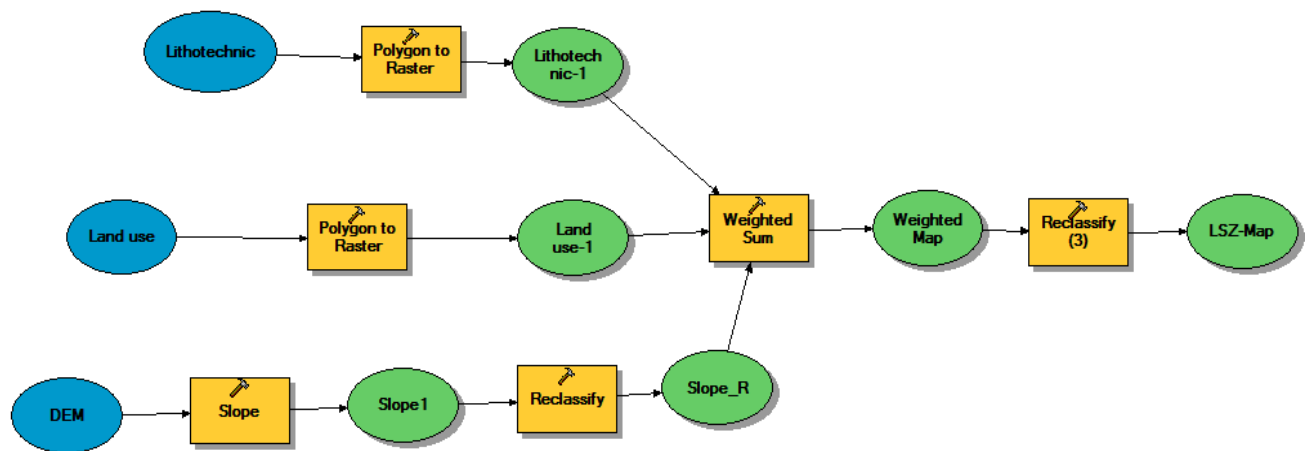


Fig 5.7: GIS-model builder of Overlay Mapping technic for landslide susceptibility mapping

(4) All the thematic maps are rasterized based on their assigned weight values and Overlay Mapping process is performed using the developed GIS model (5) finally, raw Sandslide Susceptibility Index (LSI) map showing the various zones, is produced by the overlay technique with index values range from 0 (very high susceptibility to land sliding) to 13 (non-susceptible areas) as per PAI guideline.

To reclassify this raw map into the required number of zones or classes, class boundaries with common base is necessary. In this method, class boundary recommended by the PAI guideline has been adopted to reclassify and zone the landslide susceptibility of the area of interest.

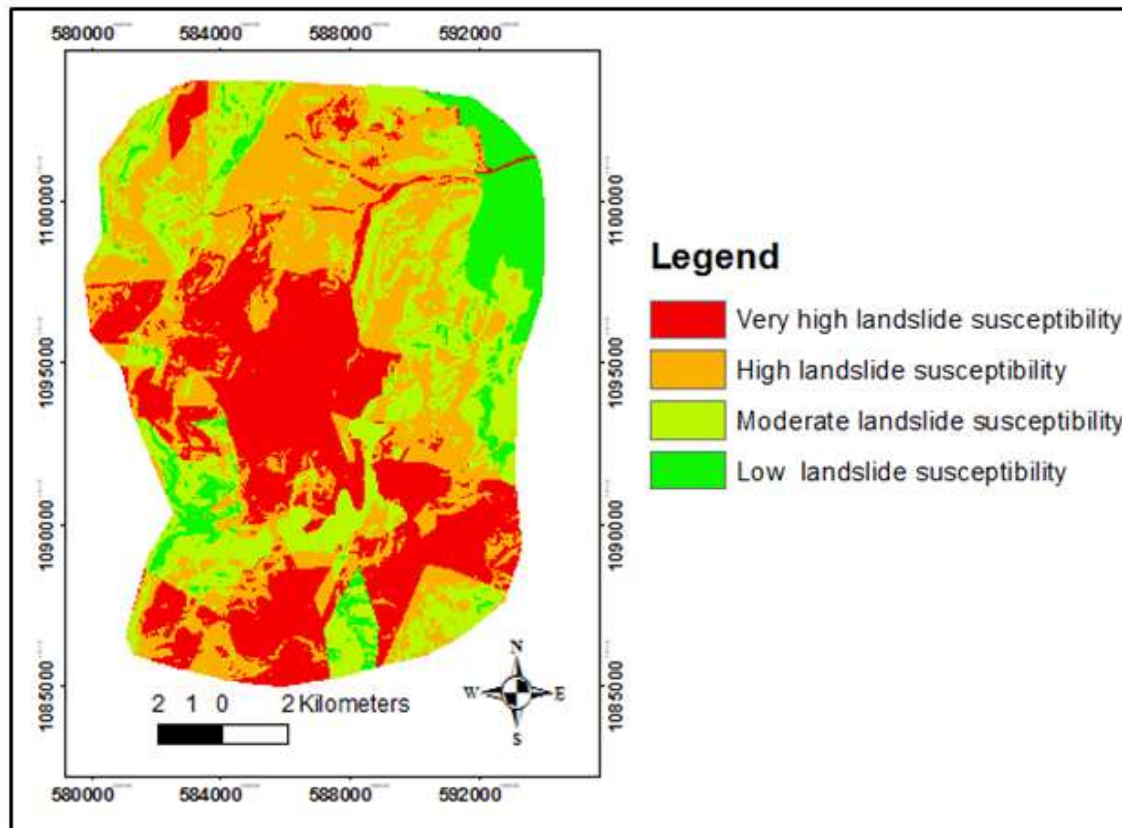


Fig 5.8: Landslide susceptibility zonation of Debresina area based on Overlay Mapping method

Thus, based on the PAI boundary classifier, four distinct Landslide Susceptibility Index (LSI) are identified (Figs 5.8 and 5.9). These susceptibility classes involve: low (9%), moderate (26%), high (33%), and very high (32%). This portrayed that about 65% of the area is susceptible to landslide.

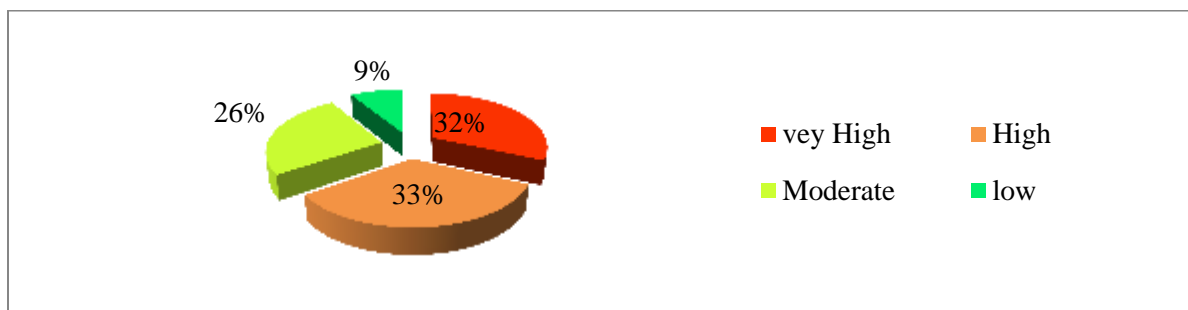


Fig 5.9: Areal coverage of the four Landslide Susceptibility Index (LSI) classes by Percent based on Overlay mapping method.

The produced landslide susceptibility map (Fig 5.8) has good agreement with the field condition. For example, the central areas where the massive landslide of September 2005 is found, as well as the southern part of the study area fall within the very high landslide susceptibility zone.

The Overlay Mapping method is therefore reasonably appropriate method in the landslide susceptibility assessment, especially it is suitable for medium and large scale landslide mapping. However, it may be limited to apply in regional scale as it needs detailed geo-mechanical characterization of lithologies consuming longer time for data collection.

Generally speaking, the overall landslide susceptibility results of this method for the study area is useful and is believed to give important information for local authorities to safeguard lives and property and improve planning and further development in the area.

5. 2. Frequency Ratio method

The most relevant input factors controlling landslides in the Debresina area of Ethiopia are given in chapter-4. All of these causative factors are further classified into a number of detailed sub-classes. Detailed landslide inventory was also carried out. The relationship between these landslide causative factors and the landslide occurrences are evaluated using GIS supported Frequency Ratio method and finally the landslide susceptibility map of the area is prepared and zoned using the obtained frequency indexes.

5.2.1 Methodology

Frequency Ratio method has been applied in the landslide susceptibility assessment and evaluation of the Debresina area. This method is used to evaluate quantitatively the relationship between the landslide distribution area and the landslide-related factors. The elements that affect slope stability and landslides are numerous and varied, and interact in complex ways (Varnes, 1984). In this study, seven causative factors involving Lithology, Proximity to fault, Land use, Slope steepness, Aspect, Elevation and Proximity to drainage have been chosen as inputs for the landslide hazard evaluation based on the site condition. The preparation of these input data can be referred in chapter 4.

After the data base has been created and all input maps are prepared, the FR was calculated for each classes of the parameter as given in equation 5.1, as has been done in similar studies (e.g. Lee and Pradhan, 2006).

$$FR = \frac{\text{area of landslide in class} / \text{area of all landslide}}{\text{area of class} / \text{entire map}} \quad (5.1)$$

The FR model is a popular quantitative method which has been recently applied with satisfactory results in several works intending to create landslide susceptibility maps (Narumon I., and Songkpt D., 2011). It is the ratio of occurrence probability to non-occurrence probability, for specific attributes (Hyun J.O, et al, 2010).

The spatial data base and the input maps have been constructed using GIS techniques, and the FR method has been applied to quantitatively describe the relationship between the landslide causative factors and the past landslide occurrences, as well as to prepare the landslide susceptibility map of the study area. The FR index of each landslide causative factor has been calculated with the help of spatial analyst techniques of ArcGIS. The weighed sums of FR values of all classes have been used to produce a landslide susceptibility map.

5.2.2. Results and Discussion

5.2.2.1 Correlations between landslides and causative factors using FR-probability model

The areal coverage of landslide occurrences in each class of causative factors is calculated by crossing with the inventory map using the ArcGIS. Then, the FR is determined by the ratio of landslide area in each class (Y in %) and total area occupation of each class (X in %) and its value is used for the correlation of each of the various factors and the landslide occurrences. The FR values of the seven chosen landslide causative parameters are demonstrated in Table 5.4. $FR < 1$ means it has less correlation than average, $FR > 1$ means higher correlation than average and $FR = 1$ means comparable to average (Lee, 2005).

The ratios of each factor's type were summed to calculate the Landslide Susceptibility Index (LSI) using the equation below:

$$LSI = \sum FR \dots\dots\dots (5.2)$$

where LSI = Landslide Susceptibility Index

FR = Frequency Ratio of each causative factor of the classes.

Table 5.4: Frequency Ratio (FR) of landslide occurrences

Factors/classes	X (% total area)	Y (% landslide area)	FR (Y/X)
Lithology			
[1] Ignimbrite (upper)	4.39	0.96	0.22
[2] Frac. Rhy. Weld tuff	4.16	6.79	1.63
[3] Alaje basalt	23.66	9.17	0.39
[4] Alluvial/Debris	5.87	11.18	1.90
[5] Basic tuff & Agglom.	21.50	4.91	0.23
[6] Colluvium-Eluvium	6.75	52.11	7.72
[7] Ignimbrite (Alaje)	5.21	1.28	0.25
[8] Resid. soil (clay & silt)	8.67	5.84	0.67
[9] Tarmaber basalt	18.56	8.88	0.48
Land Use			
[1] Forest	3.95	0.97	0.25

[2] Bushes & shrubs	15.07	5.71	0.38
[3] Bare land/sparse veget.	9.94	5.44	0.55
[4] Arable land	27.99	53.55	1.91
[5] Heterogen. Agricult. area	40.27	18.82	0.47
[6] Urban/semiurban areas	0.72	0.00	0.00
[7] River bed	2.02	14.58	7.23
Slope (in degree)			
[1] 0-5	10.6	8.2	0.82
[2] 5-10	19	18.0	0.95
[3] 10-25	52.2	55.8	1.07
[4] 25-40	16.5	16.8	1.02
[5] 40-55	1.6	0.93	0.58
[6] >55	0.1	0.04	0.33
Aspect (in degree)			
[1] NE (40)	12.71	12.64	0.99
[2] E (89)	17.95	26.80	1.49
[3] SE (134)	23.93	31.58	1.32
[4] S (180)	15.05	13.02	0.87
[5] SW (224)	6.76	3.56	0.53
[6] W (270)	4.48	1.37	0.31
[7] NW (315)	7.79	3.32	0.43
[8] N (360)	11.33	7.71	0.68
Proximity to Fault (m)			
[1] 0-400	56.03	65.72	1.17
[2] 400-600	17.28	16.98	0.98
[3] 600-800	9.55	10.06	1.05
[4] 800-1000	5.58	4.05	0.73
[5] 1000-1200	3.29	1.08	0.33
[6] 1200-1400	1.97	0.84	0.43
[7] 1400-1600	1.48	0.41	0.27
[8] >1600	4.82	0.86	0.18
Proximity to drainage (m)			
[1] 0-150	30.92	42.44	1.37
[2] 150-300	21.82	27.33	1.25
[3] 300-450	17.21	15.87	0.92
[4] 450-600	13.73	8.28	0.60
[5] 600-750	8.97	4.10	0.46
[6] >750	9.15	1.98	0.22
Elevation (m)			
[1] 1368-1500	5.52	6.19	1.12
[2] 1500-2000	44.50	38.79	0.87

[3] 2000-2500	32.47	47.36	1.46
[4] 2500-3000	16.14	7.45	0.46
[5] >3000	1.37	0.24	0.18

Lithology and landslide occurrences

Lithology is a major controlling factor for the overall slope failures in Debresina area. Especially, areas covered by the colluvial-eluvial deposits are extremely prone to landslides. The colluvium-eluvium deposit in Debresina area include heterogeneous mixture of slope wash deposits, old landslide deposits, reworked breccia, insitu developed regolith, which has variable exposed thickness varying from 5 to more than 25m (Figs 5.11 & 5.12). These are commonly affected by reactivated landslides. Other lithological groups such as alluvial deposits/debris, and fractured rhyolitic tuffs are also most sensitive to landslide occurrences having $FR > 1$ (Table 5.4 & Fig 5.10), whereas, the fine residual soils are marginally prone and the rest is less prone to landslide activity. This result is consistent with field observations.

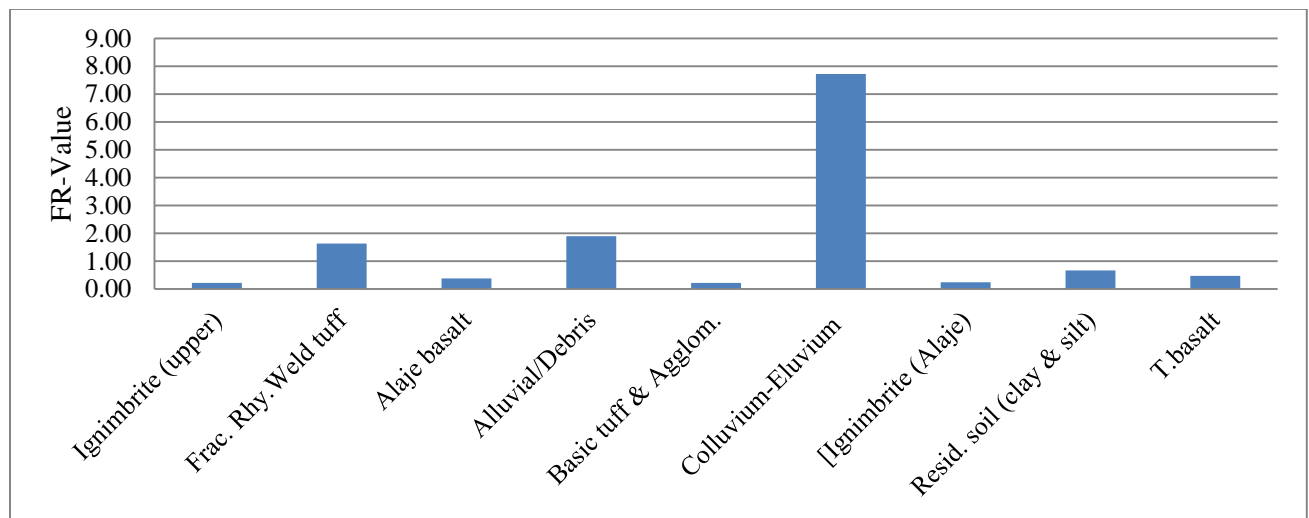


Fig 5.10: Histogram showing the FR value of the various Lithologies of the study area

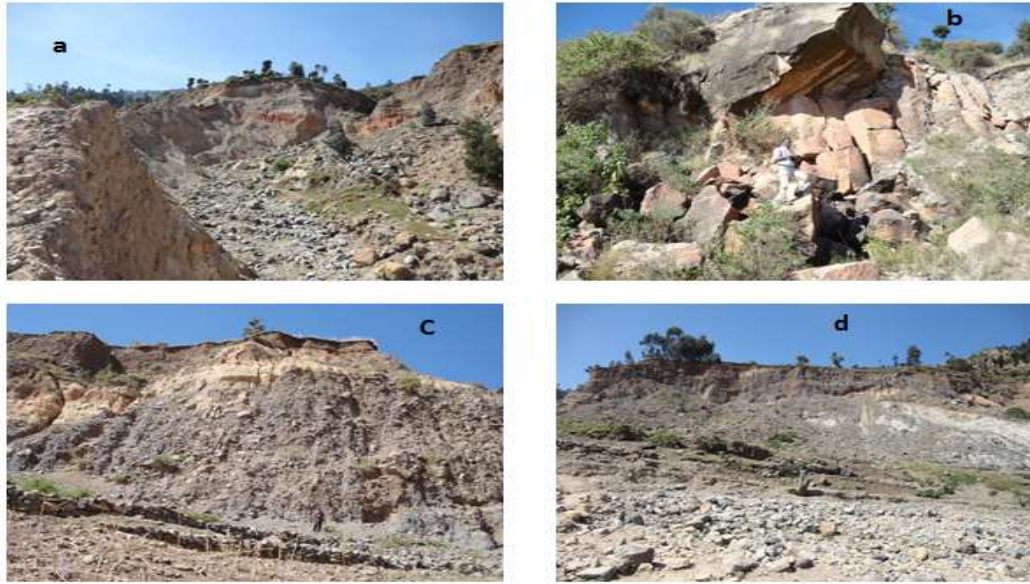


Fig 5.11: Photograph showing the landslide occurrences in thick colluvium deposit (a, c, & d) and in fractured rhyolitic ignimbrite rocks (b)

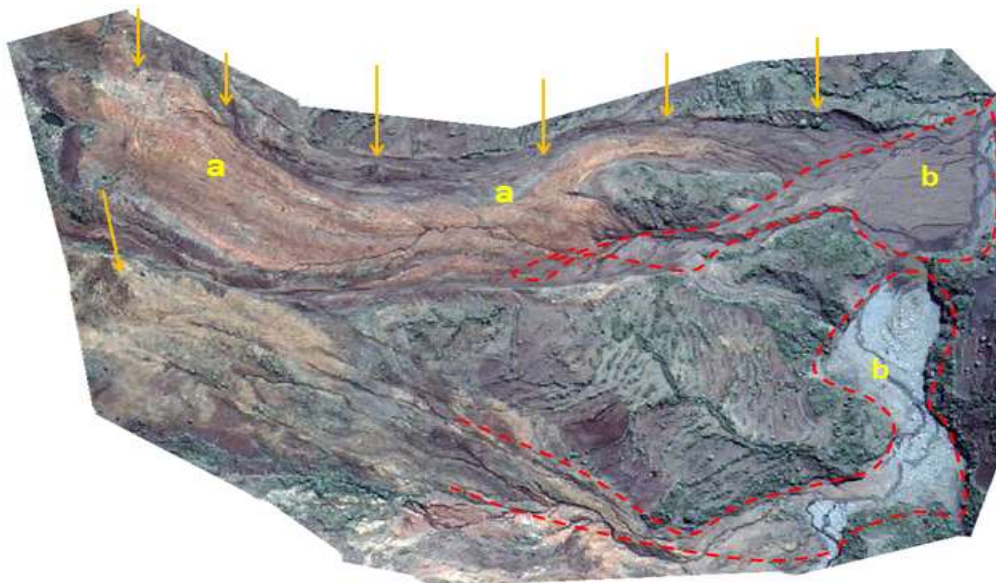


Fig 5.12: Some of the SE- facing landslide main scarp (indicated by 'a' & arrows) along the thick colluvium-eluvium deposits. At some places they are also followed by debris flows, as indicated in 'b'. (Taken from Google Earth, 2007)

Land use and landslide occurrences

The data obtained from the map regarding land use suggest that the most susceptible classes are river courses and arable lands having $FR > 1$. The bare land is marginally prone to landslide. The rest of the land use classes has low FR value and is with less contribution to sliding.

Proximity-based factors and landslide occurrences

The proximity based factors involve the distances from fault and drainage. The fault and drainage proximities show a strong correlation with landslide occurrences. That is, areas located near to fault or drainage systems more liable to slope failure than distant areas in general.

The relationship of the landslide and the proximity to faults have a general decreasing trend from very high near to the fault plane to low at the distant areas. The influence of faults is significant to the slope failure up to a distance of nearly 800m (Fig 5.13)

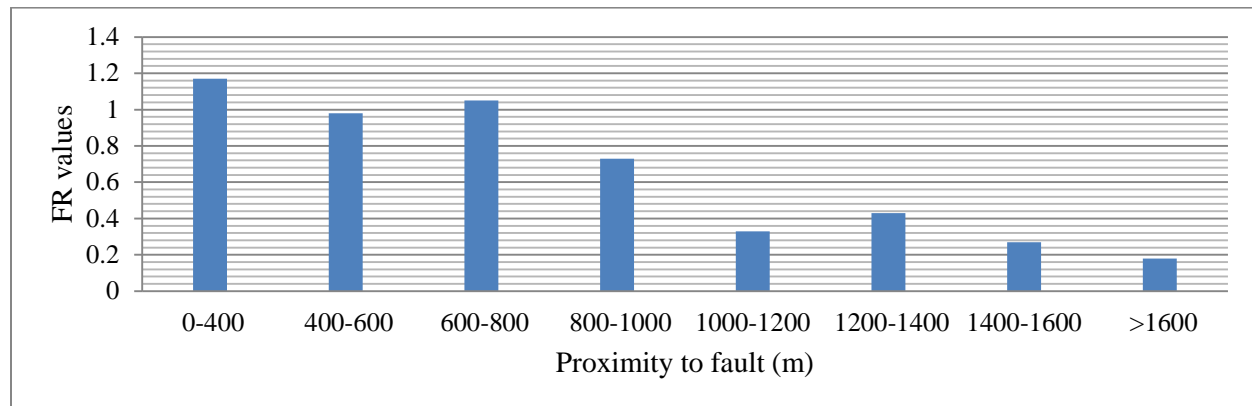


Fig 5.13: Relationship of FR values with Proximity to fault

In the case of the relationship between landslide occurrence and proximity to drainage, the probability of land sliding has a decreasing trend as one move far away from the drainage. Specifically areas found up to distances of 450 have a FR value of > 1 showing these zones are strongly susceptible to landslide (Table 5.4 & Fig5.14). This can be attributed to the fact that terrain modification caused by gully erosion and undercutting, as well as saturating the lower part of material may influence the initiation of landslides up to the distance of 450m. Thus, streams have a destabilizing effect near to their course by eroding the slopes or by until the water level increases, and such effect is especially maximum, where they are in contact with loose colluvium materials.

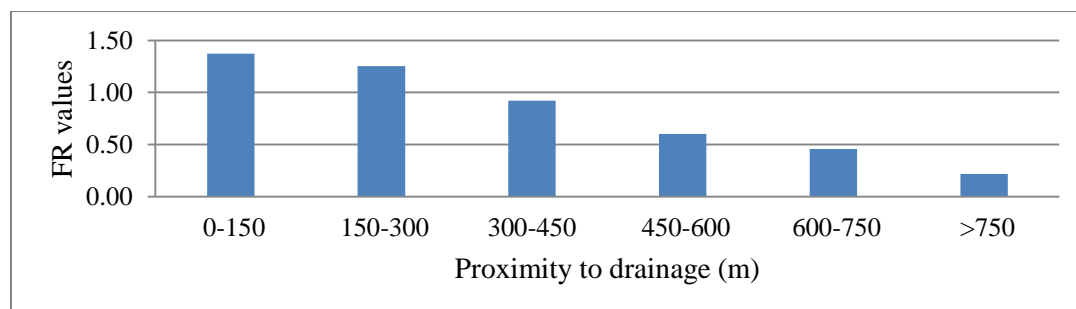


Fig 5.14: Relationship of FR values with proximity to drainages.

Topographic-based factors and landslide occurrences

Three main topographic factors such as Slope, Aspect and Elevation are evaluated in correlation to the landslide occurrences. The middle Slope angle of 10-25° and 25-40° have FR values >1 indicating the very high probability of landslide occurrences while the Slope angle 5-10° is with moderate probability while the rest have low probability of landslide occurrences (Table 5.4 & Fig 5.15). In the case of Aspect, landslides were most abundant on east facing (89°) and Southeast facing (134°) Rift margin slopes. Thus, slopes facing to the East(E) and Southeast (SE) are highly susceptible to landslides with a ratio >1; slopes facing to the North (N) and Northeast (NE) are moderately prone to landslide; whereas, the frequency of landslides was lowest on marginal slopes facing to other directions. With respect to the relationship between landslide occurrence and Elevation, it has a similar trend with Slope of the area. That is, areas with middle Elevation (2000-2500m) are highly characterised by very high landslide occurrences and have FR values greater than one: whereas the Elevations having less than 2000m varies from moderate to high slope failure and that of with greater than 2500m Elevation are characterized by low probability of landslide occurrence.

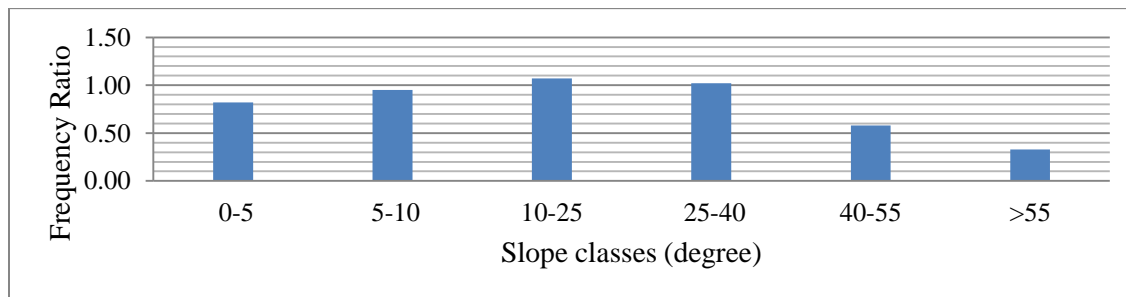


Fig 5.15: The relationship between Slope angle and FR- values

In order to enable the map interpretation, a landslide susceptibility zonation map is established by dividing the LSI values into various landslide susceptibility classes.

Finally, the raw Landslide Susceptibility Index (LSI) map was produced using equation-5.2, where the weighted sum is done by map overlay and raster calculation techniques of the ArcGIS. From the calculation, it was found that the LSI had a minimum value of 3.08 (low susceptibility), and a maximum value of 22.31 (very high susceptibility). Although common base class boundary classifiers are necessary to reclassify the raw LSI map, there are no common agreements among researchers so far. Because of this several researchers adopt their own expert opinion to develop class boundaries. For instances, mathematical GIS classifier methods that have been used in landslide classification involve manual classification (e.g. Van Westen et al. 1997; Long, et al, 2011), equal interval classification (e.g. Dai et al, 2001) or natural break classification (e.g. Fournelis, et al. 2004). In this work, the manual classifier method was adopted to reclassify the LSI values into four different susceptibility zones, according to the classification method that was proposed by Galang (2004) as cited in Long, et al, (2011).

The approach is based on the logic that an ideal classification method should satisfy the principle that higher landslide susceptibility classes should capture more or most of the landslide occurrences. Based on this rule, it can be inferred that the expected percentages of observed landslide occurrences in the low, moderate, high and very high landslide susceptibility classes are 6.7, 13.3, 26.7, and 53.3%, respectively (Long, et al, 2011).

For determining the class boundaries corresponding to percentages, the cumulative percentage of observed landslide occurrence (on y-axis) is plotted versus ranked LSI values (on x-axis) and then, the class boundaries of LSI values are obtained by intersection of the curve with the required observed landslide percentages. Accordingly, four LSI classes with boundaries of 4.5 (separating low-moderate), 7 (separating moderate - high) and 12.3 (separating high-very high) are respectively determined. The LSI values are re-classified in four zones based on these boundaries and the susceptibility map of the FR model is shown in (Fig 5.17).

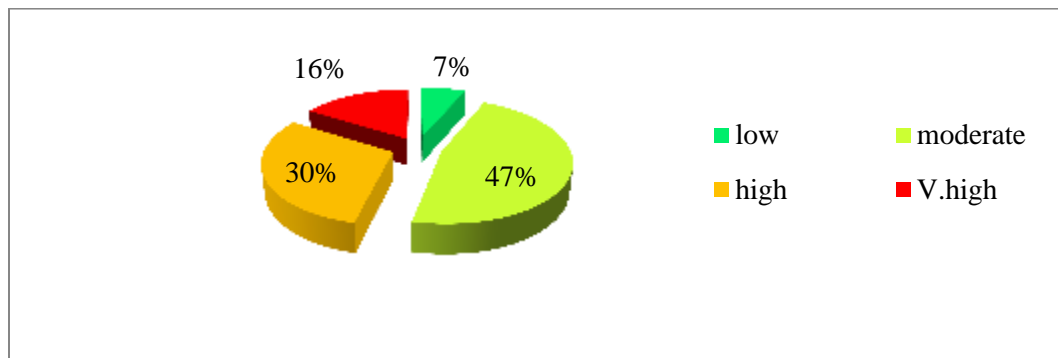


Fig 5.16: Areal coverage of the four Landslide Susceptibility Index (LSI) classes by Percent based on FR-method.

Based on the LSI values, the study area is divided into four susceptibility zones, namely very high (16.2%), high (30.2%), moderate (47.0%) and low (6.6%) susceptibility zones. Hence, according to this method, 46.4% of the total area is susceptible to landslide which is quite significant.

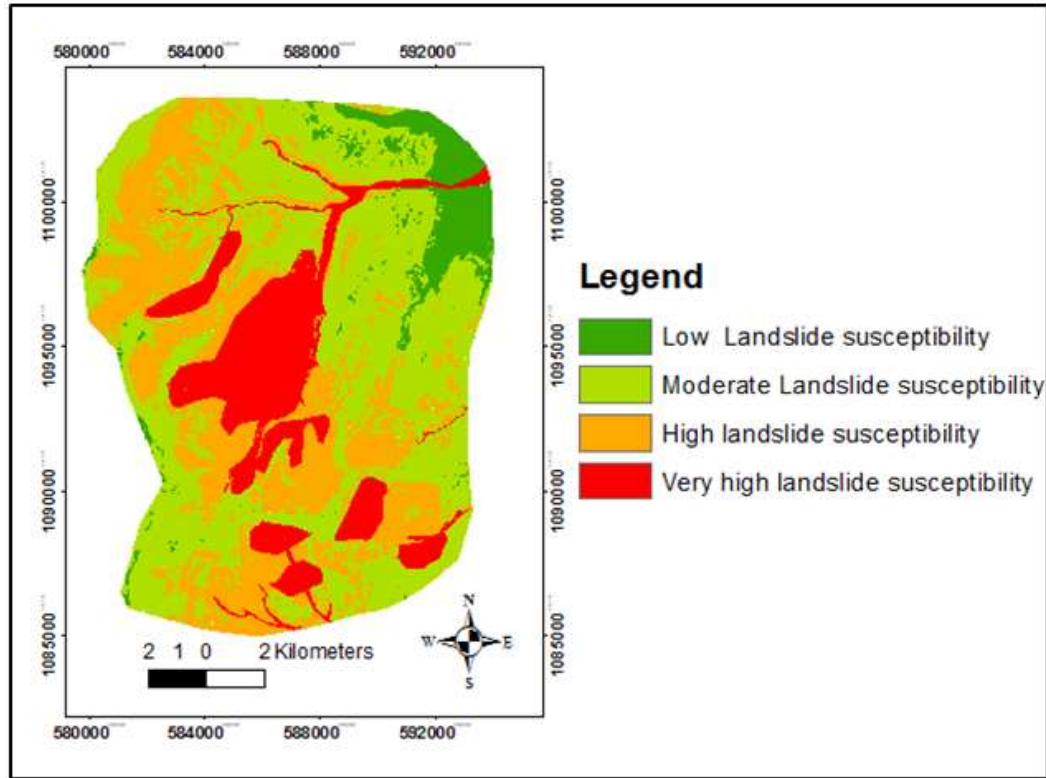


Fig 5.17: Landslide susceptibility zonation of Debresina area based on FR-method

Similar to the Overlay Mapping method, the landslide susceptibility map produced by the FR-method has reasonable prediction rate as compared with the field condition. For instance, the massive landslide of September 2005 matches within the very high landslide susceptibility zone. Moreover, this method is also very important to evaluate the contribution of the various causative factors to the landslide. This method needs detailed landslide inventory information to produce a good result. The result of verification is given in the next section of this chapter in comparison with other methods.

5.3. Analytical Hierarchical Process (AHP) method

Analytical Hierarchical Process method (AHP) as described in chapter-2 is the semi-quantitative method used in studying the influence of different landslide causative factors and susceptibility of the area. In this section, the basic principles and procedures of the AHP method is discussed, as well as causative factors are analyzed to assess the spatial landslide susceptibility distribution in the area of interest.

5.3.1 Methodology

The Analytic Hierarchy Process (AHP) was developed by T. Saaty (1980) and it is a decision-aiding tool for dealing with complex and multi-criteria decisions. AHP is a mathematical technique for multi-criteria

decision making (Saaty, 1980). The AHP has attracted the interest of many researchers mainly due to the nice mathematical properties of the method and the fact that the required input data are rather easy to obtain (E. Triantaphyllou, 1995). It provides a flexible and easily understandable way of analysing complicated problems, and allows shaping ideas and solving problems by making approximate assumptions. Therefore, it has a very high ability to structure complexity and exercise judgment.

AHP has an advantage of permitting a hierarchical structure of the criteria which provides users with a better focus on the specific criteria (factor) and sub-criteria (classes) when allocating the weight (Ishizaka A. and Labib A., (2009). Once the hierarchy is built, the decision makers systematically evaluate its different elements by comparing them to one another, two at a time, with respect to their impact on an element above them in the hierarchy. In making the comparisons, the decision makers typically use their judgments about the elements' relative meaning and importance.

The AHP converts these evaluations to numerical values that can be processed and compared over the entire range of the problem. A numerical weight or priority is derived for each element of the hierarchy, allowing diverse and often numerous elements to be compared to one another in a rational and consistent way. The AHP helps to overcome the problems with arbitrary weights and scores approaches, by its ability to enable decision-makers to derive ratio scale priorities or weights as opposed to arbitrarily assign them (Yalcin, 2007)

Because of its simplicity and robustness in obtaining weights and integrating heterogeneous data, AHP is one of the very popular multi-criteria decision methods with a wide application in many fields such as Project management (e.g. Kamal M.A., 2001), site selection and suitability analysis (e.g. Bantayan and Bishop, 1998; Mahsa H. et al, 2011; Anagnostopoulos K., 2012), regional planning (e.g. Jankowski, 1989), urban land-use planning (e.g. Dai et al, 2001; Feng and Chan., 2004), and environmental impact assessment (e.g. Ramanathan, 2001; Gregory, et al, 2005), and design and engineering (Hambali., et al, 2009; András., 2010). There is a vast literature on the applications of AHP with more than 1300 papers and 100 doctoral dissertations (Forman and Gass, 2001; also see www.expertchoice.com) as stated in Nachiappan Ramakrishnan, (2012). One of its wide applicability in recent years is in the field of landslide study. Several landslide studies have been published using the AHP approach (e.g. Yagi, 2003; Ayalew, et al, 2004; Woldearegay K., 2005; Bachri S. and Shrestha, 2010; Narumon, and Songkpt, 2010; Long and D. Smedt., 2011; Mezughi, et al, 2012).

The advantages of using AHP in a landslide analysis (Long, 2011) are: (1) all types of information can be included in the discussion process (2) judgment is structured so that all the information is taken into account; (3) discussion rules can be based on experience (4) once a consensus is reached, weights for each relevant

factor are obtained automatically by eigenvector calculation of the decision matrix and (5) inconsistencies in the decision process can be detected and, hence, corrected.

Analytical hierarchy model takes as an input the pair wise comparisons and produces the relative weights as output. To make a decision in an organized way and generate priorities, we need to decompose the decision into steps. Application of AHP to a decision problem involves four steps (Saaty, 1980; Zahedi, 1986; Saaty, 2008):

Step1: Structuring of the decision problem in a hierarchical approach

Step 2: Making pair-wise comparisons and obtaining the judgmental matrix

Step 3: Computing local weights and consistency of comparisons

Step 4: Weights Aggregations

Step-1: Structuring of the decision problem in a hierarchical approach

Modelling the problem as a hierarchy containing the decision goal, the alternative for reaching it, and the criteria for evaluating the alternatives, is the primary step in the AHP method. This step allows a complex decision to be structured into a hierarchy descending from an overall objective to various 'criteria', 'sub-criteria', and so on until the lowest level. The overall goal of the decision is represented at the top level of the hierarchy while the criteria and sub-criteria contributing to the decision are represented at the intermediate levels. Finally, the decision alternatives are positioned at the last level of the hierarchy. Although there is no clear set of procedures for generating the levels to be included in the hierarchy, Saaty (2000) indicated that a hierarchy can be constructed by creative thinking, recollection and using people's perspectives.

Step-2: Constructing pair-wise comparisons and obtaining the judgmental matrix

Once the hierarchy has been structured, the next step is to construct the pair-wise comparison matrix as proposed by Saaty (1980). The input data for problem consist of matrices of pair-wise comparisons of elements of one level that contribute to achieve the objectives of the next higher level. That is, the elements of a particular level are compared with respect to a specific element in the immediate upper level. Once the matrix is created, elements are compared pair-wise to determine their relative importance in terms of each criterion (factors) based on the scale introduced by Saaty (1980). According to this scale, the available values for the pair-wise comparisons are members of the set: $\{1/9, 1/8, 1/7, 1/6, 1/5, 1/4, 1/3, 1/2, 1, 2, 3, 4, 5, 6, 7, 8, 9\}$ (Table 5.6). The verbal judgments of each pair wise elements are transformed into numerical quantities using the scale. Usually, an element receiving higher rating is considered as superior (or more influential) compared to another one that receives a lower rating.

In order to explain the mathematical model, we are supposed to start with certain assumptions. For instance if ‘n’ represents a number of criteria or alternatives, it can be represented by n x n matrix:

$$C = (C_{ij}), (i, j = 1, 2, \dots, n)$$

As stated in Saaty (1980, 1990), each entry C_{ij} of the judgmental matrix is governed by certain rules such as (1) such matrix should be reciprocal i.e $C_{ij} = 1/C_{ji}$ for all $i, j = 1, \dots, n$. (2) when compared with itself each element has equal importance ($C_{ii} = 1$, for all i .) (3) Such matrix should be greater than zero ($C_{ij} > 0$). Moreover, such matrix is also represented by (a) diagonal elements of the matrix are always equal to 1 and lower triangle elements of the matrix are reciprocal of the upper triangle (b) the weight ratio can be defined by $w_{ij} = w_i/w_j$ for the pair wise comparison (c) The matrix have a total of $n(n-1)/2$ judgments or comparisons, where n is the number of criteria or elements.

Table5.5: illustrative pair-wise comparison matrix of elements in the AHP

Criteria	C_1	C_2	C_3	.	.	C_i	.	.	C_n
C_1	1
C_2	.	1
C_3	.	.	1
.
.
.
.
C_i	C_{ij}	.	.	.
.
.
.
.
C_n	C_{nn}

(Criteria matrix represented by ‘C’)

Table5.6: The fundamental scale of absolute numbers/Scale of Relative Importance (T.Saaty, 2008)

Intensity of Importance	Definition	Explanation
1	Equal importance	Two activities contribute equally to the objective
2	Weak or slight	
3	Weak importance of one over another	Experience and judgment slightly favor one activity over another
4	Moderate +	

5	Essential or strong importance	Experience and judgment strongly favor one activity over another
6	Strong+	
7	Very strong or demonstrated importance	An activity is strongly favored and its dominance demonstrated
8	Very, very strong	
9	Extreme importance	The evidence favoring one activity over another is of the highest possible order of affirmation
Reciprocals of above nonzero	If activity i has one of the above nonzero numbers assigned to it when compared with activity j, then j has the reciprocal value when compared with i.	A reasonable assumption
1.1–1.9	If the activities are very Close	May be difficult to assign the best value but when compared with other contrasting activities the size of the small numbers would not be too noticeable, yet they can still indicate the relative importance of the activities.

Step-3: Computing local weights and consistency of comparisons

The aim of this step is to find a set of priorities or local weights, which is the normalized Eigen vector of the elements of the matrix. Once the comparison matrices are completed, priorities can be calculated. Although different methods have been used to compute the weights or priorities in AHP, the Eigen-value technique is one of the common methods developed by Saaty (1980). The steps to compute the relative weights (Eigen vector) of a reciprocal matrix involve the following operations:

- (i) Sum of the values in each column of the reciprocal matrix.
- (ii) Divide each element in the matrix by its column total (the resulting matrix is referred to as the normalized pair wise comparison matrix and the sum of each column is 1).
- (iii) Compute the average of the elements in each row of the normalized matrix, that is, divide the sum of normalized scores for each row by the number of criteria. These averages provide an estimate of the relative weights of the criteria being compared. Since it is normalized, the sum of all elements in priority vector is 1. The relative weight (priority vector) shows relative weights among the things that we compare. The higher the weight is the more important the criteria.

Priorities or relative weights make sense only if derived from a consistent or near consistent matrices. Thus, aside from the relative weight, we can also check the consistency of reciprocal matrix. To do that, we need what is called Principal Eigen value (λ_{max}) which is an important validating parameter in AHP. It is used as a

reference index to screen information by calculating the Consistency Ratio, CR (Saaty, 2000) of the estimated vector in order to validate whether the reciprocal matrix provides a completely consistent evaluation. The Consistency Ratio is calculated as per the following steps:

(a) Calculate the Eigenvector or relative weights and largest Eigen value (λ_{max}) for each matrix of order n. Principal Eigen value (λ_{max}) is obtained from the summation of products between each element of Eigen vector and the sum of columns of the reciprocal matrix.

(b) Compute the Consistency Index(CI) for each matrix of order 'n' by the formulae:

$$CI = \frac{(\lambda_{max}) - n}{n - 1} \quad (5.3)$$

(c). the consistency ratio is then calculated using the formulae:

$$CR = \frac{CI}{RI} \quad (5.4)$$

where RI is a known Random Consistency Index obtained from a large number of simulations runs and varies depending upon the order of matrix (Table 5.7).

Table5.7: Random Consistency Index (RI) (Saaty, 1980, 2000)

n	1	2	3	4	5	6	7	8	9	10	11	12	13	14	15
RI	0	0	0.58	0.9	1.12	1.24	1.32	1.41	1.45	1.49	1.51	1.53	1.56	1.57	1.59

The acceptable CR range varies according to the size of matrix i.e. 0.05 for a 3 by 3 matrix, 0.08 for a 4 by 4 matrix and 0.1 for all larger matrices, $n \geq 5$ (Saaty, 2000). If the value of $CR \leq 10\%$, it implies that the evaluation within the matrix is acceptable or indicates a good level of consistency in the comparative judgments represented in that matrix. In contrast, if CR is more than the acceptable value, inconsistency of judgments within that matrix has occurred and the evaluation process should, therefore, be reviewed, reconsidered and improved.

Step-4: Weights aggregations

The last step is to synthesize the local priorities across all criteria in order to determine the overall final priorities of the alternatives. That is, final priorities of the alternatives can be obtained by aggregating the local priorities of elements of different levels, which are obtained in the above steps (steps 1-3). The AHP approach adopts an additive aggregation (eq'n 5.5) with normalization of the sum of the local priorities to unity (Ishizaka and Labib, .2009).

$$Pi = \sum_j w_j l_{ij} \quad (5.5)$$

where P_i : overall final priority of the alternative i (LSI in our case);

l_{ij} = local priority;

w_j = weight of the criterion j .

The specific application of the AHP method is presented below in modelling the landslide susceptibility of the study area.

5.3.1. Results and Discussion

In the evaluation of slope failure by the AHP method, the same number and types of landslide causative factors are assumed as in the case of FR method mentioned above. The details of these landslide controlling factors can be referred in chapter 4. To apply AHP method to the landslide study of Debresina area, the following procedures and approaches are followed.

1) As stated above, the considered causative factors are seven similar to the FR method. Depending on their relative influences to the landslide, each of the various causative factors was further classified into a number of significant classes. In putting priorities, weighing factors, and determining relative influences of the various factors: (a) Previous results of the FR method are considered (b) Field based expertize observation and opinions on relationship between the causative factors and landslide are used (c) Review of published literature data on the relationship of the causative factors and the landslide. Values ranging from 9 (extremely) to 1 (equally) and 1/9 (opposite extremely) are assigned based on Table 5.6 to each pair of parameters resulting a square reciprocal matrix by rating rows relative to columns as shown in Tables 5.8 (a-b).

2) Pair-wise comparisons and obtaining the judgmental matrix, consistency checks are done. Although all the mentioned factors induces landslide, their individual relative influences on the slope instabilities are different. To weigh the relative importance of the above mentioned causative factors and their subdivisions (classes) quantitatively on the initiation of the landslide, a pair-wise comparison and a judgment matrix was made based on the proposal of Saaty (1980, 2000). When comparing two attributes (layer classes or parameters in a layer), the above stated numerical relational scale is used (Table 5.6).

3) Once the comparisons matrices are made, the priorities or relative weights or Eigen vectors, as well as the Principal Eigen value (λ_{max}) are calculated following the procedures stated in step-3 above. Then,

Consistency Index (CI) and Consistency Ratio (CR) values of each developed factor or class matrices have been determined using equations 5.3 and 5.4 above. While the values of the Random Consistency Index (RI) is referred from Table 5.7.

4) Finally, the aggregation and integration of the various weights of the factors and classes to a single Landslide Susceptibility Index (LSI) is accomplished by a procedure based on the weighed linear sum (Voogd, 1983):

$$LSI = \sum_i^n W_j w_{ij} \quad (5.6)$$

where,

W_j : weight value of parameter j

w_{ij} : rating value or weight value of class i in parameter j

n : number of parameters

Table 5.8 (a): Pair-wise comparison matrixes, principal Eigenvectors (relative weights) and Consistency Ratios of various parameters (causative factors) and the data layers

	[1]	[2]	[3]	[4]	[5]	[6]	[7]	Weight (%)
[1].Lithology	1	5	4	4	2	3	9	34.2
[2] Land use	1/5	1	1/2	1	1/4	1/3	5	7.2
[3] Slope gradient	1/4	2	1	1/2	1/4	1/3	3	7.4
[4] Aspect	1/4	1	2	1	1/4	1/3	2	7.5
[5] Proximity to fault	1/2	4	4	4	1	2	7	24.5
[6] Proximity to Drainage	1/3	3	3	3	1/2	1	5	16.2
[7] Elevation	1/9	1/5	1/3	1/2	1/7	1/5	1	2.9

Lithology is the major parameter contributing to the landslide of the Debresina area followed by the faulting and drainage, which is also true from the prospective of the field observation. The area is characterized by the susceptible types of lithology i.e. thick colluvium-eluvium, intensively fractured and deeply weathered rhyolitic ignimbrites, welded tuffs, and basalts. Slope aspect and Slope gradient are the next influential parameters, with more or less equal influences on the landslide occurrences (Table 5.8a and Fig 5.18).

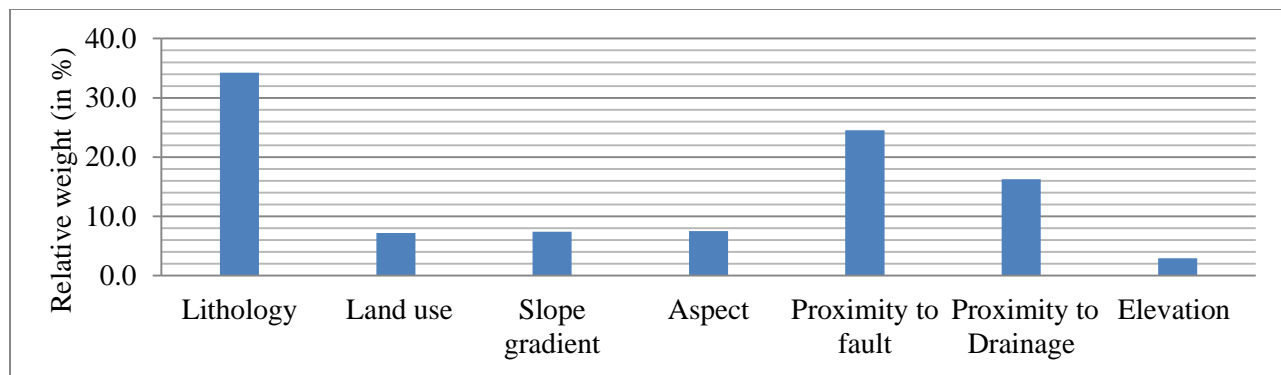


Fig 5.18: Relative influences of parameters on the landslide of Debresina

Table5.9 (b): Pair-wise comparison matrixes, principal Eigenvectors (relative weights) and Consistency Ratios of classes with in the various parameters (causative factors) and the data layers

Factors/classes										
Lithology	[1]	[2]	[3]	[4]	[5]	[6]	[7]	[8]	[9]	weight
[1] Ignimbrite (upper)	1	1/8	1/2	1/8	1	1/9	1	1/3	1/2	0.027
[2] Frac. Rhy.Weld tuff	8	1	4	1	6	1/4	6	2	3	0.161
[3] Alaje basalt	2	1/4	1	1/5	1	1/9	1	1/2	1	0.040
[4] Alluvial/Debris	8	1	5	1	6	1/4	6	3	4	0.177
[5] Basic tuff & Agglom.	1	1/6	1	1/6	1	1/9	1	1/2	1/2	0.032
[6] Colluvium-Eluvium	9	4	9	4	9	1	9	9	9	0.415
[7] Ignimbrite (Alaje)	1	1/6	1	1/6	1	1/9	1	1/2	1/2	0.032
[8] Resid. soil (clay & silt)	3	1/2	2	1/3	2	1/9	2	1	1	0.064
[9] Tarmaber basalt	2	1/3	1	1/4	2	1/9	2	1	1	0.052
Land use										
[1] Forest	1	1	1/2	1/7	1/2	1	1/9			0.043
[2] Bushes & shrubs	1	1	1/2	1/5	1/2	1	1/9			0.044
[3] Bare land/sparse veget.	2	2	1	1/3	1	2	1/9			0.079
[4] Arable land	7	5	3	1	4	2	1/4			0.199
[5] Heterogen. Agricult. area	2	2	1	1/4	1	1	1/9			0.067
[6] Urban/semiurban areas	1	1	1/2	1/2	1	1	1/7			0.058
[7] River bed	9	9	9	4	9	7	1			0.509
Slope gradient										
[1] 0-5	1	1/2	1/4	1/2	1	3				0.104
[2] 5-10	2	1	1/2	1/3	2	3				0.158
[3] 10-25	4	2	1	2	3	7				0.355
[4] 25-40	2	3	1/2	1	2	4				0.236
[5] 40-55	1	1/2	1/3	1/2	1	2				0.100
[6] >55	1/3	1/3	1/7	1/4	1/2	1				0.048
Aspect										

[1] NE (40)	1	1/2	1/3	1	2	2	2	1	0.115
[2] E (89)	2	1	1	2	3	3	3	2	0.215
[3] SE (134)	3	1	1	2	3	3	3	2	0.228
[4] S (180)	1	1/2	1/2	1	2	3	2	1	0.127
[5] SW (224)	1/2	1/3	1/3	1/2	1	2	1	1/2	0.072
[6] W (270)	1/2	1/3	1/3	1/3	1/2	1	1	1/2	0.058
[7] NW (315)	1/2	1/3	1/3	1/2	1	1	1	1/2	0.065
[8] N (360)	1	1/2	1/2	1	2	2	2	1	0.120
Proximity to Fault									
[1] 0-400	1	2	1	2	4	3	4	9	0.244
[2] 400-600	1/2	1	2	3	3	3	3	7	0.218
[3] 600-800	1	1/2	1	2	4	3	4	6	0.196
[4] 800-1000	1/2	1/3	1/2	1	3	2	3	4	0.122
[5] 1000-1200	1/4	1/3	1/4	1/3	1	1/2	1	4	0.059
[6] 1200-1400	1/3	1/3	1/3	1	2	1	2	2	0.083
[7] 1400-1600	1/4	1/3	1/4	1/3	1	1/2	1	2	0.052
[8] >1600	1/9	1/7	1/6	1/4	1/4	1/2	1/2	1	0.027
Proximity to drainage									
[1] 0-150	1	1	3	4	4	7			0.339
[2] 150-300	1	1	2	3	3	6			0.280
[3] 300-450	1/3	1/2	1	2	2	4			0.152
[4] 450-600	1/4	1/3	1/2	1	2	3			0.121
[5] 600-750	1/4	1/3	1/2	1/2	1	3			0.092
[6] >750	1/7	1/6	1/4	1/3	1/3	1			0.039
Elevation									
[1] 1368-1500	1	1	1/2	2	5				0.218
[2] 1500-2000	1	1	1/3	2	5				0.204
[3] 2000-2500	2	3	1	3	7				0.418
[4] 2500-3000	1/2	1/2	1/3	1	2				0.111
[5] >3000	1/5	1/5	1/7	1/2	1				0.050

Table 5.10 (c): Evaluation of the consistency of the preferences used for rating the parameters and classes

Factors	n	λ_{\max}	CI	RI	CR
Lithology	9	9.38	0.05	1.45	0.03
Land use	7	7.38	0.06	1.32	0.05
Slope gradient	6	6.18	0.04	1.24	0.03
Aspect	8	8.12	0.02	1.41	0.01
Proximity to fault	8	8.43	0.06	1.41	0.04
Proximity to drainage	6	6.42	0.08	1.24	0.07
Elevation	5	5.06	0.02	1.12	0.01
All data layers (parameters)	7	7.39	0.07	1.32	0.05

The average Eigen vectors (relative weight) for each factor, in the columns are initially calculated following the steps stated under step-2 above.

The produced Landslide Susceptibility Index (LSI) based on the AHP approach is calculated on the basis of a weighed-linear combination of causative factors and classes within causative factors as given in equation 5.6. From the calculation, it was found that the LSI had a minimum value of 0.492 (low susceptibility), and a maximum value of 2.294 (very high susceptibility). The susceptibility class boundaries of the AHP method are also determined using the same approach as the FR method in reclassifying the raw LSI. Accordingly, four landslide susceptibility zones are identified with class boundaries of 0.7 (separating low-moderate), 1(separating moderate-high) and 1.4 (separating high-very high). The LSI values are re-classified in four zones or classes based on these boundaries and the susceptibility map of the AHP model is shown in (Fig 5.19). According to this method, 29% and 44% of the study area is covered by the very high and high levels of susceptibility (Fig 5.20)

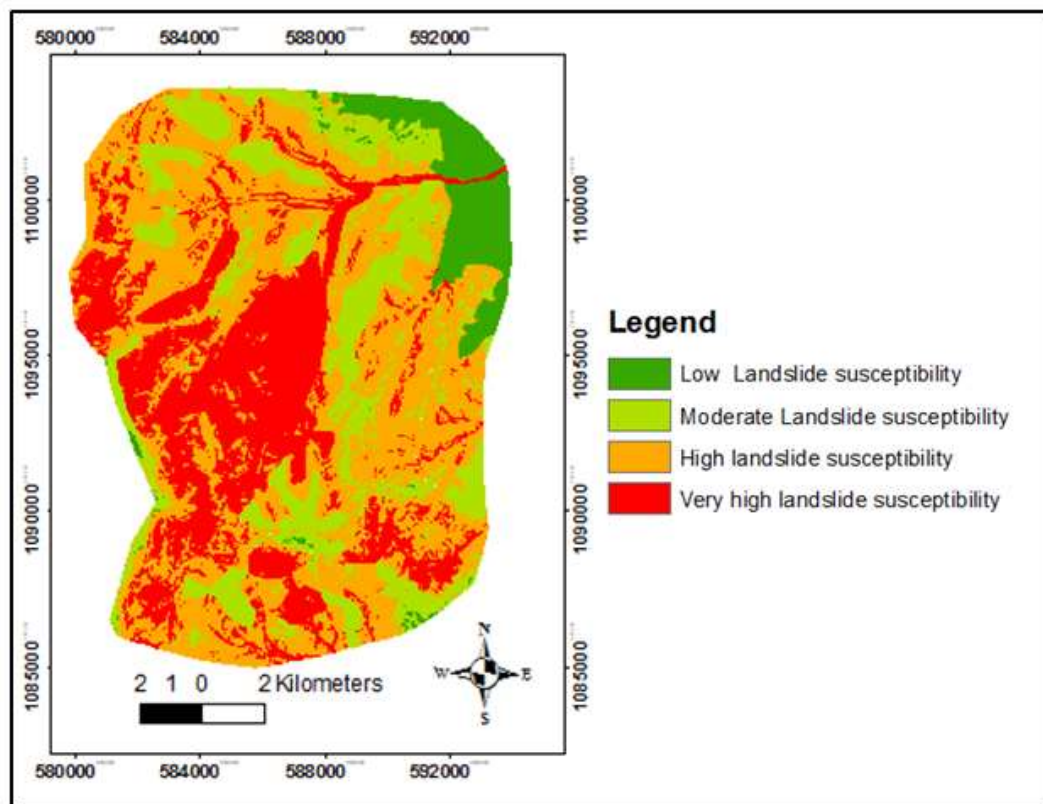


Fig 5.19: Landslide susceptibility zonation of Debresina area based on AHP method

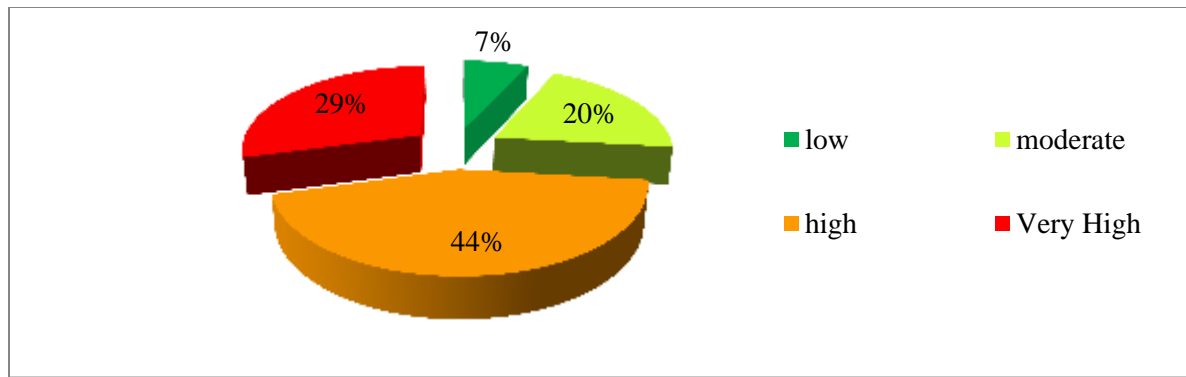


Fig 5. 20: Areal coverage of the four Landslide Susceptibility Index (LSI) classes by Percent based on AHP-method

5.4. Verification and comparison of the results of OM, FR and AHP methods

The landslide susceptibility analysis results were verified using known landslide locations, as it is usually done in related studies (Remondo et al, 2003; Lee. et al, 2005; Lee, et al, 2006; Hyum, 2009; Mezughi et al, 2012). Verification was executed by comparing the landslide inventory map with the landslide susceptibility map.

The rate curves were created and its areas of the under curve were calculated for all cases. The rate explains how well the model and factor predict the landslide. Thus, the area under curve can measure the prediction accuracy qualitatively. To create the validation curve, the computed index values of all cells in the study area were arranged in descending order and divided into 100 equal classes ranging from very highly susceptible classes to low susceptible classes. Then, the 100 classes were overlaid and intersected with known landslides to establish the percentage of landslide incidences in each susceptible class. The rate verification results appear as a line in Fig 5.21. The fitness of the rate curve can be judged by the fact that more percentage of landslides must occur in very high susceptibility zone as compared to other zones. For example, Remondo, et al (2003) states that: (1) a hypothetical “validation curve” coinciding with a diagonal from 0 to 1 would be equivalent to totally random prediction; and the further up and away the validation curve from that diagonal the better the predictive value of the model, (2) similarly, the greater the gradient in the first part of the curve the greater its predictive capability.

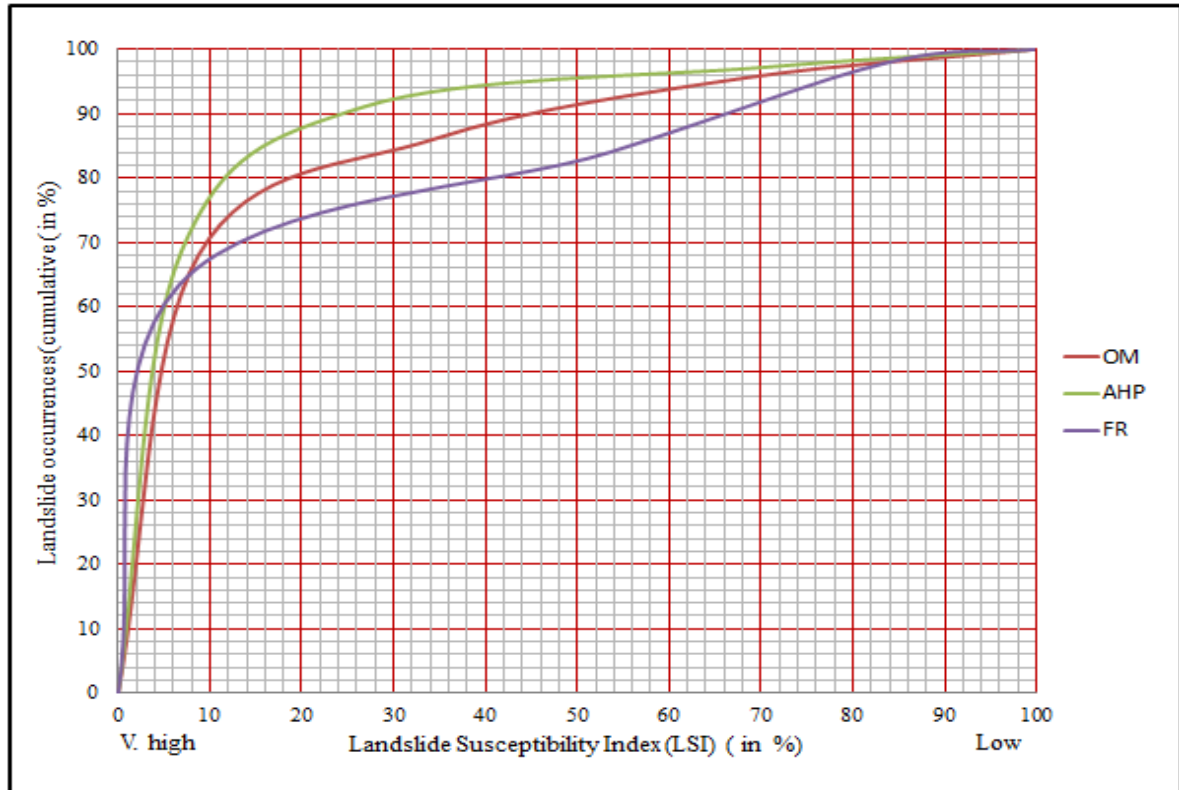


Fig 5.21: Cumulative frequency diagram showing success rate curve for susceptibility maps produced by FR, OM and AHP models (FR = prediction curve for Frequency Ratio; OM = prediction curve for Overlay Mapping and AHP = Prediction curve for Analytical Hierarchical Process method)

As can be seen in Fig 5.21, in the case of FR method, 10% class of the study area where the Landslide Susceptibility Index (LSI) had a very higher rank could explain 67% of the total landslides. In addition, the 20% class of the study area where the LSI had a higher rank could explain 74% of the landslides. In case of OM method, 10% class of the study area where the LSI had a very high rank could explain 70% of all the landslides. In addition, the 20% class of the study area where the LSI had a higher rank could explain 80% of the landslides. In case of AHP method also, 10% class of the study area where the LSI had a very high rank could explain 76% of all the landslides. In addition, the 20% class of the study area where the LSI had a higher rank could explain 88% of the landslides.

Later, the prediction of the map was validated more accurately in a quantitative manner using the Area Under the Curve (AUC) by considering that the ideal prediction will have highest AUC of 1. In this study, the AUC values were found to be 0.806, 0.846 and 0.886 for the FR method, OM and AHP methods respectively. Accordingly, it indicates that the prediction precision of the acquired maps of FR, OM and AHP are 80.6%, 84.6 % and 88.6% respectively as compared to the ideal value of 100%, which is comparatively satisfied (Fig 5.23)

The areal coverage of the various landslide classes and corresponding observed landslide percentage are also compared for all the three methods (Table 5.9 and Fig 5.22). For instance, all methods have nearly similar results at the low susceptibility zone while the result of FR method is higher at the moderate zone and lower at the very high zone as compared to the AHP and OM methods (Fig 5.22).

Table 5.11: Percentage Comparison of area occupied by each landslide susceptibility class and the susceptibility index values between OM, AHP & FR model. The LSI ranges used in the classification were assigned using manual classifier by graphing the LSI and landslide occurrences.

Landslide Susceptibility Classes				
	Low	moderate	High	Very high
Overlay Mapping method				
Area (Km ²)	19.22	56.76	73.62	69.67
Area (in %)	8.77	25.89	33.57	31.77
Observed landslide (%)	4.45	9.37	18.09	68..8
Frequency Ratio method				
Area (Km ²)	14.4	101.92	65.6	35.1
Area (in %)	6.65	46.96	30.21	16.18
Observed landslide (%)	2.03	13.92	20.61	63.4
Analytical Hierarchical Process method				
Area (Km ²)	15.03	43.22	95.24	63.66
Area (in %)	6.92	19.90	43.86	29.32
Observed landslide (%)	2.75	6.14	22.38	68.72

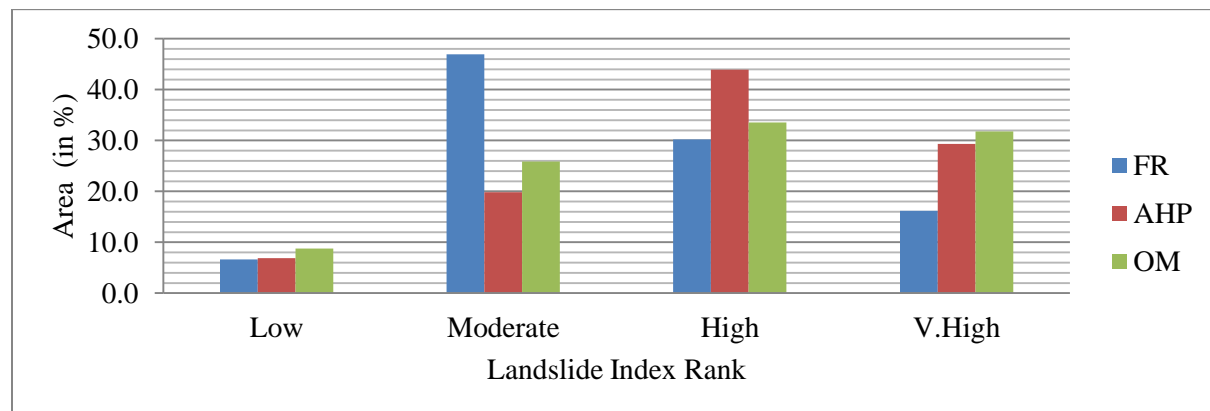


Fig 5.22: Histogram showing the relative distribution of landslide classes, for the OM, FR and AHP methods

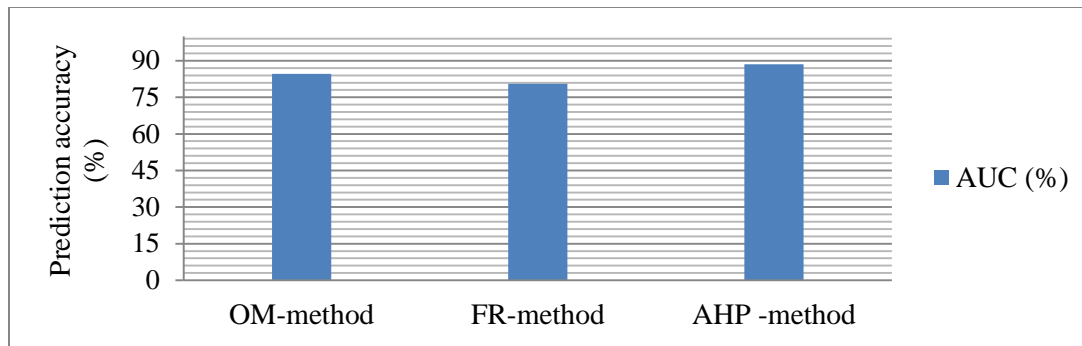


Fig 5.23: Histogram of the percentage of prediction accuracy based on Area Under the Curve (AUC) method

5.5 General characteristics and slope stability analysis of the September-2005 landslide event

The various field and laboratory description, mapping and evaluation of the landslide causative factors and landslide susceptibility analysis are presented in the previous chapters. In this section, the main interest is to elaborate the massive landslide event of the September 2005 with help of simplified and conceptualized selected sections, and conduct stability analysis assuming certain parameter. This simplified cross-section is taken along main landslide body of Yizaba Mariam which is identified as very high landslide susceptibility zone by all the three methods (OM, FR and AHP). The stability condition is checked using the Global Limit Equilibrium slope stability analysis method.

5.5.1. General characteristic of the event

The general trend of the failure planes of this massive landslide is parallel with the NNW-SSE and NNE-SSW Rift margin fault planes, having a failure length of more than 5km and width (from crown to toe) of 3km.

This massive landslide involves at the initial dominantly rock failure mass following the Rift margin faults but also incorporate a variety of earth materials (mainly the colluvium-eluvium) entrained in its path until it joins the stream. These overburden material (colluvium-eluvium) are underlain by the altered Alaje (mainly weathered tuffs) which as seen from the lower sections of the landslide scarps. The laboratory and soil classification result showed that these soils include MH, SC, SM, and CL. Thus, it is assumed that the failure surface of the landslide to be along the contact between the colluvium-eluvium deposit and underlain altered tuff. The thickness of this colluvium-eluvium material along the selected section is estimated using Geophysical Vertical Electrical Survey (VES). The estimated thickness varies from 18m to 100m averaging out to 60m. To control the geophysical results, observations and measurements have been taken along the landslide scarps lines using GPS points, DEM and Google Earth. Measured results of scar heights vary from 20m to 110m around the Yizaba and Ainemariam areas. The area of this failed mass is calculated using the

ArcGIS and is found to be 15167854m^2 . The rough volume estimation is calculated by multiplying the area and considering the minimum depth as obtained from the VES result. Therefore the minimum estimated volume of the failed mass is 303357080m^3 (i.e. approximately = $303.4 \times 10^6\text{m}^3$).

Documented historical references and studies by Evan G.S., et al (2002) illustrated that some of the massive landslides occurred in the world included the landslide of Usoy of Tajikistan in 1911 (with volume of $2000 \times 10^6\text{m}^3$), Mayunmarca of Peru in 1974 (with volume of $1000 \times 10^6\text{m}^3$), Pufu Ravine of China in 1965 (with volume of $450 \times 10^6\text{m}^3$), Yigong of China in 2000 (with volume of $300 \times 10^6\text{m}^3$), Vajont of Italy in 1963 (with volume of $292 \times 10^6\text{m}^3$) and so on. In this regard the Debresina landslide can be placed in the 4th level next to the Pufu Ravine landslide of China in terms of volume, and considered as one of massive landslides in the world.

Before directly conducting the deterministic slope stability analysis, it is crucial to qualitatively conceptualize the overall nature of landslide. Hence, the various zones (Zones I to V) of this landslide is described below in relation to the lithologies and geohydrological conditions along simplified geological cross-section as shown in Fig 5.24. The geohydrological conditons are described using the same cross-section in chapter (Fig4.8)

Zone-I

Zone-I is dominated by Tarmaber basalt flows. The vertical/sub-vertical joints and tensional fractures create a favorable condition for rainwater percolation. In some areas, inter-beds of palesol, volcanic ash/lacustrine deposits within the basalts, due to their low permeability are encouraging the emergence of springs during rainfall seasons. This section of the slope is generally acting as a recharge zone for surface as well as subsurface water flows to the down-slope areas. Rock falls and toppling are common in this zone, although they are washed away every rainy season.

Zone-II

This zone is represented mainly by the unconsolidated deposits (colluvium-eluvium) which are underlain by altered Alaje formation (various tuffs, basalts, and ignimbrites) which has low permeability. As explained above its thickness varies from 18 to 100m as estimated by the help of geophysical-VES investigation controlled by the exposed deep river cuts and scarps of the landslide.

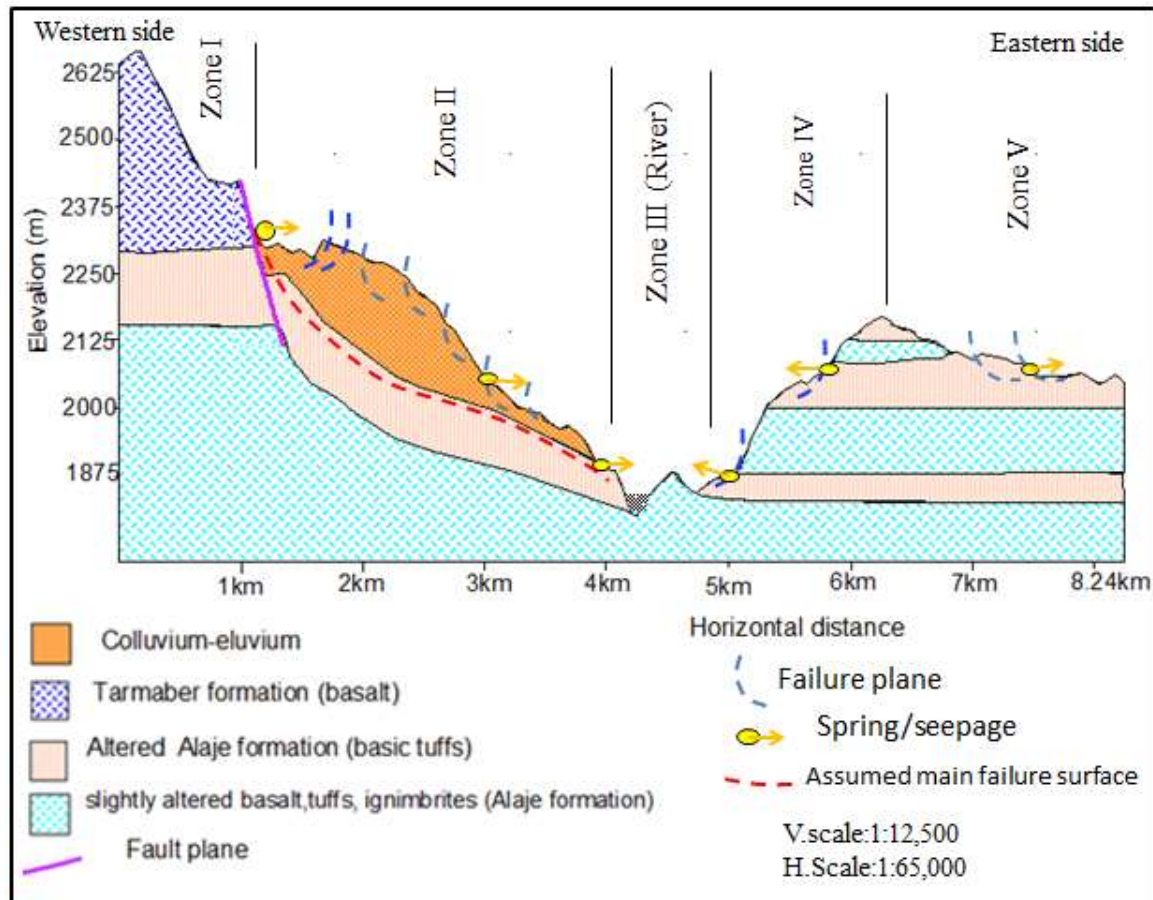


Fig 5. 24: Simplified geological cross-section across the main landslide

This section of the slope is characterized by a hummocky topography, which is associated with series of tensional fractures of en-echelon pattern. The tensional fractures and depressions have the potential to trap surface runoff and enhance groundwater recharge to the underlying mass. This zone has less well-developed drainage lines suggesting the high infiltration capacity of the colluvium-eluvium deposits. Some drainage lines that comes from zone-I disappears at the contact. Numerous springs and seepage zones emerge at the contact between the lower Alaje units, indicating that the latter are acting as barriers. In general, this section of the slope is acting not only as a zone of rainwater percolation but also as an area of groundwater accumulation from the upper sections of the slope. The head of the major landslide of the September 2005 starts at the upper fault contact with the Tarmaber basalt, and its toe is at the lower section of the Robi river channel. It has an average aerial distance of about 3km from the crown to the toe of the slide. Surface water infiltrates at the contact where the slope failure starts following the fault plane (Fig 5.25). A simplified cross-section is made along this section and the minimum safety factor is estimated.

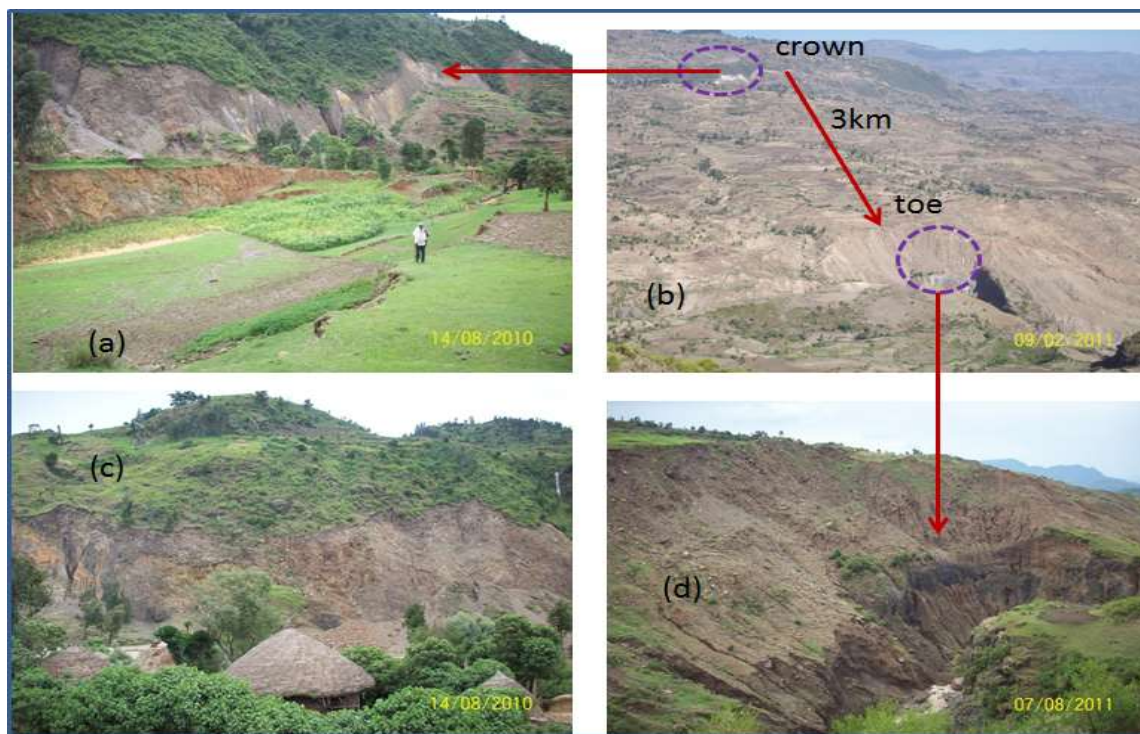


Fig 5.25: Photographs showing some characteristics of the landslide of September 2005 :(a) Zoomed photo at the crown part (b) Photo showing the distance from crown to toe of the landslide (c) Newly constructed house at the foot of the slide scarp (d) zoomed photo at the toe of the landslide

Zone-III

This zone in general is an active zone which is prone to slope instability due to the gully erosion and undercutting of the lower part of loose material in flanks of the Robi River. At this cross-section the river has a narrower section having a width of about 65m and depth of 30m. The left side of the river bank, the toe of the landslide event of September 2005, is composed by the colluvium-eluvium deposits. The right flank is dominated by weathered and fractured basaltic rock overlain by fine topsoil and pockets of colluvium-eluvium deposit. The central part of the river is full of alluvial deposit (debris) which is composed of gravel, sand, boulders, cobbles and some fines (Fig 5.26).



Fig 5.26: The nature of the various deposits and slope instability at the Robi river course and its two flanks.

Zone IV

Zone IV is dominated by Alaje formation consisting of an alternating nature of completely altered of basic tuffs/agglomerates and fractured hard rocks (either basaltic or ignimbrite). The vertical/sub-vertical joints and tensional fractures at the hard rocks create a favorable condition for rainwater percolation whereas the alternating layers of decomposed Alaje basalt/tuff or ash/paleosols within the basalts, due to their low permeability, are encouraging the emergence of springs during rainfall. This is characterized by old and reactivated landslide occurrences at the contact of the upper hard rocks and lower altered basalt/tuffs where seasonal and permanent seepage is common. In places where a gentler slope is available, a silty clay soil of 1 to 3m thick soil is available.

Zone V

This zone is topographically flat slope and hence is arable. It is covered by brownish to black color residual soil underlain by the altered Alaje basaltic agglomerates/tuff. This soil has an estimated thickness varying from 1m to 5m. The soil type includes low plastic silty clay soil (CL) to sandy silt (SM) as checked using the Unified Soil Classification system. The groundwater is shallow and shows significant variation depending on the season, i.e., from 0 m at the rainy time to 2m in the dry period. Landslide is common in this zone also. For example some residential houses (Fig 5.27, c) and the main asphalt road from Sar Amba Kidanemihret to Armaniya (Fig 5.27, a, b) have been repeatedly damaged. The footing of the poles of the National Electric Grid which passes along this zone from Addis Ababa to northern part of the country has cracked although the poles are not totally damaged to date (Fig 5.27, d).



Fig 5.27: Landslide occurrences and their impacts on Zone-V around Armania; (a) & (b) are earth slide along the road side destroying farm land also (c) Cracked house due to the landslide of August 7/2010 (d) Cracked footing of national electric grid.

5.5.2 Slope stability analysis using kinematic approach

Stereographic kinematic analysis is applied to see the impact of geological structures to the massive landslide occurrences in the study area. The kinematic analysis of the relationship of geological structures and natural slopes is used to simply indicate what kinematic modes are possible for a given slope angle without considering any lateral constraints and behavior stresses inside the unstable rock mass.

The relationship of the faults and the landslide event of 2005 are provided in Fig 5.28, a & b). The collected structural field data and slope face are also plotted using the Dip software Fig 5.29. Results show that the major part of the September 2005 landslide is a large complex landslide mainly controlled by the NNE-SSW, NNW-SSE and E-W trending Afar Rift margin faults.

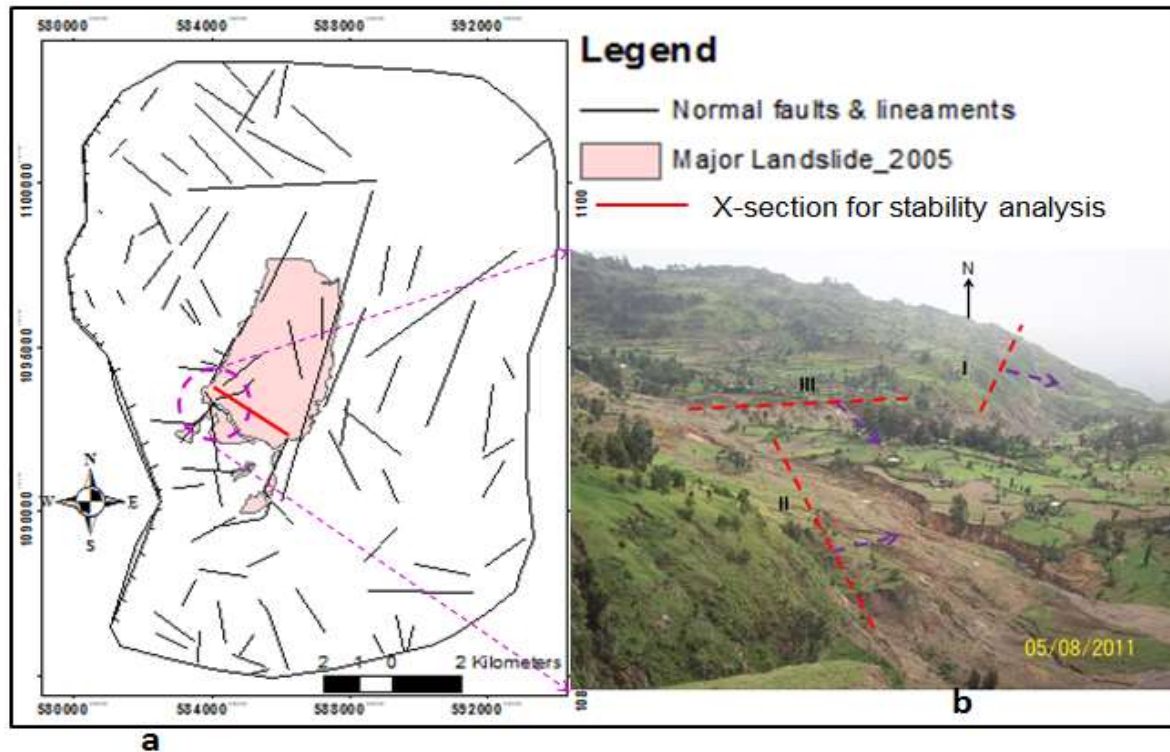


Fig 5.28: (a) diagram showing the major landslide occurred in September 2005 overlapped with the Rift margin faults (b) photograph of the landslide scarp following the trends of : (I) NNE-SSW (II) NNW-SSE & (III) E-W trending Rift margin faults

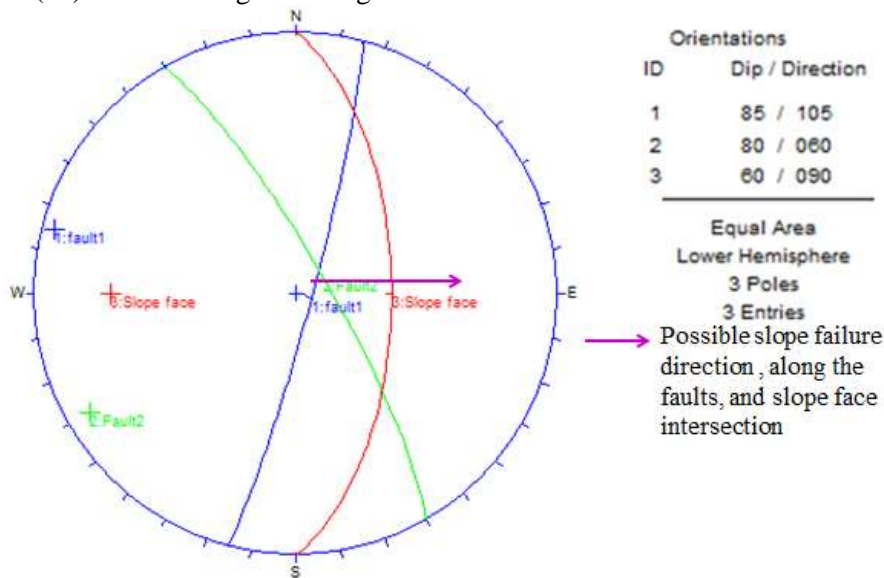


Fig 5.29: Stereographic plots of NNE-SSW, NNW-SSE trending rift margin faults and east facing slope to indicate what kinematic failures are possible

According to Hoek, and Bray, (1981) certain criteria such as the following has to be considered during the kinematic feasibility analysis: (a) The dip of the slope must exceed the dip of the potential slide plane (b)The potential slip plane must daylight on the slope plane (c) The dip of the potential slip plane must exceed the

friction angle/internal friction angle of materials and (d) The dip direction of the sliding plane should lie approximately $\pm 20^\circ$ of the dip direction of the slope

When we evaluate the Debresina landslide considering the above mentioned criteria, it combines various criteria at different parts of the length the failure plane. For example, circular/semicircular failure is common along the overburden soil or heavily fractured rock: wedge failures existed when two major structures are intersecting; plane failure following the major individual faults planes; and some toppling or rock fall when the columnar basalts are separated by steeply dipping joints. This shows that the slope failure in the area is so complex based on the various geometric arrangements of the discontinuities.

The dip of the failure plane at the junction of the three landslide scarps is variable varying from $30-75^\circ$ due to (1) the complex nature of the geological structures (2) the horizontal and the vertical variability of the lithologies and (3) surface modification of the scarps by later erosion making it difficult to fully interpret the dipping relationship of the discontinuities and the slope faces from only the surface observation.

5.5.3 Slope stability analysis using Global Limit Equilibrium (GLE) method

Slope stability analysis by means of computer software is relatively an easy duty when the slope condition and the soil parameters are known. However, understanding of the field condition and failure mechanism and thereby selection of appropriate slope stability method is not an easy task. Moreover, most slope stability analysis methods are two dimensional which simplifies the three dimensional problems into two dimensional problem from the practical point of view. Thus, with these all assumptions the slope stability of the Debresina area is checked using a Global Limit Equilibrium (GLE) method at a selected section of the landslide susceptibility map prepared using the OM, FR and AHP methods.

Practically, it is difficult to understand the three-dimension of the site as no subsurface investigations are carried out except the above mentioned geophysical VES-method. Moreover, such geophysical (VES) data acquisition and interpretation are difficult in such complicated areas without assisting borings. Thus, the simplified 2-dimension cross-section is made by the simple surface observations at a stream exposures and landslide scars integrated with the rough VES survey.

5.5.3.1 Global Limit Equilibrium (GLE) methods and general principles

Limit equilibrium study has been the most common technique for slope stability calculations. All limit equilibrium methods are based on comparison of forces and /or moments resisting instability of the mass and those that initiating instability (driving forces). These methods assume that the shear strength of the

materials along the potential failure surface are governed by Mohr-Coulomb principles to determine the shear strength (τ_f) along the sliding surface.

The shear stress at which a soil fails in shear is defined as the shear strength of the soil. The Mohr-Coulomb shear strength is usually expressed as a linear form as follows.

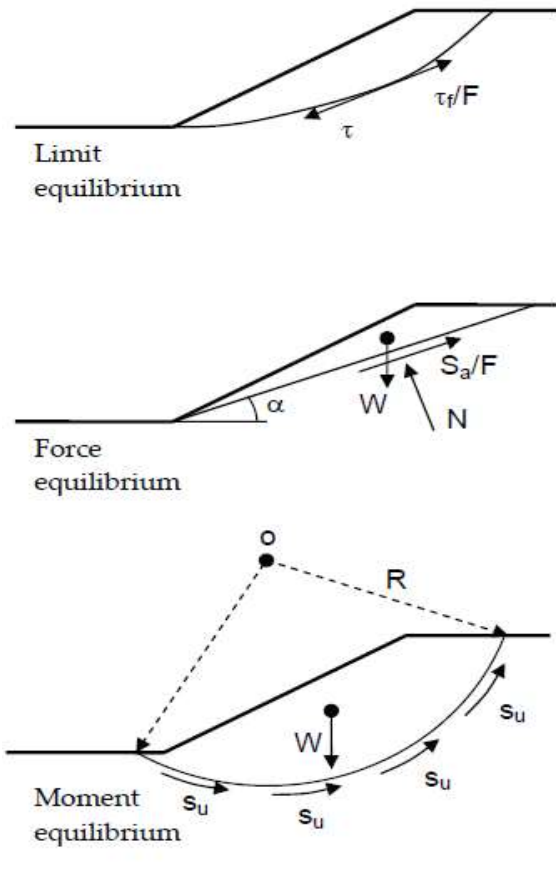
$$\text{Shear strength (available): } \tau_f = c' + \delta' \tan \phi' \quad 5.7$$

$$\text{Shear stress (mobilised): } \tau = \frac{\tau_f}{\text{SF}} = \frac{c' + \delta' \tan \phi'}{\text{SF}} \quad 5.8$$

where,

c' and ϕ' = cohesion and friction angle respectively in effective stress terms, and SF = Safety Factor.

However, the SF can be defined in three ways: Limit equilibrium, force equilibrium and moment equilibrium (Abramson, et al., 2002), which are given in Fig 5.30, as stated in Prasad (2006). The limit equilibrium definition is based on the shear strength, which can be obtained in two ways: A total stress approach and an effective stress approach. The type of strength consideration depends on the soil type, the loading conditions and the time elapsed after excavation (Prasad, 2006). As stated in the same author and references there in, the total stress strength is used for short-term conditions in clayey soils, whereas the effective stress strength is used in long-term conditions in all kinds of soils, or any conditions where the pore pressure is known. The second and third definitions are based on force equilibrium and movement equilibrium conditions for resisting and driving force and moment components respectively.



Limit equilibrium:

$$F = \frac{s_u}{\tau} \quad (\text{Total stress})$$

$$F = \frac{c' + \sigma' \tan \phi'}{\tau} \quad (\text{Effective stress})$$

Force equilibrium:

$$F = \frac{\text{Sum of resisting forces}}{\text{Sum of driving forces}}$$

$$F = \frac{S_a}{W \sin \alpha} = \frac{cL + N \tan \phi}{W \sin \alpha}$$

where,

L = total length of the sliding plane

Moment equilibrium:

$$F = \frac{\text{Sum of resisting moments}}{\text{Sum of driving moments}}$$

$$F = \frac{R \int_0^L s_u dl}{W \cdot x}$$

Fig 5.30: Various definitions of the Safety Factor (SF) (Abramson, et al. 2002) as cited in Prasad (2006).

As far as the type of methods is concerned, numerous Limit Equilibrium (LE) methods have been developed for slope stability analyses. For instance, the first method referred to as the Ordinary or the Swedish method is introduced by Fellenius (1936) for a circular slip surface. Some methods such as Bishop (1955), Janbu (1954), Morgenstern-Price (1965), and Spencer (1967) are briefed below as they can be applied in the SLIDE and Slope/w software for the limit equilibrium evaluation of slopes.

Bishop Simplified (BS) method (1955) method assumes a circular sliding surface and that the side forces on the slices are horizontal; the analysis satisfies vertical force equilibrium and overall moment equilibrium (Prasad, 2006) and references therein. It is very commonly used in practical applications for circular shear surface. This method considers the interslice normal forces (E) but neglects the interslice shear forces (T) (Abramson et al., 2002) in Prasad (2006).

Janbu Simplified (JS) method has been developed for non-circular failure surfaces, dividing a potential sliding mass into several vertical slices and the safety factor (SF) are determined by horizontal force equilibrium. Similar to the Bishop method, this method considers interslice normal forces (E) but neglects the shear forces (T).

Spencer (SP) method is the same as Morgenstern-Price except the assumption made for interslice forces. A constant inclination is assumed for interslice forces and the safety factor (SF) is computed for both equilibriums (Spencer, 1967) as stated in Prasad (2006).

Global Limit Equilibrium/Morgenstern-Price (GLE/M-P) methods (1965) also satisfies both force and moment equilibriums and assumes the interslice force function. According to this method, the interslice force inclination can vary with an arbitrary function ($f(x)$) as:

$$T = f(x) \cdot \lambda \cdot E \quad 5.9$$

where, $f(x)$ = interslice force function that varies continuously along the slip surface, λ = scale factor of the assumed function: E = interslice normal forces

A procedure of General Limit Equilibrium (GLE) was developed by Chugh (1986) as an extension of the Spencer and Morgenstern-Price methods, satisfying both moment and force equilibrium conditions (Krahn 2004; Abramson et al., 2002) in Prasad (2006).

All limit equilibrium methods are based on certain assumptions for the interslice normal (E) and shear (T) forces, and the basic difference among the methods is how these forces are determined or assumed as well as the shape of the assumed slip surface and the equilibrium conditions for calculation of the safety factor (Prasad, 2006). A summary of selected LE methods and their assumptions are presented in Table 5.10.

Table 5.12: Summary of GLE methods (modified from Nash 1987, Abramson et al. 2002) as cited in Prasad (2006)

Methods	Circular	Non-circular	$\Sigma M = 0$	$\Sigma F = 0$	Assumptions for T and E
Ordinary	√	-	√	-	Neglects both E and T
Bishop simplified	√	(*)	√	(**)	Considers E, but neglects T
Janbu simplified	(*)	√	-	√	Considers E, but neglects T
Spencer	√	(*)	√	√	Constant inclination, $T = \tan\theta E$
Morgenst-Price	√	(*)	√	√	Defined by $f(x)$, $T = f(x) \cdot \lambda \cdot E$

(*) Can be used for both circular and non-circular failure surfaces,

(**) satisfies vertical force equilibrium for base normal force, and

5.5.3.2 Selected Methods and Software

Nowadays there are several computer based geotechnical software used in the slope stability analysis. Some of the commonly used softwares in the Limit Equilibrium analysis involve the ‘SLOPE/W’, which is developed by GEO-SLOPE International Canada, and ‘SLIDE’ software, developed by Rocscience Inc Toronto Canada. In fact, SLIDE is found similar to the SLOPE/W though it has few additional features, for example groundwater analysis and back analysis for support forces. Prasad (2006) used these two software for

limit equilibrium slope stability analysis and he finally concluded that the two software computed identical safety factor within $\pm 1\%$ variations only.

In this study, SLIDE software is used for the limit equilibrium slope stability analysis the study area for the reasons that: (a) it is freely available using on line hardlock, (b) it is friendly software for user, and has similar features and functions with that of Slope/W software. Modelling in SLIDE software for the slope analysis was possible for external loading, groundwater and forces and from pseudo-static earthquakes.

The methods such as Bishop Simplified (BS), Janbu Simplified (JS), Spencer (SP), and Global Limit Equilibrium/Morgenstern-Price (GLE/M-P) methods are selected for the slope stability analysis as they are also available in the SLIDE software.

5.5.3.3 Simplified slope cross-section and input parameters

The detail field and laboratory results are already discussed in the previous chapters (in chapter 4). The input shear parameters are determined using the direct test while the unit weights are adopted from standards and handbooks of geotechnical investigation and design (e.g. Burt, 2007). The important laboratory and field features of the geologic materials present along the geological cross-section are briefed below (Fig 5.31).

- **Colluvium-eluvium (fine soil dominated):**
 - These are composed of top soils, reworked colluvium and eluvial soils of fine to gravelly size which include SC, SP, GC and CH type of soils with gravel and cobbles.
 - Their thickness, as very roughly estimated from the geophysical-VES survey varies from 5m to 45m, with average value of 25m.
 - Their cohesion (c) in KPa varies from 14 to 46, averaging to 27: their friction angle (ϕ) varies from 32 to 35⁰, averaging to 33⁰: their unit weight is referred from standard geotechnical manuals
- **Colluvium-eluvium (coarse soil dominated)**
 - These are similar to the above soils except they are coarser grains dominated. they consist of GP, SM, SC, SP. Their thickness, as very roughly estimated from the geophysical-VES survey varies from 15m to 60m, with average value of 45m.
 - Their cohesion (c) in KPa varies from 0.02 to 45, averaging to 21: their friction angle (ϕ) varies from 32 to 39⁰, averaging to 34⁰: their unit weight is referred from standards of geotechnical manuals.
- **Altered Alaje/tuff**

- These are decomposed of Alaje formation (various tuffs). These are found alternating with the hard rocks, their exposures are also found at the surface. Depending on the degree of weathering they include SC, SM, MH, CL types of soils having low permeability. Their very rough estimated thickness varies from 30 to 110m, averaging to 85m.
- Their cohesion (c) in KPa varies from 4.7 to 32, averaging to 8; their friction angle (ϕ) varies from 26° to 38° , averaging to 33° ; their unit weight is referred from standards of Geotechnical manuals.

And the rest are considered as bed rocks and hence not necessary to describe more.

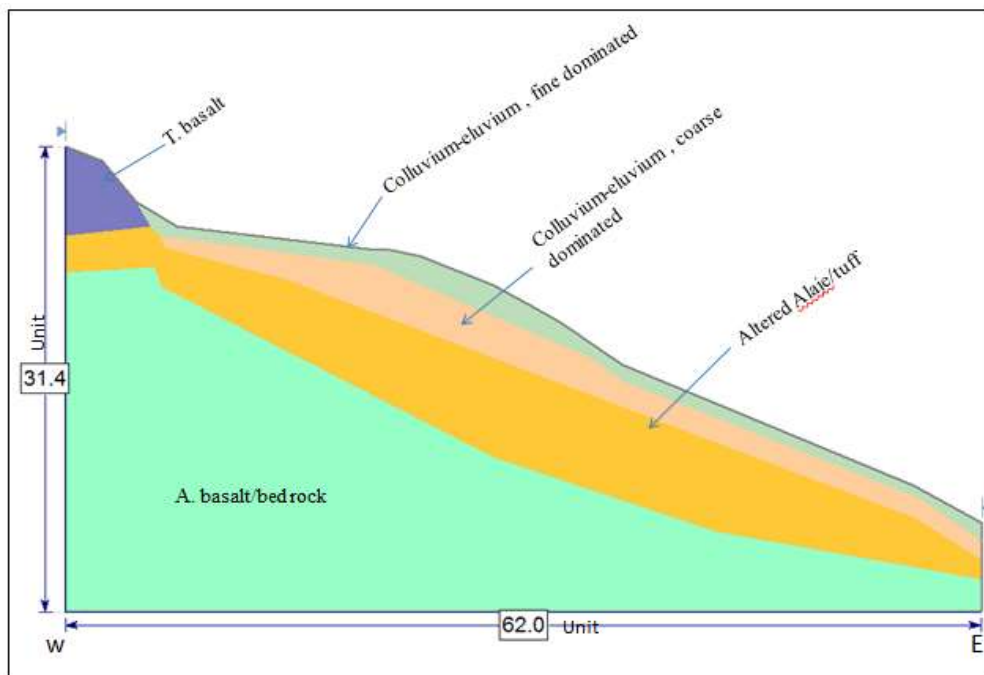


Fig 5 31: Constructed simplified geological cross-section selected for the slope stability analysis from ‘W’ (landslide crown) to ‘E’ (toe, just at the river). Note: V:S 1unit = 20m & H:S 1unit = 50m.

Regarding the earth quake coefficients of Peak Ground Acceleration (PGA) values for the Afar area of Ethiopia there are several publications and building standards with variable values ranging from 0.16g (e.g. EBCS, 1995) to 0.75g (RADIUS, 1999) for the 0.01 annual probability. In this work, the horizontal earthquake coefficient of $\alpha_h = 0.3$ is adopted for the pseudo static slope stability analysis as an average value for the study area.

5.5.3.4 Results and Discussion

To apply the softwares (e.g. SLIDE) in the evaluation of the slope stability analysis of the study area, four different conditions of loading: dry slope, wet slope, dry slope with earthquake, and wet slope with earthquake loading are considered. The load conditions analyzed are defined as:

Case I: Completely dry slope (.i.e. no GWT inside the model)

Case II: Dry slope with horizontal seismic load coefficient

Case III: Saturated slope, i.e. assumed GWT position at half of top soil layer thickness (hydrostatic pore pressure)

Case IV: Saturated slope with horizontal seismic load coefficient

The aim of considering these four various conditions are not only to evaluate the minimum Safety Factor (SF) but also to see how these various combinations of loading in the natural environment may affect the area in the future. The depth of the GWT for saturation condition is considered half of average depth of the top soil layer (at about a depth of 10m) to create similar condition with the occurrence of the landslide of September 2005 taking in to account (a) The decreasing of rainfall and associated surface runoff after mid of September in the area, (b) The comparison of monthly RF of July and August (with high RF) and that of September (with low RF) for the year 2005 (c) field observation of the position of springs at the head scarp and foot of the September 2005 landslide during the rainy and dry seasons.

To compute minimum safety factors, Mohre-coulomb failure criterion is used and the stability analysis is performed for both circular grid search composite surfaces and non-circular block search surfaces using the various method mentioned above. The calculated minimum SF are provided and compared in Table 5.11.

Table 5.13: Results of global minimum Safety Factor (SF) calculated using SLIDE software for the various combinations of conditions, Debresina area (Ethiopia).

I. Completely dry slope (no GWT inside the model)		
Surface Options	Analysis methods	Minimum-SF
Circular, grid search composite surfaces enabled	Bishop Simplified	1.996
	Janbu Simplified	1.876
	Spencer	1.990
	GLE/Morgenstern-Price	1.991
Non-circular block search	Bishop Simplified	-
	Janbu Simplified	2.053
	Spencer	2.223
	GLE/Morgenstern-Price	2.111
II. Dry slope with horizontal seismic load coefficient ($\alpha_h = 0.3$)		

Circular, grid search composite surfaces enabled	Bishop Simplified	1.087
	Janbu Simplified	1.019
	Spencer	1.091
	GLE/Morgenstern-Price	1.090
Non-circular block search	Bishop Simplified	-
	Janbu Simplified	1.191
	Spencer	1.311
	GLE/Morgenstern-Price	1.203
III. Saturated slope, i.e. assumed GWT position at half of top soil layer thickness (hydrostatic pore pressure)		
Circular, grid search composite surfaces enabled	Bishop Simplified	1.105
	Janbu Simplified	1.009
	Spencer	1.124
	GLE/Morgenstern-Price	1.118
Non-circular block search	Bishop Simplified	-
	Janbu Simplified	1.430
	Spencer	1.915
	GLE/Morgenstern-Price	1.489
IV. Saturated slope (top layer half), with horizontal seismic load coefficient($\alpha_h = 0.3$)		
Circular, grid search composite surfaces enabled	Bishop Simplified	0.564
	Janbu Simplified	0.513
	Spencer	0.607
	GLE/Morgenstern-Price	0.603
Non-circular block search	Bishop Simplified	-
	Janbu Simplified	0.938
	Spencer	0.945
	GLE/Morgenstern-Price	1.028

A slope can be classified into different susceptibility zones based on the calculated Safety Factor. For example, Pack, et al (1998) classified slopes based on Safety Factor (SF): as low landslide susceptibility (if $SF > 1.5$): moderate landslide susceptibility ($1.5 > SF > 1.25$): high landslide susceptibility ($1.25 > SF > 1$): and very high landslide susceptibility ($SF < 1$). Thus, based on the susceptibility classification of Pack, et al (1998), the calculated safety factor (SF) values for the study area (Table 5.11) demonstrate that:

(a) Low landslide susceptibility ($SF > 1.5$) - for the dry condition for both circular and non-circular failure surface

(b) Moderate landslide susceptibility ($1.5 > SF > 1.25$) - all saturated slope non-circular failure surfaces, and Spencer method in the non-circular of dry slope with earthquake load

(c) High landslide susceptibility: ($1.25 > SF > 1$) – either for the “dry slope with pseudo static seismic load” or “saturated slope conditions” under the circular surface

(c) Very high landslide susceptibility ($SF < 1$) –if the condition combines both saturated slope and seismic loads conditions at the same time.

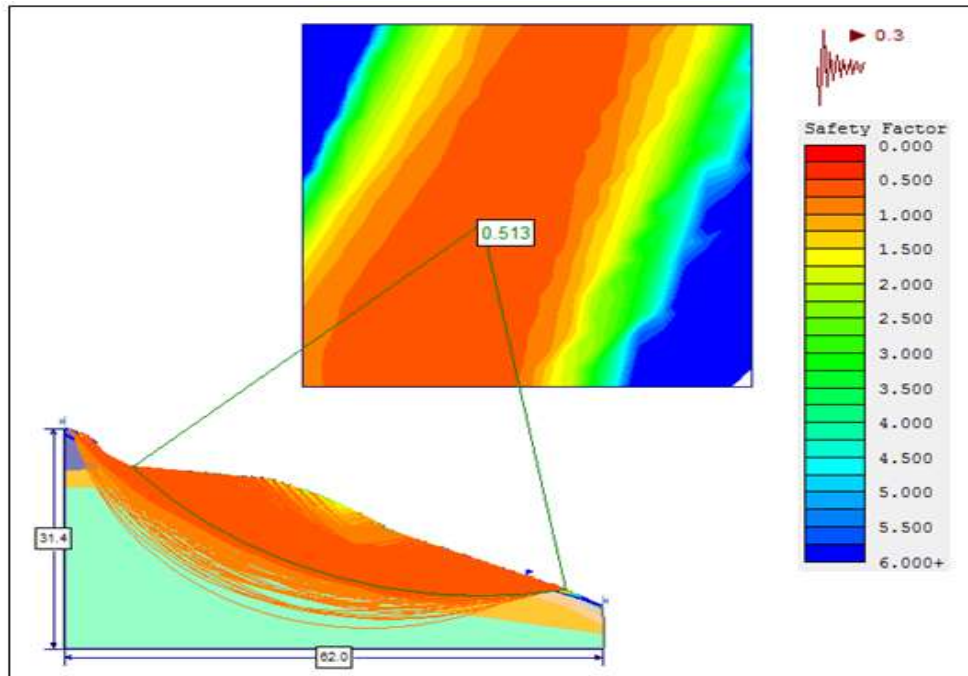


Fig 5.32: Sample interpreted global minimum Safety Factor using Janbu Simplified-method: circular failure surface under both saturated slope and horizontal seismic load coefficient value included

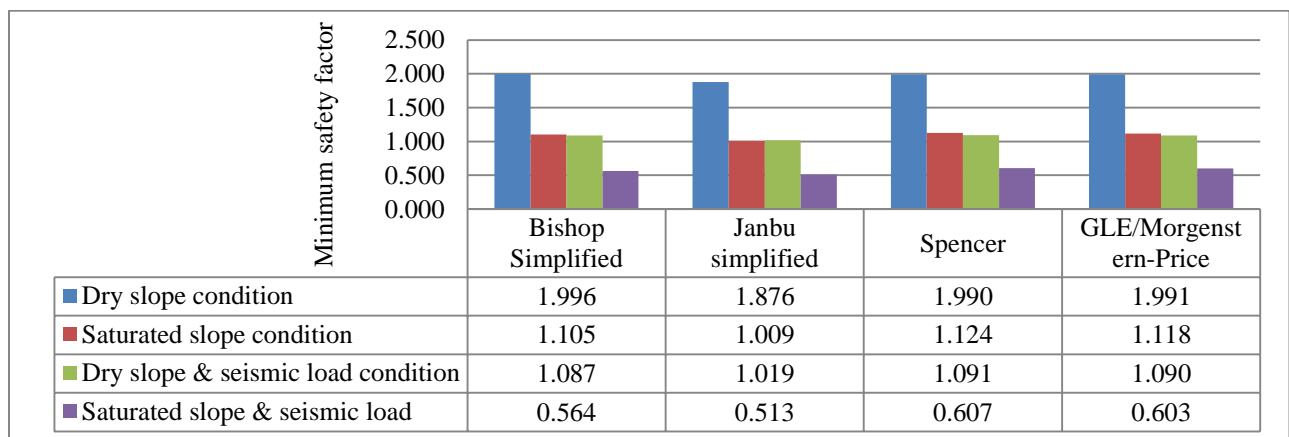


Fig 5.33: Global minimum Safety Factors for various loading conditions: using various methods and assuming circular failure surfaces.

Some concluding remarks on GLE-method:

- The BS, GLE/M-P and SP methods yield in most cases similar SF values for circular slip surfaces in all cases or conditions. However, the JS method somehow underestimated the minimum SF from other methods by around 6-10 % considering the same circular failure surface.
- In the case of the non -circular surface, the SF results show variations among the methods considering all assumed conditions, but still the difference among them is less than 10% except SP method overestimated the value up to 20% in the saturated slope condition case.
- Although, superficially the failure surfaces are complex combining circular/semicircular, planar and composite failure types following the geological discontinuities, it is assumed that the major failure surface at depth would be semi secular/circular when encountered the weak layer (altered Alaje tuffs) at depth (at about 100m). Thus, the considering the minimum SF for the circular surface could be reasonable
- The stability of the area becomes quasi-stable to unstable during the conditions where tremors of earthquake in the dry condition or increasing of the water table (saturation condition) existed, especially for those areas covered by soil layers or intensively fractured rocks which are expected to have circular failure surface. While further worst potential of slope failure possibility is created when the combination of conditions of saturation and earthquake load exists at the same time. Hence, the major landslide that occurred in September 2005 is most probably triggered by such combination of saturation and earthquake activities. This is because, the month of September in the Debresina area is the time where RF is decreased but still ground is saturated, and also several earthquakes were registered and located in the Afar rift valley and margin at that time as discussed in the previous chapters. Thus, the minimum global Safety Factor for this condition is calculated to be 0.513 (Fig 5.32) using the JS method for the circular failure surface considering the given soil parameters. However, the impact of the dynamic earth quake tremors was not included in this calculation for the lack of data and needs further analysis in the future.
- The above calculated minimum SF is performed using limited number of laboratory results and with some assumptions and therefore can only indicate the potentiality of the area for slope failure under various triggering conditions. However, in reality the geologic materials of the area are so heterogeneous laterally and vertically, requiring detailed geotechnical investigation to attain the more accurate values in the future.

6. Landslide hazard mitigation strategies and remedial measures

6.1. General

Landslides pose considerable risks to the environments, land use systems and the livelihoods of communities throughout the Ethiopian rift margins and highlands in general and in the study area in particular as development expands under pressures of increasing populations. Reactivated and new landslide occurrences are a common phenomenon in the Rift margin, especially around Debresina area due to extensional tectonic effect, high rainfall, seismic tremors, agricultural development in hazardous areas, and deforestation of landslide-prone areas. On the other hand, there is no comprehensive National Landslide Hazards Mitigation Strategy employed in Ethiopia so far. Some researchers (e.g. Woldearegay, 2005) suggested some landslide hazard mitigation strategies for the highlands of Ethiopia which include: (1) Establish an institution that could play a leading role, (2) Develop policies and guidelines on landslide risk management (3) Initiate and promote capacity building programs (4) Initiate and promote collaborative landslide hazard mapping, loss assessment and research (5) Initiate and promote landslide hazard forecasting and monitoring.

Landslide inventory and landslide susceptibility maps are critically needed and are the prerequisites for mitigation strategy of the landslide prone areas. The results and discussions provided in the previous chapters on the causative and triggering factors and susceptibility zones allow us to establish priorities that facilitate the efficient and effective use of the limited resources available for hazard mitigation in the study area. Based on this, the mitigation strategies can be grouped into structural and non-structural measures.

The overall aim of a mitigation strategy is therefore to reduce losses in the event of a future occurrence of a hazard. Thus, the main purposes of the mitigation and remedial measures of this study are to reduce: (1) the risk of death and injury to the population in the area (2) damage and economic losses imposed on public sector infrastructure, reducing losses that are likely to affect the community as whole (3) the hostile effects of the natural environmental (land degradation, loss of arable lands) and natural resources in the area of interest.

Once the landslide susceptibility mapping has been carried out and the accurate information and actual risks are identified, avoiding the problem site would become the best and easiest option. However, this option might not be the most practical one in areas where land is scarce like the case of Debresina area. Thus, it is better to see another mitigation options which are simple and economical to the site.

Thus, some of the possible non-structural and structural mitigation strategies and remedial measures which might be employed in the study area in particular and in other similar areas in general to reduce the potential impact of specific landslide hazards are provided below.

6.2 Non-structural mitigation strategies

The main step in mitigation strategy is to understand the characteristics of the hazard and causative or triggering factors. As explained in the previous chapters (chapters 1, 3, 4, and 5) the main landslide causative and triggering factors have been identified. Landslide occurrences and susceptibility maps have been produced. Characterizing and identifying the susceptibility areas into very high, high, moderate and low susceptibility areas has been accomplished.

Moreover, obtained local information indicated that the knowledge of the local community and the administrators towards the landslide hazard is very limited in the Debresina area. For this reason the landslide hazard is considered and perceived as the act of God. For example as stated in Gebresilasie (2007), about 72% of the interviewed people of the study area believed that the cause for the landslide in the landslide stricken area is by the order of God as a punishment for evil things prevailing in the area. Thus, the mitigation and remedial measures should take into consideration these conditions and beliefs. In order for mitigation and remedial measures of landslide to be feasible and sustainable, it is very crucial to note: (a) the distribution and characteristics of the landslide in the area (b) the economic capability and political realities of the country as a whole and the local community in particular (c) awareness of the local communities and administrators towards the landslide hazard (d) the type of methods to be adopted in the specific area of interest.

In such society, the remedial measures have to be taken so that they can easily be learned and implemented by institutions (governmental and non-governmental) and local communities, and at the same time result in economic benefits to the societies (woldearegay, 2005).

In this regard, some of the non-structural mitigation strategies for study area include creation of public awareness and education, pre-disaster preparedness, post-disaster recovery, establishment of early warning systems

6.2.1. Public awareness and education

Awareness and understanding of the causes, mechanisms and effects of landslides is the basis for mitigating and forecasting landslide hazards. It is therefore crucial to change the misconceptions and the present attitude of the local people by creating awareness towards the landslide and promotes capacity building programs for

all stakeholders using the scientific knowledge. This can bring a better understanding of the causes and contributing factors to land sliding. It is also crucial to formulate a mitigation measures which can reduce their vulnerability to landslides and be accepted by the affected communities. Local people, authorities/decision makers and experts should be therefore trained on landslide hazards, their mitigations and hence create awareness on society.

6.2.2 Pre-disaster preparedness

Pre-disaster preparedness is one of the hazard mitigation strategies which pursue to lessen the potential impacts of hazardous landslide processes in the area.

As landslide is a frequent activity in the area. Therefore, emergency preparedness programs are necessary to achieve a satisfactory level of readiness to respond to any emergency situation through programs that strengthen the technical and managerial capacity of governments, organizations, and communities. The local communities, authorities, nongovernmental organizations should be prepared for logistical readiness to deal with landslide disasters and can be enhanced by having response mechanisms and procedures, developing long-term and short-term strategies. The preparedness measures should also include readiness and evacuation plans; resource inventories, and so on.

6.2.3 Post-disaster recovery

Once the landslide hazard took place causing losses of life, properties and natural environments, it is necessary to recover the status to its normal previous condition and displaced people have to be returned to their home place. That is, after the emergency is brought under control, the temporary relief activities have to be changed into the normal developmental activities and the affected people have to be able to restore their lost resources and infrastructures that support them. These recovery activities should continue until all systems return to normal or better status. Information resources and services include data collection related to rebuilding, and documentation of obtained lessons.

6.2.4 Establishment of early warning systems

Early warning systems that relate the thresholds of triggering factors (RF and EQ) and the occurrences of landslide can be developed by simple registration of the date and time of occurrence of the landslide and triggering factors. This registration of landslide occurrences can be done by the local people living around the area and report it to the Woreda administrator. Then it is possible to determine the minimum thresholds of the rain fall or earthquake data, which later can be used for early warning prediction.

6.3 Structural and physical landslide hazard mitigation measures

As discussed in the previous chapters, landslides prevailed in the study area following the major structures, in areas adjacent to streams/rivers, which are affected by active stream/river incisions and gully erosion and agricultural areas. Taking into account the processes leading to instability of slopes and the social and economic conditions of the community, one or a combination of the following remedial measures are recommended: (1) Land use planning control (2) Drainage-system (3) Promote afforestation practice and reduce deforestation (4) Gully treatment and reduce stream erosion (5) Provide retaining structures, where necessary. Correction of an existing landslide or the prevention of a pending landslide is a function of a reduction in the driving forces or an increase in the available resisting forces.

Generally, a mitigation strategy can be effective and sustainable if it is easy, economically feasible, easily acceptable and participatory to the local community.

6.3.1 Land use planning

Land use planning is one of the effective and economical ways to reduce landslide losses. Especially for developing countries like Ethiopia, it is vital to establish and promote proper land-use planning and construction practices to regulate human activities that increase risk to landslides and to prevent settlement of communities in high-risk areas. It can be accomplished by: (I) discouraging or regulating new development in unstable areas or (II) removing or changing existing development. Practically, the former option is the most inexpensive and effective means for local Authorities. New developments can be forbidden and regulated in landslide-prone areas. Areas with landslide problem can be used as open space for some time or can be changed from cereal cropping pattern to commercial horticultural crops or woodland that has both income to the local community and stabilizing effect to the slope failure. On the other hand, some land uses or activities that might cause mass movement or that might be vulnerable to slope failure, such as uncontrolled irrigation, rural roads construction, uncontrolled cutting of trees can be retarded or prohibited. In general the land use planning should be updated at every planned year by preparing site-specific detailed landslide hazard maps supported by detailed geotechnical analysis.

However, peoples living at the foot landslide scarp (e.g. Yizaba and Shotel Amba) should evacuate the houses and change into another alternative site as these sites are prone to frequent occurrences of large-sized landslide and associated risks.

6.3.2 Promote afforestation practice and minimize deforestation

The destruction of forests in an area facilitates landslide (Selby, 1993). In the study area, the rises of demands for new agricultural lands are growing radically from time to time owing to the accelerated population increase. For this reason, people are cutting trees to get more agricultural lands. This long term impact of land use change from forest cover to cropland results in the extensive depletion of forests and facilitates destabilization of the slope of the study area. Therefore, to minimize the landslide, the uncontrolled tree cutting has to be prohibited and afforestation has to be promoted in the area. In this area extensive tree planting having deep rooted, combined with other measures (e.g. drainage, changing geometry of slope), may stabilize the slopes through increased support to the slope. In order to be accepted by the local community, a tree that has both slope stabilizing effect and commercial values can be selected. For example, enhancing of the eucalyptus trees planting are good examples in giving both advantages in the area. This method of mitigation strategy can be easily implemented in association to the afforestation program of the Regional government of Amhara.

6.3.3 Drainage

The application of appropriate drainage is the most effective means of mitigating landslide hazard regardless of the type of landslides due to the important role played by pore-water pressure in reducing shear strength. It is also relatively low cost method as compared with other methods. The seasonal groundwater seepages and surface water have a sound impact on triggering the landslide in the area. Hutchinson (1977) has indicated that drainage is the principal measure used in the repair of landslides, with modification of slope geometry.

For example, surface and groundwater drainage system can be one of the main mitigation mechanisms for the landslide along the main Road of Debresina-Armaniya site. As inspected during the field work, the groundwater in this area is very shallow which is highly affected by the seasonal variation. The depth of the groundwater here varies from less than 0.2m in the wet season to 1-2m in the dry season. Seepages are common at the sides of the road slope where the slope failures are common.

The surface water (seepage and springs) can be collected into a collection chamber and connected to a drainage channel to remove the water safely from the landslide zone. This water can be used for drinking water, or small irrigation activities or micro power generating or mills which are common in the area.

6.3.4 Gully treatment and reducing stream erosion

As discussed in chapter 4, the analysis of landslide with drainage proximity shows that, areas found within a radius of 150m from the streams are highly prone to landslide due to the incision effect of the streams. Significant amount of crop lands are extensively being eroded and collapsed, and because of this several farmers become landless.

Check dams are one of the known methods to protect undercutting of gullies, if properly design with appropriate drainage (spill way) and good foundation of less scouring effect are accomplished. It can be also supported with afforestation works.

6.3.5 Providing retaining wall structures

Placing retaining structures generally increases the stability of slopes by increasing the resistance to movement. These methods could be applied to mitigate the landslide that occurred at the side slope of the road cut of the Debresina-Armaniya main asphalted road and around the foundation of the main poles of National Electric Grid that pass near Armaniya village (Figs 6.1and 6.2).This method can be used in combination with the appropriate drainage system. It was observed during the field work that this retaining work is already started in some part of the mentioned road (Fig 6.1).



Fig 6.1: Construction of retaining wall along the road cut of Debresina -Armaniya main asphalt road to mitigate the potential slope failure

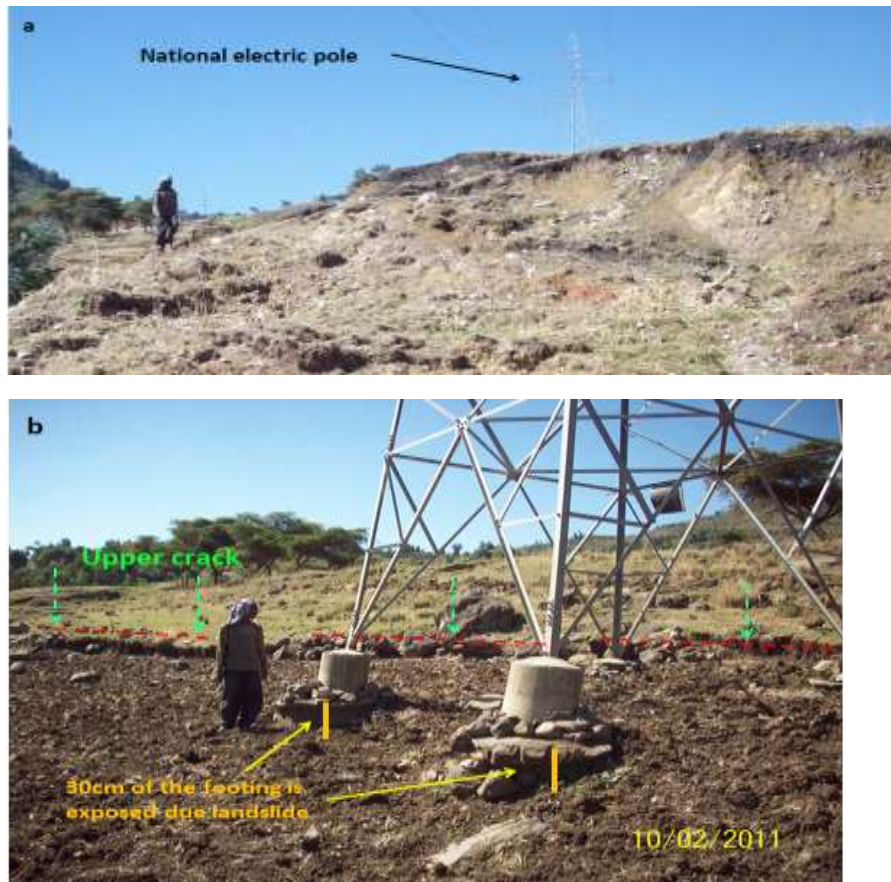


Fig 6.2: Photo showing the landslide occurrences at the foundation of the national electric grid pole at Armaniya, specific name of Tikure Chika: (a) at a distant overview and (b) zoomed view of the pole foundation

7: Conclusions and recommendations

7.1 Conclusions

The Rift margins and highlands of Ethiopia have been frequently affected by new and reactivated landslide occurrences. Debresina is one of the areas that are highly affected by such landslides found in the Northwest (NW) highlands of Southern Afar rift margin. The frequently occurring landslides have damaged the road sections, massive farm lands, local houses, crops, water sources and natural environments. For example, the September 2005 landslide event is the largest and complex event of all the landslides reported in the country so far, destructing massive agricultural lands and crops, several local houses, natural environments, and infrastructures in the study area.

This study mainly focused on the landslide study of the Debresina area, representing the Afar Rift margin, with main objectives of: (1) generating landslide inventory map (2) preparing the maps of various causative factors and evaluating their contribution to the occurrences of landslide and its frequency in the study area (3) evaluating the landslide susceptibility zoning of the area accordingly (4) suggesting landslide hazard mitigation strategies which can serve to the local community based on the final susceptibility maps of the area of interest.

All the methods and approaches used in this research included: (a) Inventory and identification of more than 160 landslides (b) remote sensing and field based detailed survey of causative factors data collection and mapping (c) Laboratory analysis of some physical and geotechnical properties of soils and rocks (d) Data analysis and evaluations using GIS-based qualitative and quantitative methods and (e) Development of landslide susceptibility map and zonation.

In this study, four different methods: Overlay Mapping (OM), Frequency Ratio (FR), Analytical Hierarchical Process (AHP) and the Global Limit Equilibrium (GLE) slope stability method were applied to identify areas susceptible to landslides in the study area. To achieve this objective, seven major landslide inducing factors were taken into consideration which includes Lithology, Proximity to faults/lineament, Proximity to drainage, Land use, Elevation, Slope, and Aspect. These factors were evaluated, and weights were assigned for each factors or classes based on the criteria of the methods used.

General features and characteristics of the Debresina area

- Debresina area is one of the areas located in the high seismic zone, with relatively high annual rainfall (1922 mm). It is characterized by gentle to steep slope gradients, dense drainage system & deep river cut and gully erosion, with elevation range of 1368 to 3100 m a.s.l. The middle and lower parts are densely populated and intensely cultivated. East and South east facing steps of flat terraces and cliffs are commonly attributed to the Afar Rift margin faults systems
- Geologically, the area is totally covered by the disturbed Tertiary volcanic terrain inter-bedded by pyroclastic materials and their weathered products (quaternary sediments) i.e. it is covered by Alaje formation (basalts, rhyolitic/trachytic ignimbrites, various tuffs, and agglomerates), Tarnaber formation (basalts) and quaternary sediments (alluvial, colluvial-eluvial deposits, fine residual soils). As part of the Afar rift margin, it is formed by the cross cutting extensional tectonics (normal faults) and hence the rocks are intensively fractured and weathered.
- It is observed that the physical and chemical weathering has played significant role in changing the stability of slopes, by forming clayey soils along fault zones and fractures. In addition, the weathering of pyroclastic material result in the production of clay-sized particles, but with little amount of clay, principally kaolinite and illite. The clay minerals such as kaolinite, halloysite, smectite, illite and the likes that can contribute to the slope failure are identified using the XRD analysis and using the Casagrande plasticity chart.
- Diffused seepages and several springs, which appear at the interface where fractured rock overlays the weathered part or where there is paleosol between the various lava flows, are common as seen at the landslide-affected sites. The area has suffered severely from mass movement problems.
- Field inspection and characterization of the September 2005 massive landslide in the area shows that: (1) it is the largest known landslide event in Ethiopia so far having an average length of 3km from crown to toe, and a width of greater than 5km, covering more than 15 km² (2) it is a very complex and composite type of failure consisting of bedrocks, debris and earth materials and has a rotational, translational and combined type of movement (3) evaluation of the faults data and slope face kinematically using the DIP software revealed that the major part of the September 2005 landslide is a large slope failure controlled by the NNE-SSW, NNW-SSE trending rift margin faults (4) in general, the occurrences of several EQ in September 2005 within the Afar rift (e.g. Hararro-Dabbahu areas) and its margins (e.g. near Ankober area) seems the most probable final triggering factor although rainfall also played a big role in bringing the slope into its marginal instable condition.

GIS-based landslide susceptibility mapping and prediction (OM, FR and AHP-methods)

Landslide susceptibility map preparation is a main step in attempting comprehensive landslide hazard management. Nowadays, such type of maps can be prepared by GIS-based qualitative and quantitative techniques. In this work both the data derived model (Frequency Ratio) and knowledge derived models (OM and AHP) were applied for the landslide susceptibility mapping of the Debresina area. As a result, the integrated methods of both data derived and knowledge derived models are shown to be useful for landslide susceptibility mapping.

Overlay-Mapping (OM) method

- The OM method is a type of heuristic (indexed) approach commonly utilized by the regional government of Sardinia (Italy) to study and evaluate hazards and risks, with their mitigation measures in the region. As a semi-quantitative method, it involves the knowledge of expertise and indexing method. This method considers only three main environmental factors such as Slope, Litho-technical and Land use factors in the evaluation process of the slope instability of an area.
- Results of the input factor analysis showed that the areas covered by colluvium-eluvium, various tuffs, clay soils, with slope range $>36\%$, land uses with arable, riverbed and poor vegetation cover are highly prone to landslide
- According to the PAI boundary classifier, four distinct Landslide Susceptibility Index (LSI) zones are identified, namely: low (9%), moderate (26%), high (33%), and very high (32%). This depicts that about 65% of the area is susceptible to landslide.
- The Overlay Mapping method is therefore reasonably appropriate method in the landslide susceptibility assessment, especially for medium and large scale landslide mapping. However, it may be limited to apply in regional scale as it needs detailed field geo-mechanical characterization consuming longer time

Frequency Ratio (FR) method

In this method, seven causative factors involving: Lithology, Proximity to fault, Land use, Slope, Aspect, Elevation and Proximity to drainage have been chosen as inputs for the landslide Susceptibility evaluation based on the site condition. The relationship between the landslide distribution area and the landslide-related factors is evaluated quantitatively using the FR methods and the results showed that: (1) The areas covered by colluvium-eluvium, debris deposits, various tuffs and clay soils, with slope range of 10° - 40° , with river course and arable type of land use, with proximity to fault of 0-600 m and to drainage of 0-300m, with elevation of 2000-2500m, with aspect to E and SE are highly prone to landslide (2) The landslide susceptibility zonation has identified four zones, namely as very high (16%), high (30%), moderate (47%) and

low (7%) zones (3) The produced landslide susceptibility map of the FR-method has reasonable prediction to the field condition, and mega landslide fall within the very high landslide susceptibility zone.

Analytical Hierarchical Process (AHP) method

The same landslides causative factors were used in the AHP method as the case in the FR method. The relative ratings assigned to the different causative factors or classes and relative weights have been calculated. The relative importance of causative factors/classes on the initiation of landslide and susceptibility of the study area is evaluated based on the relative weights, and consistencies are checked. The findings of this evaluation demonstrated that: (1) the three major influencing factors to induce land sliding activity (judged from its given weight) in the Debresina area are lithology (37.2%), proximity to fault (24.5%), and proximity to drainage (16.2 %). Then, followed by the other factors such as Aspect, Slope, and Land use having relative weight of 7.5% 7.4% and 7.2% respectively and elevation (2.9%), (2) the areas covered by: (a) colluvium-eluvium (41.5%), debris deposits (17.7%), various tuffs (16%) and residual clay soils (6.4%) (b) with slope classes 10°-25° (35.5%), 25°-40° (23.6%) and 5°-10° (15.8%), (c) land use of river course (50.9%), arable land (19.9%) and bare land (7.9%) (d) proximity to fault of 0-400m (24.4%), 400-600m (21.8%), 600-800m (19.6%), (e) proximity to drainage of 0-150m (33.9%), 150-300m (28%), 300-450m (15.2%) (f) aspect of Southeast (22.8%), East (21.5%), South (12.7%), North (12%) and (g) elevation of 2000-2500m (41.8%), 1368-1500m (21.8%), 1500-2000m (20.4%) are highly prone to landslide (3) the landslide susceptibility map generated with AHP has identified four zones, namely as very high (29%), high (44%), moderate (20%) and low (7%) zones. According to this method 73% of the area is prone to landslide.

Global Limit Equilibrium (GLE) method

A simplified geological cross-section is made along the main failed area of Yizaba to evaluate the Safety Factor. The SLIDE software has been used in the evaluation of the slope stability analysis of the study area. Four different conditions of loading; dry slope, wet slope, dry slope with external loads (earthquake), and wet slope with earthquake loading are considered. The load conditions analysed are defined as:

- **Case I:** Dry slope (.i.e. no GWT inside the model)
- **Case II:** Dry slope with external forces (e.g. horizontal seismic load coefficient)
- **Case III:** Saturated slope, i.e. GWT on the surface (hydrostatic pore pressure)
- **Case IV:** Saturated slope, with horizontal seismic load coefficient

The aim of considering these four various conditions are to evaluate the minimum Safety Factor and also to realize how these various combinations of loading may affect the natural environment in the future.

To compute global minimum Safety Factors Mohre-Coulomb failure criterion is used and the stability analysis is performed for both circular grid search composite surfaces and non-circular block search surfaces

using the various methods and loading conditions mentioned above. The calculated minimum Safety Factors are provided and compared in Table 5.11. Then, the slopes are categorized into different susceptibility zones based on results of the calculated Safety Factor as per Pack et al (1998) into: (1) Low landslide susceptibility ($SF > 1.5$) represented by the dry condition for both circular and non-circular failure surface (2) Moderate landslide susceptibility ($1.5 > SF > 1.25$) for the non-circular surfaces except in Janbu Simplified, (3) High landslide susceptibility ($1.25 > SF > 1$) for both “dry slope with pseudo static seismic load” and “saturated slope” conditions under the circular surface and (4) Very high landslide susceptibility ($SF < 1$) represented by the saturated slope with seismic load conditions. The minimum Safety Factor is calculated to be 0.513 using the Janbu Simplified method for the saturated condition with earthquake load, which has similar condition to the September 2005 massive landslide.

The calculated Safety Factors remain always greater than 1, except when a Horizontal Seismic Load coefficient is introduced into calculations; this means that according to results of the Global Limit Equilibrium analyses the earthquake has been the ultimate triggering factor of the September 2005 massive landslide

Verification and comparison of the results of OM, FR and AHP methods

Finally, results of the OM, FR and AHP methods are verified using known landslide locations (i.e. the landslide inventory map). It is therefore witnessed that:

- Small percentage of landslides are observed in the low LSI-classes while high percentage of landslides are observed in the higher LSI classes in general in all the methods. In this case the percentages of observed landslides in the low classes varies between 2 % in the FR method to 4% in the OM method while in the very high classes it varies between 63.4 in the FR method to 68.8 in the OM method indicating that landslide zonation maps can be considered as well predicted in all the methods applied.
- The rate curves were created and its areas of the under curve (AUC) were calculated for all cases. Thus, the prediction of the map was validated more accurately in a quantitative manner using the AUC by considering that the ideal prediction will have highest AUC of 1. Output maps provided by the OM, AHP, and FR methods were compared and their credibility was examined by the AUC method using known landslide locations as reference. The validations of results show that all the three methods have a satisfactory accuracy, with AHP method (88.5%) being the highest, followed by the OM method (84.6%) and FR method (80.6) being the lowest methods, as compared to the ideal value of 100%.

Consequently, the verification results showed satisfactory agreement between the susceptibility map and the existing data of landslide locations.

- The other verification method of the results, is also done by correlating all the three susceptibility maps with the massive landslide events of September 2005 (which have more than 15 km² areal coverage), occurred in the specific localities called Yizaba Mariam and Shotel Amba. In all the three maps, this area is mapped as high to very high landslide susceptibility validating the fairness of the results.

Finally as a concluding remark, all the study results of the three methods presented herein have shown the great potential of GIS-based landslide predictions. The results shown in this thesis can use as a basic data for preliminary slope management and land-use planning of the study area in particular and in other similar areas in Ethiopia in general. However, one must be careful while using these models for specific site development. This is because such specific areas need detailed investigations for site-specific decision-making.

Mitigation strategies and remedial measure options

The landslide inventory and landslide susceptibility maps of the study area, which have been prepared in this study are useful in the planning of mitigation strategy of the landslide hazard of the area. The following non-structural and structural mitigation strategies are recommended for the Debresina area to minimize losses from frequently occurring landslide hazards based on the study results.

- **Non-structural mitigation strategies for study area include:**
 - **Public awareness creation and education:** local community, authorities/decision makers and experts should be trained on landslide hazards, their mitigations and hence create awareness on society.
 - **Pre-disaster preparedness:** emergency preparedness programs such as developing long and short-term readiness strategies, communication systems, evacuations plans and resource inventories etc. are necessary to achieve a satisfactory level of readiness to respond to any emergency situation.
 - **Post-disaster recovery**-once the landslide is occurred, a restoration plan should be developed by the government and community to recover the losses to its normal condition
 - **Establishment of early warning systems:** promoting collaborative landslide hazard mapping and research work on the establishing of thresholds of triggering factors (RF and EQ) to the landslide should be developed
- **Structural and physical landslide hazard mitigation measures**
 - Taking into account the processes leading to instability of slopes and the social and economic conditions of the study area, one or a combination of the following remedial measure options

are recommended: (1) land use planning control (2) drainage-system (3) promoting afforestation practice and reduce deforestation (4) gully treatment and reduction of stream/river erosion (5) providing retaining structures, where necessary (e.g. at road sides, electric grid poles)

7.2 Future research works

The following recommendations can be provided for further action and landslide research in the Afar rift margins:

- The obtained information indicated that the knowledge of the local community and the administrators towards the landslide is very limited in the study area in that the landslide hazard is considered and perceived as the act of God. For example, as stated in Gebresilasie (2007), about 72% of the interviewed people of the study area believe that the cause for the landslide in the area is by the order of God as a punishment for evil things prevailing in the area. For such reasons the local people are not ready to do any mitigation and remedial actions. Hence, intense training that change the attitude of the people is necessary.
- Rainfall and earthquake are the main triggering factor of landslides in Afar rift margins of Ethiopia. Therefore, monitoring of: (a) rainfall and groundwater fluctuations and understanding of the hydrological process and (b) earthquake data are critical for proper hazard mappings and predictions on rift margins by establish landslide-groundwater and landslide-rainfall relationships as this could be used for developing early warnings of landslide hazards in the rift margins of Ethiopia
- Landslide and landslide generated hazards are one of the major natural hazards causing tremendous losses in the country but no attention is given to it at this time. Thus, a continuous research work on landslide and related hazards in rift margin and highland terrains is highly recommended to increase the level of understanding on both local and regional scales to finally reduce the damages and risks prevailing on intense environmental degradation and failure of major infrastructures
- Instead of the fact that there are frequent occurrences of landslides and damages in the study area in particular and rift margins in general, there is no historical record of landslide showing the time of occurrences, its magnitude, traveling distances, triggering factor, and associated damage. It is therefore crucial to establish a landslide inventory data at least in the major areas known for their landslide hazard in the country to properly address and predict the time of occurrences, expected magnitude and travel distances as well as associated damages.
- In order to evaluate better the influence of critical factors for slope instability, further detailed geotechnical investigations, geophysical and topographic survey should be performed, especially at

the major landslide of September 2005 found in Yizaba and Shotel Amba localities, which caused losses more large number of local houses, agricultural lands and infrastructure at the study area.

Part- III: Rio San Girolamo area (Sardinia, Italy)

8. General characteristic of the study area and the Campidano Rift

Rio San Giorlamo basin is the second study area, found in the margin of Campidano graben of Sardinia, Italy. Thus, chapters 8 to 12, discussed here below are about this area.

8.1. Regional geological and structural setting

The regional geology of the area is characterized by the Paleozoic basement and quaternary sediments. The Paleozoic basement, which crops out on the western edge of the Campidano graben, includes a thick metamorphic complex and granites. The former is the oldest geological unit characterized by variable degree of metamorphism and constituted by alternating metasediment (sandstones, siltstones, claystone, mudstones, and conglomerates), metavolcanics. Granites are extensively fractured at the transition to piedmont deposits and significantly altered even in depth (Barrocu, 1971) as cited in Balia, et al (2009). Out of the 24,046 km² areal coverage of Sardinia, about 55% of the territory is occupied by Paleozoic rock outcrops, and the rest 45% is occupied by lithologies related to the Mesozoic and Cenozoic formations (Carmingnani L. et al, 2001) as cited in the progetto IFFI, Regione Sardegna (2005). Further, the complex Paleozoic metamorphic rocks cover 25% while the plutonic complex covers 30%,

Quaternary sediments mainly consist of old alluvium, piedmont deposits, recent alluvium and marine sands. The old alluvium deposits are made up by fan fluvial and alluvial sediments, in turn composed of conglomerates, gravels and sands more or less compacted, often in a silty clayey ground and red in colour due to ferric oxide. Piedmont deposits are made up by coarse clastic material while the recent alluvium, the most characterizing of the plain, include alluvial, colluvial, aeolian deposits and littoral gravels. Whereas marine sands lie along the coast-line, and silty clayey deposits in the lagoon-salt works area (Carmignani, et al. 2001) as cited in Balia, et al (2009).

From a tectonic point of view (Fig.8.1), Sardinia constitutes together with Corsica a primarily Palaeozoic formation, which mainly consists of intrusive granites, intruded during the Hercynian orogenesis (300 million yrs BP: Van Dommelen,1998).These granites form a huge N-S running mountain chain, which makes up the entire central and northeastern parts of Sardinia as well as the tiny peninsula of Capo Falcone together with the accompanying island of Asinara in the extreme North-West of Sardinia (Van Dommelen, 1998).With the declining of the effects of the Hercynian orogenesis in the Tertiary era, rifting activity commenced during the Oligocene in the western Mediterranean basin, when the Corsica-Sardinia block begins its detachment from

southern France and the counterclockwise drift towards its present position. The rift valley was stretching in the N-S direction, from the gulf of Asinara to the gulf of Cagliari.

In the Middle Pliocene, a new subsidence cycle, affecting the southern part of the rift, generates the Campidano graben (Figs 8.1 and 8.2), whose filling is constituted by the same Oligocene-Miocene and Quaternary products characterizing the study area, and by Pliocene sediments. As indicated by Previous works based on several boreholes drilled for water supply, the quaternary sediments could reach a thickness of at least 150 m on the Capoterra plain, but the stratigraphy to volcano-metamorphic basement is still substantially unknown (Balìa R., et al, 2009).

Although both tectonic and volcanic activity continued until the beginning of quaternary period at the eastern half of the Campidano rift valley, their intensity gradually declined at the Pleistocene period with a nearly negligible factor in the general shaping of the Sardinian relief (Cherchi, et al, 1978; Seuffert, 1970). Extensive Holocene deposits which constitute the most recent group of geological formations dominate the two rift valleys of the Campidano and Cixerri.

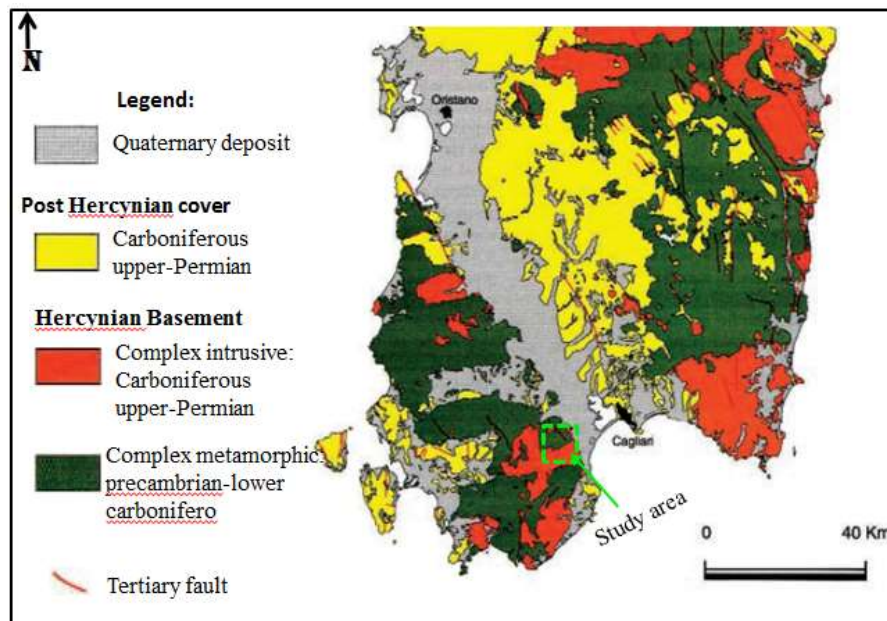


Fig 8.1: Regional geological of map sotheren and central Sardinia, including study area (adopted IFFI-2005)

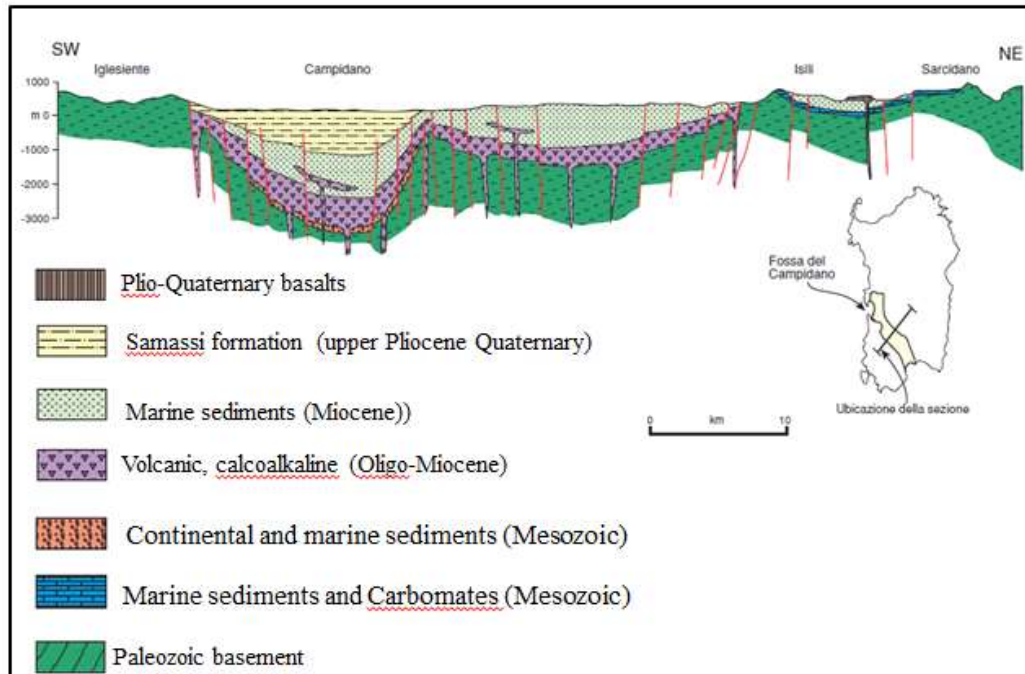


Fig 8.2: Geological cross-section across the Campidano rift based on aeromagnetic data, after Balia, et al (1991)

8.2. Physiography and climate

The regional geomorphology of the area can be grouped into several distinct landscapes and types based on nature of geology, geo-tectonic phenomena and prevailing surface processes (e.g. erosions). The region of west central Sardinia (Fig 8.3) represents all the three major Sardinia geomorphological landscapes. Broadly speaking, the region is delimited to the South and to the West by respectively the high and steep mountains of the Iglesiasiente and the Gulf of Oristano, while the northern and eastern margins are dominated by the Monte Arci massif and two vertically rising mountains. A prominent central place in the region is occupied by a vast plain, roughly orientated NW-SE, which constitutes the middle part of the much larger Campidano plain.

The low and gently rolling relief of the central Campidano is incised by two NW-wards running rivers (Riu Mannu and Riu Mògoro) and their tributaries that drain the hills and mountains on either side of the plain.

The highlands of west central Sardinia are located on either side of the Campidano plain, and are made up of mountain ridges and hills. The former are to be found both to the West of the Campidano plain, where the Monte Arcuentu and Monte Linas represent the Iglesiasiente mountain range, and to the East of it, where the Monte Arci rises somewhat isolated. The Sulcis-Iglesiente-Arburese is a territory with characteristics of irregular morphological and orographic and geological features.

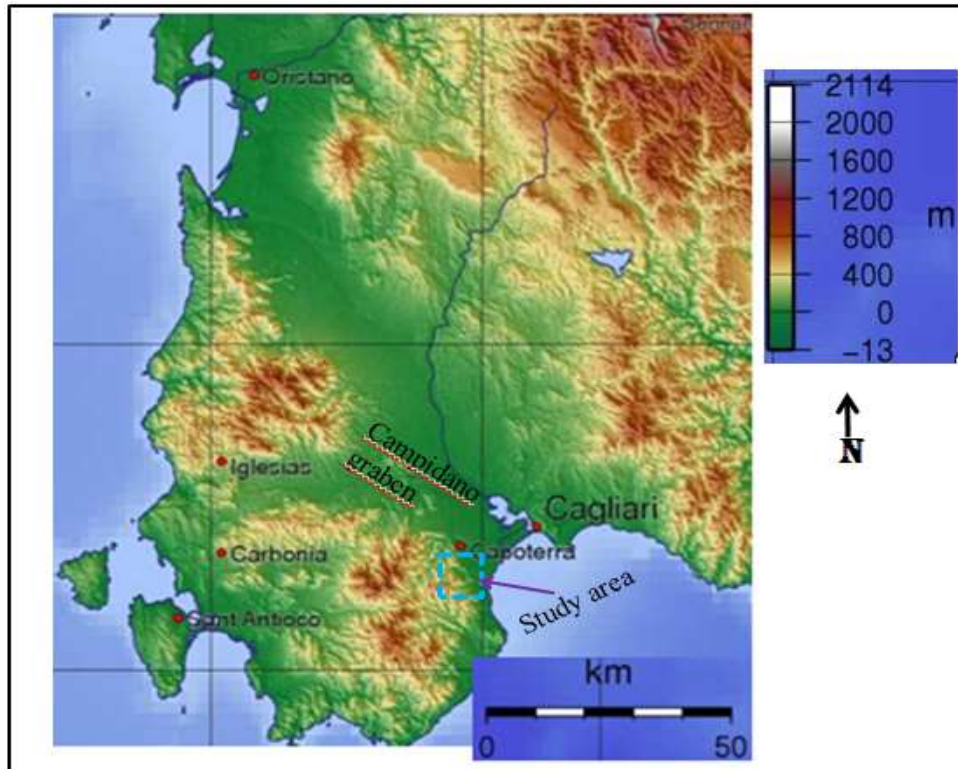


Fig 8.3: Geomorphological and structural divisions of southern and central Sardinia/from DEM

The wet period in the area extends from October to March of the year. The annual average rainfall in the rift margin represented by the Capoterra meteorological station is 533mm while that of the rift valley varies from 510mm in Decimomanu station to 526mm in Uta station. This shows that there is no significant difference like the case in Ethiopia in the annual average rainfall between the rift margins and the rift floor although the margins show a bit higher affinity. Similarly, both the rift margin and rift floor have nearly the same average minimum and average maximum temperatures ranging from 10 to 12°C and from 27 to 28°C respectively. The maximum monthly temperature is recorded in the months of July and August while the minimum temperature is in the months of January and February.

8.3 Landslide status and regional trends at the rift margin

Land slide inventories have been carried out in Italy under the project called IFFI-Project. The aim of this work was to: (a) identify and map landslides over the whole Italian territory, based on standardized criteria (b) build up a National Landslide Geographic Information System (c) provide a tool for hazard and risk assessment and land use planning. The institutions involved in the IFFI-Project are: (a) geological survey of Italy/Land Protection and Geo-resources Department, with the task of organizing and coordinating the activities, developing the guidelines, verifying the data conformity, building up a national geo-database and a

Web GIS (b) regions and Autonomous Provinces (e.g. the Sardinia Region), responsible to gather historical documents, archive data and map the areas affected by landslides.

The summary of the main points of the inventory result of the Sardinia region is provided below

8.3.1 Spatial distribution and number of landslides

In the inventory study 1,523 landslides and related processes have been surveyed, and their computerized data base with maps and tables have been created and provided (Table 8.1 and Fig 8.4).

Table8.1: Distribution of landslides in the Sardinian provinces

Province	IFFI	Landslide	Areas	Total area in Landslide (km ²)
Cagliari	409	76	167	20.895
Nuoro	631	162	245	116.67
Oristano	70	34	19	8.254
Sassari	413	45	303	41.853

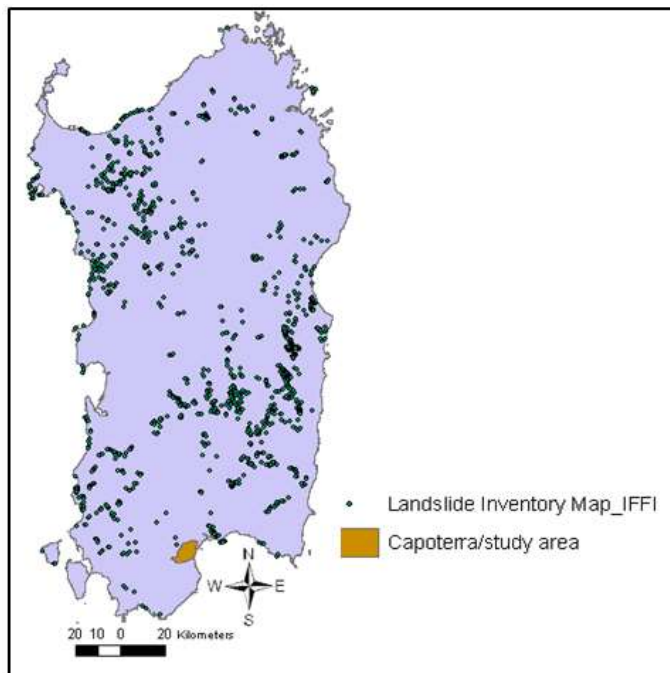


Fig 8.4: Landslide inventory map of Sardinia (adopted from Progetto IFFI-2005)

(Note: IFFI–Inventario Fenomeni Franosi in Italia)

8.3.2 Type of movement

According to the landslide inventory, the frequent and wide spread types of landslide include all types of rock fall/topple (>60%), rotational/translational slides (18%), diffused shallow landslide (10.24%), and complex failures (5.25%) (Fig 8.5).

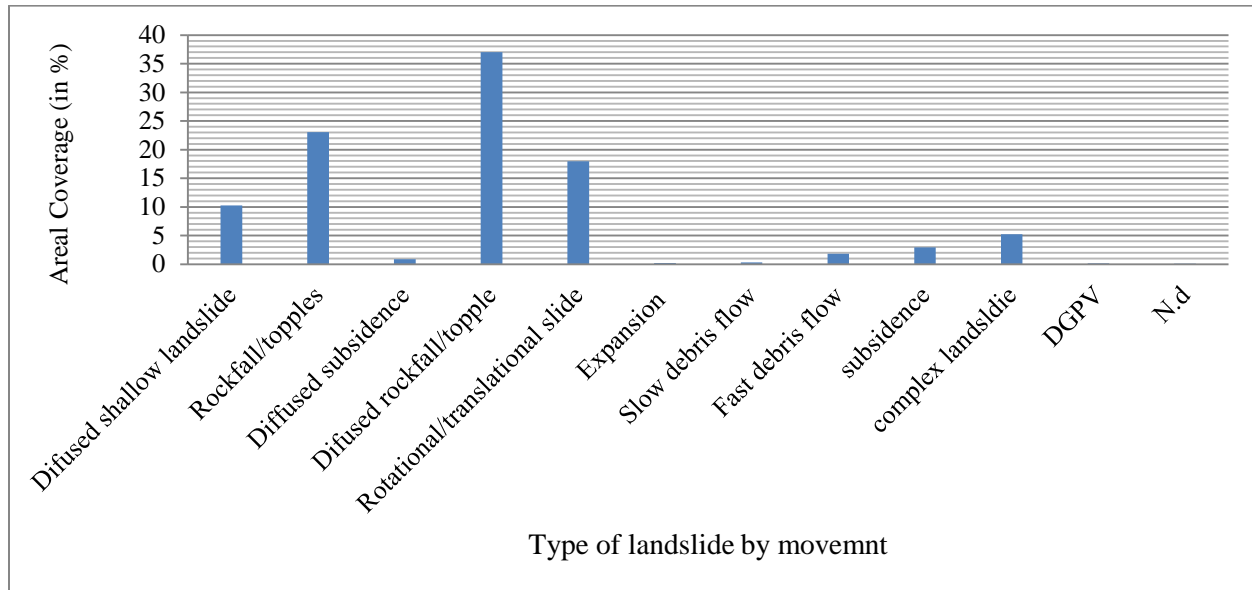


Fig 8.5: Percentage of landslides by type of movement in Sardinia (Progetto IFFI, 2005)

8.3.3 Regional distribution of landslide types by lithologies

The main lithologies prone to the various landslide processes in the region of Sardinia involves (Fig 8.6) carbonate rocks (25.11%), debris (13.28%), acidic intrusive rock (9.56%), metamorphic with few to non-foliated rocks (9.45%), metamorphic with pervasive foliation (7.51%), effusive lava and pyroclastic (6.1%) and the likes. The study area is covered by the acidic intrusive (granitic complex), Paleozoic metamorphic and debris, which are identified as regional level also as landslide prone lithologies.

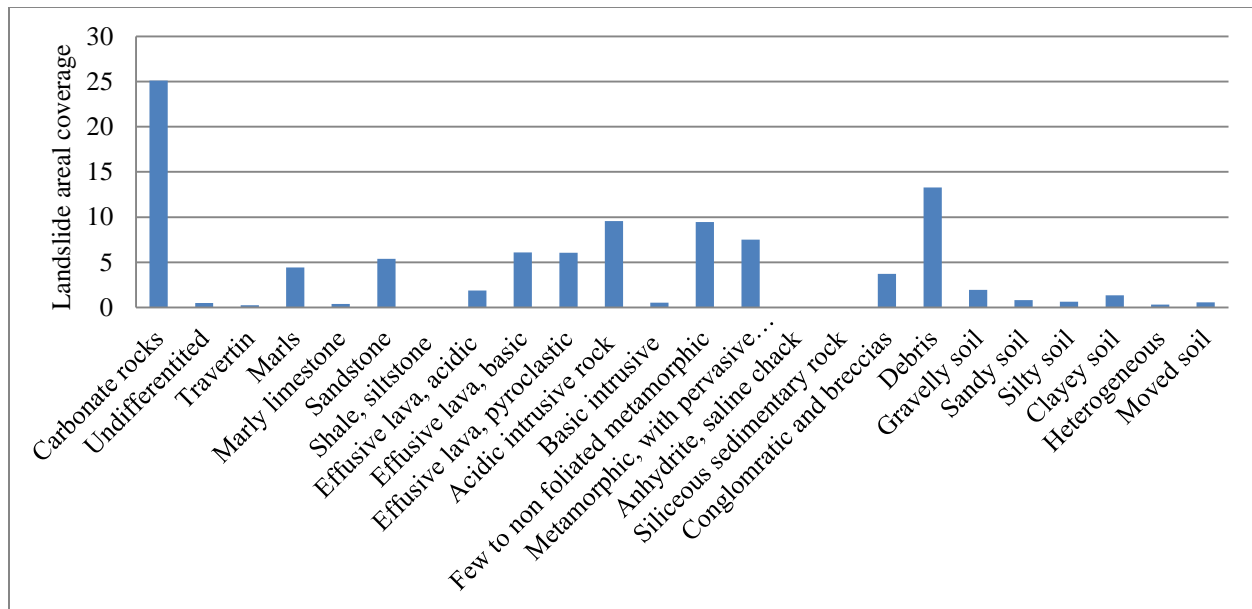


Fig 8.6: Landslide percentage by lithological classes in the Sardinia region, Italy

8.3.4 Damages caused by the landslides

The main damages identified by the IFFI-Project in the Sardinia region involve (a) more than 800 are non - differentiated (n.d), (b) about 450 roads (c) more than 100 agricultural lands and the likes (Fig 8.7).

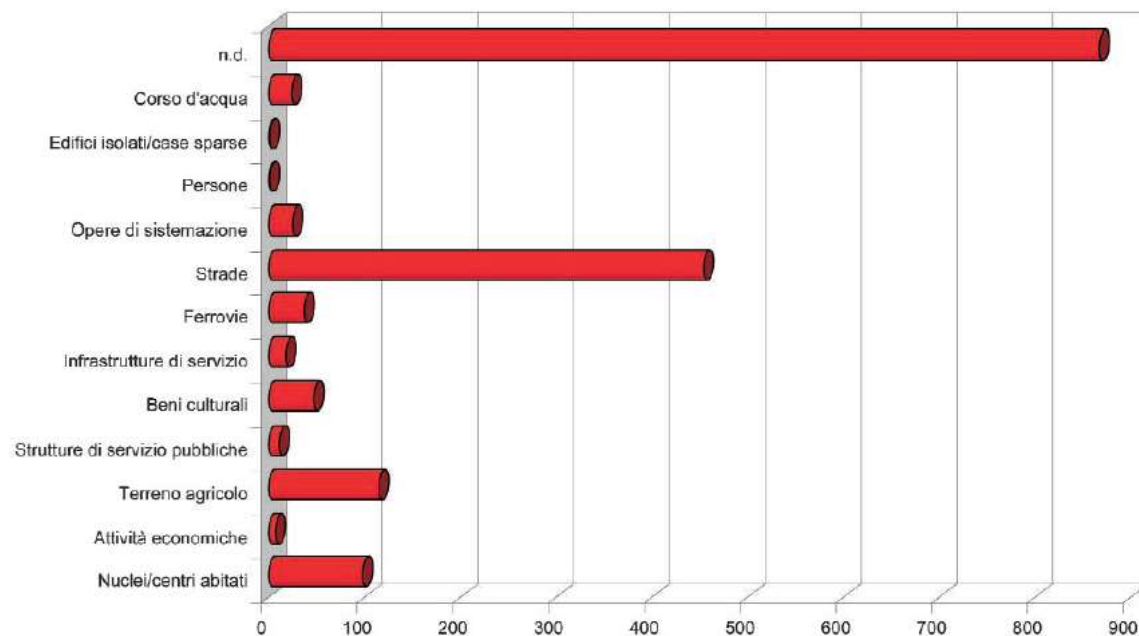


Fig 8.7: Number of landslides by type of damage.

8.3.5 Landslide Index (LSI)

The total regional Landslide Index is calculated by dividing the total landslide area to the overall regional area of the Sardinia region while the Landslide Index of the mountains and hills only are also calculated. The results are given in Table 8.2.

Table 8.2: Landslide Index values

Total area of region (km ²) (A)	Mountain/hilly areas (km ²) (B)	No. of landslides (C)	Total area of landslide (D)	Density of landslide processes (C/A)	Total regional Landslide Index % (D/A)	Landslide Index of MT/hills % (D/B)
24046	18151.45	1523	187.67	0.0633	0.78047	1.03393

8.4. Background and problem definition of R.S. Girolamo basin

Landslides are a widespread hazard in many mountainous and hilly regions of Europe and cause significant economic losses as well as human victims (Hervás J., 2003). Different historical studies (Catenacci, 1992; Trigila and Iadanza, 2008; Salvati, et al, 2010) showed that Italia is one of the European countries known for their geo-hazard, especially by various types of landslides and flooding. In the years between 1945 and 1990, landslides and floods were responsible for 3,488 (which is 45.4%) of the total 7,688 fatalities due to natural hazards in Italy and cost the national economy some 17, 000 million Euro (Catenacci, 1992).

The total areal extent of Italia is about 301,470km² and out of which 26% are alluvial plains (having an elevation <300m and slope < 3°): 43 % are hills (having slope > 3° and elevation between 300-600m) and 31% are mountains (areas having > 600m). Due to its relief, lithological and structural characteristics, Italy is a country with frequent, high and very widely spread landslide risk causing maximum disasters and the high number of victims next to earthquake (Trigila and Iadanza, 2008). A national landslide inventory has been conducted in Italy by the Institute for Environmental Protection and Research Geological Survey of Italy (³ISPRA) under the IFFI⁴ Project from 2004 to 2007. As indicated in the report of Trigila and Iadanza (2008), about 482,272 landslides inventory are surveyed covering an area of approximately 20,500 km², which is equivalent to 6.8% of the Italian territory. In the meantime, 5708 Italian municipalities (accounting 70.5% of the total number) are affected by landslides. The information obtained from the landslide inventory report is summarized below in table form.

³ ISPRA = Istituto Superiore per la Protezione e la Ricerca Ambientale.

⁴ IFFI-Inventario dei Fenomeni Franosi in Italia

Table 8.3: Types of landslides (by %) as compared with total landslide coverage in Italy (modified from Alessandro T. & Carla L., 2008)

S.N	Landslide type	% of coverage
1	rotational/translational slides	32.5
2	slow earth flows	15.3
3	rapid debris flows	14.6
4	areas affected by numerous shallow landslides	5.67
5	complex landslides	11.3
6	rock fall/topple and areas affected by them	14.6
7	non differentiated (N.d)	5.54
8	others (deep seated slide, lateral slide, sink hole)	0.49

In the landslide inventory work of Trigila and Iadanza (2008), the types of landslides were assessed in relation to the frequency distribution of the slope angle and the results show that: (1) the instability of the slopes does not increase with an increase in the slope angle and a range of slope angles has been statistically found within which there is the maximum occurrence of the landslides (2) two groups of occurrences were clearly identified from the slope-landslide frequency distributions curves (a) rapid or extremely rapid landslides such as falls/topples and rapid debris flow, have a peak at between 30° and 40° (b) slow earth flows, rotational/translational slides, complex landslides and areas affected by numerous shallow landslides have a peak at between 10° and 15°.

Landslide and flood risk of Italy was also assessed by Salvati et al, (2010) using the historical landslide and flood events that have resulted in loss of life, missing persons, injuries and homelessness in Italy, from 1850 to 2008 at both national and regional levels. According to these researchers, Italy is a country where landslides and floods killed or injured people almost every year. This landslide and flood risk study (Salvati, et al, 2010) carried out in the period 1950 to 2008 summarized that: (1) landslide events with casualties were 969 (i.e. 16.4 events /year) and flood events with casualties were 613 (10.4 events/year) (2) the number of landslide and flood events with casualties varies in the Italian regions. Landslide events with casualties ranged from 5 (0.1 event/year) in Emilia-Romagna to 231(3.9 events/year) in Campania, and flood events with casualties ranged from 8 (0.1 events /year) in Umbria to 73 (1.2 events/year in Piedmont (3) the flood risk in Italy is largest in the Piedmont and the Sicily Regions, while the lowest in the Umbria and Basilicata Regions, with the other Regions experiencing intermediate levels of landslide and flood risk (4) inspection of the historical catalogue indicated that the causes for the high landslide risk in the northern Italy (e.g. Trentino-Alto Adige) and in the southern Italy (e.g. Campania) are different. In the northern part, the landslide risk is primarily due to a combination of multiple types of fast-moving landslides, including rock falls, rock slides,

and debris flows. In the southern part, harmful landslides concentrate in the area surrounding the Vesuvius volcano, and are chiefly soil slides, debris flows, and debris avalanches that involve loose volcanic materials.

Several towns in Italy are located at the alluvial fans where debris flows and flash floods occur episodically in these alluvial fan environments. Due to this, the communities living in such area are at high risk during intense and prolonged rainfall. One of these towns is the Capoterra area where the study area is found. The study area (Rio San Girolamo Catchment) is situated in the Sardinia island of Italy and is prone to landslide generated debris flow and debris flooding. The Capoterra administration, which includes the study area, is regionally identified as one of the areas of high landslide hazardous (HG3) areas in Sardinia as stated in the Piano di Assetto Idrogeologico (PAI), carried out on the basis of Legge 18 Maggio 1989. The landslide inventory report of Trigila and Iadanza (2008) shows that, a total of 1523 landslides covering an area of 188km² are identified in the Sardinia region.

Historical records are significant for studying the overall condition (initiation, transportation, deposition, magnitude, frequency) of the debris flow and help us to be able to predict its future characteristics by relating them with various causative and triggering factors. Nevertheless, such data on the debris flow of the area of interest are not available except some event based information. For example, as obtained from regional documents of forestry and environmental surveillance (<http://www.sardegnaigitallibrary.it>) and <http://www.unpassoavanti.net/> and other sources, the Capoterra Poggio dei Pini, Pirri, Frutti d'Oro II, Montserrat, Assemini and Uta areas were stricken by flooding and debris flow hazards in the 28-29 October 1985, 14-17 October 1986, 12-13 November 1999, 5-6 April 2005, 22 October 2008. The main drainages responsible for such hazard consist of the River Santa Lucia, Rio San Girolamo, Santa Barbara that flow from the western Capoterra Mountain towards E and SE joining the Mediterranean Sea. Many small towns and villages including the study area are located at the eastern foot of the mountains and alluvial fans.

During the events of 1985 and 1986, there were no casualties except over flooding of agricultural lands but the events of 1999 and 2008 caused more strong threats to the local community. By the flooding and debris flow event of October 2008, 4 people were dead, roads, bridges, water supply and sewerage pipelines and houses of dwellers of Poggio dei Pini were destructed, and several vehicles were damaged and dragged to the Mediterranean coast. In such circumstances, the evaluation of the frequency of debris flows helps the understanding of the relations between basin conditions, with particular regard to basin morphological evolution and sediment supply processes, and debris-flow occurrence (Jackson et al., 1989).

It is, therefore, crucial to better understand and recognize: (1) the behavior and type of landslide hazard in order to design preventive strategy (2) strategies of prevention and warning signatures and to build alert systems so that expected damages on both lives and properties can be minimized.

Even though the regional landslide and flood related risks were identified by the inventory work, these problems are still continuing to damage life and properties, and devastate the environment at various localities of the country including the study area. This is due to the facts that:

- The results of studies of landslides and related hazards in one area may not be applicable to other areas as there are significant variations with the site specific catchment parameters such as geology, slope, relief, land use, precipitation regimes, governing the geo-morphometric phenomenon etc. For this reason site specific landslide investigation and characterization of the causative factors and failure mechanisms are crucial.
- Several towns in Italy, including the study area, are located at the alluvial fans where debris flows and flash floods occur episodically in these alluvial fan environments. Due to this, the communities living in such area are at high risk during intense and prolonged rainfall.
- Flow like landslide, especially debris-flows have potential discharges several times greater than clear water flood discharges from the same catchment and possess much greater erosive and destructive potential (Davies, 1997; De Scally and Owens, 2004; Jakob and Hungr, 2005). Hence, it is very important to identify the debris flow sources from that of the normal flooding in catchment.
- Most of the actions taken by the decision-makers, at various levels of the government, focuses on emergency issues instead of studying and planning preventing strategies that reduces the losses
- In the study area there is little appreciation of the threat posed by such debris phenomena, especially until the year 2008. This is exemplified by the recently constructed buildings along the fan (the green house research area and environmental protection research center)
- No susceptibility map of potential risk areas existed which could serve as an input for the preliminary mitigation planning. For this reason urbanization and intensification of infrastructures in the sloppy area is still going on.

For such reasons, understanding and evaluating of the various landslide processes and identifying of areas susceptible to landslide are quite important. Therefore, this research work intends to reduce the continuity of the landslide related problems of the study area through the identification of the potential hazards, evaluation of the various causative factors and develop the susceptibility map of the study area.

9. Description of the Rio San Girolamo area and data preparation

9.1 Location of study area

Rio San Girolamo is situated at the southern part of Sardinia, Italy found at about 20km South west of Cagliari city. It is part of the Capoterra communal administration, in the particular locality of Poggio dei Pini. Its geographic location (using WGS84) varies from 493450mE to 498900mE and 4331269 to 4335100mN (Fig9.1). As part of the Capoterra watershed, the study area belongs to the sub basin of Flumendosa-Campidano-Cixerri region.

Access to small town of Poggio dei Pini and to some part of the catchment area is possible by car but the rest most part of the study area can only be accessed on foot.

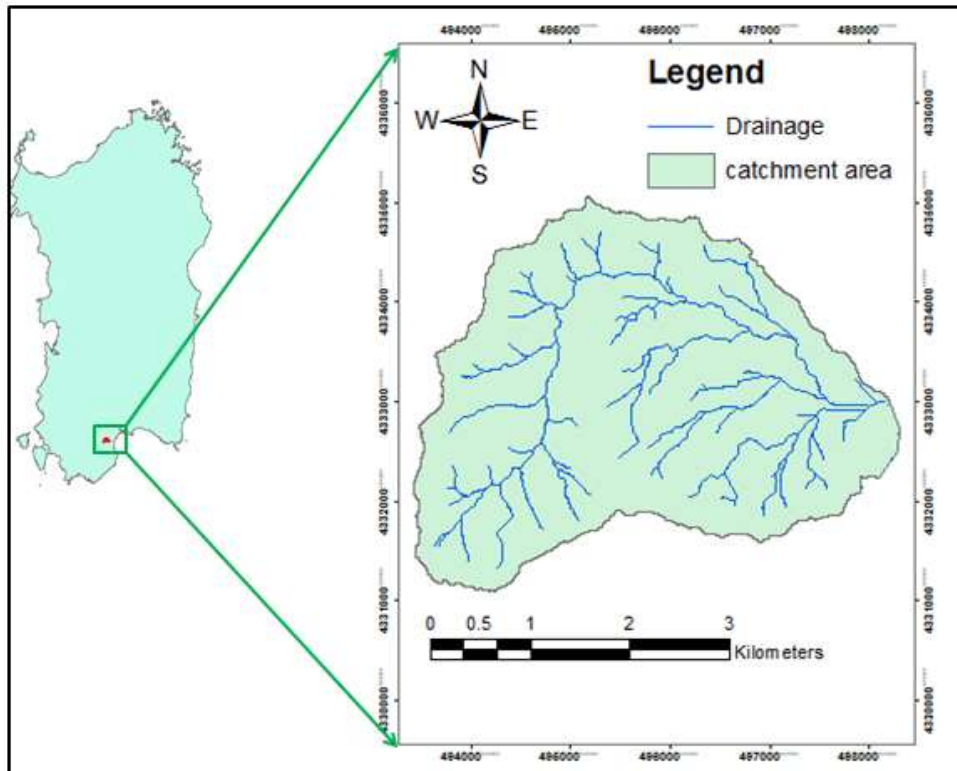


Fig 9.1: Location map of Rio San Girolamo

9.2 Triggering factor

Rainfall and rapid stream erosion on the other hand, are one of the potential triggering factors for slope failure in the R.S.Girolamo basin. However, the triggering impact of earthquake is not considered here, as in the case of Debresina area (Ethiopia) because the R.S.Girolamo area is one of the seismically inactive areas in Italy.

Italy is relatively known for its knowledge on relating the triggering factors (rainfall and earthquake) to slope failure as compared to Ethiopia and other countries. However, it is not still easy to get long term recorded historical data that relates these triggering factors to the slope failure in most places, including the study area. Thus, the event based analyses and evaluation is more focused here. Rainfall data (from the ‘‘Servizio tutela e gestione delle risorse idriche’’ of Sardinia Region) were collected to assess their triggering effect on the landslide of the study area.

1. Rainfall (RF)

Rainfalls are common triggering factors of landslides in many mountain regions. Several researchers (e.g. Caine 1980; Wilson and Wieczorek 1995; Terlien, 1998; Crozier, 1999; Glade et al, 2000; Iverson, 2000; Aleotti, 2004; Guzzetti, et al, 2004; Guzzetti, et al, 2007; Guzzetti, et al, 2008) have proposed a dependency of the minimum level of rainfall duration and intensity which might set off shallow landslides and debris flows. However, it is not only the amount of precipitation but also the amount of water that infiltrates and moves into the ground to cause a failure. To assess the triggering impact of water on the landslide of the study area, the collected rainfall data are analyzed and the geo-hydrological condition of the site is described from the field observation of surface drainages.

Hence, a monthly rainfall of four meteorological stations situated inside and outside of the study area namely, Capoterra (85 years), Decimomanu (68 years), Uta (38-years) and Elmas (14 years) are considered. The rainfall characteristic of the study area is represented by the Capoterra station. All the four stations have more or less similar amount of long term average rainfall but Uta and Capoterra stations show higher amount, especially in the months of October -December (Fig 9.2) indicating that the rift margins receives more rainfall than the central valley represented by Elmas and Decimomanu stations.

The Capoterra area is one of the areas receiving a high rainfall in the Sardinia region. The maximum rainfall is recorded in the months of October to March while the lowest ones in the months of May to September of the year (Fig9.2).

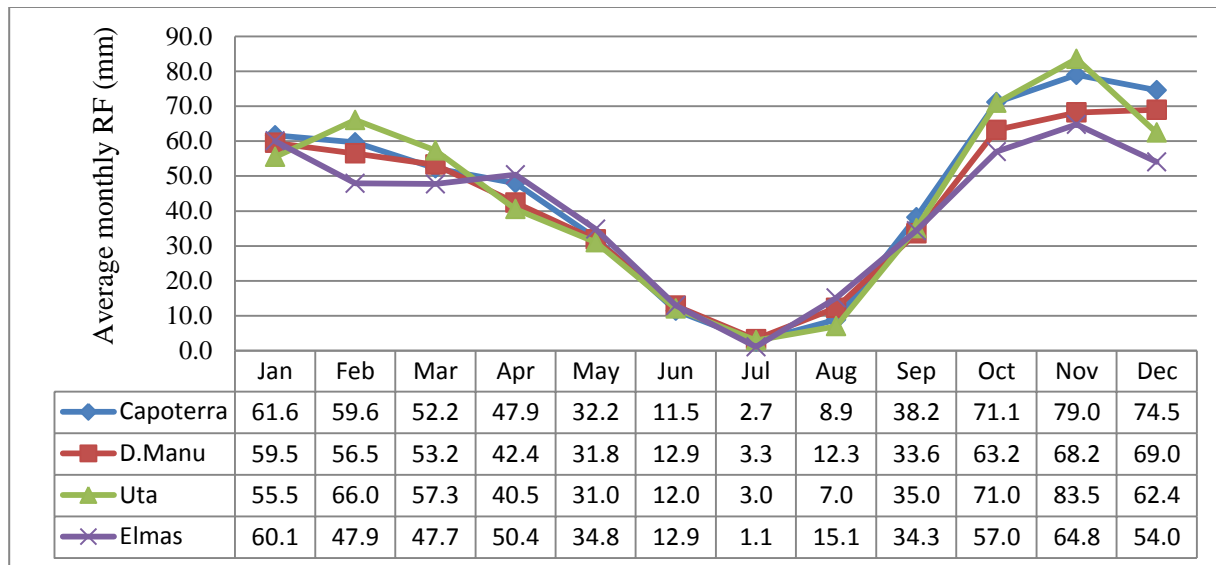


Fig 9.2: Average monthly rainfall of four stations, namely, Capoterra (85-yrs), Uta (38-yrs), Decimomanu (68-yrs), and Elmas (14-yrs)

The maximum, minimum and average annual rainfalls of the study area are 952 mm, 137 mm and 533 mm respectively. The maximum annual rainfall is recorded in the year 1936, while the minimum in the year 1948. About 43% of the recorded annual rainfalls have values greater than the average annual rainfall at the Capoterra station (Fig9.3). The monthly maximum rainfall is dominantly recorded in the months of October and November as recorded data showed.

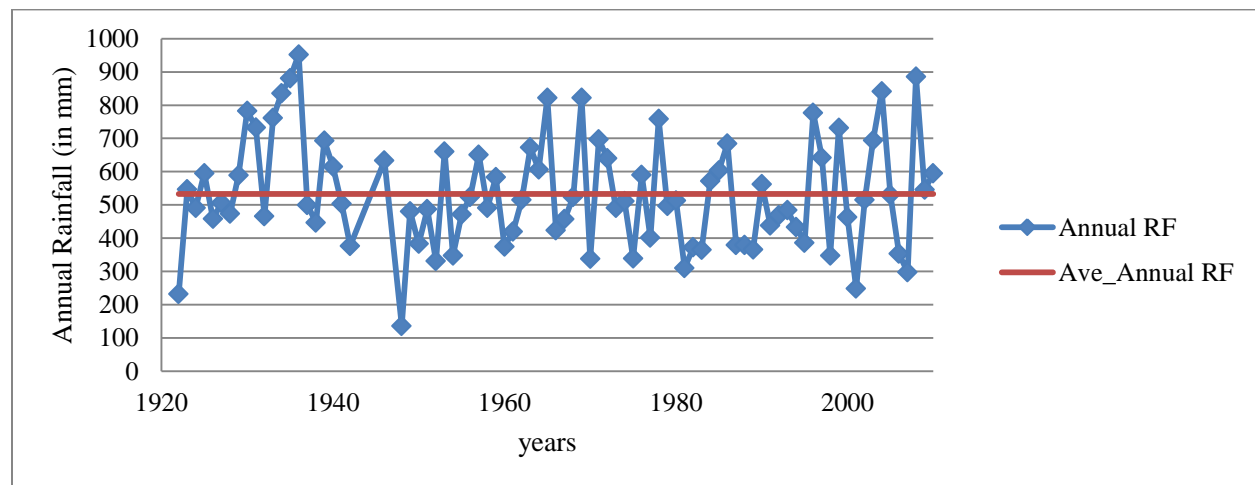


Fig 9.3: Annual rainfall of the Capoterra station for the years 1922 -2010 (85 yrs)

Although there are no well recoded historical data, some event based information sources such as documents obtained from regional documents of forestry and environmental surveillance (<http://www.sardegnaigitallibrary.it>) and <http://www.unpassoavanti.net/> and other sources indicate that

rainfall and associated stream erosion are the main triggering factor of landslides, especially the debris flow in the study area. For example, the same sources also indicated that the Capoterra Poggio dei Pini is among the few areas suffering from flooding and debris flow hazards in previous years (e.g. 1999, 2008). Rio San Girolamo and Santa Barbara are also some of the main responsible drainages for such hazard that flow from the western Capoterra Mountain towards E and SE joining the Mediterranean Sea. Many small towns and villages including the study area are located at the eastern foot of the Capoterra Mountains and alluvial fans

To realize the triggering effect of the rainfall to the above mentioned flood and debris hazards, the daily and monthly maximum rainfall for the years 1982 to 2010 are analysed. For instance, the rainfall data of Capoterra station confirms that the daily maximum rainfalls are recorded in October 27/1985 (120.4mm), November 13/1999 (195mm), April 5/2005 (94mm) and October 22/2008 (372mm) (Fig 9.4) from all the years of 1982 to 2010. The daily maximum for the rest of the years are less than 94mm, and no flooding or debris hazard is reported.

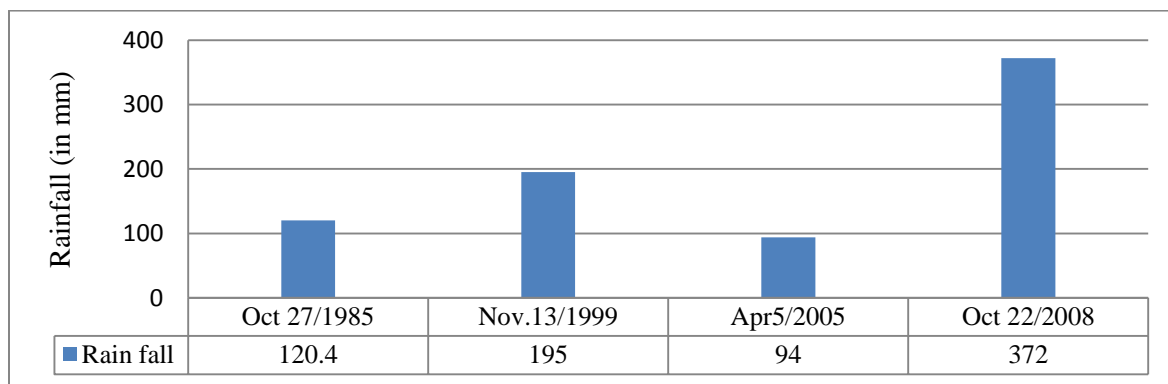


Fig 9.4: The maximum daily rainfalls that resulted in the flooding and/ or debris flow hazards in the study area

Similarly, the maximum monthly rainfalls also are recorded in the same months except for the year 1985, which its daily maximum and monthly maximum rainfalls are recorded in October March respectively (Fig 9.5).

The monthly rainfalls of the Nov. 1999 and Oct. 2008 are exceptionally more than 6 times greater than the long term average monthly rainfalls (Fig 9.4), which certainly can trigger slope instability in the area of interest.

In order for a debris flow to be initiated there could exist several factors but the main once include a good combination of catchment conditions (i.e. sufficient material sources, steep slope) and availability of sufficient amount of triggering factor (usually water). In the R.S.Girolamo area most debris heads, where debris flow initiates includes those having greater than 20° slope class, areas with greater than 400m elevation and areas where the loose talus, colluvium and fractured rocks are available. This huge amount of rainfall together with the susceptible nature of the catchment area of R.S. Girolamo triggers slope instabilities and debris flow devastating the downstream towns/villages and infrastructures.

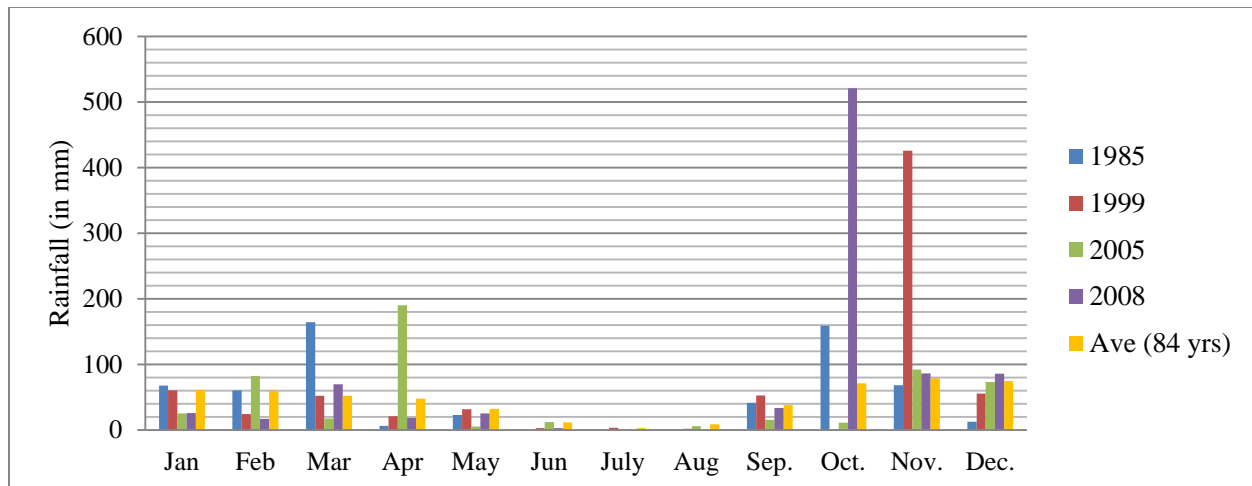


Fig 9.5: Comparison of the monthly maximum rainfall of 1985, 1999, 2005, 2008 and the average monthly rainfall for 84 years (Capoterra station)

Of all the events mentioned above, that of the Oct. 22/ 2008 was the most disastrous one. Comparison of the then rainfall event in terms of their intensity and duration is done for some station and is provided in (Table 9.1) below. The stations of Capoterra-Poggio dei Pini and Capoterra-Paese had the maximum registered rainfall intensity depicting that 93% (351.6mm) of the Poggio dei Pini and 80% (374.8mm) of the Capoterra-Paese rainfalls within 3 hours (Table 9.1 and Fig 9.6).

Table9.1: Rainfall intensity-duration data of the event of October 22/2008.

Duration (in hr.)	Intensity (mm/h)						Average Intensity (mm/hr.)
	Capoterra - Poggio dei Pini	Capoterra - Paese	S.Lucia di Capoterra	Sestu-131	Fluminimannu	Decimomannu	
0.5	234.4	249.8	108.4	82.8	44.8	50.0	128.4
1	177.4	189.1	88.0	61	38	29.0	97.1
3	117.2	124.9	75.7	33.3	21.2	12.2	64.1
6	61.9	72.1	45.6	17.9	10.6	6.9	35.9
12	31.0	36.8	23.0	9.0	5.4	3.8	18.2
24	15.8	19.4	11.5	4.5	2.7	2.1	9.3

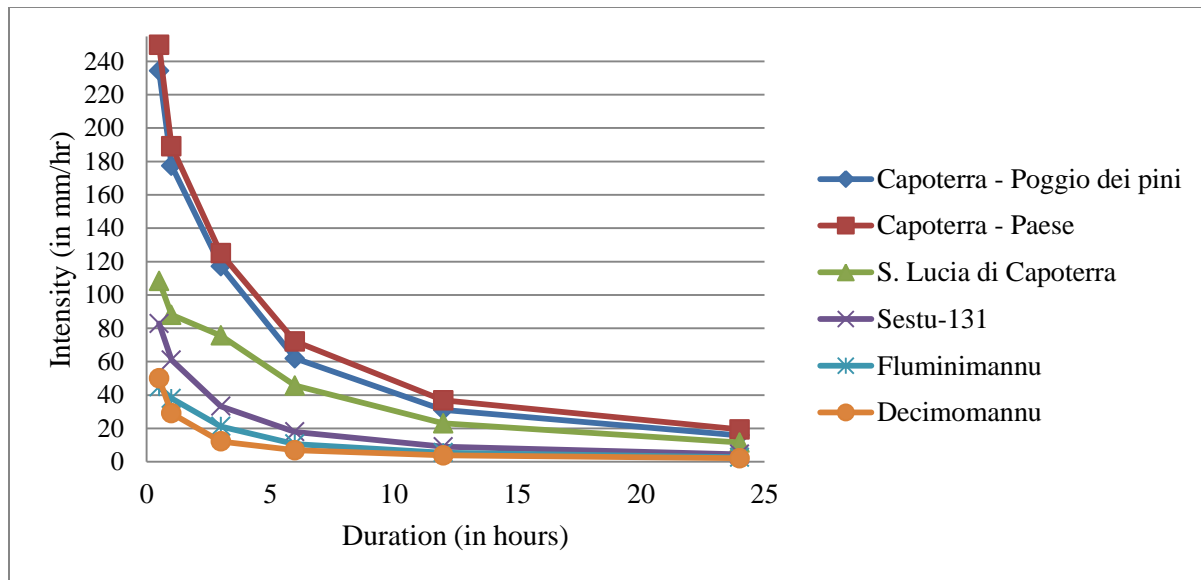


Fig 9.6: Rainfall intensity-duration relationship of the event of Oct 22/2008 for some stations including the study area

The transport of materials to the streams is associated to the correlation between debris torrent activity and moderate to heavy rainfall. Once, the sufficient water makes the sediments unstable and the source material moves into debris flows making its way into the creek.

Studies carried out by Brunetti, et al, (2010) states that rainfall events that have resulted in slope instabilities in Italy cover the range of Duration D $0.27 \text{ h} < D < 1440 \text{ h}$ (i.e. from 15min to 60 days), with the majority of the events in the range $12 \text{ h} < D < 20 \text{ h}$, and span the range of rainfall mean Intensity I $0.15 \text{ mmhr}^{-1} < I < 150 \text{ mmhr}^{-1}$, with the majority of the events in the range $0.5 \text{ mmhr}^{-1} < I < 10 \text{ mmhr}^{-1}$.

For the October 22/2008, the Intensity-Duration of the 6-various station including the study area is given in Table 9.1 and Fig 9.6 and their average curve given in Fig 9.7. The threshold curve of Intensity-Duration can be expressed using a simple power law form (equation 9.1).

$$I = \alpha D^{-\beta} \quad 9.1$$

where I is the rainfall mean intensity (in mm/hr.), D is the Duration of the rainfall event (in hr.), α is a scaling constant (the intercept), and, β is the shape parameter that defines the slope of the power law curve.

Similarly, the threshold of average rainfall intensity-Duration curve for the event of October 22/2008 as recoded in the six stations is expressed using equation 9.2. Any rainfall intensity-Duration values that fall above the line can trigger shallow landslide in the study area.

$$I = 99.08D^{-0.671}$$

9.2

Regional (and even more local) ID thresholds to generate landslide are usually higher than national (or global) thresholds (Guzzetti, et al., 2007).

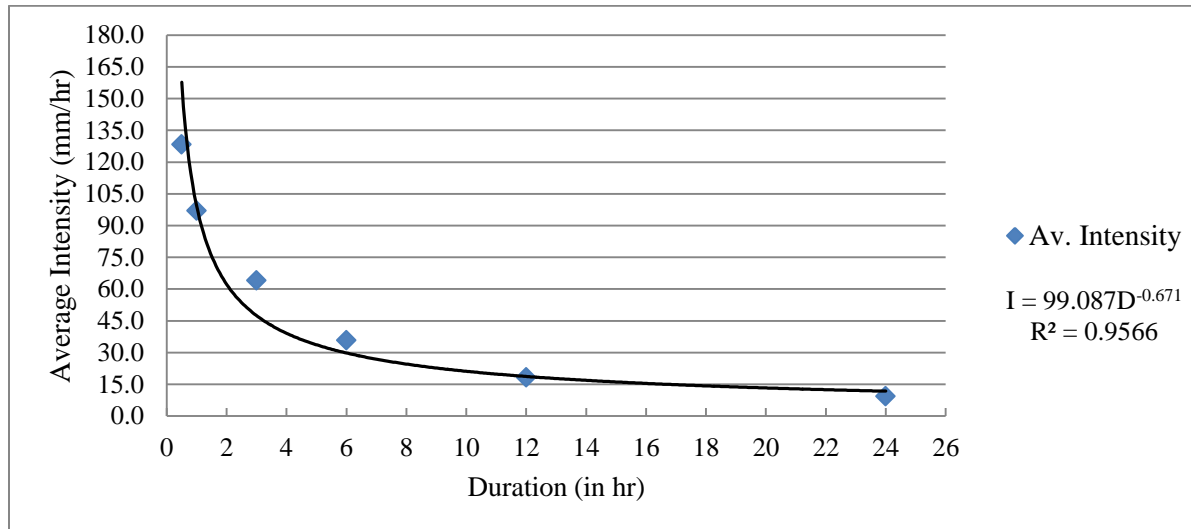


Fig 9.7: Average rainfall Intensity-Duration relationship of event of Oct. 22/2008 for 6 stations including the study area

The amount of heavy rainfall event of October 2008 (an amount equal to five million cubic meters in three hours as estimated by hours rough calculation) has descended on the mountain causing mudslides and landslides and giant boulders have moved away from steep slopes, dragging from the slopes of Mount Santa Barbara million cubic meters of rock, sand and earth causing incredible destruction in the valley and changing the appearance of the landscape (www.Capoterra.et; Corpo Forestale e di Vigilanza Ambientale, 2008). Fig 9.8 illustrates some of the situations of that of the event of October 2008 in the Poggio dei Pini of Capoterra area.



Fig 9.8: Debris flow nature and its effect of Oct. 22/2008 (a) the turbulence nature of the debris flow (b) collapsed bridge by the debris flow (c) damaged car (d) research center collapsed by the then debris flow

Although the occurrence of debris flows is irregular, comparison of the historical rainfall data before and after the events of October 2008 shows that the low rainfall periods in the catchment favors the accumulation of materials from the shallow landslides (rock fall, debris and earth slide) and weathering for longer years and if these are flowed by the heavy rainfall period, the debris flow is expected. For example, Fig 9.9 demonstrates that there is a substantial accumulation of debris materials in the catchment of R.S. Girolamo even after the event of 2008. These recently accumulated debris materials in the catchment are a potential danger for the people living at the downstream (e.g. Poggio dei Pini) of this catchment area in the near future when heavy or high intensity rainfall occurs.



Fig 9.9: The figure demonstrates accumulations of debris materials after the 2008 event of R.S.Girolamo: I and II represented the debris slide originated from talus of the metamorphic rocks; III-shows the debris (talus) slide from the granitic rock and IV show the accumulated debris at the river bed of Santa Barbara.

9.3 Properties of rocks and soils

9.3.1 General

Referring to the regional tectonic setting of Sardinia, the study area is found at the contact zone between the Arburese unit and the Sulcis Iglesiente unit. As stated in different publications such as Leone (1973) Cocco (1974), Barca (1981,1982 and 1991) cited in Barca, et al (2009) and others, regionally the study area is covered by (1) the Paleozoic metamorphic basement which consists of the two successive formations called the “Arenare di San Vito (SVI)” belonging to the Arburese unit (overlying unit) and Pala Manna formation (PMN) belonging to the Iglesiente - Sulcis units (underlying unit) (2) complex granitic intrusions consists of two different units: the units of Villacidro intrusive and intrusive units of Santa Barbara with some quartic hydrothermal dikes and basic dykes (Fig 9.12) as in Barca et al, (2009) and references there in (3) quaternary sediments that include the recent sediments such as the alluvial and colluvium deposits, found at the stream beds and areas with relatively lower slopes.



Fig 9.10: Position of the ‘PMN’ and ‘SVI’ formations in relation to the regional stratigraphic succession of Paleozoic metamorphic basement (modified from Barca, et al, 2009) (PMN=Pala Manna; SVI=Arenare di San vito; MPS=formazione di Mason Porcus; MUX= formazione di Genna Muxerru; RSM= formazione di San Marco; DMV=Formazione di Domusnovas; MRI=Formazione di Monte Orri; AGU=Formazione di Monte Argentu)

The geological and geotechnical properties of the rocks and the soils are more discussed and elaborated based on the field and laboratory works as follows.

9.3.2. Field survey and laboratory tests of geologic materials

Geology is one of the landslide causative factors that are considered as main input map of susceptibility of the study area. For this reason, some physical and geotechnical tests and measurements have been carried out on the rocks and soils of the study area to describe their litho-technical properties. Summary of activities are provide in Table 9.2.

Table 9.2: Summary of field and laboratory works

Tests on rocks		
S.N	Type of test	Number of samples/tests
1	Physical tests (density, water absorption)	66 tests on 16 samples
2	Point load tests	40
3	Schmidt hammer reading measurements	>215
Physical, index and geotechnical tests on soils		
4	Atterburg limit (LL,PL, PI)	23
5	Grain size test	25
6	Moisture content	11
7	Direct shear test	6

9.3.2.1 Lithological, physical and geotechnical properties of rocks

Paleozoic metamorphic basement

Lithologically, the Paleozoic metamorphic basements found in the study area are more or less similar. The ‘‘Arenare di San Vito (SVI) is composed of alternation of fine to medium grained meta-sandstone and meta-siltstone while the ‘‘Pala Manna formation’’ (PMN) is composed of an alternation of meta-sandstone, laminated quartzite and meta-siltstone. Some sedimentary relict structures like lamination are also observed in some parts. The areal coverage of the metamorphic basement is 6.5% (4% PMN and 2.5% SVI formations) and is found in the left flank of the R.S. Girolamo River. Besides, to their lamination they are also affected by secondary fractures and thus they are main sources of debris deposits. They are exposed at upper part of the left side of the catchment forming cliff, dipping vertical to sub-vertical (Fig 9.11).



Fig 9.11: Palaeozoic metamorphic basement exposure (a) Lamination structure (b) Cliffs of the meta-sandstone rock (c) Vertical to sub vertical dipping of the meta-siltstone and (d) Debris accumulation from metamorphic basement

Complex Granitic intrusions

These complex granitic intrusions are similar in texture and structure although they have different composition (Barca, et al, 2009). This complex lithological contains the various granitic intrusions such as the Santa Barbara and Villacidro granitic rocks and the quartzite hydrothermal dikes and the basic dikes (Fig9.12). These complex granitic intrusions have a total areal coverage of 83.3% (74% of VLD, 9% SBB and 0.3% dikes) of the study area. In the study area these units are mapped as one lithologic unit in the course of the litho-technical mapping of the area for the purpose of the landslide susceptibility analysis.

The intrusive unit of S.Barbara are found at the top part of the S.Barbara Mountain. Compositionally, they vary from tonalitic-granodioritic to microgranodioritic with biotite. That is, composition of the S. Barbara intrusive varies from tonalitic to granodioritic with some xenolith of metamorphic rocks. All varieties of the S.Barbara intrusive are found in the study area but the dominant are the microgranodioritic one. According to Barca et al, (2009) and references therein, the major mineral composition includes phenocryst of plagioclase (40%), quartz and orthoclase, biotite (15%), subordinates of amphibole immersed in the ground mass, as well as magnetite, apatite, zircon as accessory minerals.

The Villacidro intrusive includes micromonzogranite to sieno-monzogranitic more or less leucocratic reddish to whitish red colour, medium to coarse grains, having a k-feldspar crystal size of 1-2cm. Their major mineralogical components are phenocrysts of plagioclase, orthoclase, quartz, biotite and amphibole (Hornblende) but its volumetric percentage varies depending on the type of the intrusive unit. In the study area, these units are relatively more weathered and have developed into residual soil where the topography allows.

Most rock falls and /or toppling start from the fractured cliff forming granitic rock, especially from the drainage of the S. Barbara Mountains.



Fig 9.12: Various granitic exposures showing: (I). Fractured granitic intrusion (SBB), (II). Weathered granitic intrusion (VLD) (III). Basic dikes within the S. Barbara unit, (IV).Fractured granitic and their accumulated debris material

From the field observation, they are affected by 2-3 sets of joint sets, with vertical to sub-vertical dip angles and nearly N-S, E-W and NNE- SSW general trends. These discontinuities have high contribution to the rock falls in this rock exposure.

Quaternary/recent sediments

These consists of the alluvial deposits, slope/colluvium, and residual depoists. The alluvial deposits dominality are found following the drainage lines, banks and valleys where the relatively flat topography is available. Those alluvials are composed of course grained materials such as gravels, sands,cobbles,boulders with very low amount of fine soils (Fig 9.13, a & b). This indicates that the streams that initiate their flowing from the slided land are very rich in debris and are with erosive power damaging farmland and other infrastructures.The exposure thickness of the alluvial deposit at the river bank varies from 1m to 4m and have relatively more fines than the alluvials found at the river bed (Fig 9.13,c).

While the slope deposits/colluvium are found at the foots of the stepped cliffs, ridges, flat hilltops.They are mixed and loose sediments deposited from rockfall or topple from the rock exposure. The slope deposits originated from the granitic rock exposure are dominated by large boulders that reach up to 2m diameter boulder while those originated from the metamorphic basement are dominated by the cobbles and gravels. In general the slope deposits are prone to debris slide and debris flow.

The fine dominated residual soils with no noticeable gravity movements are mapped and described separately and they bottomed by their parent rock. At the top they are covered by the organic rich soil (Fig 9.13,d).

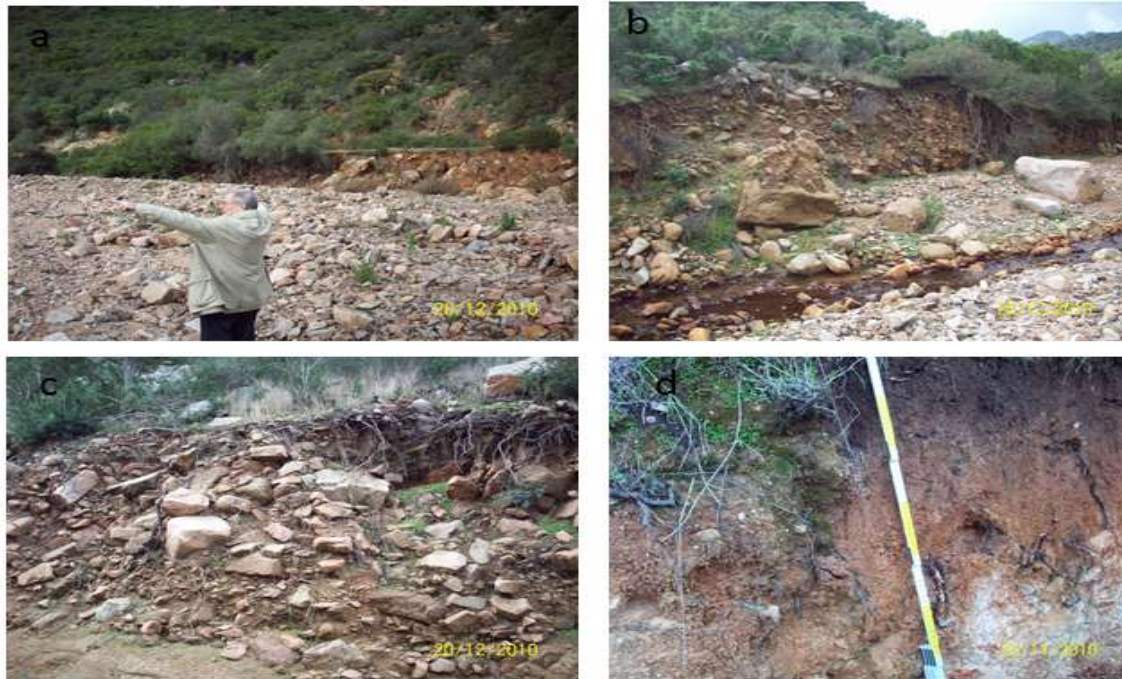


Fig 9.13: The various types of quaternary unconsolidated sediments (a) and (b) alluvial deposits at the river bank and river floor (c). colluvium dominated (d) Residual soil

A. Physical and geotechnical properties of rocks

Some physical (density, water absorption) and unconfined compressive strength tests are carried out on some of the rocks. The unconfined compressive strength is estimated using both the Point Load and the Schmidt hammer test. The physical tests and Point Load test have been carried out at the laboratories of the departments of Territorial Engineering and Earth Science of Cagliari University.

Point load & Schmidt hammer tests and unconfined compressive strength (UCS)

Rock strength is one of the parameters used in the litho-technical characterization of rock masses for landslide susceptibility analysis. In this work, Schmidt hammer and Point Load test were used to determine the UCS rocks of the study area. These methods are economical and useful to reasonably estimate the rock strength. These tests give reasonably accurate results besides to their economic and fast behavior. Numerous studies have demonstrated widespread agreement that these tests provide comparable results with those obtained with a much more complicated and expensive uniaxial compression test if we used them carefully and strictly. The Schmidt hammer gives a measure of the bounce of the hammer against the rock wall and this

measurement is converted into the corresponding value of uniaxial compression using the standard graph shown in Fig 4.17 in chapter-4

During the field work more than 215 Schmidt hammer readings have been taken in various rock units in 20 locations, 11 reading at each point and the values have been averaged out. Densities of rocks is also been determined in the laboratory as it is one of the factors used to convert the Schmidt hammer rebound values in to the corresponding values of uniaxial compression. Finally, the UCS of the rocks is calculated considering the average rebound number, position of hammering, and the density of rocks. The total reading measurements taken in the granitic intrusion have been 143 while that of metamorphic rock have been 72 readings. Thus, results show that the calculated minimum, maximum and average UCS of the granitic rock of study area are 18, 205 and 81 MPa respectively while that of the metamorphic rock (meta-sandstone) is 26, 75 and 49 MPa for the minimum, maximum and average respectively (Fig 9.14).The Schmidt hammer measurements have been taken only in the rocks with degree of weathering from grade-I (fresh rock) to grade - III. Rock units weathered to grade IV and above give nearly zero-value of rebound reading and are considered as engineering soil.

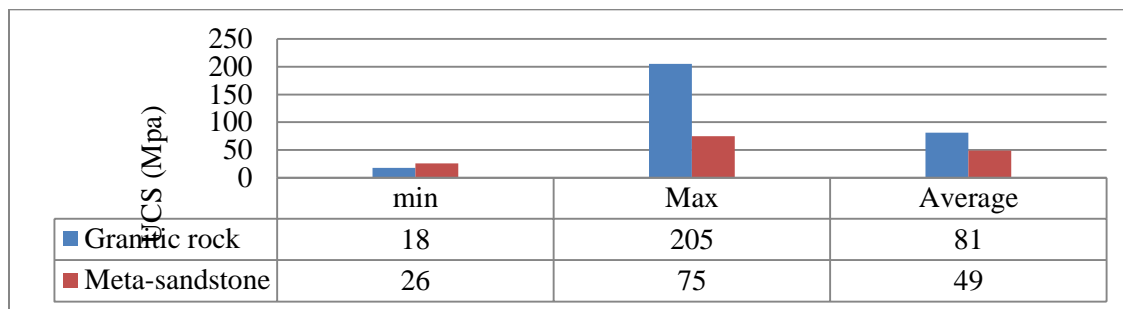


Fig 9.14: Calculated minimum, maximum and average values of Unconfined Compressive Strength (UCS) of rocks from Schmidt hammer rebound

The difference between the minimum and maximum rock strength is high in the granitic rock due to high differential weathering of the granitic rocks. The negative impact of the degree of weathering on the strength of granitic rocks of the R.S. Girolamo area is given below in Fig 9.15. Both the Point Load and the Schmidt hammer results showed similar trends.

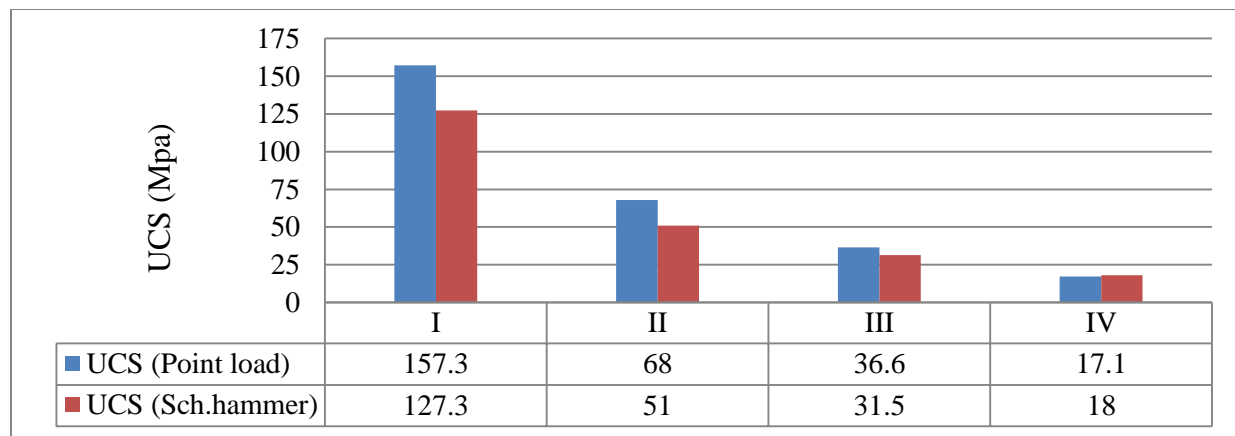


Fig 9.15: Degree of weathering versus Unconfined Compressive Strength of granitic rocks of the study area (NB: The numbers I, II, III and IV represents degree of weathering i.e. I= 'fresh', and IV= 'highly weathered' and UCS = average values in each degree of weathering)

Some rock samples are also collected and tested using the point load strength test to determine and compare the UCS with that of the Schmidt hammer. The point load strength testing is carried out following the procedures outlined in ISRM (1985). In this work irregular rock samples are collected for the test and calculations (Table 9.3) are carried out by applying the size correction and equivalent core diameter based the recommendation of ISRM (1985).

Table 9.3: Example showing how the Unconfined Compressive Strength (UCS) is calculated from Point Load test for the R.S.Girolamo area, Sardinia.

	W_a	D	P	De^2	De	I_s	F	I_{s50}	UCS
S. code	mm	mm	KN	mm^2	mm	Mpa	mm	Mpa	Mpa
S26	77	57	15.9	5591.1	74.8	2.9	1.2	3.4	82.0
S27	78	57	41.9	5663.7	75.3	7.4	1.2	8.9	213.3
S28	120	76	6.4	11617.8	107.8	0.5	1.4	0.8	18.6
capt_01_Rgt	87	81	28.6	8977.1	94.7	3.2	1.3	4.3	102.1
capt_02_Rgt	45	70	29.9	4012.7	63.3	7.5	1.1	8.3	199.0
capt_03_Rmt	62	80	39.5	6318.5	79.5	6.2	1.2	7.7	184.8
capt_04_Rmt	62	80	23.9	6318.5	79.5	3.8	1.2	4.7	112.0
capt_05_Rmt	33	80	16.1	3363.1	58.0	4.8	1.1	5.1	122.5

(W_a = average width of sample; D = thickness of sample; P = applied load; De = equivalent diameter of sample; I_s = point load strength; F = size correction factor; $I_{s(50)}$ = point load strength index)

The Point Load tests were conducted both on a perpendicular and parallel to the orientation of the grains or foliation of the rock samples to check the mechanical anisotropy. Results of the rocks, especially the

metamorphic rocks have shown a strong mechanical anisotropy in rock strength at least in two directions (Fig 9.16).

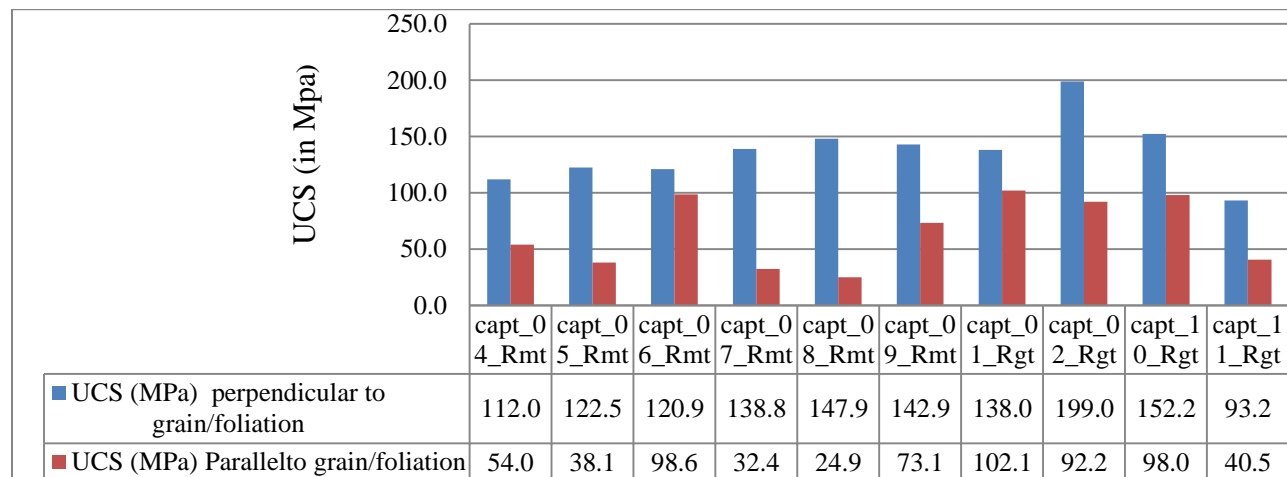


Fig 9.16: Strength variation of rocks for Point Load measurements parallel and perpendicular point load measurements to the grain/foliation alignment

Similarly, when the strength values of the point load is compared, the, maximum and minim value are recorded by the granite due to the difference in degree of weathering in the samples, but the difference between minimum and the maximum of the samples of the meta-sandstone rock is lower indicating the samples are relatively fresh (Fig 9.17). In the field rock fall/topples are common in both the granitic intrusion and metamorphic rocks of the study area.

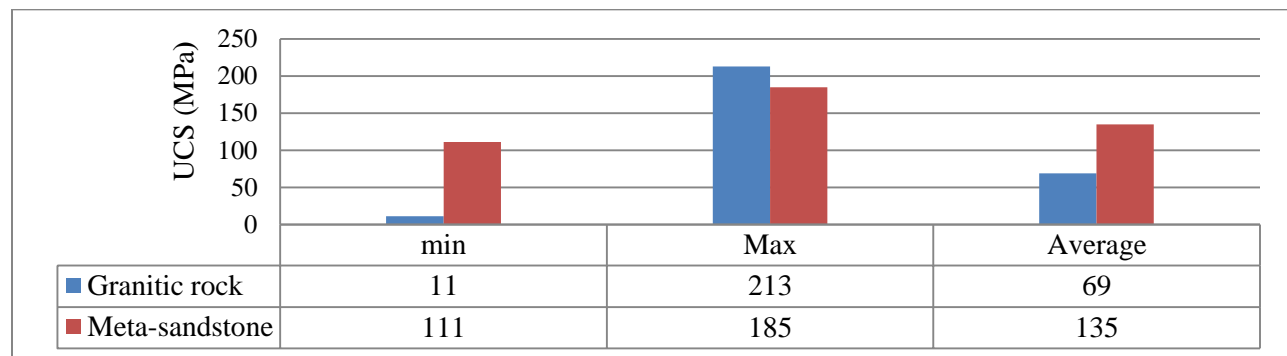


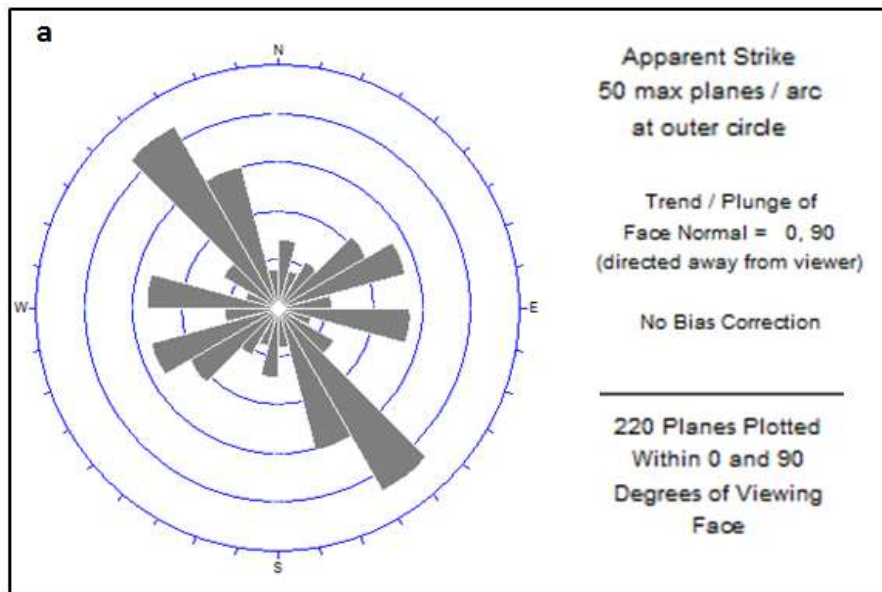
Fig 9.17: Summary Unconfined Compressive Strength from point load (the number of samples tested for granite is 34 samples and for metamorphic is 6 samples)

Hydraulic properties of rocks

To estimate the hydraulic characteristics of the rock mass of R.S.Girolamo, similar methodology and approach is used as in the case of the Debresina area of Ethiopia. Thus, to estimate the hydraulic conductivity of the fractured rock masses of the study area, the characteristics of the discontinuities such as orientation, spacing, opening and the likes have been collected during the litho-technical mapping of the area together

with other joint characteristics. About 220 discontinuity measurements (dip angle, dip direction, spacing, and opening) from the granitic rock exposure and 34 measurements on the metamorphic basement have been carried out. The characteristics of the discontinuities are summarized below. To visualize the general trends of the discontinuities, some of the collected data are plotted on rose diagram (Fig 9.18, a, & b).

Rose diagram is a method of displaying the relative statistical prevalence of various directional trends, e.g. strike direction of discontinuities. In this case, the rose diagram for some of the measured discontinuities in the area has been prepared using the dip angle and dip direction. The rose diagram depicts that the number of joints direction wise and frequency in a group-interval is represented along the radial axis, the length of petals becoming a measure of relative dominance of the trend. The directions are grouped in 10° interval (Fig 9.18). The strike petals possess a mirror image about the center of the rosette.



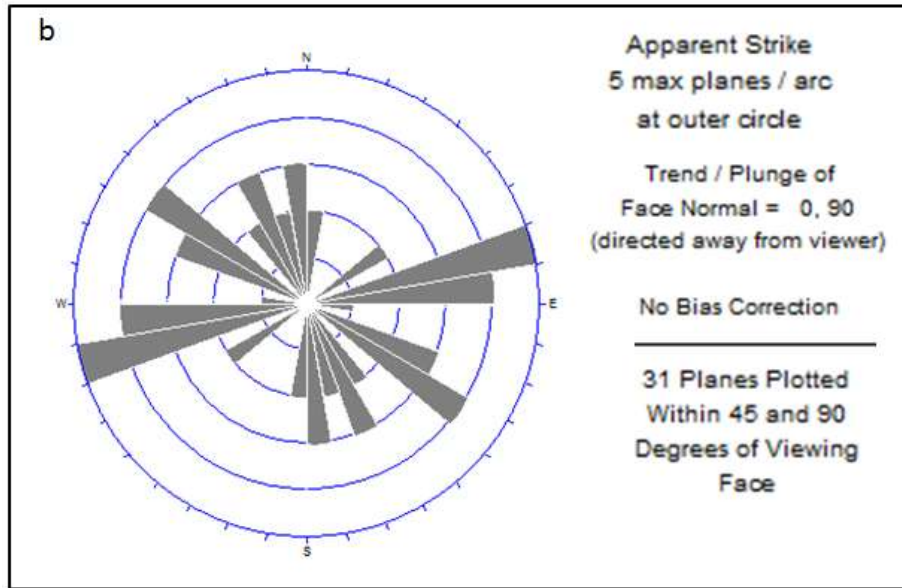


Fig 9.18: Rose diagram of strike trends of discontinuities showing their relative prevalence for (a) granitic intrusion and (b) Metamorphic basement

The estimation of hydraulic conductivity in different directions can lead to different results due to different fracture parameters such as spacing and aperture values (A.El-Naqa.2000). The methodology of Snow (1969) and Louis (1974) as stated in A.El-Naqa (2000) was used which is based on: (a) selection of typical outcropping rocks (b) recording of geometrical characteristics of discontinuities, and (c) calculation of the hydraulic conductivity of a single joint and of the rock mass as a whole. In collecting the pertinent discontinuity data, the scan line techniques of Piteau (1973) was used. The discontinuity parameters measurements were done following to the norms given by Italian Geological services guide line (Amanti et al, 1992) and also the International Society of Rock Mechanics (ISRM, 1978): orientation, number of joints sets, spacing, aperture, roughness, fill material, and hydraulic conditions.

Two to four sets of systematic joints are recognized in the rock masses of the granitic rock and metamorphic rock outcrop besides to the non-directional fractures. The dip angle of the systematic sets of joints on both rock units is variable but mostly dipping vertical to sub vertical. The dominant joint sets in the granitic rocks dips towards SW, WNW and ESE while dominant joints in the metamorphic are similarly dipping towards SW and SSE.

Sample geometrical characteristics discontinuity measurements carried out for the granitic are provided in Table9.4. The hydraulic conductivity of the rock masses of the study area is estimated using the equations 1.2 to 1.6 provided in chapter 1(section 1.4) and the result is summarized in table below.

Table 9.4: Discontinuity characteristics and estimation of hydraulic conductivity of rock masses in Granitic rock outcrop.

Parameter	Discontinuity sets		
	J1	J2	J3
Orientation	Nearly N-S (trending)	Nearly E-W	NW-SE
Spacing(m)	0.12 to 0.5m (Ave. = 0.29m)	0.05 to 1.06m (Av. 0.27m)	0.05 to 1m (Av. =0.25m)
Opening (m)	0.002m	0.001m	0.0015
K(m/sec)	0.006161	0.000827	0.003015

The estimated hydraulic conductivity of the rock masses in the granite rocks outcrop varies from 8.27×10^{-4} m/sec to 3.015×10^{-3} m/sec with an average value of 3.335×10^{-3} m/sec. Similarly the hydraulic conductivity of the fractured metamorphic rock in the area is estimated using the same calculation and the result varies from 2.223×10^{-3} m/sec to 1.417×10^{-1} m/sec.

9.3.2.2 Physical and geotechnical properties of soils

To evaluate the physical and geotechnical properties of soils, laboratory tests such as grain-size distribution analysis, Atterberg tests and direct shear tests were performed for soil samples collected from landslide-affected areas. The laboratory tests have been conducted in the Geotechnical Laboratory of the Department of Territorial Engineering of Cagliari University) and Geotechnical Laboratory of Cagliari Province of Sardinia, Italy.

Particle Size Distribution and Atterberg Limits of soils

Generally, soils of the R.S. Girolamo are classified as coarse grain soils because the grain size analysis result showed that their courser grains content is more than 50%. Thus, they have a very low consistency limits (LL, PL and PI), or else they are mostly non plastic (Table 9.5).

The Atterburg limits and the grain size laboratory analysis results provided in Table 9.5 indicated that these soils have: (i) more than 40% of the analysed samples non plastic (NP) (ii) the maximum Liquid Limit value of 32% (iii) the maximum Plastic Limit of 31%, and (iv) Plasticity Index ranges from non-plastic to 13% showing the soils in general are low plastic nature (v) the grain size analysis result showed that more than 68% of the samples have less than 5% fines (silt and clay) content (vi) the soil type according to the Unified Soil Classification (USC) system varied between poorly graded sand with gravel (SP) to well graded sand with gravel (SW).

Table9.5: Grain-size characteristics, Atterberg limits and classification of soils of R.S.Girolamo area

S.N	Sample code	Gradation			Atterbug limits			Coefficients		soil type (USC)
		%gravel	%sand	finest (Clay & silt)	LL	PL	PI	Cu	Cc	
1	Capt-01 -RS	39	58.5	2.5	31	21	10	16	1.2	SW
2	capt-02 -RS	19	79	2	28	17	11	10	0.05	SP
3	capt-03 -RS	24	71	5	20	18	2	10	0.5	SP-SM
4	Capt-04 -RS	11.8	85	3.2	23	20	3	10.7	0.3	SP
5	capt-05 -RS	17	80	3.3	NP	NP	NP	8.8	0.07	SP
6	capt-06 -RS	23.4	74	2.6	NP	NP	NP	5.1	2.7	SP
7	Capt-07 -RS	23.7	74	2.3	27	18	9	10	1.1	SW
8	capt-08 -RS	9	85.2	54	22	19	3	10	0.71	SM
9	capt-09 -RS	24	75	1	30	25	5	4.9	2.7	SP
10	capt-10-RS	4	92.4	3.6	NP	NP	NP	9.3	1.2	SW
11	Capt-11 -RS	9	87.3	9	30	25	5	8.8	0.06	SP-SM
12	Capt-12 -RS	25.6	72	2.5	NP	NP	NP	9.3	1.7	SW
13	Capt-13-RS	8	85	7	NP	NP	NP	10	1	SW-SM
14	Capt-14 -RS	8	86	6	NP	NP	NP	10.8	1	SW-SM
15	Capt-15 -RS	14	85.6	0.4	23	17	6	8.4	0.06	SP
16	Capt-16 -RS	7.6	86.4	6	28	26	2	12.5	0.9	SP-SM
17	Capt-17 -RS	9	82	9	?	?	?	13.3	0.42	SP-SM
18	Capt-18 -RS	7	82	11	NP	NP	NP	15	1	SW-SM
19	Capt-19 -RS	21	74	5	NP	NP	NP	14.7	1.5	SW-SM
20	Capt-20 -RS	24	72	4	NP	NP	NP	9.3	2.33	SW
21	Capt-21 -RS	22	76	2	29	18	11	9.3	1.5	SW
22	Capt-22 -RS	9.7	83.6	6.7	28	23	5	15	1.12	SW-SM
23	Capt-23 -RS	14	85	1	32	19	13	6.25	1.7	SW
24	Capt-24 -RS	10.4	89.4	0.2	36	31	4	6.7	0.05	SP
25	Capt-25 -RS	10.7	89	0.3	NP	NP	NP	10	0.07	SP

(LL= Liquid Limit; PL= Plastic Limit; USC = Unified Soil Classification; SM = silty sand; SW=well graded sand with gravel; SP= poorly graded sand with gravel; SW-SM = well graded sand with silt & gravel; SP-SM = poorly graded sand with silt & gravel; NP = non plastic)

Shear strength parameters of soil

The shear strength of soil has been also assessed using the direct shear test (ASTM D3080) of 6 soil samples to calculate the safety factor of the area from a remolded sample (Table 9.6). The test has been conducted at 1kg, 2kg and 3kg vertical forces, for each soil samples and the value of shear stress at failure has been plotted against the normal stress for each test. The shear strength parameters are then obtained from the best line fitting the plotted points. A number of specimens of the soil have been tested, each under a different vertical force. Results show that the Cohesion (C) value of the soils of the study area varies from 6.87 to 47.12 kpa and the angle of internal friction (ϕ) varies from 38.8 to 43.2°.

Table 9.6: Shear strength parameters of soils (from direct shear test) of R.S. Girolamo area, Sardinia

	Code	C (kpa)	ϕ (degree)
1	Capt-04	47.12	34.4
2	Capt-06	43.91	38.8
3	Capt-11	26.37	42.5
4	Capt-13	10.64	43.2
5	Capt-19	6.87	42.5
6	Capt-21	31.04	36.3

Permeability of soils

The hydraulic conductivity of the soils of the study area is estimated based on the soil classification. That is soils are classified using the Unified Soil Classification (USCS) system. Analysed results of the USC displayed that the soil types include SP, SW, SM, SP-SM, and SW-SM types of soils.

The hydraulic conductivity (permeability) values of the soils are estimated using the Hazen's formula indicated in chapter-1 (equation 1.1) as the soils are coarser grain soils in which the Hazen's formula can be applied. Calculated values of the Hazen's formula are compared with the standard (ASTM and BS standards) and showed reasonable results. Accordingly, the lowest hydraulic conductivity value is calculated to be 6.40×10^{-5} m/sec for the poorly graded sand with silt and gravel (SP-SM) soil, while the maximum value (1.68×10^{-3} m/sec) is calculated in the poorly graded sand (SP) soil types Fig 3.19).

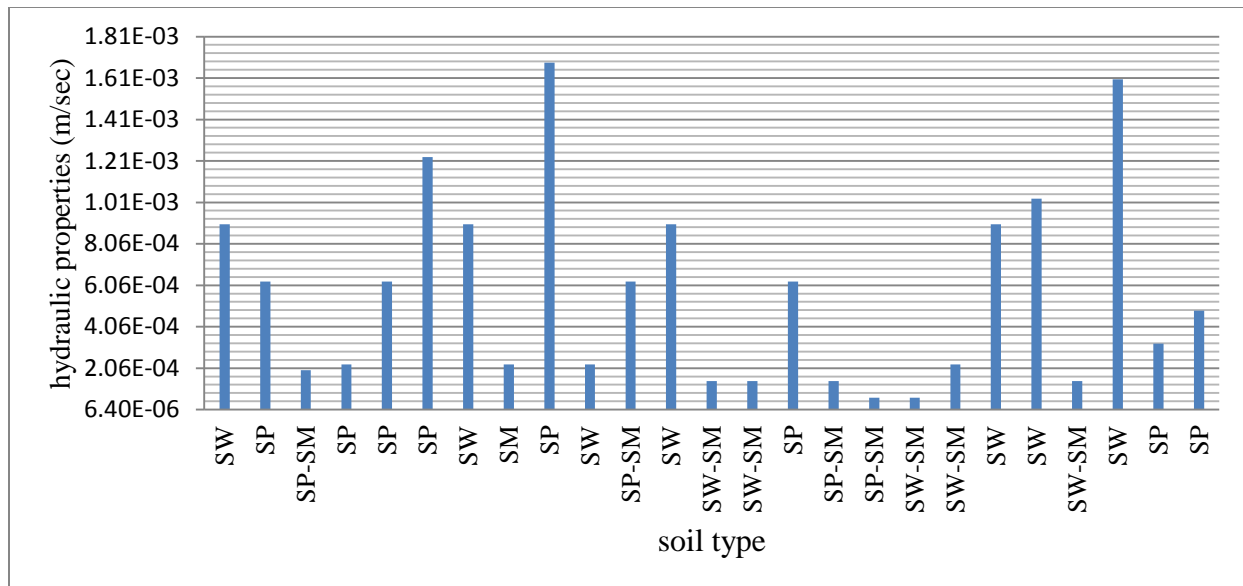


Fig 9.19: Hydraulic conductivity values of the various soils of the study area as Calculated by Hazen's formula

9.4. Landslide inventory and input data preparation and mapping

9.4.1. Landslide inventory mapping

As delineation of past landslide occurrences is useful for the prediction of future patterns of instability, landslide inventory of the study area has been executed through the direct field survey supported by the interpretation of orthophotoes and Google Earth, and then digitized directly into inventory map using GIS. The common types of landslide in the area includes rock fall/topple, debris slides and debris flow.

These slope failures were related to geological, topographical, and climatic conditions, thus, they can often facilitate the prediction of locations and conditions of future landslides. A total of more than 108 landslides are identified and out these 27 are debris flow, 42 are debris slide and 39 are rock fall/topple, but with no information on the date of occurrence.

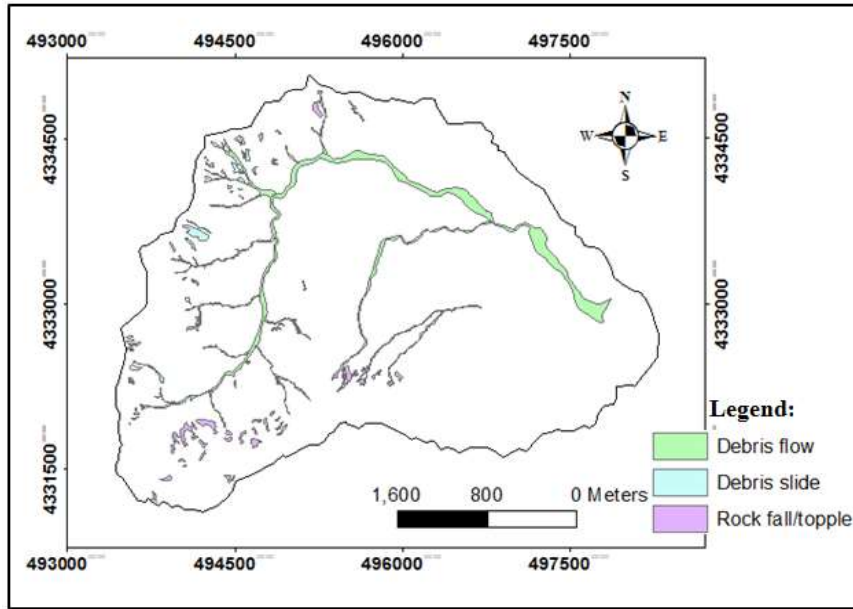


Fig 9.20: Landslide inventory map of R.S. Girolamo, Sardinia, Italy.

The inventory map is used in the Frequency Ratio method for analysis and verification of the susceptibility prediction of the various landslide analysis methods used by this study. For this reason, it is important to determine the location and area of the landslide accurately when preparing the landslide susceptibility maps. About 4.5 % of the total catchment area of the study area is affected by the landslides. Comparing the areal coverage of the landslide types, 11%, 14% and 75% are respectively occupied by the debris slide, rock fall/topples and debris flow (Fig 9.21).

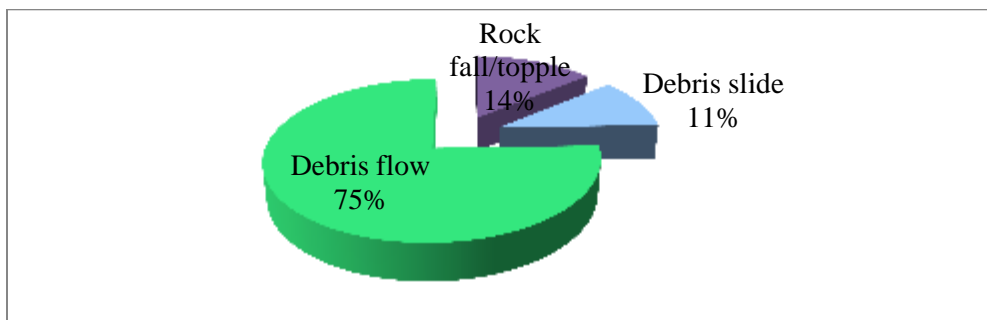


Fig 9.21: Landslide types and their percentage of area coverage

9.4.2 Input map preparation

In the case of the R.S.Girolamo, six relevant causative factors are selected as inputs for the models of landslide susceptibility evaluation and compare the degree of influence for each possible factor and their sub-classes i.e. slope, aspects, elevation, and distance from streams, land use, and lithology.

9.4.2.1 Slope gradient

Slope is very regularly used in landslide susceptibility studies by numerous researchers and is also considered in this study. Hence, the slope map of R.S. Girolamo area is derived from the 10m resolution DEM using the slope function of the spatial analyst of ArcGIS 9.3. The slope map is prepared in the form of a raster map with the same pixel size as the DEM. A map of slope classes is generated by separating the slope angles into five different classes considering the weighting system of PAI (Fig 9.22): (a) slope class-1 ($<10^0$), (b) slope class-2 ($11-20^0$), (c) slope class-3 ($21-35^0$), (d) slope class-4 ($36-50^0$), and (e) slope class-5 ($>50^0$). In the area of interest, the steep slopes are covered by the granitic and metamorphic rock outcrops which are potential sources of rock falls and/or topple while the gentler slopes are characterized by the debris accumulation.

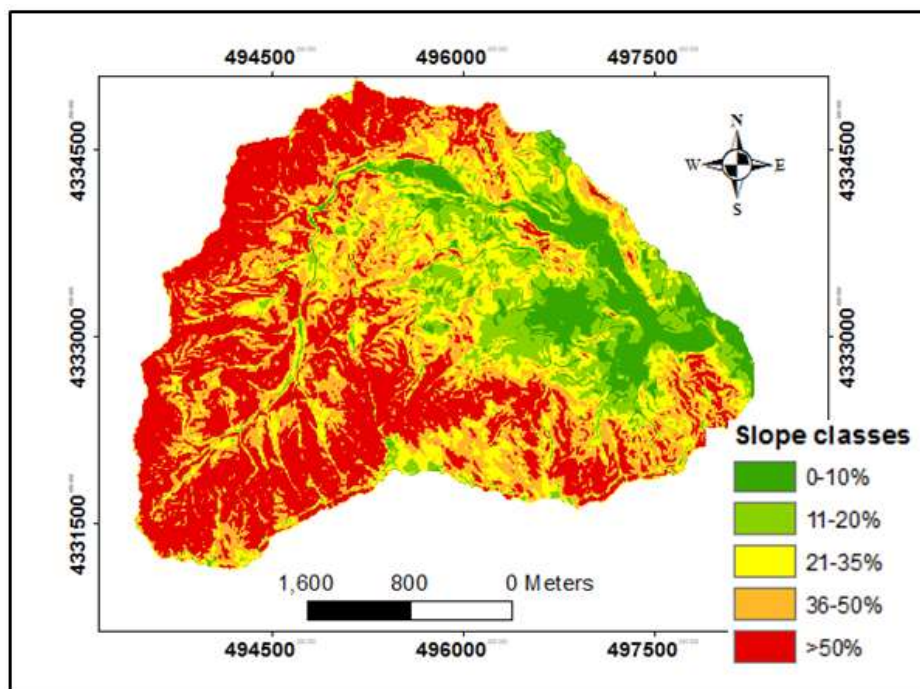


Fig 9.22: Slope gradient map of the study area

Fig 9.23 below designates that slope classes $>50\%$ and $36-50\%$ are the dominant ones in terms of areal coverage and characterized by slope instabilities. While the slope class $0-10\%$ have smallest areal coverage and are areas of debris deposition.

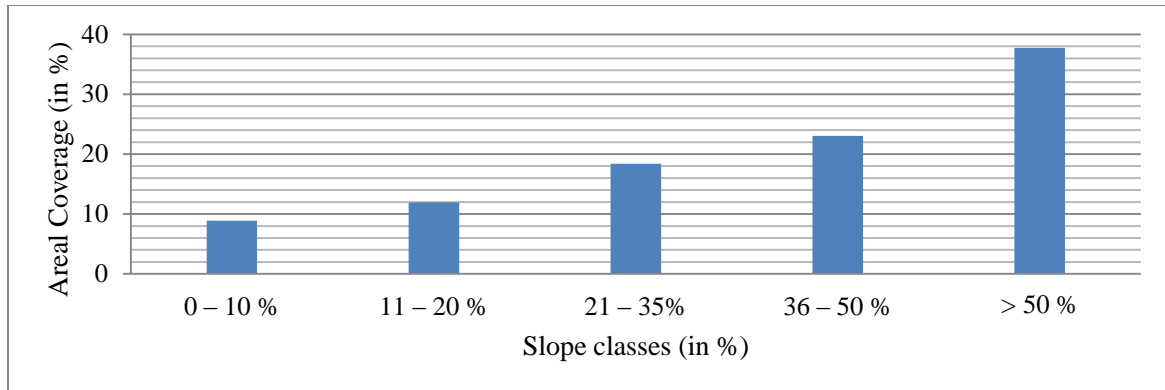


Fig 9.23: Percentage of areal coverage by the different slope classes

9.4.2.2 Slope aspect

Aspect is another landslide controlling factor considered in the landslide susceptibility assessment of R.S.Girolamo catchment as is also considered in several similar studies. Aspect simply refers to the orientation to which a mountain slope faces and can make very significant influences on its local climatic factors such as amount of rainfall which in turn influences the occurrences of landslides. Aspect related parameters such as exposure to sunlight, drying winds, rainfall (degree of saturation), and discontinuities may control the occurrence of landslides (Dai & Lee, 2002).

Hence, the slope aspect of the study area is derived from the 10m DEM. The derived aspect map was further reclassified into 8-distinctive classes (Fig 9.24). The catchment of R.S. Girolamo is a nearly circular shape having a slope face (aspect) to every direction. Thus, rock fall and/or topples and debris slide occurred in most slope face with dominant one being W, N, NW facing slope aspects. However, the aspects of NE, E and N have dominant areal coverage having 21.3%, 18.5% and 14.2% respectively (Fig9.25).

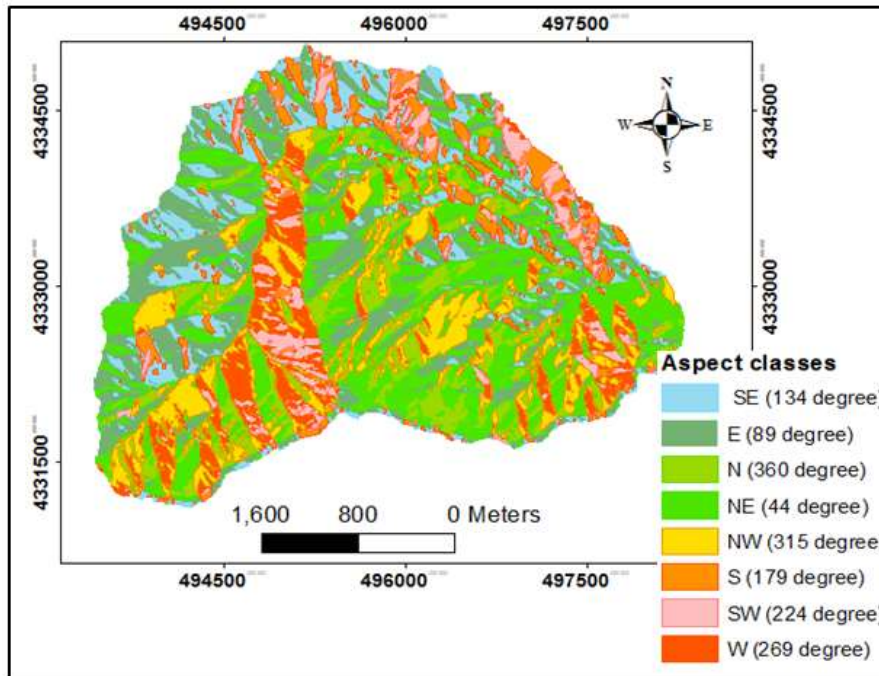


Fig 9.24: Slope aspect map of the study area

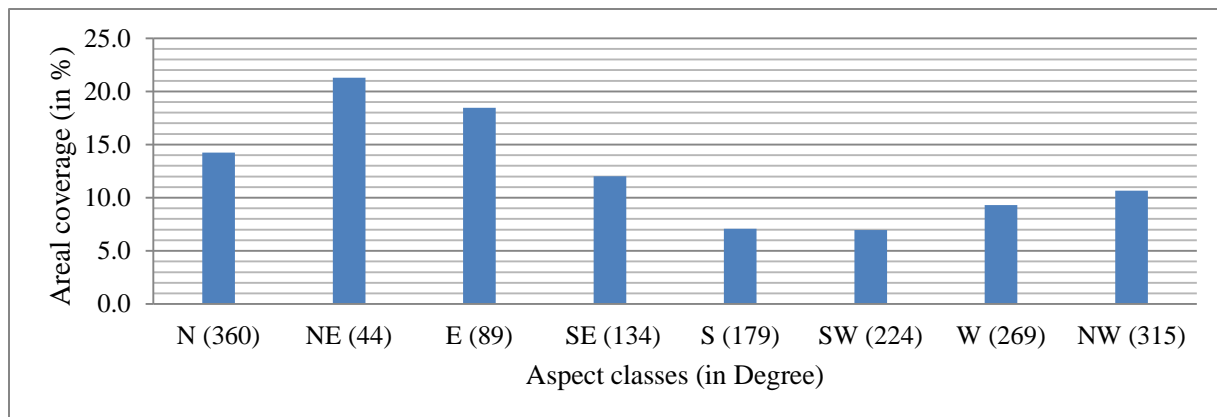


Fig 9.25: Percentage of areal coverage by the different classes of aspects, R.S.Girolamo, Sardinia

9.4.2.3. Elevation

Elevation is another selected useful landslide causative factor. To correlate landslide occurrence for different relief classes, the elevation map has been prepared from the 10m DEM map with help of ArcGIS9.3 and categorized into 5-class ranges (Fig 9.26). The influence of elevation to landslide is often reflected also as indirect relationships or by means of other causes. For example in the study area, lithological variations and degree of weathering that plays an important role in land sliding, is closely related with elevation. The elevated areas are covered by the fractured rock outcrop while the lower areas with the recent sediments. The spatial variability of rainfall is also dependent on the elevation.

The minimum elevation in the area of interest is 52m, while the maximum is 738m. Elevation classes in the range of 52-150m and 150-300m and 300-450m covers 28.6%, 30 % and 23.9 of the total area respectively, while the elevation greater than 450m has smallest areal coverage (Fig 9.27). More than 53% of the landslide distribution is found within the elevation class range of 300-450m followed by the elevation class range of 450-600m which contains 31% of the landslide occurrences.

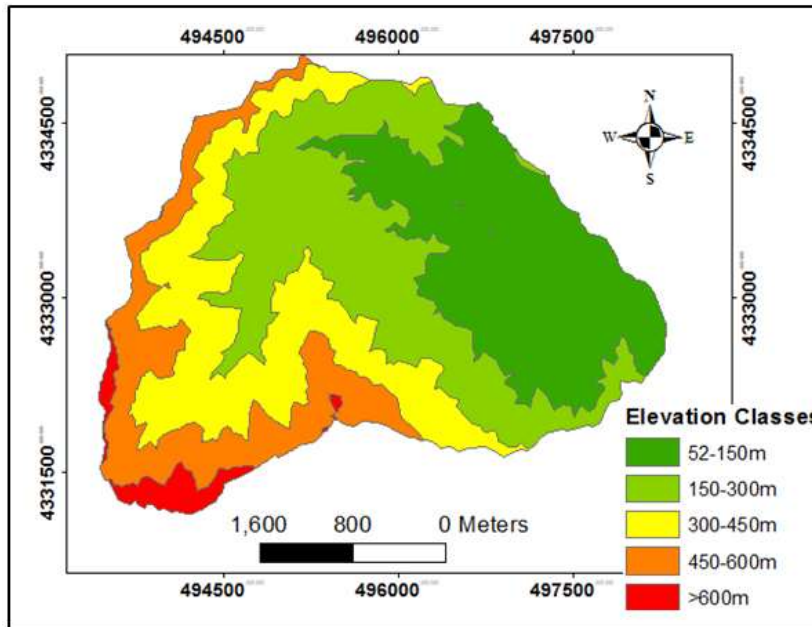


Fig 9.26: Elevation map showing the various classes of R.S. Girolamo area

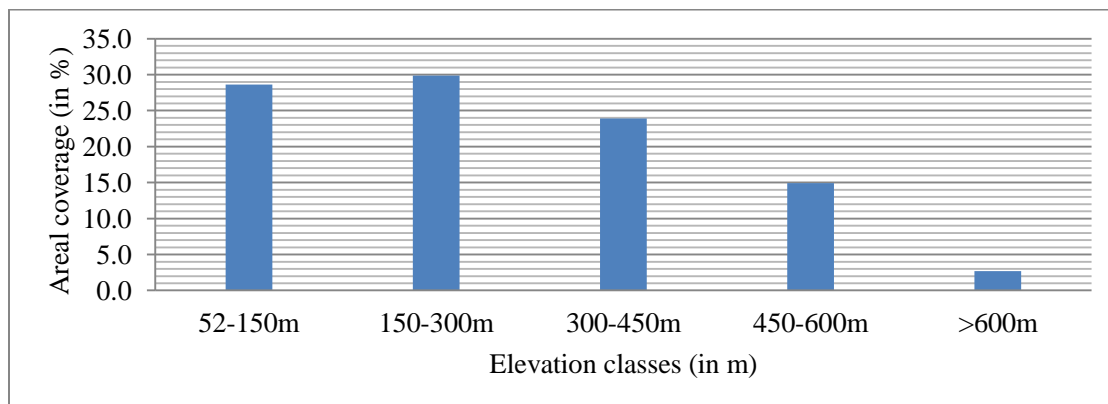


Fig 9.27: Percentage of areal coverage by the different classes of elevation

9.4.2.4 Proximity to drainage

Field observation showed that streams have a significant role in the superficial slope instability of the study area by toe erosion and hence proximity to stream is considered as one of the major factors for the landslide study. Consequently, the drainage map has been prepared from the 10m DEM with the help of Archydro 9.3.

Unlike the Debresina area, most drainage of the R.S.Girolamo has a shallower river bed due to the relatively shallower thickness of soil. However, the catchment area is dissected and eroded by dense first and second order streams which trigger the debris flow initiation. They also have an over steepening of the lower sections of the slopes and removal of materials that provided support at the toe causing slope instability.

The prepared map was divided into five different drainage proximity zones (Fig 9.28) and more than 54% and 30% of the study area respectively is found within the range of 0-100m and 100-200m distance from the drainage, and about 94% of the landslides occur in these areas.

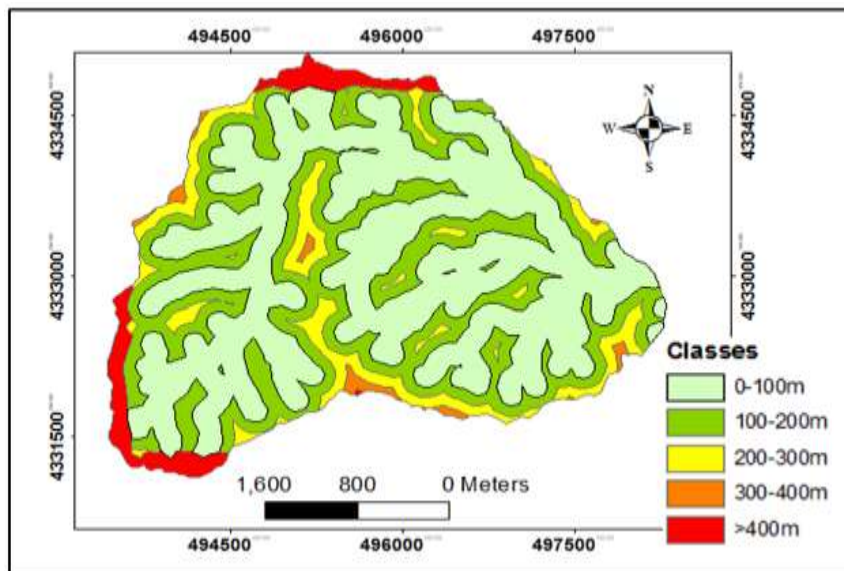


Fig 9.28: Drainage proximity map of the R.S Girolamo area

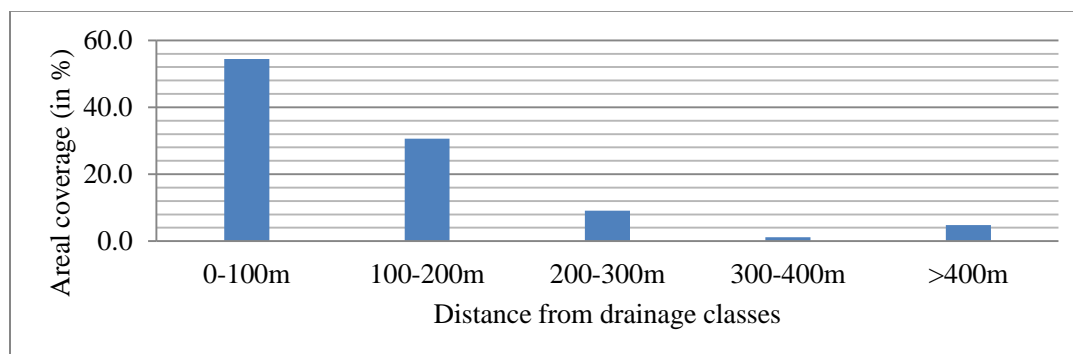


Fig 9.29: Proximity to drainage versus areal coverage, R.S. Girolamo, Sardinia

9.4.2.5. Land use

Land-use is another important causative factor in the landslide evaluation of the area. The land use map of the study area has been prepared from the modification of the regional land use map of region of Sardinia, field work, Google Earth, orthophotos of 2006 (Fig 9.30). In this study, eight land use classes have been identified

with the dominant involving mixed scrub land/bush (55%), forest (13%), residential fabrics, urban and suburban areas (10%), bare rock outcrop (9%), river course & reservoir areas (8%), and so on (Fig 9.31).

The bare rock out crops are potential sources of the rock falls and/or toppling and debris and boulder sliding while lower regions (up to slopes $< 20^\circ$) have comparatively higher human influence. People in this region are still involved in some house and road constructions towards the foot of the mountains. This may aggravate the landslide phenomena in the future. On the other hand, huge amount of debris materials are being protected from moving down temporarily by the forest and mixed scrub lands. Nevertheless, they can be easily moved by runoff during heavy rainfall or if there is forest fire in the future.

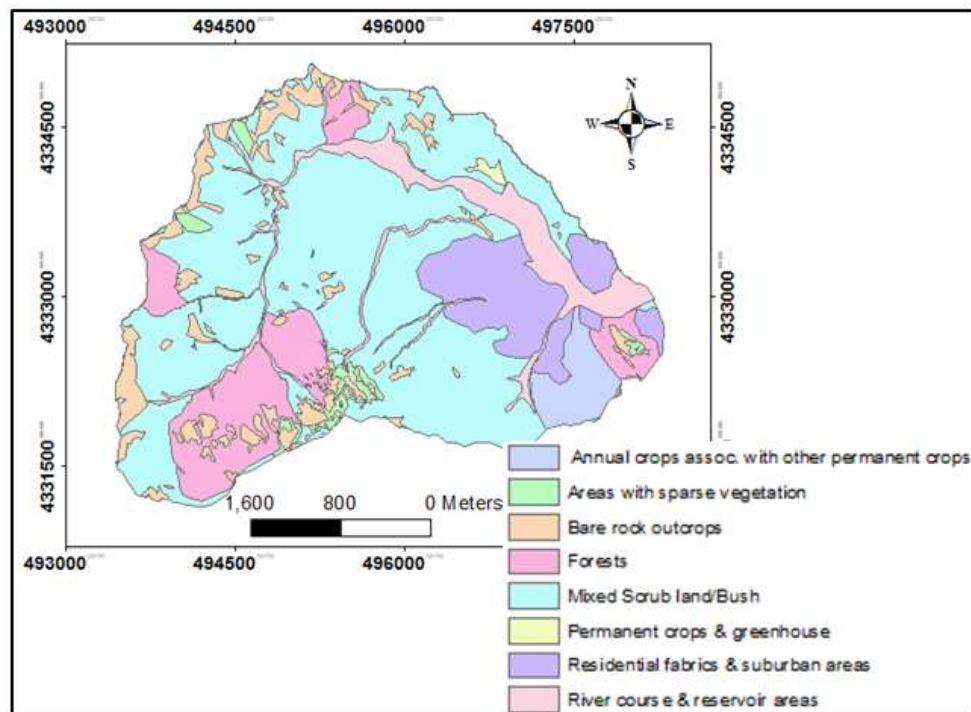


Fig 9.30: Land use map of the study area

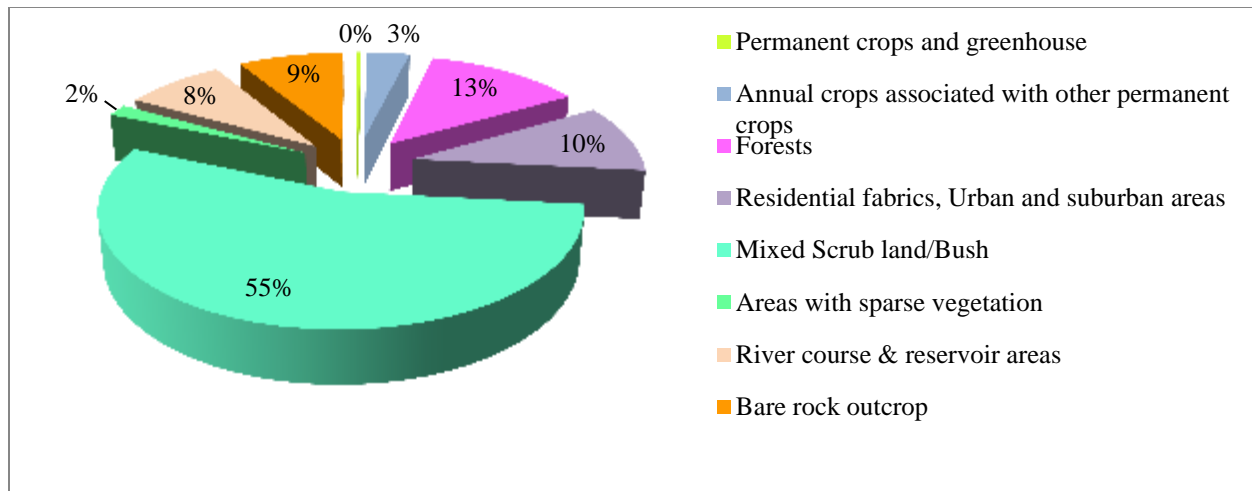


Fig 9.31: Percentage of areal coverage by the different land use classes

9.4.2.6 Lithology/Litho-technical mapping

It is strongly accepted that lithology significantly influences the occurrence of landslides due to the fact that lithological variations often lead to a difference in the strength and permeability of rocks and soils. Thus, similar to the land use the lithological map of the study area has been prepared from intense field survey, interpretation of various orthophotoes, Google Earth, supported by the existing regional geological map of Capoterra sheet 565 (1:50,000 scale), and some laboratory works as described in the previous chapters.

The main rock formations that cover the catchment area, as described in chapter-9 under section 9.3 are the Paleozoic metamorphic basement and complex granitic intrusions. Under here, more focus is given to the litho-technical mapping and the lithologies and further description in term of their degree and depth of weathering, fracture, texture and the likes is done based on a format modified from guideline developed by the Italian Geological Services (Amanti M., et al,1992). For instance, the fresh and slightly weathered rock outcrops are separately mapped while the highly weathered parts of the granitic and /or the metamorphic rocks are mapped as soils. The recent sediments are also further divided in to alluvial, colluvium-alluvium, colluvium and talus based on the textural, depositional mechanisms, morphological nature of the area.

The physico-mechanical parameters such as degree and depth of weathering, orientation and spacing of discontinues, unconfined compressive strength, hydraulic nature, compaction and cementation of each lithologies, have been described and measured in 180-GPS points during the fieldwork based on the mentioned guideline. The estimated depth of weathering has been measured from gully and ridge exposure using the meter tape, While Schmidt hammer, compass and GPS have been used to measure the compressive strength, joint characteristics and

locations respectively. These physic-mechanical descriptions are already described above in chapter-9 and the lithological map is given in Fig 9.32 below.

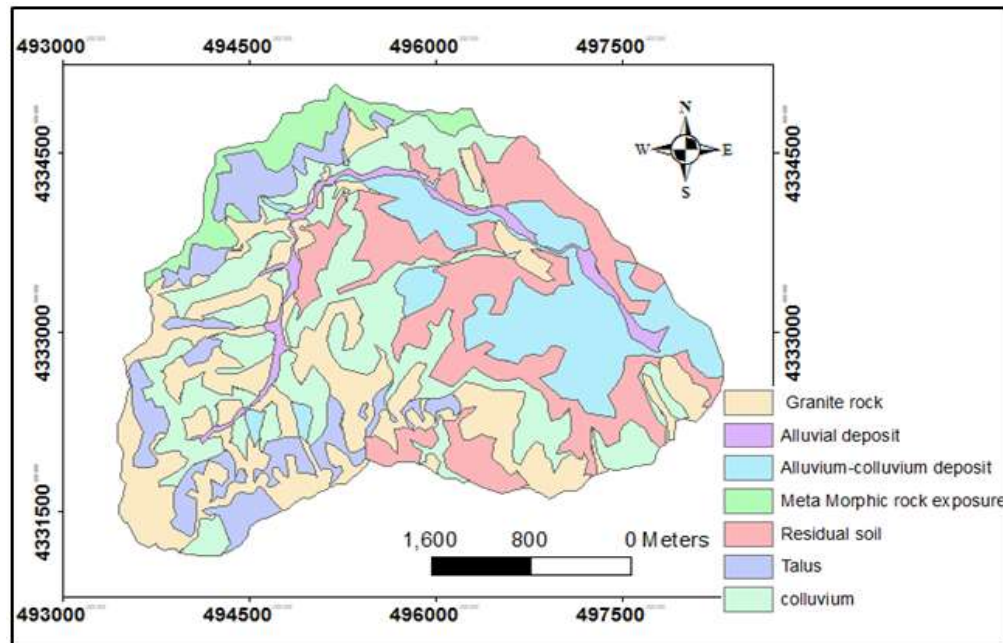


Fig 9.32: Lithologic map of the study area

Considering the detailed classification of the lithologies (or litho-technical map), about 29% of the catchment is covered by the rock outcrops (5% metamorphic & 24% granitic rock) and 71 % of the area is covered by recent sediments including the residual soils (Fig 9.33. Out of these the granitic rocks are main sources of rock fall and/or topple while the talus and alluvial sediments are the main sources of debris slide and debris flow respectively.

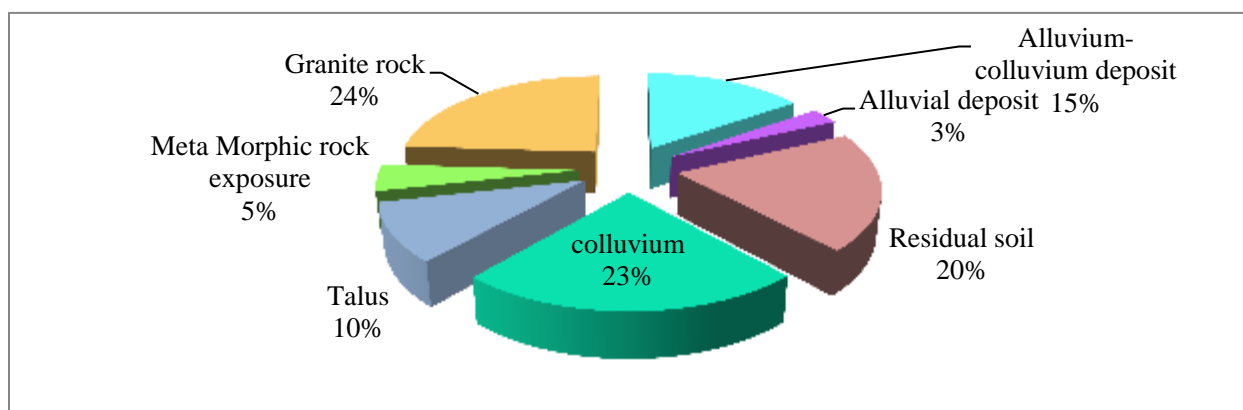


Fig 9.33: Percentage of areal coverage by the different lithologic units

10. GIS- based landslide susceptibility mapping and analysis of R.S.

Girolamo area

Landslide susceptibility zoning involves the spatial distribution and rating of the local environmental conditions according to their tendency to produce landslides. It should consider all land sliding which can affect the study area and include landslides which are above the study area but may travel onto it, and landslides below the study area which may retrogressively fail up-slope into it (Fell R., et al, 2008).

As has seen in the descriptive section of the methodologies to assess landslide hazards, there are several approaches useful in analyzing the potential hazards. Most of the approaches currently used in assessing and mapping landslide susceptibility are based on an accurate evaluation of the spatial distribution of both the landslide causative factors and/or of the landslides. The same methods (OM, FR, AHP, and GLE) are adopted to analyze and evaluate the potential slope stability problems in the R.S.Girolamo basin. It is envisaged also to test the applicability of the various methods for landslide susceptibility of different environments. The short introduction of each of these methods and their application can be referred to chapters 2 and 5.

10.1. GIS-based Overlay Mapping techniques (OM)

10.1.1. Methodology

The Overlay Mapping method is a type of heuristic approach utilized by the regional government of Sardinia (Italy) to study and evaluate hazards and risks, with their mitigation measures in the region. The general principles and background information of this method can be referred in chapter-5 under section 5.1.1, as already described there.

Based on the requirement of the method three main environmental factors such as Slope gradient, Litho-technical and land use factors of R.S.Girolamo are prepared to be used for appraisal process of the slope instability of the area. These input data and thematic maps are collected and processed based on guideline of the Italian Geological Services (Amantii M., et al, 1992) in a similar manner as stated in section 5.1.1. Classification of the factors into classes or sub-classes is accomplished; numeric weights were assigned to each factors /classes considering their field findings and influence to the slope instability. Finally, various processes of data preparation of the input maps and overlay mapping are done with the help of ArcGIS 9.3 as given in the flow chart in chapter-5 (Fig 5.1). In this part, the processes and procedures related to the landslide

susceptibility of Overlay Mapping, their results and implications will be discussed and addressed as specific to the catchment of R.S.Girolamo area.

10.1.1.1. Weighed slope map

The Slope map and its different slope classes of the study area are given in chapter-9, section 9.4.2.1. Under this part; weights are assigned to the five slope classes according to the guideline of PAI. As per the PAI system, the weight to be assigned for the slope varies from -2 (steepest slope) to +2 (flat area) as referred in Table10.1. The maximum areal coverage (37.8 %) falls in the higher slope class range of >50% while the minimum coverage (8.9%) lies in the slope class range of 0-10%. About 61 % of the study area is covered by the slope range of 36-50% and >50% whose weights are assigned by -1 and -2 (Table10.1 and Fig10.1).

Table10.1: Weights of the different classes of slope gradients of R.S. Girolamo using PAI weight.

Slope classes (deg)	Equivalent Slope classes (%)	Weights	Areal coverage (%)
0 - 6	0-10 %	2	8.9
7-11	11-20 %	1	11.9
12-19	21-35%	0	18.4
20 -26	36-50 %	-1	23.1
> 26	> 50 %	-2	37.8

The weighed slope map of the study area is made in the GIS environment (Fig10.2).

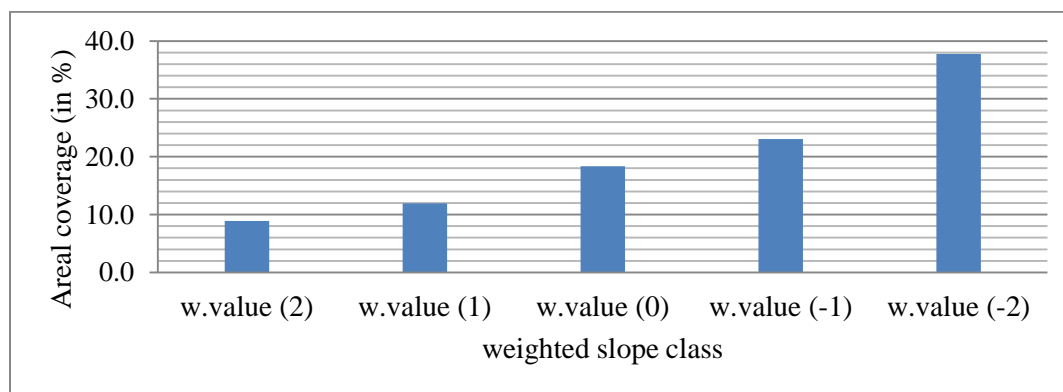


Fig 10.1: The percentage areal coverage of the various weighed Slope classes based on PAI weighing system. (w.value = weighted values)

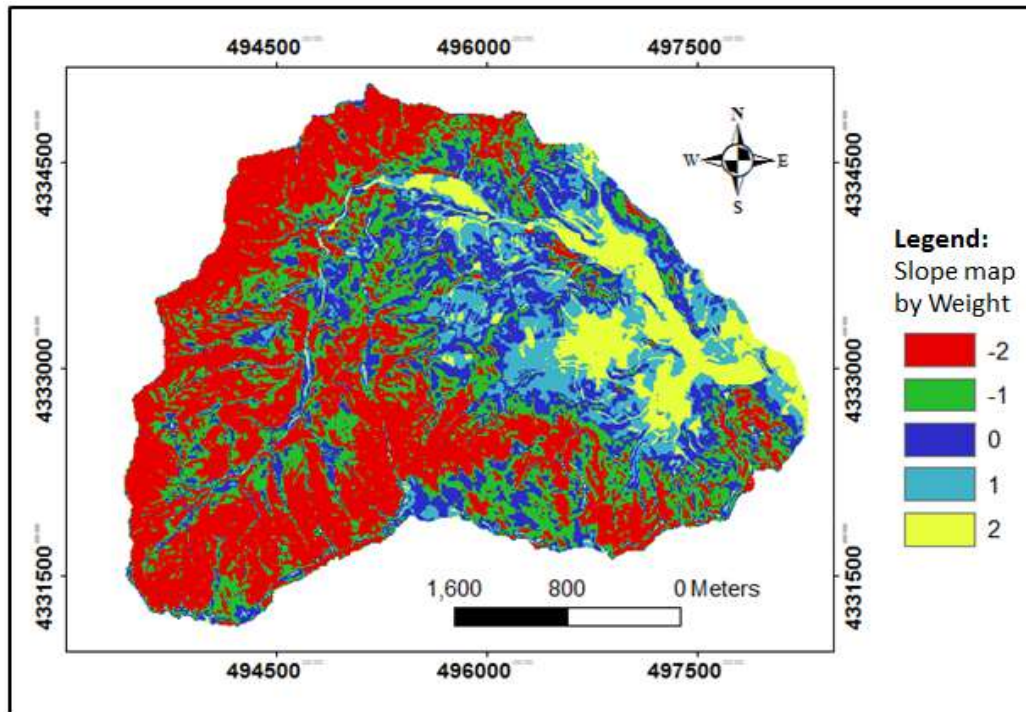


Fig 10.2: Weighed slope map of the study area

10.1.1.2 Weighed land use map

The Land use map of the study area and its various classes are presented in section 9.4.2.5 above. Eight land use classes has been identified, with mixed scrub land/bush, forests, and residential fabrics/ urban areas being the main land use units covering 54.72%, 12.8 % and 10.07% respectively (Table10.2). From the field observation, landslide occurrences are pronounced at the forests, river courses and bare rocks compared to the other types of land use classes. Weights are assigned for each identified land use classes as per the PAI guideline, which vary between +2 (e.g. forest land use) to -2 (e.g. arable land, river bed) and the weight values for the rest of the classes (Table10.2).Then the land use map is rasterized using the weighted value and prepared in a way suitable for the Overlay Mapping process (Fig10.3).

Table10.2: Areal coverage of various Land uses and their assigned weights, R.S.Girolamo

Land use classes	Area (in %)	Weight
1 Permanent crops and green house	0.34	0
2 Forests	12.80	2
3 Annual crops associated with other permanent crops	3.51	-2
4 Residential fabrics, Urban and suburban areas	10.07	1
5 Mixed Scrub land/Bush	54.72	1
6 Areas with sparse vegetation	1.72	0
7 River course & reservoir areas	8.16	-2

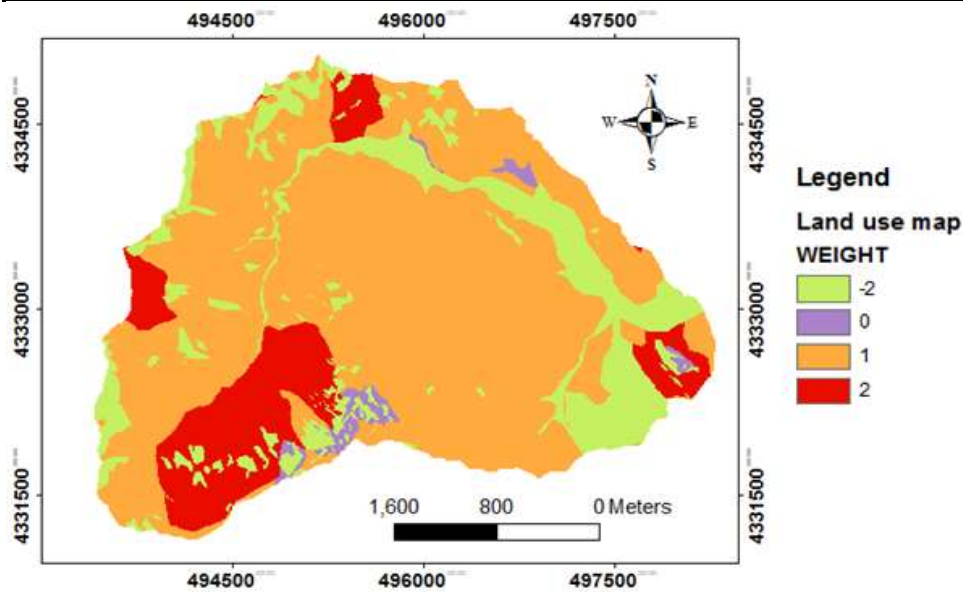


Fig 10.3. Rasterized weighed land use map of the study area

10.1.1.3. Weighed Litho-technical map

Similarly, the Litho-technical map and the Lithological classes of R.S.Girolamo area are given in chapter-9 section 9.4.2.6. According to Overlay Mapping method, litho-technical factor is one of the most decisive factors in the slope instability assessment. It incorporates several lithological and mechanical parameters to be addressed in detail in the field.

The evaluation of the litho-technical parameters, the division into classes and weighing processes was performed following the same instructions of the Italian Geological services and the PAI weighting systems as stated in chapter-5 section 5.1.1.3. All the litho-technical parameters have been collected in 180-field station points and weight is assigned. Normalization of the field litho-technical weight is also done using the same graph and equation shown in Fig 5.5 of chapter5 as per the PAI guideline. Sample calculation of normalization is given Table10.3. Details of the normalization process can be referred under section 5.1.13.

Table10.3: Example of calculated litho-technical weights in two stations of R.S Girolamo

Lithology	granitic rocks			
Stations	11		18	
GPS locations	4332403 (mE)	495630	0497719 (mE)	4332382 (mN)
	Classes	weight	Classes	weight
Degree of weathering	II	3	III	2
Depth of weathering	I	4	II	3
Spacing of discontinuity	II	3	III	2
Orientation of discontinuity	II	3	II	3
Compressive strength	I	4	III	2
Permeability	III	2	III	2
Sum of weights	19		14	
Weight of PAI	6.7		4.6	

In a similar way as shown in the table 10.3, all the weights are calculated in the 180 stations and the weighted litho-technical map is produced (Fig 10.5), which is the major input map for the Overlay Mapping method. Then after some editing and crosschecking, the polygon litho-technical map is rasterized for the overlay mapping process (Fig10.5).

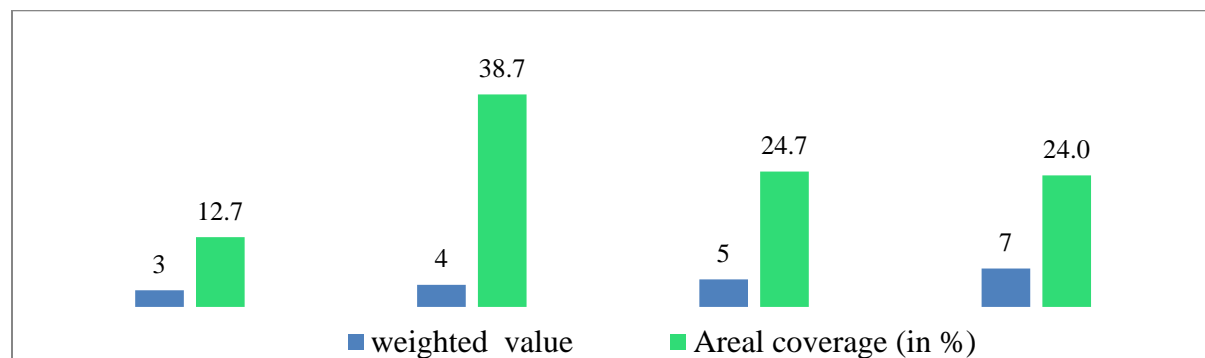


Fig 10.4: Histogram of areal coverage of each weighed of litho-technical classes based on PAI weighing system

More than 76% of the total area is covered by lithologies having a weighted value of 3 to 5 (Fig10.4). This means that most lithologies of the study area are weathered and liable to slope instability problems. However, the depth of weathering of R.S.Girolamo is shallow as compared to the Debresina area of Ethiopia.

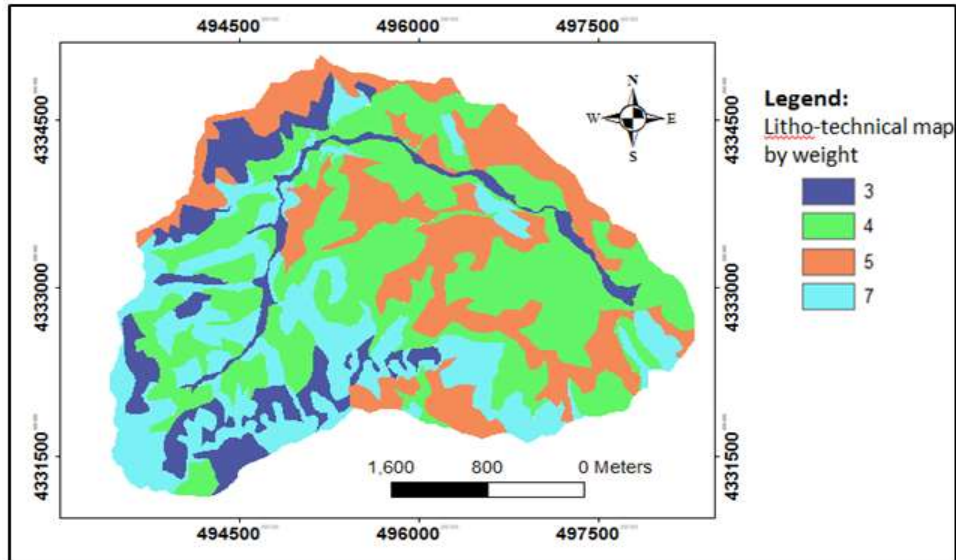


Fig 10.5: Weighed Litho-technical map of study area

10.1.2 Results and discussion

To prepare the landslide susceptibility of the study area based on Overlay Mapping approach: (1) selection and mapping of the causative factors such as Slope (Fig10.2), Land use (Fig10.3) and Litho-technical (Fig10.5) is performed (2) thematic data layers are categorized among different classes and corresponding weights are assigned (3) GIS based Overlay Mapping model is using the model builder of ArcGIS 9.3. The flow chart used for the overlay model preparation of the study area is shown in chapter5 of Fig 5.8, similar to the Debresina area (4) All the thematic maps are rasterized based on their assigned weight values and Overlay Mapping process is performed using the developed GIS model (5) finally, raw Landslide Susceptibility Index (LSI) map showing the various zones is produced by the overlay. Resulting LSI values range from -1 (very high susceptibility to land sliding) to 11 (non-susceptible areas) as per PAI guideline.

To reclassify this raw map into the required number of landslide susceptibility zones or classes of the study area, the class boundary of PAI guideline has been applied.

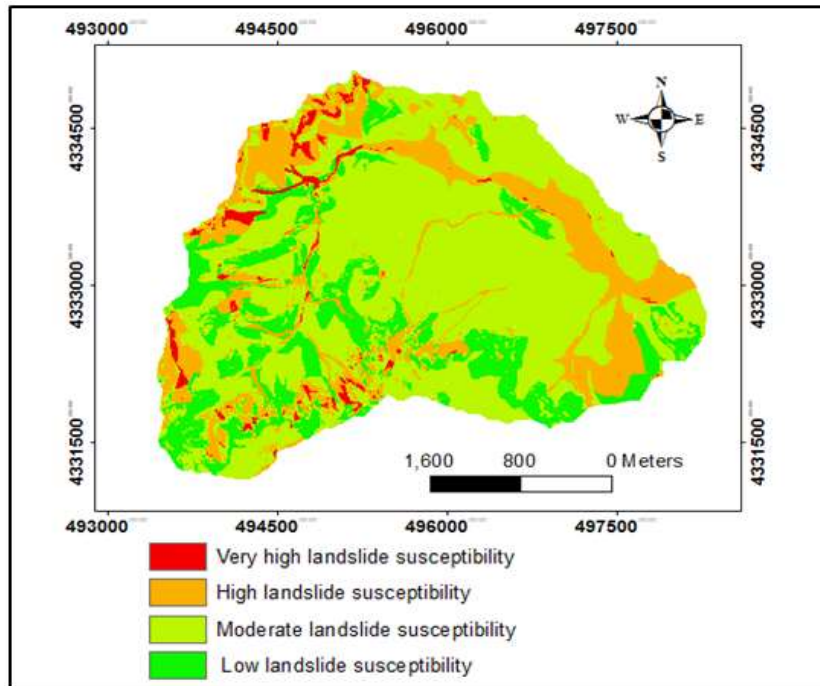


Fig 10.6: Landslide susceptibility zonation of R.S. Girolamo area based on Overlay Mapping method

Thus, based on the PAI boundary classifier, four various Landslide Susceptibility Index (LSL) has been identified (Figs10.6 and 10.7). These susceptibility classes involve: low (18%), moderate (59%), high (21%), and very high (2%). This depicts that about 23% of the area is susceptible to landslide.

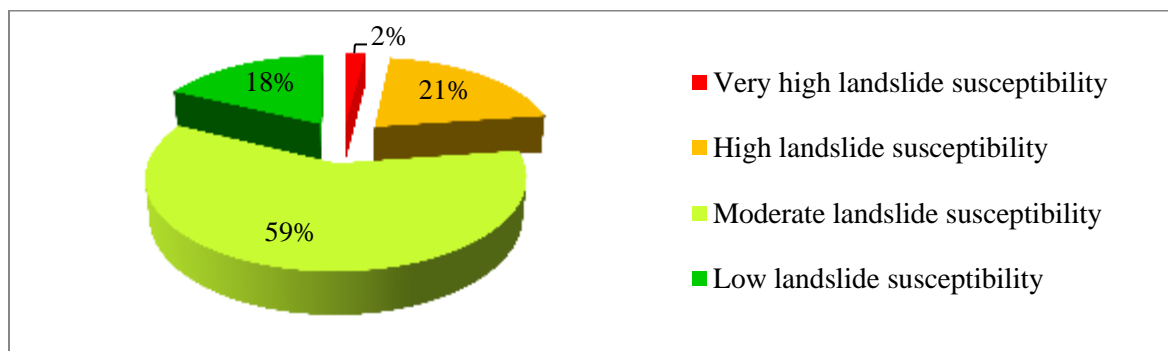


Fig 10.7: Areal coverage (in %) of the four Landslide Susceptibility Index (LSI) classes based on Overlay mapping method.

The produced landslide susceptibility map (Fig10.6) has good agreement with the field condition. The Overlay Mapping method and is therefore reasonably appropriate method in the landslide susceptibility assessment, especially it is suitable for medium and large scale landslide mapping.

Generally speaking, the overall landslide susceptibility results of this method for the study area is useful and is believed to give important information for local authorities to safeguard lives and property and improve planning and further development in the area.

10.2. Frequency Ratio (FR) method

The most relevant input factors controlling landslides in the R.S. Girolamo area (margin of Campidano graben) of Sardinia (in chapter 9, section 9.4.2) include Lithology, Proximity to drainage lines, Land use, Slope, Aspect and Elevation. Each of these causative factors are further classified in to a number of detailed classes. Comprehensive landslide inventory is also conducted. The relationship between these landslide causative factors and the landslide occurrences are evaluated using the GIS supported Frequency Ratio method and finally the landslide susceptibility of the area is prepared and zoned using the obtained frequency indexes.

10.2.1 Methodology

Similarly to the Debresina area of Ethiopia, FR method has been also applied in the landslide susceptibility assessment and evaluation of R.S Girolamo area. The details of this methodology can be referred in part II of section 5.2.2 as it is explained there.

To apply the FR method of landslide evaluation for the study area, the spatial data base and the input maps of the study area have been constructed using GIS techniques. After the data base was created and input maps preparation was completed, the FR value was calculated for each classes of the parameter as given in equation 5.1, as has been done in similar studies (e.g. Lee and Min, 2001; Lee and Pradhan, 2006),

The FR index of each landslide causative factor has been calculated with the help of spatial analyst techniques of ArcGIS9.3. The weighed sums of FR values of all classes have been used to produce a landslide susceptibility map.

10.2.2. Results and discussion

10.2.2.1 Correlations between landslides and causative factors using FR probability model

The areal coverage of landslide occurrences in each class of causative factors is calculated by crossing with the inventory map using the ArcGIS. Then, the FR is determined by the ratio of landslide area in each class (Y in %) and total area occupation of each class (X in %) and its value is used for the correlation of each of the various factors & the landslide occurrences. The FR values of the six chosen landslide causative

parameters are demonstrated in Table10.4. When $FR < 1$ means it has less correlation than average, $FR > 1$ means higher correlation than average and $FR = 1$ means comparable to average (Lee, 2005).

The ratios of each factor type were summed to calculate the Landslide Susceptibility Index (LSI) using equation (5.2).

Table10.4: Frequency Ratio (FR) of landslide occurrences of R.S. Girolamo

Factor/classes	X (% total area)	Y (% landslide area)	FR (Y/X)
Land use			
[1] Permanent crops and greenhouse	0.34	0	0.00
[2] Annual crops associated with other permanent crops	3.51	0	0.00
[3] Forests	12.80	50.7	3.96
[4] Residential fabrics, Urban and suburban areas	10.02	0.1	0.01
[5] Mixed Scrub land/Bush	54.72	9.6	0.18
[6] Areas with sparse vegetation	1.73	2.2	1.28
[7] River course & reservoir areas	8.16	23.4	2.86
[8] Bare rock outcrop	8.72	14.1	1.61
Lithology			
[1] Alluvial deposit	2.75	13.46	4.90
[2] Alluvium-colluvium deposit	15.32	2.47	0.16
[3] colluvium	23.39	7.51	0.32
[4] Granite rock	23.97	68.44	2.86
[5] Metamorphic rock exposure	4.54	0.27	0.06
[6] Residual soil	20.11	0.55	0.03
[7] Talus	9.92	7.30	0.74
Proximity to Drainage			
[1] 0-100m	54.38	70.92	1.30
[2] 100-200m	30.60	23.35	0.76
[3] 200-300m	9.07	0.36	0.04
[4] 300-400m	1.16	0.06	0.06
[5] >400m	4.80	5.30	1.10
Elevation			
[1] 52-150m	28.64	5.57	0.19
[2] 150-300m	29.85	9.60	0.32
[3] 300-450m	23.92	53.44	2.23
[4] 450-600m	14.91	31.19	2.09
[5] >600m	2.68	0.21	0.08
Aspect			
[1] N (360 degree)	14.23	21.95	1.43
[2] NE (44 degree)	21.28	16.80	0.91

[3]	E (89 degree)	18.46	15.65	0.83
[4]	SE (134 degree)	12.00	7.16	0.59
[5]	S (179 degree)	7.09	6.34	0.83
[6]	SW (224 degree)	6.96	5.28	0.70
[7]	W (269 degree)	9.30	14.92	1.49
[8]	NW (315 degree)	10.67	11.89	1.25
Slope				
[1]	0-10%	8.9	2.11	0.24
[2]	11-20%	11.9	0.86	0.07
[3]	21-35%	18.3	1.42	0.08
[4]	36-50%	22.9	2.16	0.09
[5]	>50%	38.0	93.45	2.46

Lithology & landslide occurrences

Lithology is one of causative factor for the overall slope failures in R.S.Girolamo area. Especially, areas covered by the alluvial deposits, fractured granite and talus are prone to debris flow, rock fall and debris slide respectively (Figs10.9 and 10.10). The FR -values of the alluvial deposits and fractured granite are greater than one showing they are prone to the landslide phenomena while that of talus is near to one indicating its potentiality to the slope failure (Table10.4 and Fig10.8). The alluvium-colluvium deposit of R.S. Girolamo area include a heterogeneous mixture of loose slope wash deposits, old landslide deposits, which has variable thickness varying from 1 to more than 3.5m. These are commonly affected by gully erosion followed by small debris slide and debris flow as observed during the field work.

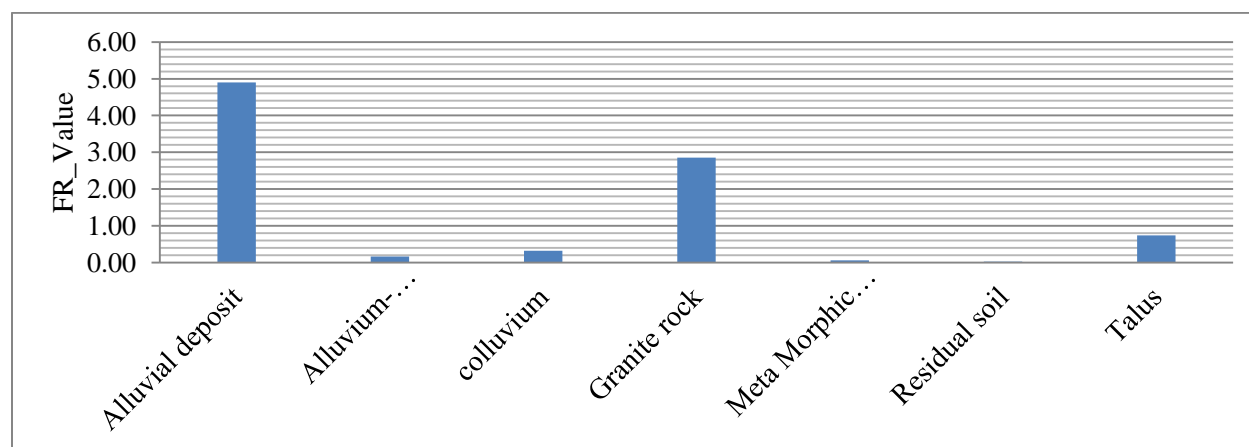


Fig 10.8: Histogram showing the FR values of various lithologies of the study area



Fig 10.9: Photographs showing the various lithologies and landslides: (a) fractured granite rocks which are liable to rock falls (b) talus deposit which are prone to debris slide (c) non-channelized debris flow containing woods and rock boulders (d) channeled debris flow along the streams of R.S. Girolamo catchment



Fig 10.10: Rock fall derived talus deposits at the foot of the fractured granite rock exposure and NNW-SSE trending lineaments (taken from Google Earth of 2011)

Land use & landslide occurrences

The data obtained from the map regarding land use suggest that the most susceptible classes are pockets of the forested area, river courses, bare rock out crop or areas with less vegetated having $FR > 1$. The vegetated areas (forests) are being destructed by the channelized and non-channelized debris flows as well as rock falls. The rest has low FR value and are with less contribution to sliding.

Proximity to drainage and landslide occurrences

The drainage proximities show a strong correlation with landslide occurrences, especially within the distances range of 100m (Table10.4). This can be attributed to the fact that terrain modification caused by gully erosion and undercutting, as well as saturating the lower part of material may influence the initiation of landslides up to the distance of mainly 100m. This indicates that stream has a destabilizing effect near to their course by eroding the slopes or by until the water level increases and such effect especially is maximum, where they are in contact with loose colluvium materials.

Topographic-based factors and landslide occurrences

Three main topographic factors such as slope, aspect and elevation are evaluated in correlation to the landslide occurrences. The slope class having an inclination of more than 50% has FR values > 1 indicating that this zone is highly prone to landslide occurrences than the other slope classes (Table10.4 and Fig10.11). In the case of slope aspect, landslides were most abundant on North facing (360°), West facing (269°), Northwest facing (315°) and Northeast (44°) slopes. Thus, slopes facing to the mentioned slope aspects are highly susceptible to landslides with a FR values > 1 (Table10.4). With respect to the relationship between landslide occurrence and elevation factor, landslide occurrences are common in the elevation range of 300 to 450m as the FR value is greater than one (Fig10.12).

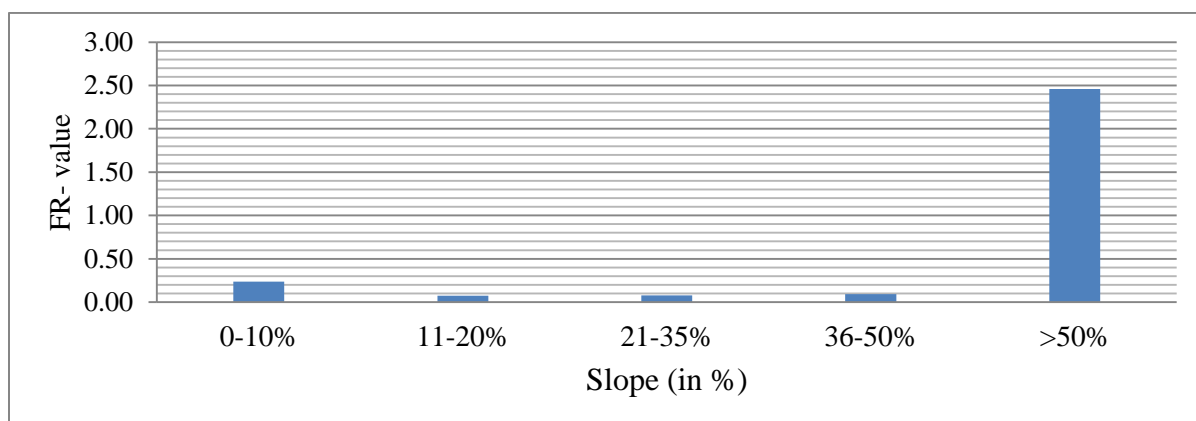


Fig10.11: The relationship between Slope gradient and FR values

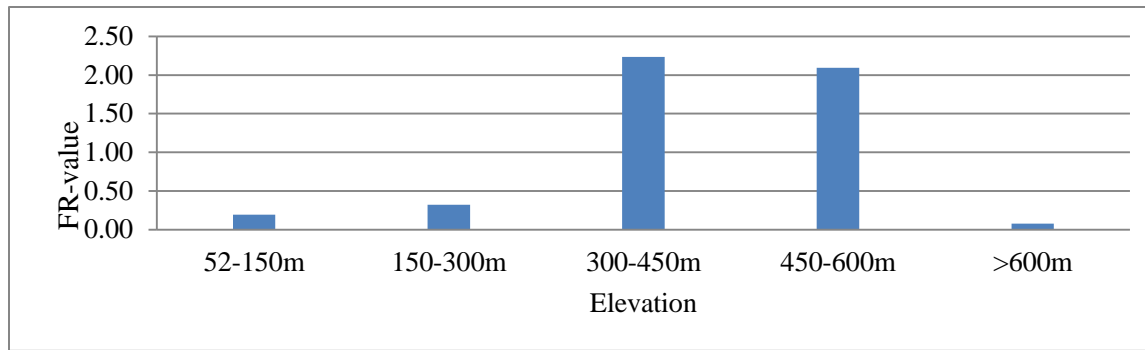


Fig 10.12: The relationship between Elevation and FR values

In order to enable the map interpretation, a landslide susceptibility zonation map is established by dividing the LSI values into various landslide susceptibility classes.

Finally, the raw landslide susceptibility index map was produced from the obtained values given by equation-1, where the weighted sum is done by map overlay and raster calculation techniques of the ArcGIS. From the calculation, it was found that the LSI had a minimum value of 0.94 (low susceptibility), and a maximum value of 15.51 (very high susceptibility). To reclassify this raw map into the required number of zones or classes, boundaries with common base is necessary. Similar to the Debresina area (section 5.2.2), manual classifier method was adopted to reclassify the LSI values into four different susceptibility zones, according to the classification method that was proposed by Galang (2004) as cited in Long, et al (2011). The basic principle of this approach is that higher landslide susceptibility classes should capture more or most of the landslide occurrences. Based on this rule, it can be inferred that the expected percentages of observed landslide occurrences in the low, moderate, high and very high landslide susceptibility classes are 6.7, 13.3, 26.7, and 53.3%, respectively (Long, et al, 2011).

For determining the class boundaries corresponding to percentages, the cumulative percentage of observed landslide occurrence (on y-axis) is plotted versus ranked LSI values (on x-axis) and then, the class boundaries of LSI values are obtained by intersection of the curve with the required observed landslide percentages. Accordingly, four LSI classes with boundaries of 3.88 (separating low-moderate), 7.8 (separating moderate-high) and 11.6 (separating high-very high) are respectively determined. The LSI values are re-classified in four zones or classes based on these boundaries and the susceptibility map of the FR model is shown in (Fig10.14).

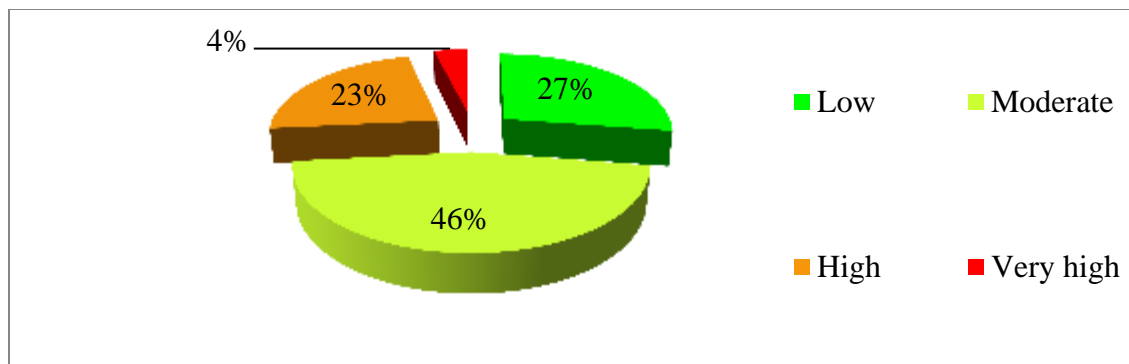


Fig 10.13: Areal coverage of the four landslide susceptibility index (LSI) classes by percent based on FR method.

Based on the LSI values, the study area is divided into four susceptibility classes (or zones), namely very high (3%), high (22%), moderate (45%) and low (30%) susceptibility zones. The classified landslide susceptibility FR method map depicts that 25% of the total area is susceptible to landslide.

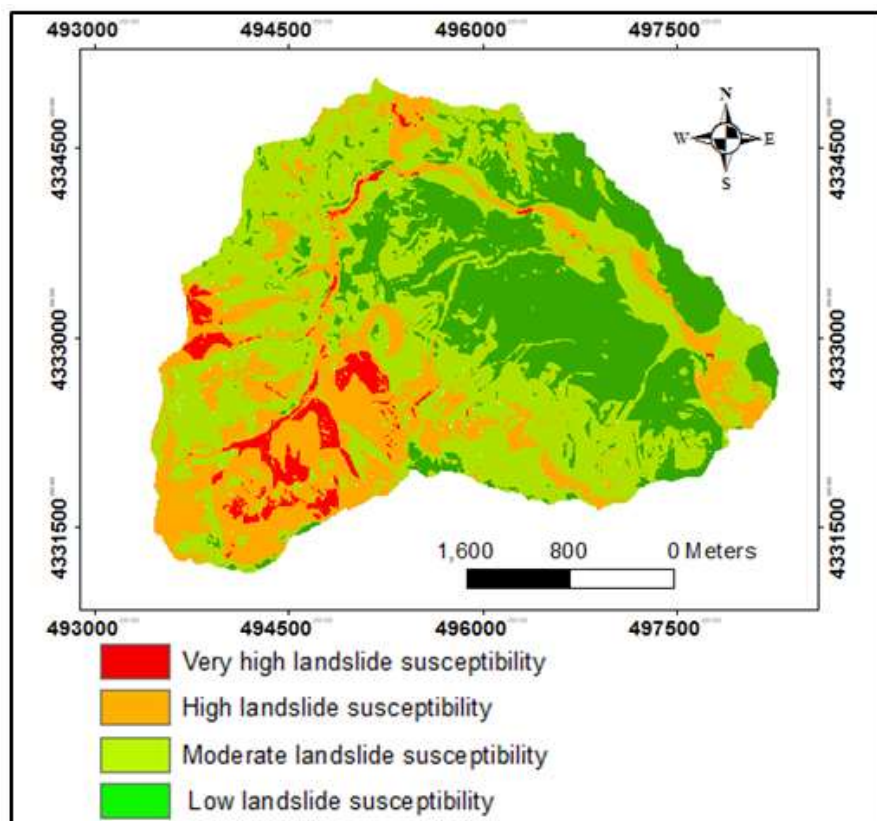


Fig 10.14: Landslide susceptibility zonation of R.S. Girolamo area based on FR-method

Similar to the Overlay Mapping method, the produced landslide susceptibility map of FR-method has reasonable prediction that fits to the field condition. Besides, to the susceptibility mapping this method is very

important to evaluate the contribution of the various causative factors to the landslide. The accuracy of this method increases if the landslide inventory is comprehensive and detail. Verification of the result is given in the next section of this chapter in comparison with other methods.

10.3. Analytical Hierarchy Process (AHP) method

10.3.1 Methodology

As the case in the Debresina area (Ethiopia), the AHP method is also applied to evaluate and prepare the landslide susceptibility map of the R.S Girolamo area, Sardinia. In this section of the thesis, only the specific application of the AHP method is discussed, as the general concepts, principles, and procedures of the AHP method is already discussed in the chapter 5.3.1.

To apply the AHP method at the R.S Girolamo basin, the same six input factors are considered as the case applied in the FR method above. All the collected data were converted in to map and rasterized with grid of 10 m x10 m cells using the spatial analyst of GIS environment for the use with AHP technique. Following the principles, rules and steps of AHP method stated in the previous chapters (chapter 5.3.1) and considering also their relative influence on slope instabilities, each of the various causative parameters were classified into a number of significant classes.

The relative significance of each causative factors and each of their class to the slope instability has been quantitatively determined based on the concepts and techniques of AHP method which includes: (1) construction of pair-wise comparisons and obtaining the judgmental matrix that included rating each factor and each class within a factor in relation to their relative influence on the initiations of the slope instability. When comparing two features (layer classes or causative factors in a layer), the numerical relational scale is used (section 5.3.1 in Table 5.6) and the verbal judgments of each pair wise elements is transformed into numerical quantities. Usually, an element receiving higher rating is considered as more influential compared to another one that receives a lower rating, (2) calculation of the priorities or relative weights, as well as the principal Eigen value (λ_{max}) are performed for each factor and for each class following the procedures of AHP method stated in section 5.3.1. Then, Consistency Index (CI) and Consistency Ratio (CR) values of each developed factor or sub-class matrices have been determined using equations 5.3 and 5.4. While the values of the Random Consistency Index (RI) is referred from Table 5.7 in section 5.3.1, (3) aggregating and combining of the weights for the different factors to obtain a single index, which depicts landslide susceptibility, is accomplished using the equation 5.6.

10.3.2. Results and discussion

The constructed pair-wise comparison matrix and obtained judgmental matrix that included rating each factor and each class within a factor in relation to their relative influence on the slope instability is provided in Table 10.5 (a, b, & c). The consistency of the weights and ratings are evaluated by taking the principal eigenvectors of each matrix and calculating the consistency index and consistency ratio. The values shown in Table 10.5 revealed that all the CR values are less than 0.1 and therefore this confirmed that the preferences used to produce the comparison matrixes are consistent. The LSI map is established according to equation 5.6.

Table 10.5 (a): Pair-wise comparison matrixes, relative weights of various parameters (causative factors) and the data layers of R.S. Girolamo

	[1]	[2]	[3]	[4]	[5]	[6]	Relative weight (%)
[1] Proximity to Drainage	1	2	4	5	6	7	41
[2] Lithology	1/2	1	2	3	5	5	24
[3] Land use	1/4	1/2	1	2	2	3	13
[4] Slope gradient	1/5	1/3	1/2	1	2	5	11
[5] Elevation	1/6	1/5	1/2	1/2	1	3	7
[6] Aspect	1/7	1/5	1/3	1/5	1/3	1	4

As per the results of the AHP method, proximity to drainage is the major parameter contributing to the landslide of the R.S. Girolamo area followed by the lithology and land use, which is also true from the perspective of the field observation. The area is characterized by the several debris rich streams. Slope gradient and elevation are the next influential parameters, with more or less equal influences on the landslide occurrences (Table 10.5 and Fig. 10.15).

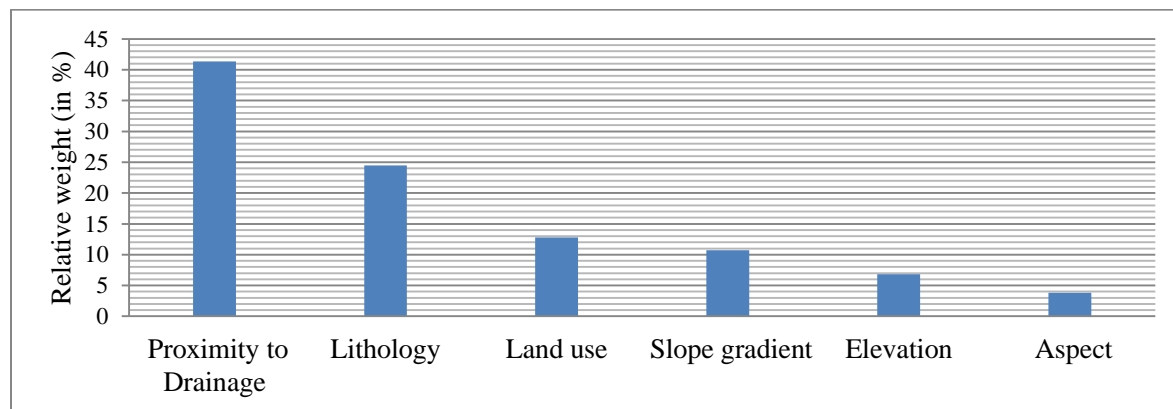


Fig 10.15: Relative influences of causative factors on the landslide of R.S. Girolamo

Table 10.6 (b): Pair-wise comparison matrixes, principal Eigenvectors (relative weights) of classes within the various parameters (causative factors) and the data layers of R.S. Girolamo

Factors/classes	[1]	[2]	[3]	[4]	[5]	[6]	[7]	[8]	Relative weight
[1] Permanent crops and greenhouse	1	1/2	1/4	1/3	1/5	1/6	1/8	1/7	0.02
[2] Annual crops asso. with other permanent crops	2	1	1/5	1/4	1/5	1/7	1/9	1/7	0.03
[3] Forests	4	5	1	1/3	1/2	1/2	1/5	1/4	0.05
[4] Residential fabrics, Urban and suburban areas	3	4	3	1	1/2	1/3	1/7	1/4	0.06
[5] Mixed Scrub land/Bush	5	5	2	2	1	1/4	1/7	1/5	0.07
[6] Areas with sparse vegetation	6	7	2	3	4	1	1/5	1/3	0.11
[7] River course & reservoir areas	8	9	5	7	7	7	1	4	0.37
[8] Bare rock outcrop	7	7	4	4	5	3	1/4	1	0.18
Lithology									
[1] Alluvial deposit	1	3	5	4	6	7	2		0.35
[2] Alluvium-colluvium deposit	1/3	1	3	2	4	5	1/2		0.16
[3] colluvium	1/5	1/3	1	1/2	2	3	1/5		0.07
[4] Granite rock	1/4	1/2	2	1	3	5	1/3		0.11
[5] Meta Morphic rock exposure	1/6	1/5	1/2	1/3	1	2	1/5		0.04
[6] Residual soil	1/7	1/5	1/3	1/5	1/2	1	1/7		0.03
[7] Talus	1/2	2	5	3	5	7	1		0.25
Proximity to drainage									
[1] 0-100m	1	3	5	7	9				0.51
[2] 100-200m	1/3	1	3	5	7				0.27
[3] 200-300m	1/5	1/3	1	2	4				0.12
[4] 300-400m	1/7	1/5	1/2	1	2				0.07
[5] >400m	1/9	1/7	1/3	1/2	1				0.04
Elevation									
[1] 52-150m	1	1/2	1/4	1/6	1/6				0.05
[2] 150-300m	2	1	1/3	1/5	1/7				0.07
[3] 300-450m	4	3	1	1/2	1/4				0.15
[4] 450-600m	6	5	2	1	1/2				0.28
[5] >600m	6	7	4	2	1				0.45
Aspect									
[1] N (360 degree)	1	2	3	5	6	7	1/2	1/2	0.18
[2] NE (44 degree)	1/2	1	2	4	5	6	1/2	1/3	0.13
[3] E (89 degree)	1/3	1/2	1	3	4	5	1/3	1/4	0.09
[4] SE (134 degree)	1/5	1/4	1/3	1	2	3	1/5	1/6	0.04
[5] S (179 degree)	1/6	1/5	1/4	1/2	1	2	1/6	1/7	0.03

[6]	SW (224 degree)	1/7	1/6	1/5	1/3	1/2	1	1/7	1/5	0.03
[7]	W (269 degree)	2	2	3	5	6	7	1	1/3	0.20
[8]	NW (315 degree)	2	3	4	6	7	8	3	1	0.31
Slope										
[1]	0-10%	1	1/5	1/6	1/7	1/8				0.04
[2]	11-20%	5	1	1/2	1/3	1/4				0.12
[3]	21-35%	6	2	1	1/2	1/3				0.17
[4]	36-50%	7	3	2	1	1/2				0.23
[5]	>50%	8	4	3	2	1				0.44

Table10.7 (c): Evaluation of the consistency of the preferences used for rating the parameters and classes

Factors	n	λ_{\max}	CI	RI	CR
[1] Proximity to Drainage	5	5.25	0.05	1.12	0.05
[2] Lithology	7	7.28	0.04	1.32	0.03
[3] Land use	8	8.52	0.07	1.41	0.05
[4] Slope gradient	5	5.39	0.08	1.12	0.07
[5] Elevation	5	5.18	0.04	1.12	0.03
[6] Aspect	8	8.62	0.08	1.41	0.05
All data layers (parameters)	6	6.33	0.05	1.24	0.04

The average Eigen vectors (relative weight) for each factor are initially is calculated following the steps stated under 5.3.1

The produced Landslide Susceptibility Index (LSI) of AHP approach is calculated on the basis of a weighted linear combination of causative factors and classes within causative factors as given in equation 5.6. From the calculation, it was found that the LSI had a minimum value of 0.94 (low susceptibility), and a maximum value of 1.97 (very high susceptibility). Therefore the higher the index, the more susceptible the area is to landslide. The produced raw map is reclassified into required number of zones or classes. The LSI class boundaries of the AHP method are also determined using the same approach as the FR-method. Accordingly, four landslide susceptibility zones have been identified with class boundaries of 0.64 (separating low-moderate zone), 1.08 (separating moderate-high zone) and 1.52 (separating high-very high zone). The LSI map of the AHP model is shown in (Fig10.16). According to this method, 1.3% and 27% of the area is covered by the very high and high levels of landslide susceptibility respectively while the percentage of areal coverage for each susceptibility class is shown in Fig10.17.

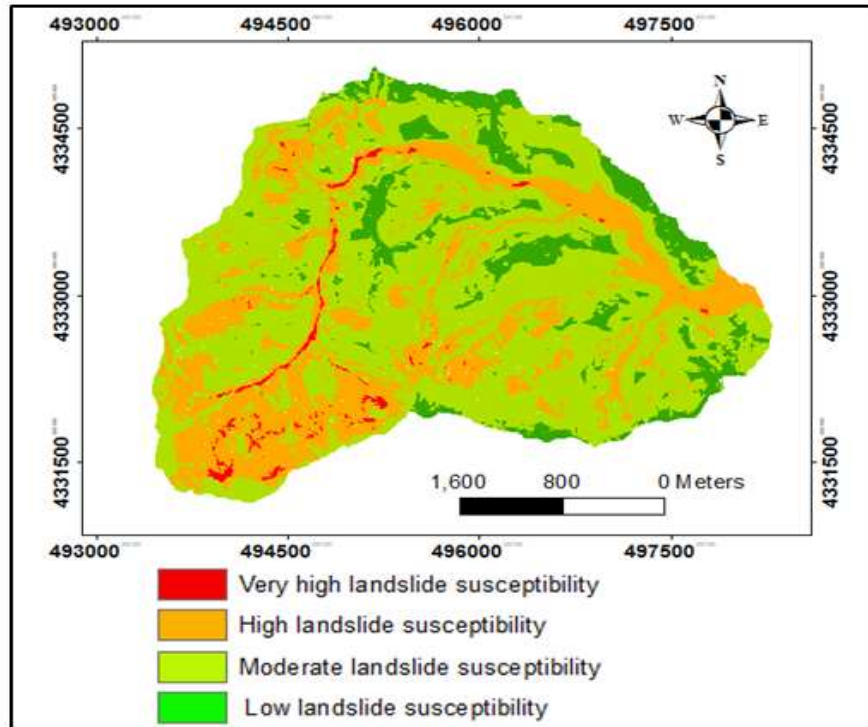


Fig 10.16: Landslide susceptibility zonation of R.S.Girolamo area based on AHP- method

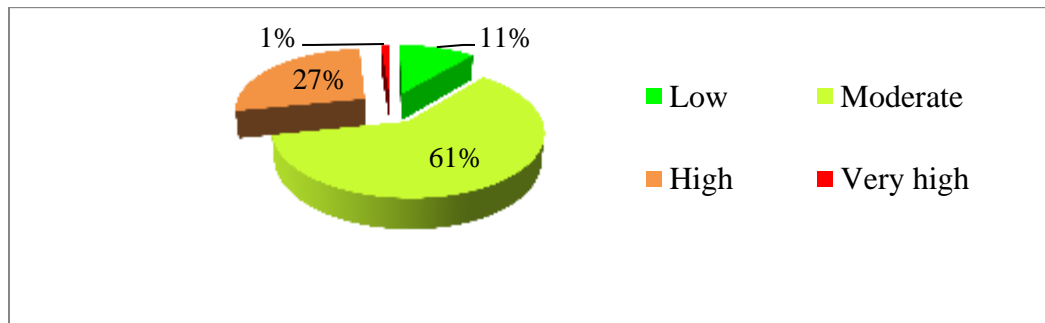


Fig 10.17: Areal coverage of the four Landslide Susceptibility Index (LSI) classes by Percent based on AHP- method

10.4 Verification and comparison of the results of OM, FR and AHP methods for R.S. Girolamo area

The landslide susceptibility analysis results have been verified using known landslides as applied in Ethiopian project (section 5.3.2). The rate curves were created and its Areas of the Under Curve (AUC) were calculated for all cases. The validation curve is created using the same procedures as described in section 5.4 of Debresina area. The rate verification results appear as a line in Fig10.18. The fitness the rate curve can be

judged by the fact that more percentage of landslides must occur in the high susceptibility zone as compared to other zones.

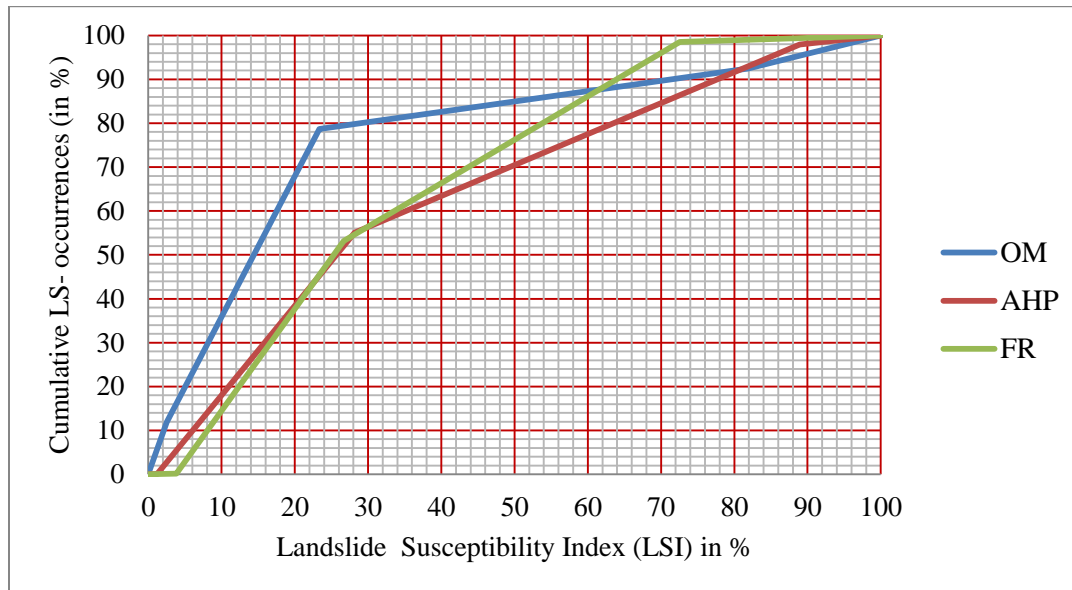


Fig 10.18: Cumulative frequency diagram showing success rate curve for susceptibility maps produced by FR, OM and AHP models (FR = prediction curve for Frequency Ratio; OM = prediction curve for Overlay Mapping and AHP = prediction curve for Analytical Hierarchical Process method)

As can be seen in Fig10.18, in the case of FR-method used 27% class of the study area where the landslide hazard index had very high and high ranks could explain more than 53% of all the landslides. In case of OM method, 23% class of the study area where the LSI had very high and high ranks could explain 78% of all the landslides. In case of AHP method also, 28% class of the study area where the LSI had very high and high ranks could explain 54% of all the landslides.

Later, the prediction of the map was validated more accurately in a quantitative manner using the Area under the Curve (AUC) by considering that the ideal prediction will have highest AUC of 1. In this study, the AUC values were found to be 0.670, 0.686 and 0.775 for the AHP method, FR and OM methods respectively. Accordingly, it indicates that the prediction precision of the acquired maps of FR, OM and AHP are 67%, 68.6 % and 77.5% respectively as compared to the ideal value of 100%. Although all the three methods have comparatively satisfactory results, the OM method shows more accuracy in the case of the R.S.Girolamo area (Fig10.20).

The areal coverage of the various landslide classes and corresponding observed landslide percentage are also compared for all the three methods (Table10.6 and Fig.10.19). In general all the three methods show relatively similar values in all susceptibility zones as compared with the results of Debresina. However, there

are still some differences among them. For example, FR-method shows a little higher value at the low susceptibility zone and lowers at the moderate zone than the AHP and OM methods (Fig10.19).

Table10.8: Percentage of area occupied by each landslide susceptibility class Compared to the Landslide Ssusceptibility Index values between OM, AHP & FR model. The LSI ranges used in the classification were assigned using manual classifier by graphing the LSI and Landslide occurrences.

Landslide Susceptibility Index Classes				
	Low	moderate	High	Very high
Overlay Mapping method				
Area (Km ²)	2.2	7.1	2.5	0.3
Area (in %)	18.0	59.0	21.0	2.0
Observed landslide (%)	7.6	13.7	66.8	11.9
Frequency Ratio method				
Area (Km ²)	3.3	5.6	2.8	0.5
Area (in %)	27.5	45.9	22.8	3.8
Observed landslide (%)	0.14	53.03	45.34	1.49
Analytical Hierarchical Process method				
Area (Km ²)	1.34	7.39	3.28	0.14
Area (in %)	11.07	60.76	26.97	1.19
Observed landslide (%)	0.06	54.96	42.89	2.08

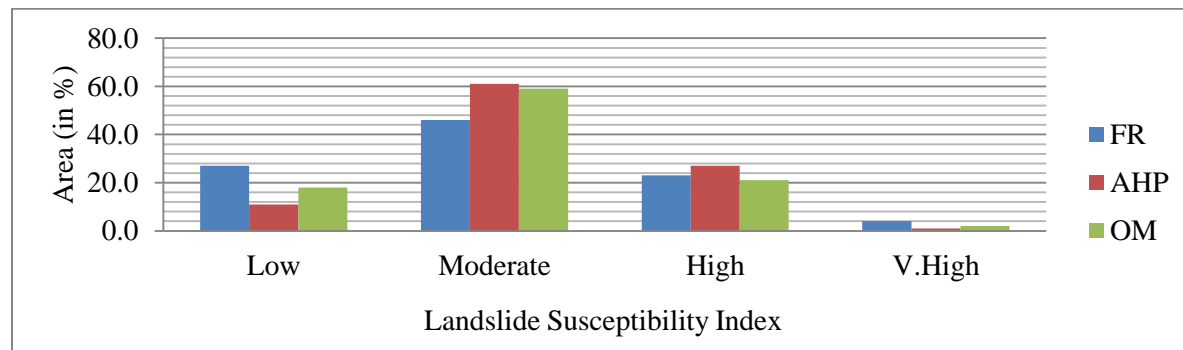


Fig 10.19: Histogram showing the relative distribution of landslide classes, for the OM, FR and AHP methods for R.S. Girolamo area

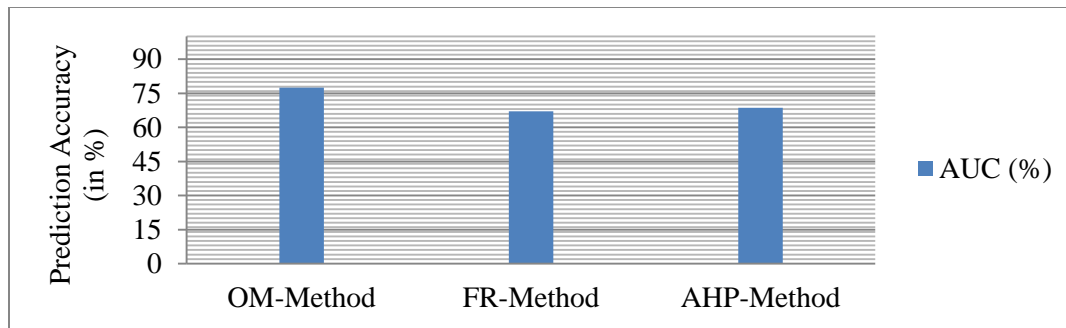


Fig 10.20: Histogram showing the percentage of prediction accuracy comparison of the three methods based on Area Under the Curve (AUC) method for R.S. Girolamo area

10.5. General characteristics of the event and deterministic slope stability approach

The events that took place on the 12-13th November 1999 and 22-23th October 2008 indicated that the R.S. Girolamo catchment is a potential site for shallow flow like landslide and flooding hazards. This chapter presents detailed description of characteristics and failure mechanisms of landslides in R.S. Girolamo catchment, by taking some typical cross-sections at selected area

10.5.1. General characteristic of the event, focusing on that of October 2008

Rock falls/topples, debris slides, and debris flow/ floods are the major types of slope failures observed in the catchment area of R.S.Girolamo (Sardinia).

A typical slope profiles have been selected at the left side of the R.S.Girolamo (Fig10.21a) and at the Santa Barbara sub-catchment following a small stream for detailed investigations (Fig10.21.b). Though the down-slope variation is not sharp, the slope profiles are divided into zones (I-IV) in (a) and (b) of Fig10.21).

An assessment of the lateral and vertical distributions of rocks and soils, the mechanisms of the various slope failure, the geo-hydrological condition of the area, field examinations of unstable slopes and features revealing of the mechanisms of failures, kinematic analysis of discontinuities have been carried out along these selected typical profile (Fig10.21, a & b).

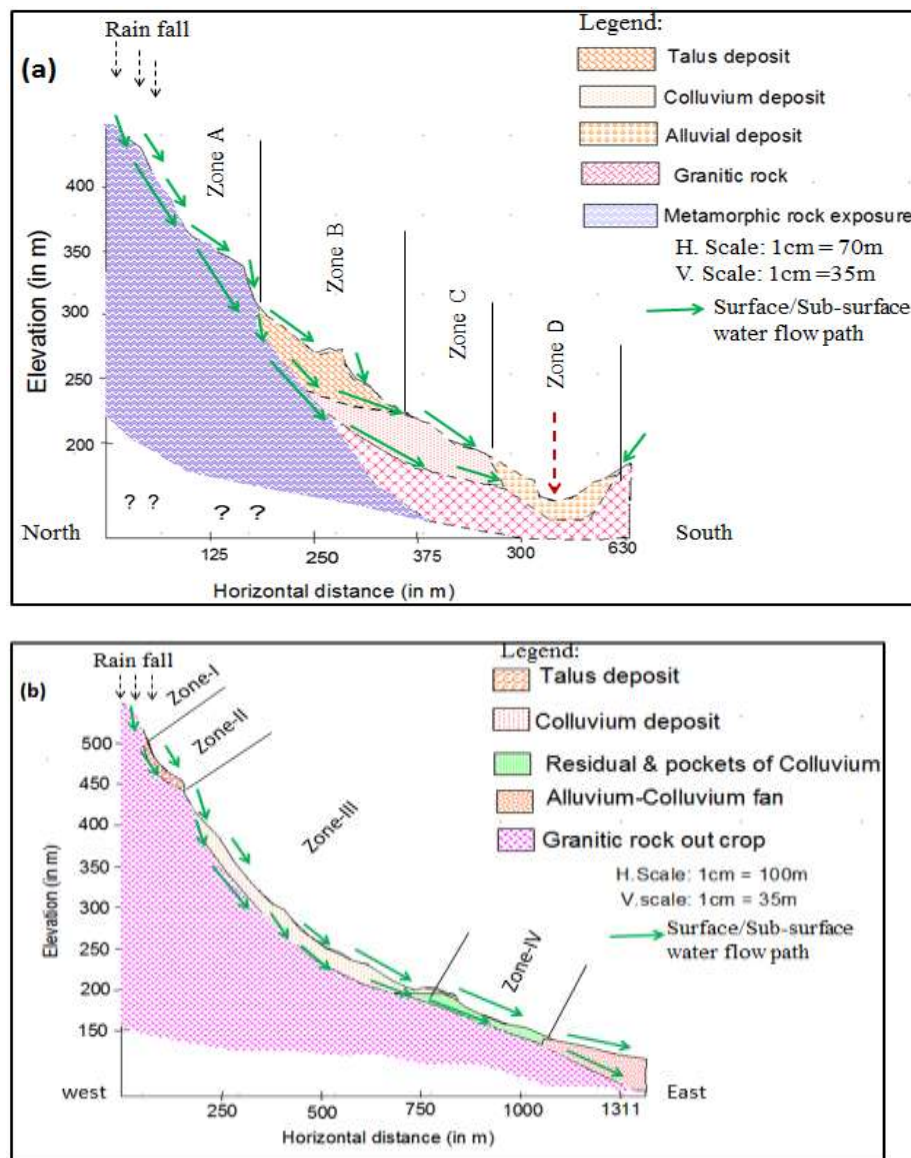


Fig 10.21: Typical slope profile along: (a) the left side of the R.S. Girolamo and (b) a small creek at the Santa Barbara sub-catchment

10.5.1.1 Rock fall/Topples and Kinematic Approach

Rock fall/topple are prevailed on steep hill slopes where competent fractured rocks (granitic rock and/or basement metamorphic) exposure exists (zones-I & zone A, in Fig10.21). These are controlled by the systems of discontinuities. The open nature of these discontinuities at the rock outcrop of zone-I and A, favors for the percolation of rainfall thereby triggering the rock falls (Fig10.22). The measured sizes of the failed blocks of granitic rock varied from about 0.2m^3 to 2m^3 while the blocks of metamorphic origin is less than 0.5m^3 due to the closely spaced joints.



Fig 10.22: Rock falls from the jointed granitic rocks, at the steep slope of the study area (S.Barbara Sub-catchment)

The kinematic analysis of the relationship of geological structures and natural slopes has been applied to examine what kinematic modes are possible for a given slope angle inside the unstable rock mass of the study area. It requires the detailed evaluation of rock mass structures and geometry of existing discontinuities contributing to block instability. Discontinuities data of the study area has been represented on a stereographic projection. Stereonets are useful for analyzing discontinuous rock blocks. Program DIPS allows for visualization of structural data using stereonet, determination of the kinematic feasibility of rock mass and statistical analysis of the discontinuity properties. Two joints with J1 (65/145), J2 (86/070) and the steepness of the natural slope (70/100) are plotted on stereonet using the Dip software (Fig10.23). The result shows the possibility of rock falls towards east-southeast.

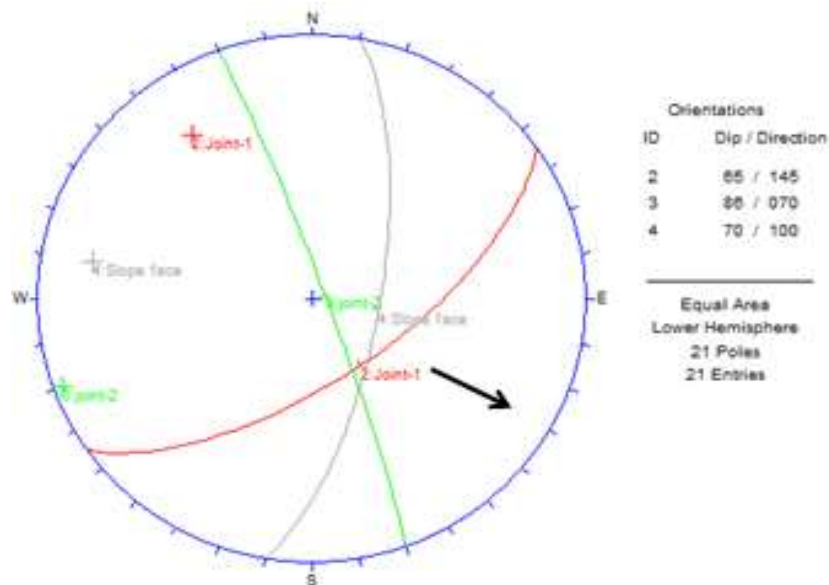


Fig 10.23: Stereogram plots of joints of the study area

10.5.1.2 Debris slide

The zones II and B in Fig10.21 are covered by angular debris materials dominated by boulders accumulated from the rock falls. Debris slide that initiates from the talus deposits are common mass movement in these zones (Fig10.24). Their run out distances is less than 50m. The debris flow starts from these deposits during heavy rainfall.



Fig 10.24: Debris slide from the granitic sources (a) and metamorphic sources (b)

10.5.1.3 Debris flow/flood

Debris flow/flood is a very common mass wasting process in the catchment and is the potential hazard for the dwellers downstream. As indicated in Fig10.21,a & b, the debris flow initiates from the interface of Zones-II and Zone-B; transported through zones III-IV and zone-C and finally deposited at zones beyond.

The evaluation of the frequency of debris flow helps the understanding of the relations between basin conditions, with particular regard to basin morphological evolution and sediment supply processes, and debris-flow occurrence (Jackson et al., 1989). Although there is no exact clear cut about the occurrences and behavior of debris flow, various researchers (Andrew w., et al, 2011) states that the occurrence of a debris flow requires large volumes of sediment to be available, either on slopes or in a stream channel, and steep slopes to allow rainfall and/or stream flow of sufficient intensity to mobilize the sediment. In this context, the R.S.Girolamo catchment is characterized by steep slope gradients and loose sediment availability which are ready to produce debris flow when heavy rainfall is available. Slope instabilities and debris flows may occur at the R.S.Girolamo basin in the near future when there will be heavy rainfall resulting in a runoff that exceeds a threshold value.

Material involved in the debris flow of the study area includes the unconsolidated heterogeneous materials such as talus/ colluvium deposit, alluvial deposits and saprolite/residual soils and woods. The characteristics of various slope failure mechanisms are described below with the help of Google image (Fig10.25).

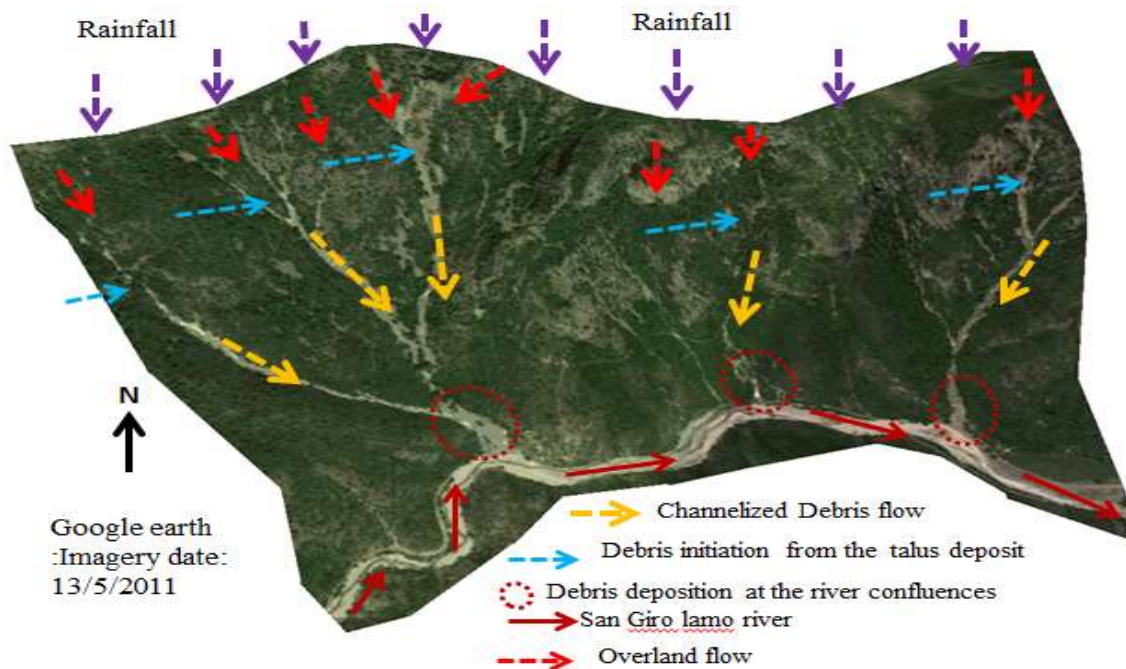


Fig 10.25: Characteristics of landslide initiated debris flow at the left side of the river R.S. Girolamo

A number of studies have pursued to identify catchment morphometric variables such as Catchment area (e.g. de Scally and Owens, 2004), Melton Ratio (e.g. Jackson, et al, 1987; de Scally and Owens, 2004; Wilford, et al, 2004; Andrew W. & T. Davies, 2011), Watershed Length (e.g. Wilford, et al. 2004; Andrew W. & T. Davies, 2011) for the preliminary identification of basins and fans susceptible to debris-flows. Those various studies have also distinguished thresholds of Melton Ratio (R) which are capable of differentiating of fluvial dominated basins from those dominated by debris-flows. For instance, Jackson, et al, (1987) identified a Melton Ratio (R) threshold value of 0.30 to distinguish between basins prone to flooding ($R < 0.30$) and those prone to debris-flows ($R > 0.30$). Wilford, et al. (2004) also followed similar approach but incorporated another term called ‘debris flood’ and new threshold value in their work to distinguish between debris flood and debris flow .i.e. a threshold value of $R < 0.30$ has recognized as normal flood-prone watershed; thresholds between R-values of 0.3 to 0.6 are prone to debris flood, while a threshold value of $R > 0.60$ was established for debris-flow prone basins.

Debris flow and/or flood prone areas are delineated and identified using direct field survey and relating to certain morphometric parameters of the R.S. Girolamo catchment following the principles used by Jackson, et al. (1987), Wilford, et al, (2004) and Andrew, et al, (2011). During the field survey, the sediment deposit signatures of each of the micro drainages of the R.S. Girolamo catchment are studied to classify basins by their sediment deposit.

Delineation of the drainage network of micro-catchments and extracting of their morphometric parameters such as catchment area, watershed length, minimum and maximum elevation for each of micro-catchments are determined to know the contribution of debris from each micro-catchment using the spatial analyst of Arc GIS 9.3. Then, the extracted morphometric parameters were exported into a Microsoft excel spreadsheet where Melton Ratio and relief for each of the micro catchments were calculated and prepared for subsequent analysis. The overall catchment area, having total area of about 12 km^2 , is divided into 16-micro catchments with areal extent varying from 0.104 km^2 to 2.9 km^2 (Fig10.26).

Melton Ratio (R) has been calculated within Excel using the formula:

$$R = \frac{H_b}{\sqrt{A_b}} \quad 10.1$$

where H_b is basin relief (difference between maximum and minimum elevations in the basin) and A_b basin area, after Melton (1965).

The results show that two of the micro catchments are prone to conventional flooding (have $R < 0.3$); seven of the micro-catchments are prone to debris flood (R is between 0.3 and 0.6) while seven of them are prone to debris flow ($R > 0.6$) (Figs 10.26 and 10.27).

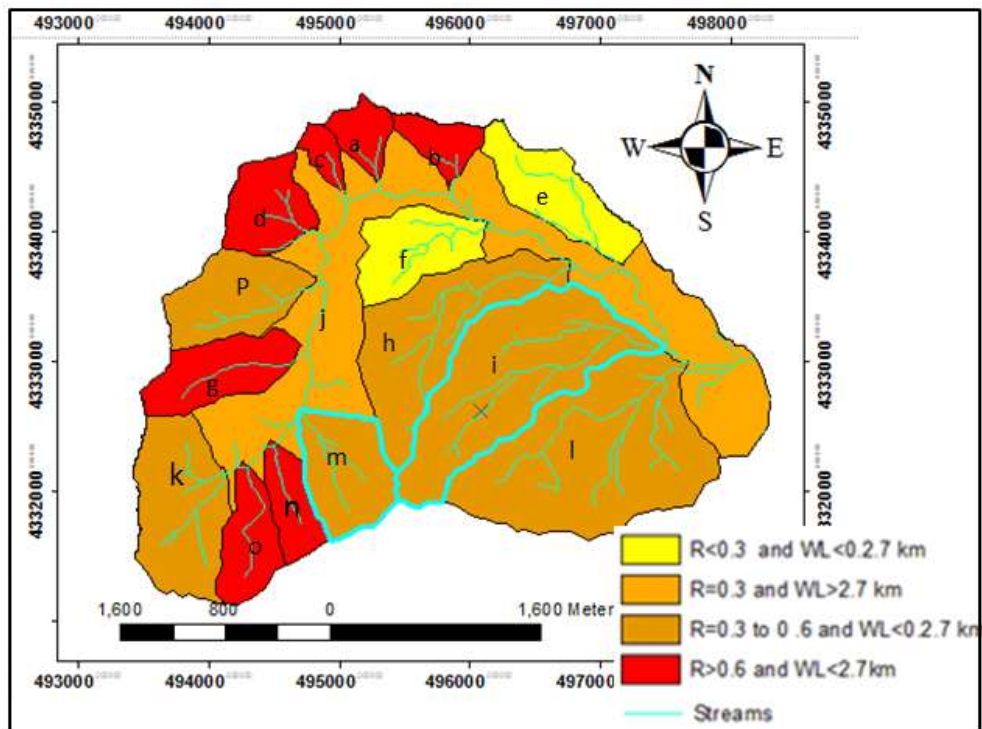


Fig 10.26: Micro-catchments identified as debris flow, debris flood and fluvial floods in the R.S. Girolamo area, based on Melton Ratio methods.

The availability of the debris flow and debris flood and conventional flood in the study area has been checked also by field observations using some criteria like geomorphic and sedimentary characteristics of debris flows, debris floods and fluvial floods which are developed by (e.g. Davies 1997; Jakob and Hungr, 2005) as cited in Andrew et al (2011). Thus, from the field observation two, five and nine micro-catchments are identified fluvial, debris flood, and debris flow respectively. Both the field observation and morphometric approach of identification have similar results except in two micro catchments ('m' and 'i' in Fig 10.26). From the field observation, these two micro-catchments ('m' and 'i') are identified as debris flow although the morphometric approach categorised them as debris flood.

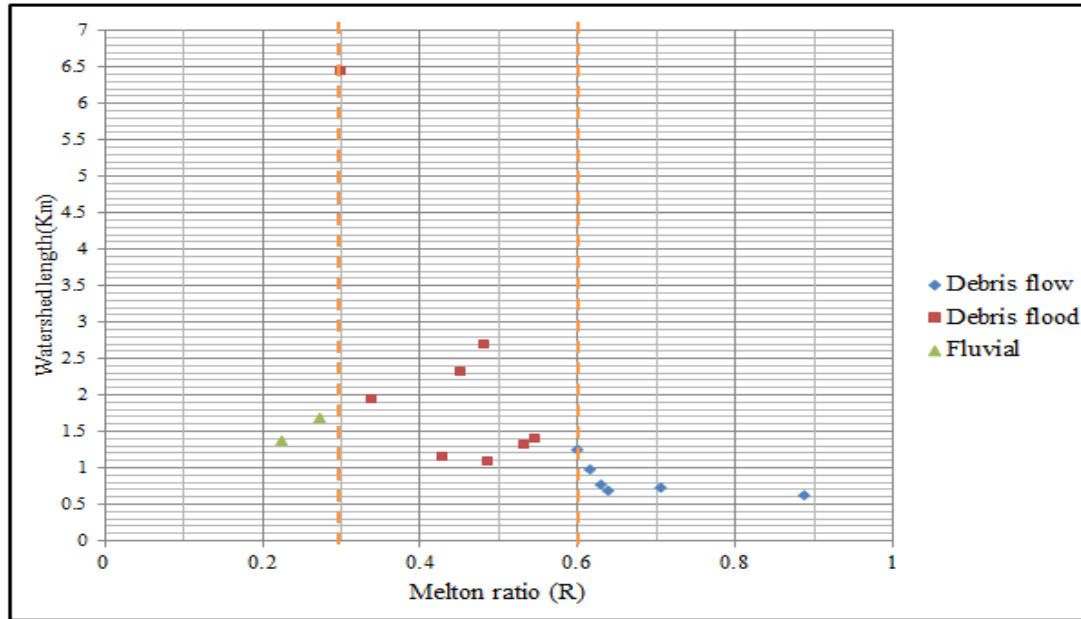


Fig 10.27: Scatter plot using Melton Ratio and Watershed Length with class limits for debris flow, debris flood and fluvial flood.

10.5.3 Slope stability analysis using Global Limit Equilibrium (GLE) method

The same methodology, procedure and software are applied in this section also as the case in Debresina area (Ethiopia) for the geotechnical slope stability study. Thus, the general principle of the GLE of the various methods and the software are presented under section 5.4 and can be referred there. In here, slope stability analysis is given below at the selected cross-section (Fig 10.21,b). The shear parameters of the residual soils are obtained from the direct shear test in the laboratory where as the shear parameters of the talus some of the alluvium-colluvium is adopted from standard manuals.

10.5.4 Results and discussion

To apply the software (e.g. SLIDE) in the evaluation of the slope stability analysis of the study area, two different conditions of loading; Dry slope and wet slope are considered. The case with earthquake loading condition is not considered in this analysis as the area under study is not prone to such conditions.

The load conditions analysed are defined as:

Case I: Dry slope (.i.e. no GWT inside the model)

Case II: Saturated slope, i.e. GWT on the surface (hydrostatic pore pressure)

The calculated results are presented in table below.

Table10.9: Results of global minimum Safety Factor (SF) calculated using SLIDE software for the various combinations of conditions, R.S. Girolamo area (Sardinia)

I. Dry slope (no GWT inside the model)		
Surface Options	Analysis methods	Global minimum :SF
Circular, grid search composite surfaces enabled	Bishop Simplified	1.08
	Janbu Simplified	1.02
	Spencer	1.06
	GLE/Morgenstern-Price	1.06
Non-circular block search	Bishop Simplified	-
	Janbu Simplified	2.04
	Spencer	2.23
	GLE/Morgenstern-Price	2.23
II. Saturated slope, i.e. GWT on the surface (hydrostatic pore pressure)		
Circular, grid search composite surfaces enabled	Bishop Simplified	0.356
	Janbu Simplified	0.298
	Spencer	0.374
	GLE/Morgenstern-Price	0.384
Non-circular block search	Bishop Simplified	-
	Janbu Simplified	0.970
	Spencer	1.234
	GLE/Morgenstern-Price	1.257

Thus, based on the susceptibility classification of Pack et al (1998), the calculated Safety Factor (SF) values for the study area (Table10.7) revealed that:

- (a) The dry slope condition with non-circular failure surface have low landslide susceptibility (SF >1.5). That is, the slope is stable.
- (b) all methods in the case of dry slope condition and assuming a circular failure surfaces as well as Spencer and GLE/M-P methods in saturated slope condition with non-circular surface have high landslide susceptibility ($1.25 > SF > 1$). That is, the slope is marginally stable or quasi stable.
- (c) Saturated slope with circular surface for all methods, and saturated non circular surface of the Janbu simplified method have very high landslide susceptibility ($SF < 1$). That is, the slope is completely unstable under the wet condition (Fig10.28).

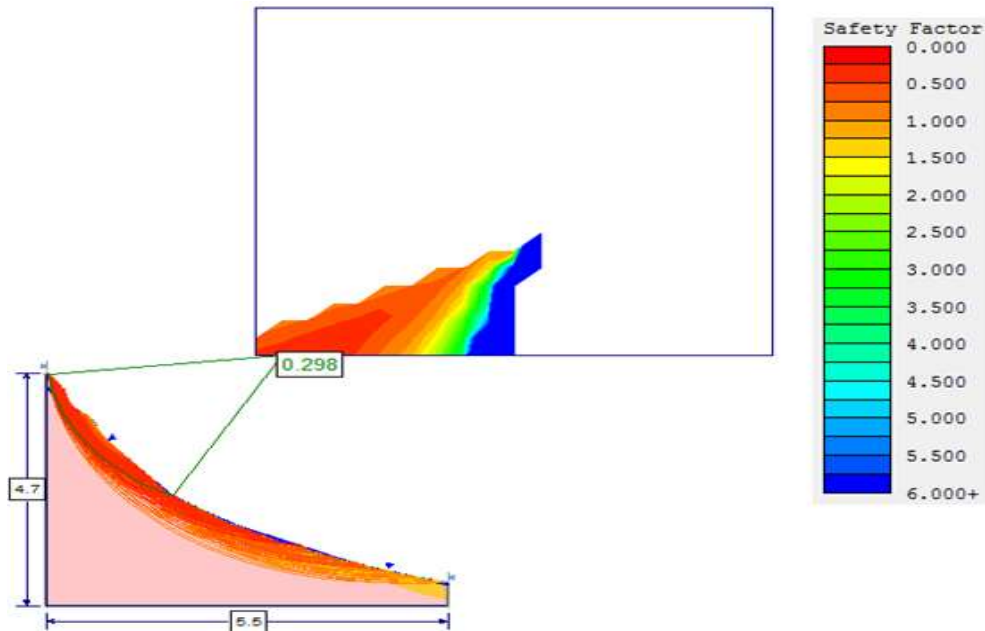


Fig 10.28: Global minimum Safety Factors using circular failure surface with Janbu simplified method. (cross-section from Santa Barbara to down town town)

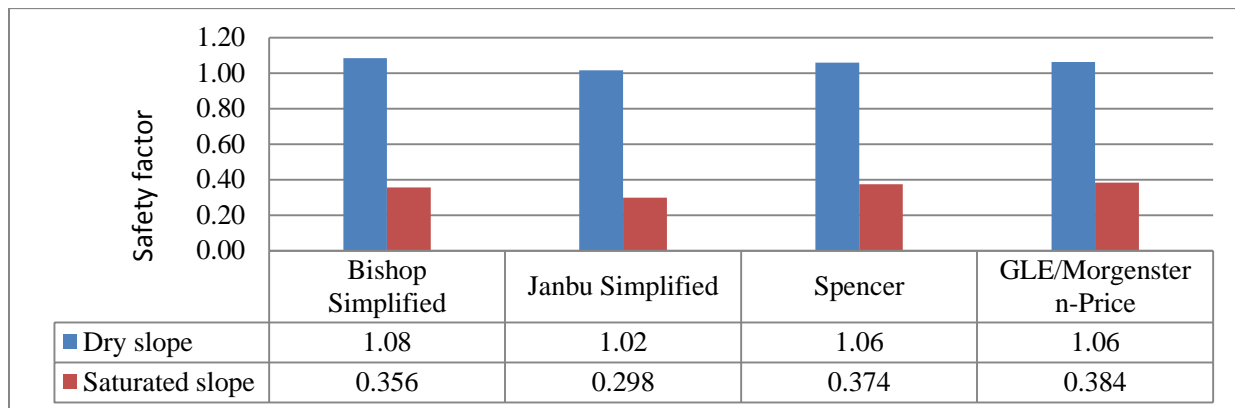


Fig 10.29: Histogram illustrating global minimum Safety Factor (SF) for the various loading conditions: using various methods and assuming circular failure surfaces

Some concluding remarks:

- The calculated minimum SF values show that the area is unstable under both the dry and saturated conditions based on the susceptibility classification of Pack et al (1998). In fact, the slope becomes extremely prone to failure when saturated. This is also confirmed from the field observation i.e. the debris slide are moving even in the dry condition in the steep slopes (Fig10.24,a&b).
- The simplified Bishop (BS), GLE/Morgenstern-Price and Spencer methods yield in most cases similar SF values for circular slip surfaces in the dry slope condition. However, Janbu simplified (JS)

method underestimates the SF by 4-6 % from from the other methods. Whereas, Spencer and GLE/M-P methods have similar SF values but BS and JS methods underestimate by 7% and 20% respectively for the circular saturated slope Fig10.29).

- In the case of the circular surface, Spencer and GLE/M-P methods have similar SF values in both the dry and saturated conditions but JS underestimates the value from 8% in the dry slope to 20% in the saturated condition.
- The area becomes highly prone to slope failure during the saturated conditions, especially for those areas covered by colluvium and boulders of talus materials. As can be referred in Table10.7, the Safety Factor (SF) values calculated in the dry and the saturated conditions have quite significant difference. For example, the SF in the dry season is reduced by 65 to 70% in the wet season for the circular surfaces while it reduces 55-80% for the non-circular failure surfaces. This displays that the triggering effect of the water in slope failure of R.S.Girolamo area is quite significant and can be exemplified by the event of October 2008.
- The above calculated minimum safety factors were performed using limited laboratory results and assumptions. Therefore, it only indicates the potentiality of the area for slope failure under various triggering conditions (presences or absence of water). However, in reality the geologic materials of the area are so heterogeneous both laterally and vertically, requiring details of geotechnical investigation to attain the more accurate values in the future.

11. Landslide hazard mitigation strategies and remedial options

11.1. General

Previous events (e.g. the events of 1999 and 2008) clearly demonstrated that the watershed of R.S. Girolamo is prone to shallow and flow like landslides and floods that usually tends occur in the wet season. Although Italy is known for its natural hazard (e.g. landslide and flooding), it has an accumulated long time experience on what natural hazards are and how to mitigate them. For this reason Italy has established civil protection institutes both at national and regional levels which regulates the geo-hazards and develop guidelines. For example, a national landslide inventory has been conducted in Italy in general by the Institute for Environmental Protection and Research Geological Survey of Italy (ISPRA⁵) under the project IFFI⁶-from 2004 to 2007. Thus, Italy is one of the developed countries with a better geo-hazard mitigation capacity. However, because of the dynamic nature of the geo-hazard phenomena and a regional nature of the developed guideline, continuous research work and improving of the guidelines and mitigation measures are necessary.

Landslide inventory and susceptibility maps are critically needed for the mitigation strategy of the landslide prone areas. To assess the possible mitigation measures for landslide hazard in the study area, the potential landslide occurrences are delineated and identified, mapped and their nature is discussed in the previous chapters of this study. This helps us to establish the priorities that facilitate the efficient and effective use of the limited resources available for hazard mitigation in the study area. Mitigation strategies can be grouped into structural and non-structural measures. Specific mitigation measures are recommended within each group as they relate to different hazards.

11.2 Non-structural mitigation strategies

11.2.1 Pre-disaster preparedness

As part of Italy, the Sardinia region in general has relatively better experience and capacity in this regard. The communities are also well aware of the natural disasters. However, the natural disasters are dynamic, frequent and destructs live and properties in a very short time. Therefore, pre-hazard emergency preparedness programs are always necessary to achieve a satisfactory level of readiness to respond to any emergency situation through programs that strengthen the technical and managerial capacity of governments, organizations, and communities.

⁵ ISPRA =institutio Superiore per la Protezione e la Recerca Ambientale.

⁶ IFFI-inventario Fenomenon Frana Italia

Short-term and long-term preparedness measures that should include readiness plans, warning systems, emergency communications systems, evacuations plans; resource inventories, emergency personnel/contact lists and public information/education. As with mitigations efforts, preparedness actions depend on the incorporation of appropriate procedures in national and regional development plans.

11.2.2 Post-disaster recovery

Once the landslide hazard is happened, it is necessary to have some immediate temporary relief activities. After the emergency is brought under control, the temporary relief activities have to be changed into the normal developmental activities and the affected people have to be able to restore their lost resources and infrastructures that support them. Both short and long term recovery actions which include returning vital life-support systems to minimum operating standards; temporary housing; public information; health and safety education; reconstruction; and economic impact studies.

11.2.3 Establishment of early warning systems

Early warning systems that relate the occurrences of landslide and the thresholds of triggering factors (e.g Rain fall) can be developed by simple registration of the date and time of occurrence of the landslide. This registration landslide occurrences can be done by the local people living around the area and report it to the local administrators. Then it is possible to determine the minimum thresholds of the triggering factors by relating with the rainfall data, which later can be used for early warning prediction of the landslide in the study area.

11.3 Structural and physical landslide hazard mitigation measures

As has been discussed in the previous chapters, landslides are prevailed in areas adjacent to streams/rivers, due to active stream/river incisions and gully erosion and agricultural areas. Taking into account the processes leading to instability of slopes and the social and economic conditions of the country, one or a combination of the following structural/physical landslide remedial measures such as: (1) land use planning: (a) further development activities should be protected at the very high/high landslide prone areas (b) forest fire & cutting should be minimized (2) engineering design: (a) proper drainage-system on the surface water (b) river training & gully treatment to reduce further erosion (3) bridge design scouring depth of foundation, abutment erosion & dimension to pass the amount of maximum debris flow should be properly addressed

12. Conclusions and recommendations

12.1 Conclusions

The hilly and mountainous areas of Campidano graben of Sardinia have been frequently affected by landslide and landslide generated landslide hazards. R.S. Girolamo is one of the areas that are highly affected by such landslide found in the SW and southern margin of Campidano graben. The frequently occurring landslides and flooding have casualties in the downstream dwellers. For example considering only the landslide and flooding events of Oct.2008,4-people are dead, bridges/roads, pipelines and sewerage lines are damaged.Besides, several houses of dwellers of Poggio dei Pini were destructed and many vehicles were damaged and dragged to the Mediterranean.

This part of the study also has the same objectives and methodologies with that of Debresina area (Ethiopian project). Therefore, there is no need to repeat them here as they are already mentioned in that section of the thesis. In the landslide susceptibility evaluation of the R.S.Girolamo area, six major landslide inducing factors were taken into consideration which includes Lithology, Proximity to Drainage, Land use, Elevation, Slope, and Aspect. These factors were evaluated, and weights have been assigned to each factor or classes based on the criteria of the methods used.

General features and characteristics

- RS.Girolamo area is one of the areas with relatively high annual rainfall (533mm) in the Sardinia region. It is characterized by gentle to steep slope gradients, dense drainage system & gully erosion, with elevation range of 52 to 738 m a.s.l. The flat areas, at the outlet of the catchment are occupied by small towns and farm activities.
- Geologically, about 6.5% and 83.3% of the catchment area is covered by metamorphic basement and granitic intrusions and their residual products respectively while the rest 10 % is covered by the colluvium/talus, alluvial and colluvium-alluvium deposits. The rock outcrops are intensively affected by cross cutting fractures having variably dipping angle that made it liable to failure.
- Field inspection and laboratory analysis (grain size and Atterburg limit tests) show that most soils in the catchment are categorized as coarser soils because they have more than 50% coarser grain component from the laboratory result. More than 90% of the alluvial and the colluvial soils are gravely and sandy soils with negligible amount of fines. While grain size analysis result of the residual soil showed that more than 68% the samples have less than 5% fines (silt and clay) content and with very low to non-plastic nature. The soil types according to the Unified Soil Classification

(USC) system vary between poorly graded sand with gravel (SP) to well grade sand with gravel (SW). This indirectly indicates that the mechanical weathering is more dominant process than chemical weathering and no chance of clay soil is formed.

- There are no significant seepages and springs in the catchment area and hence the main landslide triggering processes are the surface run off and erosions.
- Landslide inventory carried out by this study depicts that more than 108 landslide and related phenomenon are mapped in the study area consisting of rock fall/toppling, debris slide and debris flow having aerial coverage percentage of 14%, 11% and 75 % respectively. The rock fall and/or topples are controlled by the NW-SE, nearly E-W and nearly N-S trending major fractures

GIS-based landslide susceptibility mapping and prediction (OM, AHP and FR methods)

Similar to the Debresina area, landslide susceptibility map preparation and evaluation has carried out using the GIS based OM, FR and AHP methods. Besides, the GLE is also applied at selected section for the slope stability calculation.

Overlay Mapping (OM) method

- This method needs only three main environmental factors such as Slope, Litho-technical and Land use factors in the evaluation process of the slope instability of an area. According to the analysis findings: (1) the areas covered by talus, alluvium-colluvium, with slope range of >36%, land uses with bare rock and/or less vegetated, river course are highly prone to landslide (2) four distinct LSI are identified namely: low (18%), moderate (59%), high (21%), and very high (2%). This depicts that about 23% of the area is susceptible to landslide and landslide generated phenomena.

Frequency Ratio (FR) method

In this method, six causative factors such as Lithology, Slope, Land use, Aspect, Elevation and Proximity to drainage have been chosen as inputs for the landslide hazard evaluation based on the site condition. According to quantitative evaluation and correlation between the landslide distribution area and the landslide causative factors using the FR method: (1) areas covered by alluvium, granite, talus and colluvium, with slope range >50%, with forest, river course and bare rock or less vegetative type of Land use, with distance of 0-100 m from drainage, with elevation of 450-600 m, with Aspect to N, NW, S and west are highly prone to landslide (2) the landslide susceptibility zonation has identified four zones, namely: very high (4%), high (23%), moderate (46%) and low (27%) zones.

Analitical Hierarchical Process (AHP) method

The same six causative factors are used in the AHP method also. Although these factors dominantly controlled the slope failure in the catchment, their relative influence in inducing landslide is different. The relative influences of each causative factors and/or classes to the landslide are evaluated by the AHP method. The final analyzed result displayed that: (1) the three top influencing factors to induce land sliding activity in the R.S.Girolamo catchment comprise proximity to drainage (41%), lithology (24%), and land use (13%). Then, followed by the other factors such as slope, elevation and aspect having relative weight of 11%, 7% and 4% respectively (2) areas covered by:(a) alluvium (35%), talus (25%), alluvium-colluvium (16%) and granitic rock (11%), (b) with Slope classes >50% (44%), 36-50% (23%) and 21-35% (12%), (c) land use of river course (37%), bare land (18%) and with sparse vegetation (11%) (d) proximity to drainage of 0-100m (51%), 100m-200m (27%), 200-300m (12%), (e) aspect of northwest (31%), west (20%), north (18%), north east (13%) and (f) elevation of >600m (45%), 450-600m (28%), 300-450m (15%) are highly prone to landslide (3) the landslide susceptibility map generated with AHP has identified four zones, namely as very high (1.3%), high (27%), moderate (61%) and low (11%) zones. According to this method 28% of the area is prone to landslide.

Global Limit Equilibrium (GLE) method

- Under this method, the minimum SF of the slope is calculated using Bishop Simplified, Janbu Simplified Spencer, and Morgenstern-Price methods for selected cross-section. Consequently, the area is: (1) stable under the dry slope condition and non-circular surface (2) quasi-stable under the dry circular surface and saturated non dry surface (3) completely unstable under the wet slope condition with circular surface
- The calculated minimum SF for the dry slope condition is 1.02, while for the wet slope is 0.298 using the Janbu Simplified method showing there is a maximum reduction (70%) of the SF from dry to wet conditions.

Verification and comparison of the results of OM, FR and AHP methods

The results of the landslide susceptibility of R.S.Girolamo were verified using known landslide location. To verify the result, observed landslides in different landslide susceptibility classes and rate curves (AUC) are used.

- In most landslide studies, the observed landslides in different LSI classes are usually considered as the key factor for result evaluation. Comparing of the areal coverage of observed landslides in the four LSI-classes of each method, shows that small landslides are observed in the low LSI-classes and the high percent of landslides are observed in the higher classes in general and this depicts that landslide zonation maps can be considered as well predicted in all the methods applied.

- The rate curves were created and its areas under curve (AUC) were calculated for all cases. Thus, the prediction of the map was validated more accurately in a quantitative manner using the AUC by considering that the ideal prediction will have highest AUC of 1. The validation of results show that all the three methods have a satisfactory accuracy, with OM method (77.5%) being the highest, followed by the FR- method (68.6%) and AHP method (67%) being the lowest methods, as compared to the ideal value of 100%. Generally, the verification results showed all the three methods have comparatively satisfactory results.
- Finally, the results shown in this thesis can use as a basic data for preliminary slope management and land-use planning of the study area in particular and in other similar areas in Sardinia in general. However, additional detailed investigations might be necessary for specific site development and decision-making.

Mitigation strategies and Remedial measure options

Italy/Sardinia in general and the study area in particular have a better geo-hazard mitigation capacity than Ethiopia in that: (a) its population are well conscious of the problem, (b) civil protection institutions responsible for such mitigation measures and strategies are established (c) it is by far in a better status in both financial and technological wise than Ethiopia. However, because of the dynamic nature of the geo-hazard phenomena and a regional nature of the developed guideline, continuous research work and improving of the guidelines and mitigation measures are necessary. Thus, based on the landslide inventory and susceptibility maps of the study area, non-structural measures such as pre-disaster preparedness, post-disaster recovery, establishment of early warning systems as well as structural mitigation/physical strategies such as land use planning control, drainage-system, promotion of afforestation practice, gully treatment/river training and providing guiding or diverting retaining structures are some of recommended strategic measures in the R.S. Girolamo area to minimize losses from frequently occurring landslide hazards.

12.2 Future research works

The following recommendations can be provided for further action and landslide research in the margin of Campidano graben:

- Rainfall is the main triggering factor of landslides in R.S.Girolamo catchment. Therefore, monitoring of rainfall and understanding of the hydrological process is critical for proper hazard predictions by establishing landslide-rainfall relationships as this could be used for developing early warnings of landslide hazards in the study area and its surroundings.

- The study area in particular and other similar catchments at the margins of Campidano graben as a whole are characterized by steep slopes and continue as highly prone environments in terms of slope stability whereby any external factors such as heavy rainfall, active erosion, and excavation works could lead to the initiations of landslides. It is therefore worthwhile to carry out proper land use planning and management before intervention of developmental works
- Further detailed geotechnical investigations should be performed in the catchment area in order to evaluate better for the influence of critical factors for slope instability, with especial emphasis on debris flow velocity, maximum magnitude and run out distance determination which are helpful for the design of mitigation measures.
- Regular inspection of the availability and condition accumulated sediment in the catchment to update the existed mitigation strategies and/or measures should be carried out either yearly or following a debris-flow. Checking of a debris-flow prone streams and creeks (e.g. creeks in the S.Barbara sub catchments, R.S. Girolamo stream) is essential to evaluate the situation of the catchment and the status of the existing mitigation measures. The efficiency of these measures should then be appraised following to an event so that weak elements in the mitigation concept or safety system can be identified and further measures can be planned accordingly.

Remarks on the similarities and differences of the two distant study areas

The two study areas, Debresina (Ethiopia) and R.S. Girolamo (Sardinia) are found on the mountains and hills of the margins of the Afar rift valley and Campidano graben respectively. Both of them are affected by landslide and landslide-generated hazards. Their similarities and/or differences are presented below considering the general situations of the two sites, triggering and causative factors, and the obtained analysis results and mitigation strategies.

- Geologically Debresina is covered by various tertiary volcanic rocks inter-bedded with pyroclastic materials & quaternary sediments, and is also found in the Afar rift margin active in volcanic, extensional faulting and earthquake. Whereas R.S.Girolamo is covered by Paleozoic metamorphic rocks, complex granitic intrusion & quaternary sediments and is found in the tectonically less active Campidano rift since the beginning of the quaternary period. Thus, the current landslide and landslide-generated hazards in the Debresina are associated to both internal earth processes (e.g. earthquake, faulting, and volcanism) and surficial geo-hydrologic process (rainfall-runoff, rapid erosion) while in the case of R.S.Girolamo they are associated mainly to the surface process such as the rainfall-runoff and active erosion.
- More than 77% the areal coverage of the landslide is complex/composite slide and debris/earth slide in the Debresina area, while about 75% of areal coverage of the landslide types in R.S. Girolamo is flow like landslide (debris flow)
- Earthquake seem the most probable triggering factor for the September 2005 landslide event of Debresina (Ethiopia), while rainfall is the main triggering factor for the landslide event of R.S.Girolamo basin (Sardinia).
- The rainy period in Debresina (Ethiopia) have short durations (mostly June to August) and have bimodal nature, while in R.S.Girolamo is prolonged (mostly October to March).The annual average precipitation of Debresina is 1922mm and that of R.S. Girolamo is 533 mm. The mean monthly RF of Debresina (Ethiopia) and R.S.Girolamo (Sardinia) have nearly similar value in the months of November, December, January and February and for the rest of the months the monthly RF of Debresina is greater than that of R.S.Girolamo from 38% in October to 99% in July (Fig 12.1). Therefore, Debresina area is affected by high RF and high erosion every rainy season and hence with less possibility of debris deposit in the steep slope of the catchments. On the other hand, the

R.S.Girolamo has relatively lower RF, runoff and erosion every year favoring the accumulation of debris in the steep slopes of the catchment area. In such condition when the maximum probable RF is happened, the occurrence of debris flow is inevitable in the R.S.Girolamo.

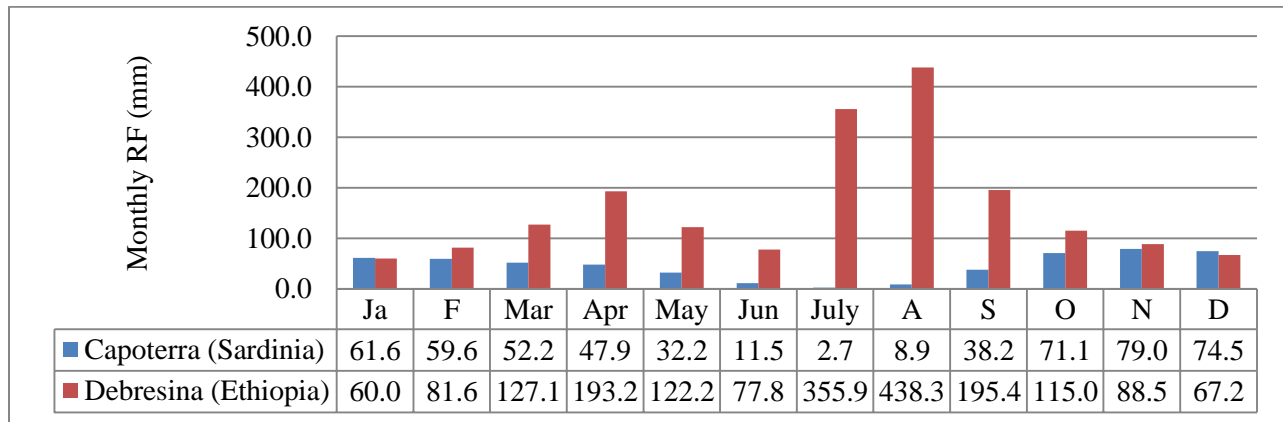


Fig 12.1: Mean monthly rainfall comparison of the two study areas, Debresina (average of 44years) and R.S.Girolamo (Capoterra station, average of 84 years)

- The study results identified that the major influencing landslide causative factors in Debresina area are lithology (34.2%), proximity to fault (24.5%), proximity to drainage (16.2%), and the least is elevation (2.9%). Whereas in R.S. Girolamo, the top landslide influencing factors are proximity to drainage (41%), lithology (24%), land use (13%), slope (11%) and the least is aspect (4%).
- Analysis of all methods (OM, FR and AHP) more or less show similar result that in the Debresina site an area is susceptible to slope failure if it is: (a) covered by lithology of colluvium-eluvium, debris deposits, various tuffs and clay soils; have slope range of 10°-40°; land use of river course, arable and poorly vegetated land; have proximity to fault of 0-600m; proximity to drainage of 0-300m ; have elevation of 2000-2500m and with an aspect to E and SE, (b) whereas in the R.S. Girolamo an area is prone to landslide if it has a lithology of alluvium, talus, granite and colluvium; have a slope class of >26°; have land use of river coarse, forest and bare rock; have proximity to drainage of 0-100m ; with elevation of 450-600m and having an aspect of facing N, NW, NE and S wards. These analysis results revealed that landslide inducing class ranges of each causative factor are different in each study areas (i.e. Debresina and R.S.Girolamo) in all cases except in the land use classes which more or less have similar impact on the slope failure of both sites.
- The prediction accuracy of the OM, FR and AHP methods in both study areas (Debresina and R.S.Girolamo) is compared based on Area Under the Curve (AUC) method as seen in Fig12.2. Results showed that the percentage of prediction accuracy of the methods in general is higher at the Debresina area (Ethiopia) than in R.S.Girolamo (Sardinia). This could be mainly attributed due to the

prevalent landslide types in each study areas. As mentioned above, the dominant landslide types in Debresina site are the complex slides and debris/earth slides whereas in the R.S.Girolamo dominant one are the flow-like landslides (e.g. debris flow) and rock falls. Therefore, it can be suggested that the applicability of these methods for the susceptibility analysis of the flow-like landslide (e.g. debris flow) and rock falls/topples are relatively lower than in the other types of landslide types.

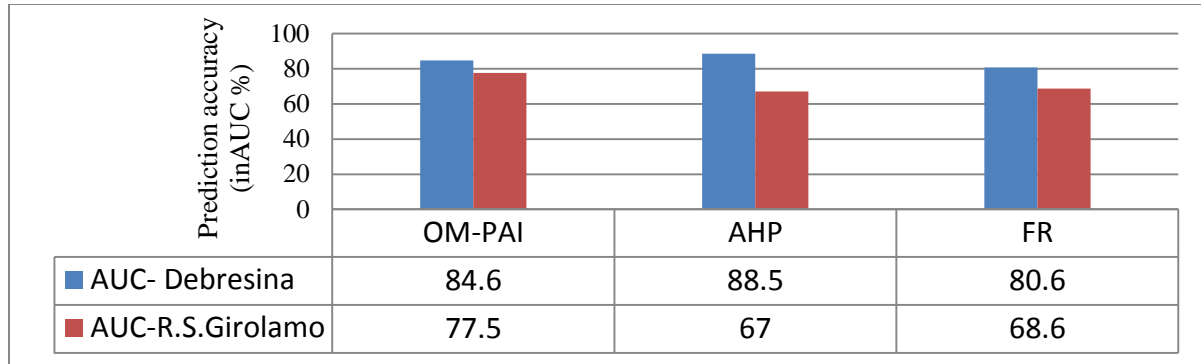


Fig 12.2: Histogram showing the percentage of prediction accuracy comparison of the three methods based on Area under the Curve (AUC) method for R.S. Girolamo (Sardinia) and Debresina areas (Ethiopia)

- In the GLE method of circular failure surface, the reduction of the SF from the dry slope to the saturated slope condition for the Debresina area (Ethiopia) is 43-45% but in the case of R.S. Girolamo the reduction SF reaches 64-71%. This clearly displays that the triggering impact of water for slope failure is more in the R.S. Girolamo than in the Debresina area.
- Although the landslide and related hazards still existed in both study areas, the position of prevention towards the hazards is quite different in both areas owing to the developmental difference of the two countries, Ethiopia and Italia. Thus, in R.S. Girolam (Sardinia) landslide and related hazard prevention measures are better institutionalized and hence, with better territorial management and public awareness of the hazard. Where as in Debresina (Ethiopia), no responsible institution and poor territorial management exist, and people have no idea how to prevent landslide hazards.

References

- Abebe B., Dramis F., Fubelli G., Umer M., Asrat A., (2010). Landslides in the Ethiopian highlands and the Rift margins. *Journal of African Earth Sciences* 56: 131–138
- A El-Naqa, (2000). The hydraulic conductivity of the fractures intersecting Cambrian sandstone rock masses, central Jordan. Hashemite Univ., Institute of Lands, Water & Environment, Depart of Water Management & Environment, Zerqa, Jordan
- Afar consortium, (2012). Magmatic Rifting & Active Volcanism Conference. Addis Ababa, Ethiopia; 11-13 January 2012
- AGS, (2000). Landslide risk management concepts and guidelines, Australian Geom. Society (AGS), Subcommittee on landslide risk management
- Al-Arifi N.S., Al-Humidan S.M., and Al-Bassam A.M., (2012). Time independent seismic hazard analysis of the Afar depression. *Scientific Research & Essays* Vol.7 (14): 1494-1500.
- Aleotti P. and Chowdhury, R., (1999). Landslide hazard assessment: summary review and new perspectives, *Bulletin of Eng. Geology and the Env*, 58:21-44.
- Aleotti P., (2004). A warning system for rainfall-induced shallow failures. *Eng. Geology*, 73:247-265.
- Alexander D., (1993). *Natural Disasters*. UCL Press and Chapman & Hall, New York, 632pp
- Amantii M., et al., (1992). Linee guida per la relizzazione di una cartografia della pericolosità geologica connessa ai fenomeni di instabilità dei versanti alla scala 1:50,000; Progetto CARG. Presidenza del consiglio dei ministri servizio geologico.
- Anagnostopoulos K., & Vavatsikos A., (2012). Site Suitability Analysis for Natural Systems for Waste water Treatment with Spatial Fuzzy Analytic Hierarchy Process. *Jour. of Water Resour. Plann. Manage.* 138, 125
- Anbalagan R., (1992). Landslide hazard evaluation and zonation mapping in mountainous terrain. *Eng. Geology*, 32: 269-277
- András F., (2010). The Use of the AHP in Civil Engineering Projects. MEB 2010- 8th Inter. Conf. on management, Enterprise and benchmarking, June 4-5, Budapest, Hungary
- Andrew W., Davies T., (2011). Identification of alluvial fans susceptible to debris-flow hazards. *Landslides*, 8:183-194
- Asfaw L., (1986). Catalogue of Ethiopian Earth Quakes, Earth quake parameters, Strain release and Seismic risk, Geophy. Obser, Faculty of Science, Addis Ababa University.
- Aulitzky H., (1980). "Preliminary two-fold classification of debris-torrents". In: Proceedings of 'Interpraevent' Conference. Austria, Bad Ischl 4:285-309, translated from German by G Eisbacher.
- Ayalew L., (1999). The effect of seasonal rainfall on landslides in the highlands of Ethiopia, *Bull Eng Geol Env*. 58: 9-19, Q Springer-Verlag
- Ayalew L., Yamagishi H., (2003). Slope failures in the Blue Nile basin, as seen from landscape evolution perspective. *Jour. of Geomor.* 1361, 1-22
- Ayalew L., Yamagishi H., (2004). Slope movements in the Blue Nile basin, as seen from landscape evolution perspective. *Geomorphology*, 57:97-116.
- Ayele A., et al., (2007). The volcano-seismic crisis in Afar, Ethiopia, starting September 2005. *Earth & Planetary Sci. letters* 255: 177–187

- Ayele A., et al., (2009). September 2005 mega-dike emplacement in the Manda-Harraro nascent oceanic rift (Afar depression), Geophysical Research letters, VOL.36, L20306, doi: 10.1029
- Ayenew T., Barbieri G., (2005). Inventory of landslides and susceptibility mapping in the Dessie area. Northern Ethiopia, Eng. Geology 77:1-15
- Bachri S., and Shrestha R.P., (2010). Landslide hazard assessment using analytic hierarchy processing (AHP) and GIS in Kaligesing mountain area of Central Java Province Indonesia; 5th Annual Inter. Workshop & Expo on Sumatra Tsunami Disaster & Recovery
- Bagyaraj M. & Gurugnanam B., (2011). Significance of Morphometry Studies, Soil Characteristics, Erosion Phenomena and Landform Processes Using RS and GIS for Kodaikanal Hills. A global biodiversity hotspot in Western Ghats, Dindigul district, T.Nadu, South India. Rese. Jour. Envir. & Earth Sci., 3(3):221-233
- Balia R., et al., (2009). Assessment of the Capoterra coastal plain (southern Sardinia, Italy) by means of hydrogeol. and geophy. studies. Hydrogeol. Jour., 17: 981-997
- Bantayan N.C., Bishop ID., (1998). Linking objective and subjective modeling for land use decision-making. Landscape and urban planning 43:35-48.
- Barberi F., and Varet J., (1977). Volcanism of Afar: Smallscale plate tectonics implications: Geological Society of America Bulletin, v. 88: 1251-1266
- Barbieri G., and Cambuli P., (2009). The weight of evidence statistical method in landslide susceptibility mapping of the Rio Pardu Valley (Sardinia, Italy): 18th World IMACS / MODSIM Congress, Cairns, Australia
- Barca S., & Maxia M., (1982). Assetto stratigrafico e tettonico del Paleozoico del Sarrabus occidentale. In Guida alla Geologia del Paleozoico sardo. Guide Geologiche Regionali. Soc. Geol. It., 87-93.
- Barca S., Serri R., Rizzo R., Forci A., Calzia P., Pertusati P.C., (2009). Note Illustrative della Carta Geologica d'Italia alla scala 1:50.000, foglio 565, CAPOTERRA. I S P R A, Sardegna, Italy.
- Bathrellos G.D., Kalivas D.P., Skilodimou, H.D., (2009). GIS-based landslide susceptibility mapping models applied to natural and urban planning in Trikala, Central Greece Estudios Geol., 65(1):49-65
- Bell F.G., (1999). Geological hazards: their assessment, avoidance, and mitigation. E & FN Spon, Routledge, London, 648pp.
- Bell F.G., (2007). Engineering Geology, 2nd Edit, Butterworth-Heinemann, UK: 593pp
- Bekele A., et al., (2010). Landslides in the Ethiopian highlands and the Rift margins. J. African Earth Sci 56:131-138
- Beyene A., Abdelsalam M. G., (2005). Tectonics of the Afar Depression: A review and synthesis. Jour. of African Earth Sciences 41, 41-59.
- Bettina N., Birgit T., (2007). Landslide susceptibility assessment using "weights-of-evidence" applied to a study area at the Jurassic escarpment (SW-Germany), Geom. Vol. 86:12-24
- Bloch A., & Braun B., (2005). Economic assessment of landslide risks in the Swabian Alb, Germany research framework & 1st results of homeowners' & experts' surveys. N. Hazards & Earth Syst Sci. 5: 389-396.
- Bonam-Carter G.F., Agterberg F.P., Wright D.F., (1989). Weights of evidence modelling: a new approach to mapping mineral potential: Statistical Application in the Earth Sci, ed. F.P. Agterberg and G.F. Bonam-Carter; Geol. Survey of Canada, Paper 89-9:171-183
- Brabb E.E., (1984). Innovative approaches to landslide hazard mapping. Proc. 4th Inter. Symp. on landslides, Toronto, 1: 307-324.

- Brayshaw D., and Hassan M.A., (2009). Debris flow and Sediment recharge in gullies. *Geom.* 109:122-131
- Brunetti M.T., et al., (2010). Rainfall thresholds for the possible occurrence of landslides in Italy. *N.Hazards Earth Syst. Sci.*, 10:447-458
- Burt G. L., (2007). *Hand book of geotechnical investigation and design tables*. Taylor & Francis/Balkema: London, UK, 356pp
- Caine N., (1980). The rainfall intensity-duration control of shallow landslides and debris flows. *Geogr. Ann.* A62:23-27
- Calcaterra D., Parise M., and Palma B., (2003). Combining historical and geological data for the assessment of the Landslide hazard: a case study from Campania, Italy *Natural Hazards and Earth System Sciences* 3: 3-16, European Geosciences Union
- Carrara A., (1983). Multivariate models for landslide hazard evaluation. *Mathematical Geology*, 15(3):403-426.
- Carrara A., et al., (1991). GIS Techniques & statistical models in evaluating landslide hazard. *Earth Surface Proces. & Landform* 16:5: 427-445.
- Carrara A., Cardinali M., Guzzetti F., Reichenbach P., (1995). GIS technology in mapping landslide hazards. In: Carrara A, Guzzetti F (eds.), *GIS in Assessing N.Hazards*. Kluwer Academic Publis., Dordrecht, The Netherlands:135-175.
- Carrara A., Guzzetti F., Cardinali, M. and Reichenbach P., (1999). Use of GIS Technology in the Prediction and Monitoring of Landslide Hazard. *Natural Hazards*, 20:2-3:117-135
- Catenacci V., (1992). Il dissesto geologico e geoambientale in Italia dal dopoguerra al 1990. *Memorie Descrittive della Carta Geologica d'Italia*, XLVII.
- Chigira M., (2000). Geological structures of large landslides in Japan, *Jo. Nepal Geol. Soc.* 22: 497-504.
- Chowdhury R., et al., (2010). *Geotechnical Slope Analysis*. Taylor & Francis Group, London, UK, 751PP
- Clark M.J. and Samall R.J., (1982). *Slopes and Weathering*. London, Cambridge University Press, 112pp.
- Coccozza T., Schafer K., (1974). Cenozoic Graben Tectonics in Sardinia. *Rend.Sem. Fac. Sc. Univ. Cagliari*, suppl.vol.43:145-162
- Conoscenti C., Maggio C.D. and Rotigliano E., (2008). GIS Analysis to assess landslide susceptibility in a fluvial basin of NW Sicily (Italy). *Geom.* 94:325-339
- Cornforth D.H., (2005). *Landslide in practice: investigations, Analysis, and Remedial/preventative Options in soils*. John Wiley & Sons, Inc., Hoboken, New Jersey, Canada, 622pp
- Crozier M.J., (1986). *Landslides: causes, consequences and environment*. Croom Helm, London, 252pp.
- Crozier M.J., (1996). Magnitude frequency issues in landslide hazard assessment. In: Mausbacher, R. & A. Schulte (eds): *Beitrage zur Physiogeographie.-Barsch Festschr., Heidelberg Geogr. Arb.* 104:221-236
- Crozier M.J., Glade T., (1999). Frequency and magnitude of landsliding: fundamental research issues. E. Schweizerbart'sche Verlags buchandlung
- Crozier M.J. and Glade T., (2005). Landslide hazard and risk: issues, concepts and approach. In: Glade, T., Anderson, M.G. and Crozier, M.J. (eds.) *Landslide risk assessment*. John Wiley: 1-40.
- Cruden D.M., (1991). A simple definition of a landslide. *Bull. of the Int. Asso. Eng. Geology*, 43:27-29.
- Cruden D.M., (2000). Some forms of mountain peaks in the Canadian Rockies controlled by their rock structure, *Quat. Int.* 68-71: 59-75.

- Cruden D.M. and Hu, X.Q., (1996). Hazardous modes of rock slope movement in the Canadian Rockies, *Env. Eng. Geosci.* 2, 507-516
- Cruden D.M., and Varnes D.J., (1996). "Landslide types and processes". In: Turner, A.K. and Shuster, R.L. (eds) (1996). *Landslides investigation and mitigation. Special report 247:36-75.* Transportation Research Board, Washington, D.C., US National Research Council
- Dahal R.K., Hasegawa S., Yamanaka M., Dhakal S., Bhandary N.P., Yatabe R., (2009). Comparative analysis of contributing parameters for rainfall-triggered landslides in the Lesser Himalaya of Nepal, *Environmental Geology*, 58(3):567-586
- Daniel M., Dejene H., and Abrham M., (2010). *Geology of Debre Birhan area. Geological survey of Ethiopia, Ministry of mines and energy of Ethiopia: 70pp*
- Daniele de W., & Stefano M., (2011). Assessment of debris flow magnitude in small catchments of the Lombardy Alps: the Val gola case study, Vol.2:9-15
- Dai F.C, Lee C.F, Zhang XH., (2001). GIS-based geo-environmental evaluation for urban land-use planning: a case study. *Eng. Geology* 61:257-271.
- Dai F.C., and Lee C.F., (2002). Landslide characteristics and slope instability modeling using GIS, Lantau Island, Hong Kong. *Geom.* 42:213-228
- Dietrich E.W, Reiss R, Hsu M.L, Montgomery D.R., (1995). A process-based model for colluvial soil depth and shallow landsliding using digital elevation data. *Hydrol. Proc.*, 9:383-400.
- De Scally F.A, Owens I.F., (2004). Morphometric controls and geomorphic response on fans in the Southern Alps, New Zealand. *Earth Surf Proc. Land* 29:311-322
- Dikau R., Brunsden, D., Schrott L. and Ibsen M.L., (1996). *Landslide recognition, Identification, Movement and Courses.* Wiley & Sons, Chichester, etc., 251pp.
- Dovera, Mancini, Salis (2000) *Attività di individuazione e di perimetrazione delle aree a rischio idraulico e geomorfologico e delle relative misure di salvaguardia*
- EBCS-8, (1995). *Code of Standards for Seismic Loads*, Ministry of Works and Urban Development, Addis Ababa, Ethiopia
- Ebinger C.J., et al., (1993). Late Eocene–Recent volcanism and faulting in the southern main Ethiopian rift: *Geol. Society, London, Jour.* v.150:99-108
- Evans S.G., Aitken J.D., Wetmiller R.J., and Horner R.B. (1987). A rock avalanche triggered by the Oct. 1985 North Nahanni Earthquake, District of Mackenzie, N.W.T., Can. *Jo. Earth Sci.* 24:176-184.
- Fauque L., and Tecligharian P., (2002). Villavil rockslides, Catamarca Province, Argentina, In: S.G. Evans and J.V. De Graff (eds.), *catastrophic landslides: effects, occurrence, and mechanisms*, *Geol. Soc. Am. Rev. Eng. Geol.*, v. XV: 303-324.
- Fell R., et al., (2008). On behalf of the JTC-1 Joint Technical Committee on Landslides and Engineered Slopes; *Eng. Geology*, 102:99-111
- Feng C.C., & CHAN E.H.W., (2004). Application of AHP in Decision making on urban use: A case study of Chao-Hu city Development in China. *The Inter. Jour. of Construction management*: 93-110
- Foumelis M., Lekkas E, Parcharidis I., (2004). Landslide susceptibility mapping by GIS-based qualitative weighting procedure in Corinth area. *Bull Geol Soc Greece*, 36:904-912
- Galang J.S., (2004). A Comparison of GIS Approaches to slope instability zonation in the central Blue Ridge Mountains of Virginia. MSc thesis, Faculty of Virginia Polytech. Institute and State Univ., Blacksburg, Virginia. 99pp.

- Gete Z., (2010).A Study on Mountain Externalities in Ethiopia, FAO final report, Ethiopia
- Giannis T.Tsoufias, Costas P., Rachaniotis N.P., (2004).Aggregating and evaluating the results of different Environmental Impact Assessment methods. *Eco. Indicators*, 4:125-138
- Giovanni P., (2008).Relazione sulle precipitazioni del giorno 22-Ottobre-2008 nella Sardegna centro-meridionale, Regione Autonoma della Sardegna Assessorato Dellavori Pubblici Servizio Difesa del Suolo
- Grandin R., et al., (2009).September 2005 Manda Hararo-Dabbahu rifting event, Afar (Ethiopia): Constraints provided by geodetic data, *Jour. of Geophy. Research*, vol.114
- Gebresilassie A., (2007).The Social, economic and environmental impacts of landslides in the high lands of Ethiopia. MSc Thesis, Faculty of Dry Land Agriculture and natural resources, Mekelle Univ.
- Glade T., Crozier M.J, Smith P., (2000).Applying probability determination to refine landslide-triggering rainfall thresholds using an empirical “Antecedent Daily Rainfall Model”.*Pure Appl Geophys*, 157(6/8):1059-1079
- Glade T., Anderson M., Crozier J.M., (2005).Landslide Hazard and Risk. West Sussex PO19 8SQ, England, 834pp
- Gouin P., (1979).Earthquake History of Ethiopia and the Horn ofAfrica. International Development Research Centre (IDRC), Ottawa, Ont., 258 pp.
- Gregory A.K., et al., (2005).Application of Multicriteria Decision Analysis in Environmental Decision Making. *Integrated Envir. Assessment and Management*, vol.1:95-108
- Gritzner L.M., Marcus W.A., Aspinall R., & Custer S.G., (2001).Assessing landslide potential using GIS, soil wetness modeling and topographic attributes, Payette River, Idaho. *Geom*, 37:149-165.
- Guzzetti F., Cardinali M., and Reichenbach P., (1996).The influence of structural setting and lithology on landslide type and pattern, *Env. Eng. Geosci*. 2:531-555.
- Guzzetti F., Carrara A., Cardinali M. & Reichenbach P., (1999).Landslide hazard evaluation: an aid to a sustainable development. *Geom*, 31:181-216.
- Guzzetti F., and Tonelli G., (2004).Information system on hydrological and geomorphological catastrophes in Italy (SICI): a tool for managing landslide & flood hazards, *N.Hazards Earth Syst. Sci.*, 4:213-232
- Guzzetti F., (2005).Review and Selection of Optimal Geological Models Related to Spatial Information Available, Risk-Advanced Weather forecast system to Advise on Risk Events and management Action 1.14,IRPI CNR, Perugia, Italy
- Guzzetti F., et al., (2006).Estimating the quality of landslide susceptibility models. *Geom.*, 81:166-184.
- Guzzetti F., Peruccacci S., Rossi M., & Stark, C. P., (2007).Rainfall thresholds for the initiation of landslides in central and southern Europe, *Meteorol. Atmos. Phys.*, 98:239-267.
- Guzzetti F., Peruccacci S., Rossi M., & Stark C.P., (2008).The rainfall intensity-duration control of shallow landslides and debris flows: an update, *Landslides*,5(1):3-17
- Hambali A., Sapuan S.M., Ismail N., and Nukman Y., (2009).Application of analytical hierarchy process in the design concept selection of automotive composite bumper beam during the conceptual design stage. *Scientific Research and Essay* vol.4:198-211
- Hayward N., and Ebinger C.J., (1996).Variations in the along-axis segmentation of the Afar Rift System: *Tectonics*, v.15:244-257.

- Hendron A.J. & Patton F.D., (1985).The Vajont Slide: a geotechnical analysis based on new geological observations of the failure surface: U.S. Army Engineer Waterways Experiment Station, Technical Report GL-85-5, 2 volumes.
- Hervás J. (Ed.), (2003).Lessons Learnt from Landslide Disasters in Europe. EUR 20558 EN, European Commission, Ispra, Italy, 91pp.
- Hode R.A.L., & Freeze R.A., (1977).Ground water flow systems and slope stability, Canadian Geot.Jour., 14: 466-476
- Hoek E., and Bray J.W., (1981).Rock slope engineering, 3rd ed., Institution of Mining & Metal., London, 402pp
- Hoffman, et al., (1997).Timing of the Ethiopian flood basalt event and implications for plume birth and global change: Nature, v. 389:838-841
- Hudson J.A., and. Harrison J.P., (1997).Engineering rock mechanics, an introduction to the principles. Elsevier Sci. Ltd, UK: 458pp
- Hungr O., Morgan G.C., & Kellerhals R., (1984).Quantitative analysis of debris torrent hazards for design of remedial measures. Can. Geotech. J. 21:663-677
- Hungr O., Evans S.G., Bovis M., & Hutchinson J.N., (2001).“Review of the Classification of landslides of the flow type”. Environ. and Eng. Geosci., VII: 221-238
- Hutchinson J.N., (1995).Keynote paper: Landslide hazard assessment.In L.slides, Proc.of VI. Inter. Symp.on Landslides, Feb., Christchurch, New-ZealandA.A.Balkema, Rotterdam, The Netherlands, 3:1805-1841.
- Hutchinson J.N., (1987).Mechanisms producing large displacements in landslides on pre-existing shears, Mem. Geol. Soc. of China, 9:175-200
- Hutchinson J.N., (1988).Morphological and geotechnical parameters of landslides in relation to geology and hydrology. In: Landslides, Bonnard C(ed.). Proc. 5th Inter. Symp. on Landslides 1988, Lausanne, Balkema, Rotterdam,1:3-35.
- Hyun-J.O., Lee S., Soedradjat G., (2010).Quantitative landslide susceptibility mapping at Pemalang area, Indonesia, Environ Earth Sci, 60:1317-1328
- Iverson R.M., & Reid M.E., (1992).Gravity-driven groundwater flow and slope failure potential: Elastic effective-stress model: Water Resources Research, v.28:925-938.
- Ishaku J.M., Gadzama E.W., & Kaigama U., (2011).Evaluation of empirical formulae for the determination of hydraulic conductivity based on grain-size analysis.J. of Geol. & Mining Research Vol.3:105-113.
- Ishizaka A., & Labib A., (2009).Expert choice: Benefits and limitations. Operational research society Ltd. Vol. 22, (4):201-220
- ISRM, (1985).Suggested methods for determining point load strength ISRM commission on testing methods, working group on revision of the point load test method. Int.jrn. of rock min Sci. and geomech. Abst22: 51-60
- Jakob M., (1996).Morphometric and geotechnical controls of debris flow frequency and magnitude in southern British Columbia. PhD thesis; the University of British Columbia: 241pp
- Jackson L.E, Kostaschuk R.A, MacDonald G.M., (1987).Identification of debris-flow hazard on alluvial fans in the Canadian Rocky Mountains. Rev Eng. Geol., 7:115-124
- Jackson L.E., Hungr O., Gardner J.S., and Makay C., (1989).Cathedral Mountain debris flows, Canada, Bull. IAEG 40:35-54

- Jankowski P., (1989).Mixed-data multi-criteria evaluation for regional planning: a systematic approach to the decision-making process. *Environment and planning A* 21:349-362
- Kamal M.A-Subhi Al-Harbi, (2001).Application of the AHP in project management. Vol.19:19-27
- Kazmin V., (1975).Explanatory Note to the Geology of Ethiopia. Addis Ababa, Ethiopia: Ethiopian Institute of Geological Surveys. Bull.no.2
- Kebede F., and Kulhnek O., (1991).Recent seismicity of the East African rift system and its implications. *Phys.Earth Planet. Inter.*, 68:259-273.
- Kebede F., T.Van Eck, (1997).Probabilistic Seismic Hazard Assessment for the Horn of Africa based on seismotectonic regionalization.*Tectonophy.* 270:221-237
- Keefer D.K., (2002).Investigating landslides caused by earthquakes-a historical review. *Surveys in Geophy.*23:473-510.
- Krejci O., et al., (2002).Slope movements in the Flysch Carpathians of Eastern Czech Republic triggered by extreme rainfalls in 1997:a case study. *Physics and Chemistry of the Earth*, 27:1567-1576.
- Kumar R.S., Kumar A.K., Lohani R.K., and Singh R.D., (2000).Evaluation of geomorphological characteristics of a catchment using GIS. *GIS India*, 9(3):13-17
- Lee S., Min K., (2001).Statistical analysis of landslide susceptibility at Youngin, Korea. *Environ. Geol.* 40, 1095–1113
- Lee S., Ryu J.H., Min K., & Won J.N., (2004).Landslide susceptibility analysis using GIS and artificial neural network. *Earth Surface Proc. and Landforms*, 28(12):1361-1376.
- Lee S., (2005).Application and cross-validation of spatial logistic multiple regression for landslide susceptibility analysis. *Geosci*, 9(1):63-71.
- Lee S., & Nguyen T.D., (2005).Probabilistic landslide susceptibility mapping in the Lai Chau province of Vietnam: focus on the relationship between tectonic fractures & landslides, *Env. Geol.*, 48:778-787
- Lee S., & Pradhan B., (2006).Probabilistic landslide hazards and risk mapping on Penang Island, Malaysia. *Earth Syst.Sci.*, 115(6):661-672.
- Leta A., (2007).Landslide Susceptibility Modeling Using Logistic Regression and Artificial Neural networks in GIS: a case study in Northern Showa area, Ethiopia. MSc Thesis, Addis Ababa university earth science department: 75pp
- Long N.T., (2008).Landslide susceptibility mapping of the mountainous area in a Luoi district, Thua Thien Hue Province, Vietnam. PhD thesis, Faculty of Engineering, Vrije Universiteit Brussel: 229pp.
- Long N.T., & De Smedt F., (2011).Application of an analytical hierarchical process approach for landslide susceptibility mapping in A Luoi district, Thua Thien Hue Province, Vietnam; *Environ Earth Sci*, 10, 011-1397
- Marco B., Giancarlo D.F., Carlo G., and Lorenzo M., (2002).Assessment of shallow land sliding by using a physically based model of hill slope stability. *Hydrogeol. Process.*16:2833-2851
- Mahsa H.A., et al., (2011).Site Selection Using Analytical Hierarchy Process by GIS for Sustainable Coastal Tourism. *Inter. Conf. on Environ.& Agricul. Eng., IPCBEE* vol.15, IACSIT Press, Singapor
- Mehrdad S., et al., (2011).Deterministic Rainfall Induced Landslide Approaches, Advantage and Limitation, Vol.16, Bund. U 1620, EJGE
- Mehrnoosh J., et al., (2009).Landslide susceptibility Evaluation and factor effect analysis using probabylsitic frequency ratio Model. *Euroepan Jour., Scien. Research.*vol.33:654-668

- Mengesha T., Tadiwos C. & Workineh H., (1996). Explanation of the Geological Map of Ethiopia, Scale 1:2,000,000, 2nd edition. Addis Ababa: The Federal Democratic Republic of Ethiopia.
- Mezughi T.H., et al., (2012). Analytical hierarchy process method for Mapping Landslide Susceptibility to an Area along the E-W Highway (gerik-Jeli), Malaysia. *Am. J. Environ. Sci.* 5:13-24
- Midzi V., et al., (1999). Seismic hazard assessment in eastern and southern Africa. *Annali Di Geophysica* Vol.42, N6
- Millard T.H., Wilford D.J., & Oden M.E., (2006). Forest research Technical Report, Coast Forest Region 2100 Labieux Road, Nanaimo, BC, Canada, Geomo. 250:751-7001
- Mohr P.A., (1962). The Geology of Ethiopia. Addis Ababa, Ethiopia: University. Coll. of Addis Ababa Press, 268pp
- Mohr P., (1983). The Ethiopian Flood Basalt Province. *Nature*, v.303:577-584.
- Muthu K., Petrou M., (2007). Landslide-Hazard Mapping Using an Expert System and a GIS. *IEEE Transactions on Geosci. & Remote sensing*, 45(2):522-531
- Narumon I., and Songkpt D., (2010). Analytical hierarchal for landslide susceptibility mapping in lower Mae chaem watershed, northern Thailand. *Suranaree J. Sci. Technol.* 17(3):277-292.
- Neaupane K.M., Piantanakulchai M., (2006). Analytic network process model for landslide hazard zonation. *Eng. Geology*. 85 (3-4):281-294.
- Nettleton I.M., et al., (2005). Debris flows from the perspective of the Scottish Highlands. *Proc, 11th Inter. Conf. on Landslides*, Norway, 1-10 Sept. 2005
- Pack R.T., Tarboton D.G., & Goodwin C.N., (1998). The SINMAP approach to terrain stability mapping. In: *Proc. of 8th Cong. of the Inter. Ass. of Eng. Geol.* Vancouver, British Colum, & Canada: 1157-1165
- Pradeep K.R., Tiwari P.C., & Charu C.P., (2011). Morphometric Analysis of Third order River Basins using High Resolution Sat. Imagery and GIS Technology: Special Refer. to N. Hazard Vulnerability Assessment, Vol.3:2094-1749
- Prasad A., (2006). Slope Stability Evaluations by Limit Equilibrium and Finite Element Methods. PhD thesis. Norwegian University of Science and Technology, NTNU: 146pp
- Pierson T.C. & Costa J.E., (1987). "A rheological classification of sub-aeria sediment-water flows". *Geol. Society of America Reviews in Eng. Geology*, 7: 1-12
- Pik R., et al., (1998). The northwestern Ethiopian Plateau flood basalts: classification and spatial distribution of magma types. *Jour. of Volcanology and Geothermal Research* 81:91-111
- Price D.G., (2009). *Engineering geology, Principles and Practice*. Springer-Verlag Berlin Heidelberg: 460pp
- Progetto IFFI, Regione Sardegna (2005). *Assessorato della Difesa dell'Ambiente*, Sardinia
- RADIUS Group (1999). IDNDR RADIUS Project, Addis Ababa Case Study, Final Report.
- Ramanathan R., (2001). A note on the use of the analytic hierarchy process for environmental impact assessment. *Jour. of Environ. Management*, 63: 27-35.
- Remondo J., et al., (2003). Landslide susceptibility models utilising spatial data analysis techniques. A Case study from the Lower Deba Valley, Guipúzcoa (Spain). *N. Hazards*, 30:267-279.
- Richard E.G., (2005). Guide lines for the Geologic evaluation of debris flow hazards on alluvial fans in Utah. *Hutahutah geological Survey, Miscellaneous Publication* 05-6.
- Rickenmann D., & Zimmermann M., (1993). The 1987 debris flows in Switzerland: documentation and analysis. *Geom.*: 8:175-189.

- Rowland J., et al., (2007). Fault growth at a nascent slow spreading ridge: 2005 Dabbahu rifting episode, Afar, *Geophys. Jour.Int.* 171(3):1226-1246
- Saaty T.L., (2000). The fundamentals of decision making and priority theory with the analytic hierarchy process, Vol VI, 2nd edn. RWS Publications, Pitsburg
- Saaty T.L., (2008). Decision making with the analytic hierarchy processes, *Int.J.Services, Sci.*, Vol.1:83-98
- Salvati P., Bianchi C., Rossi M., and Guzzetti F., (2010). Societal landslide and flood risk in Italy. Istituto di Ricerca per la Protezione Idrogeol., Consiglio Nazionale delle Ricerche, Perugia, Italy
- Santiago B., (2006). Changes in land cover and shallow landslide activity: a case study in the Spanish Pyrenees, Preprint of the article published in *Geom.*, 74:196-206.
- Schuster R.L., & Highland L.M., (2001). Socio economic and environmental impacts of land slide in the western hemisphere. U.S. Geological Survey, U.S.A.
- Selby M.J., (1993). *Hillslope Materials and Processes*, 2nd ed. Oxford University Press: New York, 451pp.
- Sidle R.C., & Ochiai H., (2006). *Landslides: processes, prediction, and References* 202 landuse. American Geophys. Union, Washington, D.C. Water Resources Monograph No.18:312pp.
- Soeters R. & van Westen C.J., (1996). Slope instability recognition, analysis and zonation. In: Turner, A.K. and Schuster, R.L., (eds.), *Landslide investigation and mitigation*, National Research Council, Transportation Research Board Special Report 247:129-177.
- Schuster R.L., and Highland L.M., (2001). *Socioeconomic and Environmental Impacts of Landslides in the Western Hemisphere*. U.S. Geological Survey Open-File Report 01-0276: 47pp
- Süzen M.L., & Doyuran V., (2004). A comparison of the GIS based landslide susceptibility assessment methods: multivariate versus bivariate. *Envi. Geology*, 45:665-679
- Takahashi T., (1981). Debris-flow. *Annual Reviews in Fluid Mechanics*, 13:57-77
- Takahashi T., (2007). *Debris flow Mechanics, Prediction and Countermeasures*, Taylor & Francis Group, London, UK: 465pp
- Tefera M, Chernet T, Workeneh H., (1996b). *Explanation to Geological Map of Ethiopia*. Scale 1: 2,000,000: second ed. Ethiopian Institute of Geol. Surveys, Addis Ababa, 69pp
- Temesgen B., Mohammed M.U., Korme T., (2001). Natural hazard assessment using GIS and remote sensing methods, with particular reference to the landslides in the Wondogenet area, Ethiopia. *Phys. Chem. Earth.*, 26 (9):665-675.
- Tesfaye S., Harding D.J., Kusky T.M., (2003). Early continental breakup boundary and migration of the Afar triple junction, Ethiopia. *Geol. Society of America Bull.* 115:1053-1067.
- Tien-C.C., et al., (2012). Limitation of hillslope debris flow affected by Chi-Chi Earthquake. Taiwan. *Proc. of the Inter. Symp. On Eng. Lessons Learned from the 2011 Great East Japan E.quake*, March 1-4, 2012, Tokyo, Japan
- Turner A.K., & Schuster R.L., (1996). *Landslides: investigation and mitigation*. Transport Research Board Spec. Rep. 247. Washington, D.C., National Academy of Sci. 36-75.
- Thiery Y., et al., (2007). Landslide susceptibility assessment by bivariate methods at large scales: Application to a complex mountainous environ. *Geom.*, 92(1):18pp.
- Trigila A., and Iadanza C., (2008). *Landslides in Italy*, Special Report 83/2008, ISPRA. Institute for Environmental Protection and Research Geol. Survey of Italy/Land Protection and Geo-resources Department, Monitoring Plans, Risk assessment and Data Collection Unit, Rome

- Ulrich K., et al., (2008).GIS-based landslide susceptibility mapping for the 2005 Kashmir earthquake region, *Geom.*101, 631-642UNISDR- Inter. Strategy for Disaster Reduction: www.unisdr.org/we/inform
- UNISDR, (2009).Global assessment report on disaster risk reduction: risk and poverty in a changing climate
- Vahidnia M.H., Alesheikh A.A., Alimohammadi A., and Hosseinalie F., (2009).Landslide Hazard Zonation Using Quantitative Methods in GIS. *Intern. Journal of Civil Eng.*, Vol.7, No. 3:176-189
- Van Dommelen P.A, (1998).A comparative study of colonialism and rural settlement in first millennium B.C west central Sardinia. *Archaeological Studies Leiden Univ, Faculty of Archaeology, The Netherlands*
- Van Westen C.J, Rengers N, Terlien M.T.J, Soeters R., (1997).Prediction of the occurrence of slope instability phenomena through GIS based hazard zonation. *Geol Rundsch* 86(2):404-414
- Van Westen C.J., Van Asch T.W.J., Soeters R., (2006).Landslide hazard and risk zonation - why is it still so difficult?. *Bulletin of Eng. Geology and the Envir.* 65:167-184.
- Varet J, and Gasse F., (1978).Geology of central and southern Afar (Ethiopia and Djibouti Republic): Paris, Editions du Centre National de la Recherche Scientifique, Report, 124pp, and map, scale 1:500,000
- Varnes D.J., (1978).Slope movement types and processes. In: Schuster RL, Krizek RJ (eds.), *Landslides: Analysis & Control*.Natio. Aca. of Sci,Transport. Resear. Board, W.DC, Special Rept.176:11-35.
- Varnes D.J., (1984).Landslide hazard zonation: a review of principles and practice. *Commission on landslides of the IAEG, UNESCO, N.Hazards*, No.3: 61pp.
- Varnes D.J., (1996).Landslide Types and Processes. In: Turner, A.K., and R.L.Schuster (eds), *Landslides: Investigation and Mitigation*, Transportation Research Board Special Report 247, National Research Council, Wasington, D.C. N.Academy Press
- Wang W.N., Chigira M., and Furuya T., (2003).Geological and geomorphological precursors of the Chiu-fen-erh-shan landslide triggered by the Chi-Chi earthquake in central Taiwan, *Eng. Geol.*69: 1-13
- Wilford D.J, et al., (2004).Recognition of debris flow, debris flood and flood hazard through watershed morphometric. *Landslides* 1:61-66
- Wilson J. P. & Gallant J.C., (2000).Terrain Analysis: Principles and Applications, John Wiley and Sons, New York: 479pp
- Woldearegay K., (2005).Rainfall-triggered landslides in the northern highlands of Ethiopia: Characterization, GIS-based Prediction and Mitigation. PhD Thesis. Facul. of Civil Eng. Graz Univ. of Techno.,176pp
- Wright T., et al, (2006).Magma maintained rift segmentation at continental rupture in the 2005 Afar diking episode, *Nature*, Vol 442|20
- Wu Jishan, (1992).Characteristics of erosion and deposition from debris flows. *Institute of Mountain Disasters and Environment, Chinese Academy of Sci., Chengdu, China*
- Yagi H., (2003).Development of assessment method for landslide hazards by AHP. In: Abstract vol. of the 42nd annual meeting of the Japan Landslide Society: 209-212.
- Yalcin A., (2007).GIS-based landslide susceptibility mapping using analytical hierarchy process and bivariate statistics in Ardesen (Turkey). *Catena*, 72(1):1-12.
- Yalcin A., and Bulut F., (2007).Landslide Susceptibility Mapping Using GIS and Digital Photogrammetric Techniques: A Case Study from Ardesen (NE-Turkey),” *Natural Hazards*, 41: 201-226
- Yalcin A., Reis S., Aydinoglu A.C., Yomralioglu T., (2011).A GIS-based comparative study of frequency ratio, analytical hierarchy process, bivariate statistics and logistics regression methods for landslide susceptibility mapping in Trabzon, NE Turkey, *ELSEVER, Catena* 85:274–287

- Yin K.J., and Yan T.Z., (1988).Statistical prediction model for slope instability of metamorphosed rocks. Proc. 5th Inter. Symp. on Landslides, Lausanne, Switser, 2:1269-1272
- Zahedi F., (1986).The analytic hierarchy process, a survey of the method and its applications. Interfaces 16(4): 96-108.
- Zanettin, B. & Justin Visentin, E., (1974).The volcanic succession in central Ethiopia, 2: The volcanics of the western Afar and Ethiopia rift margins.Memorie degli Istituti di Geologia e Mineralogia dell'Universita di Padova 31: 1-19.
- Zanettin B., et al., (1978).Volcanic Succession, Tectonics and Magmatology in Central Ethiopia. Istituto di Mineralogia e Petrologia, Universita di Padova,Padova, Italy.
- Zanettin B., (1992).Evolution of the Ethiopian Volcanic Province. Atti Della Accademia Nazionale Dei Lincei, Rome.

Annexes:

Annex-I: Description of parameters used in the litho-technical mapping (modified from the guideline of Italian Geological Services (Amanti et al, 1992) and weight values of PAI guideline (Dovera et al, 2000)

(A) For rock units

1. Degree of weathering:

Classes	Degree of weathering	Weight
1	I-II	4
2	III-IV	3
3	V	2
4	VI	1

Table used for the field description of degrees of rock mass weathering (after BS-5930, 1981).

Degree	term	Description/Field recognition
VI	Soil	All rock material is converted to soil. The mass structure and material fabric is destroyed. There is a large change in Volume, but the soil has not been significantly transported.
V	Completely weathered	All rock material is decomposed and/or Disintegrated to soil. The original mass structure is still largely intact
IV	Highly weathered	More than half of the rock material is decomposed or disintegrated to a soil. Fresh or discolored rock is present either as a discontinuous framework or as core stones
III	Moderately weathered	Less than half of the rock material is decomposed or disintegrated to a soil. Fresh or discolored rock is present either as a continuous framework or as core stones.
II	Slightly weathered	Discoloration indicates weathering of rock material and discontinuity surfaces. All rock material may be discolored by weathering.
I	Fresh rock	No visible sign of rock material weathering; perhaps slight discoloration on major discontinuity surfaces.

(2) Depth of weathering

Classes	Depth of weathering	Weight
1	$Z < 1\text{m}$	4
2	$1\text{m} < Z < 3\text{m}$	3
3	$3\text{m} < Z < 5\text{m}$	2
4	$Z > 5\text{m}$	1

Z = depth of weathering

3. Spacing of discontinuities

Classes	Spacing of discontinuities	Weight
1	$> 100\text{cm}$	4
2	$30-100\text{cm}$	3
3	$30-5\text{cm}$	2
4	$< 5\text{cm}$	1

4. Orientation of discontinuities

Classes	Orientation of discontinuities	Weight
1	Against the slope to horizontal	4
2	Vertical	3
3	Parallel to the slope and steeper inclination than the slope	2
4	Parallel to the slope and smaller inclination than the slope	1

5. Compressive strength

Classes	Compressive strength		Weight
	Compressive strength (in kg/cm ³)	Point load (Is 50)	
1	$\delta_c > 40 \text{ kg/cm}^3$	>10MPa	4
2	$20 \text{ kg/cm}^3 < \delta_c < 40 \text{ kg/cm}^3$	4-10MPa	3
3	$10 \text{ kg/cm}^3 < \delta_c < 20 \text{ kg/cm}^3$	2-4MPa	2
4	$\delta_c < 10 \text{ kg/cm}^3$	1-2MPa	1

(6).permeability

Classes	Permeability	Weight
1	highly permeable ($k > 10^{-3} \text{ m/sec}$)	4
2	Medium permeability ($10^{-5} \text{ m/sec} < k < 10^{-3} \text{ m/sec}$)	3
3	Low permeability ($10^{-9} \text{ m/sec} < k < 10^{-5} \text{ m/sec}$)	2
4	Very low permeability ($k < 10^{-9} \text{ m/sec}$)	1

(B) Additional description for unconsolidated lithologies/soils

(1) Degree of cementation

Class	Degree of cementation	Description	Weight
1	Highly cemented	The sample cannot be broken up with fingers	4
2	Moderate cemented	The sample breaks only if it is impressed with a strong finger pressure	3
3	Weak cemented	The sample can be broken under light compression by finger pressure	2
4	Very weak cemented	The sample can be easily broken by finger	1

(2). Thickness of the unconsolidated material (debris) – is the same as depth of weathering

(3). Compactness of unconsolidated materials

Classes	Degree of compactness	Weight
1	very compact	4
2	Compact	3
3	weak	2
4	Very weak	1

Annex-II: Weighing system of PAI guideline

Weights of the different classes of Slope gradients PAI guideline (Dovera et al 2000)

Slope classes (in %)	Weights
0 - 10 %	2
11 - 20 %	1
21 - 35%	0
36 – 50 %	-1
> 50 %	-2

Weights of the different classes of Land use based on PAI guideline (Dovera et al, 2000)

<i>Sigla</i>	<i>Classi di uso del suolo</i>	<i>Impendenza</i>	<i>Peso</i>
111	<i>Tessuto urbano continuo</i>	<i>mediocre</i>	<i>0</i>
112	<i>Tessuto urbano discontinuo</i>	<i>mediocre</i>	<i>0</i>
121	<i>Aree industriali e commerciali</i>	<i>mediocre</i>	<i>0</i>
122	<i>Reti stradali e ferroviarie e spazi accessori</i>	<i>minima</i>	<i>-1</i>
124	<i>Aeroporti</i>	<i>mediocre</i>	<i>0</i>
131	<i>Aree estrattive</i>	<i>nulla</i>	<i>-2</i>
133	<i>Aree in costruzione</i>	<i>minima</i>	<i>-1</i>
211	<i>Seminativi in aree non irrigue</i>	<i>nulla</i>	<i>-2</i>
221	<i>Vigneti</i>	<i>nulla</i>	<i>-2</i>
222	<i>Frutteti</i>	<i>mediocre</i>	<i>0</i>
231	<i>Prati stabili</i>	<i>mediocre</i>	<i>0</i>
242	<i>Sistemi colturali particellari complessi</i>	<i>minima</i>	<i>-1</i>
243	<i>Aree prevalentemente occupate da colture agrarie</i>	<i>nulla</i>	<i>-2</i>
311	<i>Boschi di latifoglie</i>	<i>massima</i>	<i>+2</i>
312	<i>Boschi di conifere</i>	<i>massima</i>	<i>+2</i>
313	<i>Boschi misti</i>	<i>massima</i>	<i>+2</i>
321	<i>Aree a pascolo naturale e prateria d'alta quota</i>	<i>mediocre</i>	<i>0</i>
322	<i>Brughiere e cespuglieti</i>	<i>buona</i>	<i>+1</i>
324	<i>Aree vegetazione boschiva e arbustiva in evoluzione</i>	<i>buona</i>	<i>+1</i>
331	<i>Spiagge, dune, sabbie</i>	<i>nulla</i>	<i>-2</i>
332	<i>Rocce nude, falesie, rupi e affioramenti</i>	<i>nulla</i>	<i>-2</i>
333	<i>Aree con vegetazione rada</i>	<i>minima</i>	<i>-1</i>
411	<i>Paludi</i>	<i>nulla</i>	<i>-2</i>
511	<i>Corsi d'acqua, canali e idrovie</i>	<i>nulla</i>	<i>-2</i>
512	<i>Bacini d'acqua</i>	<i>nulla</i>	<i>-2</i>

Classes of potential instability based on PAI guideline ((Dovera et al, 2000)

<i>Classe di instabilità</i>	<i>Descrizione</i>	<i>Pesi</i>	
		<i>da</i>	<i>a</i>
<i>1</i>	<i>Situazione potenzialmente stabile</i>	<i>10</i>	<i>12</i>
<i>2</i>	<i>Instabilità potenziale limitata</i>	<i>7</i>	<i>9</i>
<i>3</i>	<i>Instabilità potenziale media</i>	<i>4</i>	<i>6</i>
<i>4</i>	<i>Instabilità potenziale forte</i>	<i>1</i>	<i>3</i>
<i>5</i>	<i>Instabilità potenziale massima</i>	<i>-3</i>	<i>0</i>